# Thermal History of Parts of the Lewisian Gneiss Complex, N.W. Scotland.

Andrew Charles Barnicoat B.Sc. ( Leeds ).

Ph.D

Universtiy of Edinburgh

1982

Dedicated to my wife and parents for unflagging support throughout.

## Abstract

The Scourian complex consists of a complex suite of rocks which are of mixed origin. Obvious metasediments and metaigneous rocks occur with 'grey' gneisses of equivocal origin. All of these rocks underwent deformation and metamorphism between 2.7 and 2.6 Gyr. Owing to re-equilibration during slow cooling from high temperatures, it is not possible to be certain of peak metamorphic conditions, but the cores of coarse-grained crystals record that temperatures were at least 1000°C and pressures were in excess of 14kbar (1.4 Gpa). These conditions fall in the medium-pressure sub-facies of the granulite facies as defined by an analysis of reactions in the system $CaO-MgO-Al_2O_3-SiO_2$. The highest grade conditions are recorded by coarse, highly exsolved sub-calcic ferroaugite and pigeonite in a metamorphosed ironstone. Garnet-clinopyroxene equilibration temperatures for coarse-grained intergrowths are also about 1000°C. Major and rare earth element analyses indicate that these intergrowths originated as high-alumina amphiboles. The highest pressures are recorded by assemblages formed by the later breakdown of garnet in basic rocks.

An examination of the initial content and activity of water in the rocks of the Scourie complex indicates that partial melting of both acid and basic rocks was important in generating the geochemical depletion

observed in the Scourie complex.

Numerical thermal modelling suggests that the cause of the Scourian metamorphism was tectonic thickening rather than heat from cooling plutonic rocks as geochronological data indicates an extended period (>200 Myr) between igneous activity and the peak of metamorphism.

Later tectonic activity, emplacing the rocks of the Scourie complex to higher levels (above amphibolite facies rocks) caused re-equilibration, notably the breakdown and subsequent regrowth of garnet in basic rocks. Scourie dykes were emplaced into the still hot and deeply buried crust; conditions were about 600°C and 6 kbar (0.6 Gpa). Subsequently, the complex underwent additional deformation due to gravitational re-adjustment of the unstable situation of granulites overlying less dense amphibolites.

## Contents

## List of figures

## List of tables

I declare that this is all my own work with the exception of Chapter 3 which has been published in an earlier form as a paper with Prof. M J O'Hara ( Mineralogical Magazine Vol.43 ).

Signed .....

A.C.Barnicoat.

## Abbreviations and constants used

### Minerals

Minerals are generally abbreviated to three letters and end-members to two.

| | | | |
|---|---|---|---|
| qtz | quartz | plg | plagioclase |
| ksp | alkali feldspar | opx | orthopyroxene |
| cpx | clinopyroxene | gnt | garnet |
| spn | spinel | amp | amphibole |
| kya | $Al_2SiO_5$ polymorph | ilm | ilmentite |
| mag | magnetite | olv | olivine |

| | | | |
|---|---|---|---|
| An | anorthite | ab | albite |
| en | enstatite | fs | ferrosilite |
| di | diopside | hd | hedenbergite |
| CaTs | Calcium tschermaks molecule ($CaAl_2SiO_6$) | | |
| CaEs | Calcium eskolas molecule ($Ca_{1/2}AlSi_2O_6$) | | |
| py | pyrope | gr | grossular |
| al | almandine | M5C | $Mg_{5/3}Ca_{1/3}Al_2Si_3O_{12}$ |
| sp | spinel | tr | tremolite |
| hb | hornblende | fo | fosterite |

### Abbreviations of thermodynamic terms

| | |
|---|---|
| $\Delta G_{(P,T)}$ | Gibbs free energy change at P bars and T K |
| $\Delta H_{(P,T)}$ | Enthalpy change at P bars and T K |
| $\Delta S_{(T)}$ | Entropy change at T K |
| $\Delta V$ | Volume change |
| $\Delta v_s$ | Volume change of solids |
| $X_n^m$ | Thermodynamic mole fraction of n in phase m |
| $A_{n,id}^m$ | Ideal activity of n in phase m |
| $A_n^m$ | Activity of n in phase m |
| $\gamma_n^m$ | Activity coefficient of n in phase m |
| K | Equilibrium constant |
| R | Gas constant, 8.3 J $mol^{-1}$ $K^{-1}$ |

### General abbreviations

| | |
|---|---|
| C | Heat capacity at constant pressure |
| $\varrho$ | Density |
| K | Themal conductivity |
| REE | Rare earth elements |
| HREE | Heavy rare earth elements |
| hfu | Heat flow units = 41.8 $mWm^{-2}$ |
| hgu | Heat generation units = 0.418 $\mu Wm^{-3}$ |
| EDS | Energy-dispersive probe analysis |
| MWDS | Manual wavelength-dispersive probe analysis |
| AWDS | Automatic wavelength-dispersive probe analysis |
| nd | Not detected |
| na | Not analysed |

Lens cap used in photographs is ca. 55mm across.

## Acknowledgements

I would like to thank Prof. MJ O'Hara for suggesting the topic for research, and for allowing me the time to complete it. I would also like to thank Dr. B Harte and Prof MJ O'Hara for valuable advice and supervision. NERC provided a research studentship for the first two years of this work, and assistance to attend the theoretical petrology course at Manchester.

I am grateful to Dr. PG Hill, Mr. C Begg and Dr. S O'Hara for assistance with microprobe analyses, and to Dr. N Walsh of King's College, London for performing ICPS analyses of eight specimens for major and rare-earth elements.

Dr. R Powell of Leeds University gave advice on error analysis and he, Dr. WR Fitches and Mr J Ridley were helpful in discussion of various points.

Mr D Jenkins quickly and efficiently produced the plates and the UCW computer unit freely gave advice and the use of equipment used in producing the text.

Finally I would like to express my gratitude to Bill Fitches and my wife, Christine, for much assistance during the final stages of preparing this thesis.

# Chapter 1 Introduction

The Scourian portion of the Lewisian complex of NW Scotland is the most intensively investigated portion of Archaean rocks in the world. Investigations have ranged over many aspects, including field relations, structure, petrology, geophysics , and more recently geochemistry. Until the mid 1970's, no serious attempt to elucidate metamorphic conditions (and leading on from this to quantify the thermal history ) had been published. This thesis is particularly concerned with the metamorphic and thermal history, but attention is also paid to their relationships with other areas of investigation and to the presentation of a coherent geological history. The area around Scourie is ideally suited for this investigation as it shows various features whose P-T conditions of formation can be estimated, and which can be dated relatively by field criteria and 'absolutely' by radiometric methods.

## 1.1 Geological Setting

The geology of the Lewisian complex has recently been reviewed by Watson (1975) and Bowes (1978). The mainland Lewisian has been divided into two separate rock groups, the Scourian and Laxfordian complexes (fig.1.1). They are distinguished primarily by the deformational state of early Proterozoic dykes (the 'Scourie dykes')

Fig. 1.1 Map of N.W. Scotland showing the outcrop of the Lewisian gneiss and major areas of Scourie and Laxford complexes.

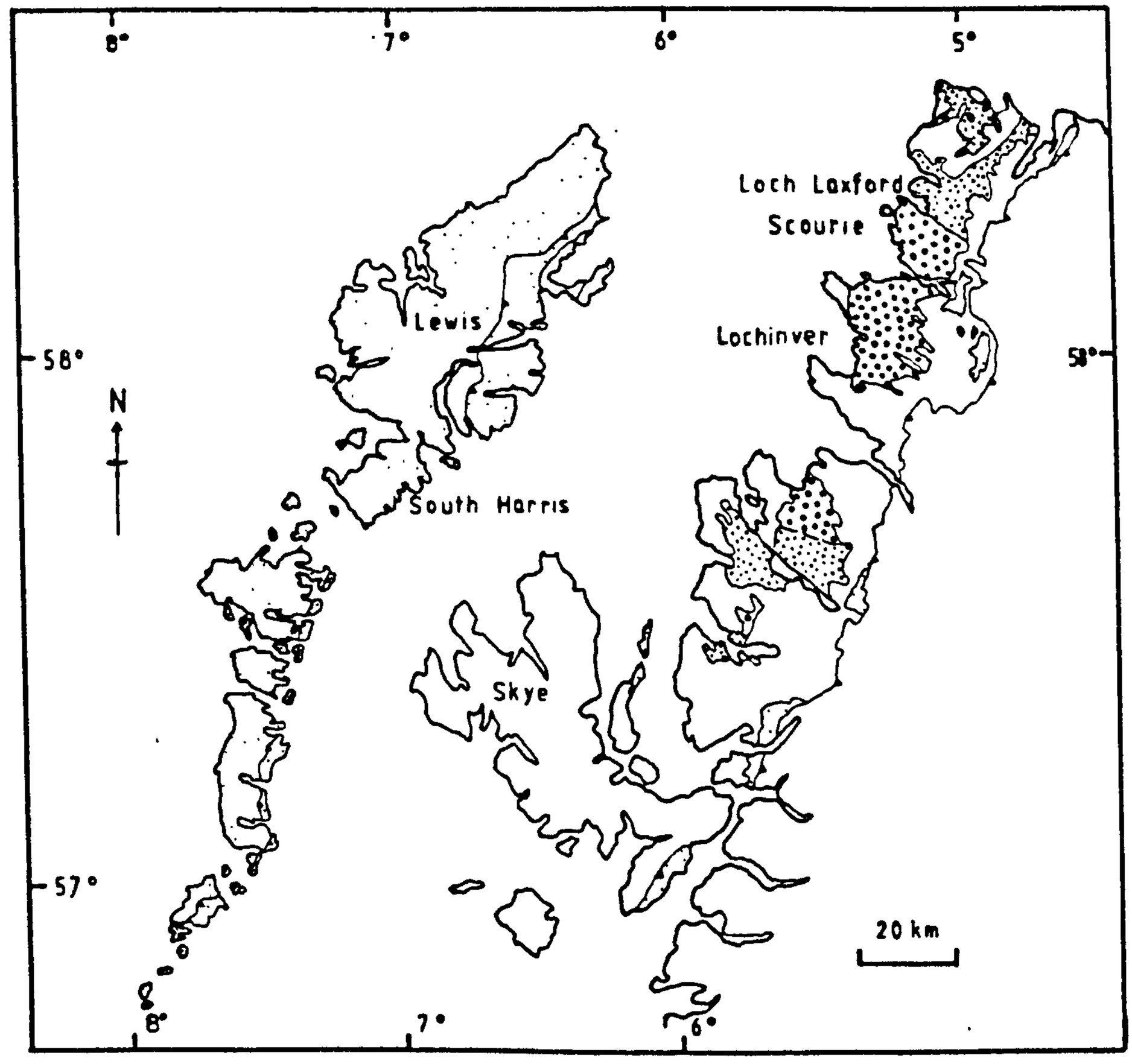
8°
7°
6°
5°
58°
57°
N
Lewis
South Harris
Skye
Loch Laxford
Scourie
Lochinver
20 km
Scourie Complex (extensive areas only)
Laxford Complex
Undifferentiated Lewisian
Post Lewisian rocks
Major thrusts

which cut across much of the Lewisian. All of the rocks (including those of the Laxfordian complex) date back to at least 2.8 Gyr (Moorbath et al.,1969, Hamilton et al, 1979). The geochronological framework of the Outer Isles is at present unclear as rocks in South Harris, long considered to be Scourian, now appear to be no older than 2.2 Gyr (Dr RA Cliff, personal communication 1982).

The Scourian complex, with which this thesis is concerned, is dominated by granulite facies quartzo - feldspathic gneisses and their retrogressed equivalents. An important minor constituent of the Scourian is a series of basic - ultrabasic masses, which are in some cases associated with undoubted metasediments (Davies, 1974).

Various origins have been proposed for the quartzo - feldspathic gneisses : greywackes, intermediate volcanics and Cordilleran plutonic rocks, individually or together are the most frequently suggested precursors. The basic - ultrabasic masses are usually described in terms of plutonic rocks, altough some authors do not rule out an extrusive origin. These questions are discussed further in Chapters 7 and 9.

A flat-lying foliation, imposed on the complex by a high-grade tectonothermal event, has obliterated any evidence of early, primary features or early history as envisaged by Davies (1975), by analogy with Greenland. Isotopic evidence (Chapman and Moorbath, 1977), however, suggests that there was only a very limited pre - 2.8 Gyr

crustal residence time for these rocks.

The geography and geology of the Scourie area is summarised in fig.1.2.

## 1.2 Previous work

### 1.2.1 Early work

The earliest comprehensive study of the Lewisian of the NW Highlands was published in 1907 (Peach et al.). The broad two - fold division of the Lewisian complex into what are now called the Scourian and Laxfordian was recognised at this stage, and amplified by Sutton and Watson (1951) who studied the areas around Scourie and Torridon. The petrology of the complex , especially the basic rocks, was studied by O'Hara (1960, 1961b, 1965). He also investigated the petrology of the Scourie dykes (1961a, 1962), and demonstrated that the dykes were emplaced under amphibolite facies conditions, thereby implying that the rocks of the Scourie complex remained deep - seated at this time, contrary to the views of Sutton and Watson (op. cit.). At about the same time, Giletti et al (1961) provided the first radiometric dates of Lewisian rocks, demonstrating the Archaean age of the Scourie complex. Evans (1965) and Evans and Lambert (1974) recognised that pre - Scourie dyke amphibolite facies metamorphism occurred in certain localised parts of the Scourian complex, notably around Lochinver and north of Tarbert. This phase of activity has been called the Inverian.

Subsequent work has been relatively specialised, and

Fig. 1.2a The area between Loch Laxford and Lochiver.

Fig. 1.2b The Geology of the Scourie area showing the distribution of basic-ultrabasic masses and Scourie dykes.

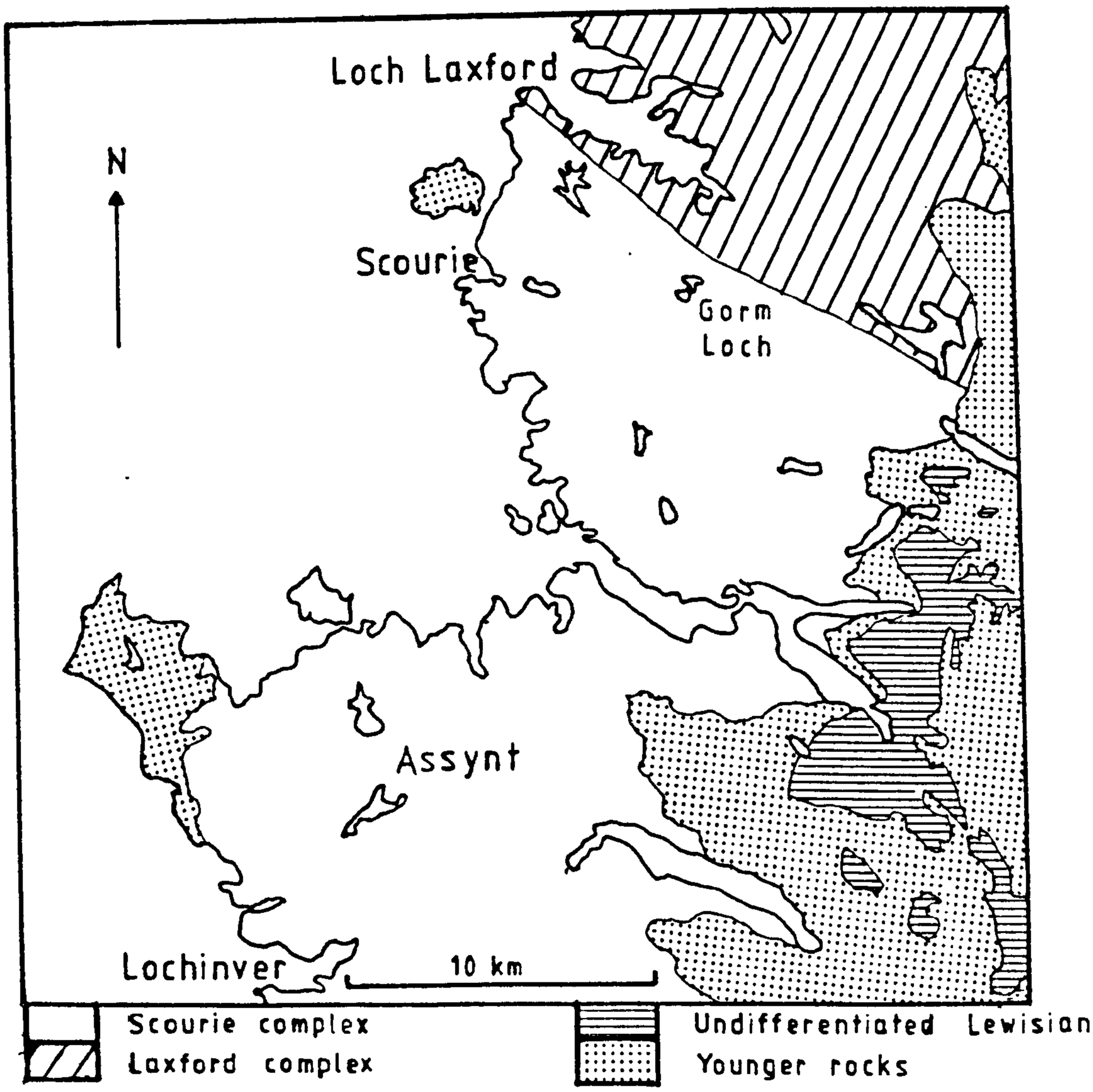
Loch Laxford
N
Scourie
Gorm
Loch
Assynt
Lochinver
10 km
Scourie complex
Laxford complex
Undifferentiated Lewisian
Younger rocks

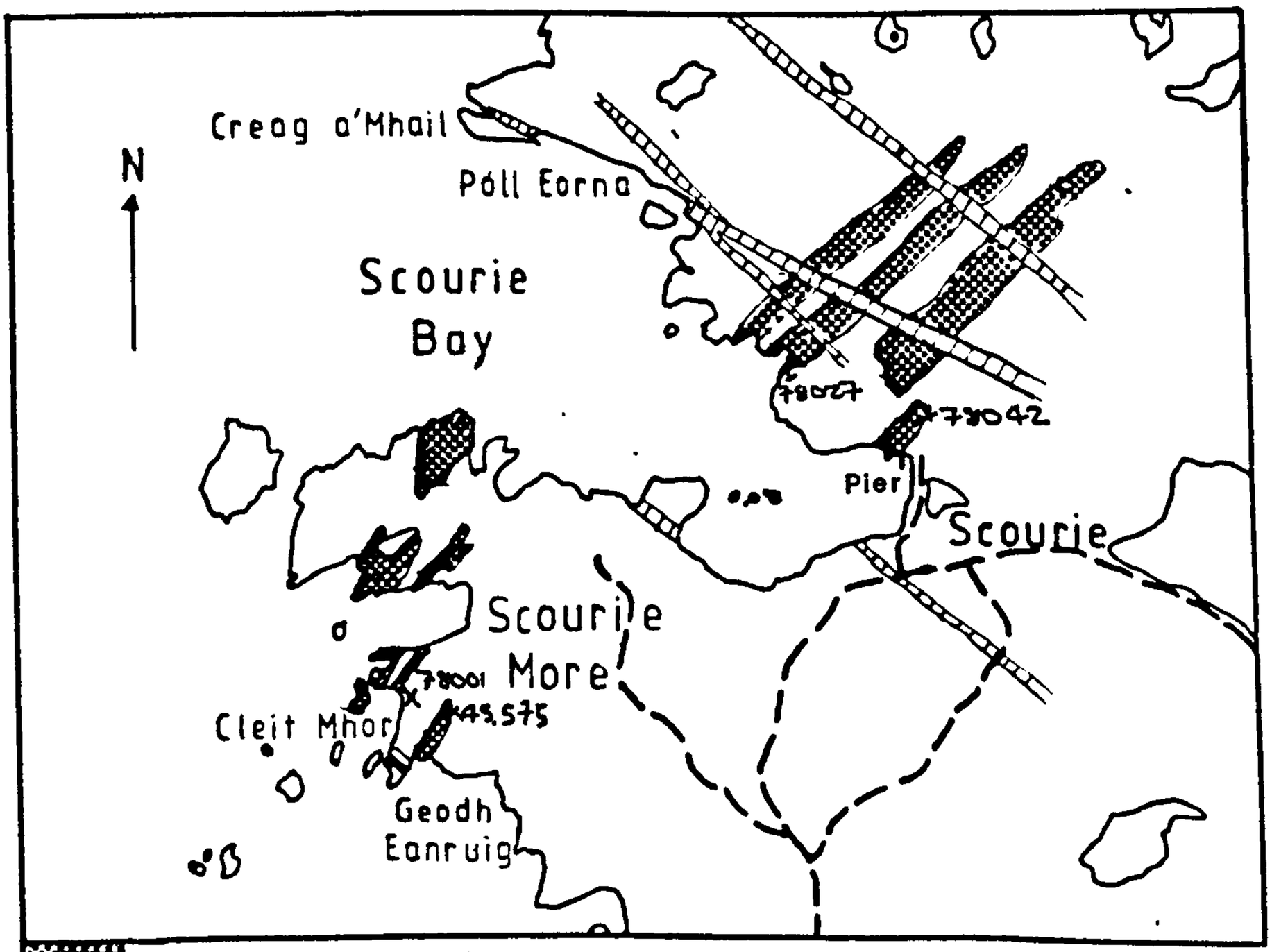
Creag a'Mhail
Pòll Eorna
N
Scourie
Bay
Pier
Scourie
Scourie
More
Cleit Mhor
Geodh
Eanruig
Basic - ultrabasic masses
Scourie dykes
1 km

will be described under various headings.

1.2.2 Structural and Geophysical work

In the fifteen years since the first work on the Inverian, research on the Lewisian has concentrated on the earlier events (i.e. granulite facies metamorphism and earlier, termed 'Badcallian' by Park, 1970). Geophysical surveys across the Scourian - Laxfordian boundary by Bott et al. (1972) suggested the presence of a large fold . Detailed mapping by Beach et al. (1974), Coward (1974), Beach (1974) has modified this suggestion and indicates that kernels of rocks undeformed since the Scourian are surrounded in three dimensions by zones of later (Inverian and Laxfordian) reworking. Furthermore, Beach et al (op. cit.) suggest that the rocks of the Scourie 'block' may have been tectonically emplaced in their present position, possibly during the Laxfordian. Davies (1978) has provided evidence implying that this emplacement may have occured, or at least started, during the Archaean (see Chapter 9).

1.2.3 Geochronolgy

Subsequent to the initial work of Giletti et al.(1961), Moorbath et al. (1969) and Chapman and Moorbath (1977) used Pb - Pb whole rock techniques to demonstrate that a period of U depletion occurred throughout the Lewisian 2.6 Gyr ago. U - Pb dating of zircons by Pidgeon and Bowes (1972) suggests that the granulite facies metamorphism was at about 2.69 Gyr. Hamilton et al.(1979) used Sm - Nd dating on whole rocks,

to obtain an age of 2.92 ± 0.05 Gyr. They interpreted this as representing the time at which the precursors (igneous forerunners) of the whole Lewisian complex crystallised. They also said that the rocks could only have had a short crustal residence time (<200 Myr) prior to this.

In addition to providing a Pb - Pb date, Chapman and Moorbath (op. cit.) also tested and rejected the hypothesis of Davies (1975) that certain parts of the Scourie complex (the 'Uamhaig' gneisses) were the equivalent of the much older Amitsoq gneisses of Greenland. Very recently, Humphries and Cliff (1982) published Sm-Nd mineral data from rocks from Scourie, suggesting mineral growth at ca. 2.62 ± 0.12 Gyr and cessation of isotopic diffusion at about 2.49 ± 0.03 Gyr.

Chapman (1979) has dated the Scourie dyke swarm at 2.39 ± 0.02 Gyr using Rb - Sr whole rock techniques.

### 1.2.4 Geochemistry

The geochemistry of the Lewisian , especially the Scourian ,has been extensively investigated over the past decade. The initial work of Sheraton (1970) has been followed by that of many workers, notably Holland and Lambert (1973, 1975), Sheraton et al (1973), Tarney (1976), Tarney and Windley (1977), Weaver and Tarney (1980), Rollinson and Windley (1980a,b), Pride and Muecke (1980,1981). Most effort has been devoted to ascertaining the main processes governing the geochemistry of the acid gneisses, and to their environment of formation. Several

origins for these gneisses have been suggested: notably greywacke-type sediments, andesitic volcanics and calc-alkaline plutonic rocks. Most authors have favoured the third alternative (eg Holland and Lambert, op. cit.; Rollinson and Windley, op. cit.; Weaver and Tarney, op. cit.), although they differ in the explanation given for the difference in chemistry between the Scourian rocks and their modern analogues. Rollinson and Windley, and Weaver and Tarney explain these differences (exemplified by the very low levels of K and U and very high K/Rb values of the Scourian rocks) by invoking the passage of mantle-derived $CO_2$-rich ichors through the Lewisian rocks. Holland and Lambert favour a mechanism whereby the Scourian rocks crystallised from a magma at depth directly to a charnokitic mineralogy, and the residual liquid (rich in K,U and with a low K/Rb value ) escaped to higher levels. The latter model is not easily distinguished chemically from a partial melting model as favoured by Pride and Muecke (op. cit.). Further discussion of this topic is given in Chapter 9 .

### 1.2.5 Metamorphism

The earliest work concentrating on the metamorphic petrology was by O'Hara (1960, 1961a,b, 1965). O'Hara (1967b) also produced the first estimate of the P - T conditions for the Scourian granulite facies metamorphism; $P_{Max.}$ = 17kbar, $T_{Max.}$ = 1000°C, estimated on the basis of pyroxene parageneses. In 1969, in a detailed study, Muecke concluded that $P_{Max.}$ = 8Kbar, $T_{Max.}$ = 800°C.

Since then, techniques of estimation of P-T conditions in granulite-facies rocks have improved markedly, although problems of identifying equilibrium assemblages and their time of origin (Harte et al., 1981) remain. Several authors have recently pursued P-T estimates. Rollinson (1979, 1980a) has examined magnetite-ilmenite relationships in granulites and trondhjemites, and estimated equilibration temperatures at various stages, including a high temperature 'igneous' event . His sequence of events is presented in table 1.1. These results must be treated with caution, however, as some ilmenite grains have Mn contents of up to 8.3% and there may well be non-ideal solid-solution relations between ilmenite and a manganese end-member. In another paper (1980b) he has used plagioclase-scapolite and plagioclase-clinopyroxene equilibria to constrain peak granulite facies conditions. Savage and Sills (1980) proposed a two stage granulite facies metamorphim on the basis of garnet reaction textures. The estimates of maximum P - T conditions of these and other authors are listed in table 1.2.

1.2.5.1 O'Hara's 1977 model

In 1977, O'Hara proposed a comprehensive metamorphic evolution of the Scourie complex, with a series of eleven demonstrable stages (table 1.3). In broad outline, he proposed a continuous evolution involving a long and complex path from the surface, through a prograde sequence of events to a granulite facies peak (at which

Table 1.1 The metamorphic history of the Scourie complex proposed by Rollinson (1979*, 1980a†, 1980b$^{\Delta}$).

| | T | P | Activity of oxygen |
|---|---|---|---|
| Magmatic event | 1035-890°C* | - | Slightly above NNO* |
| Metamorphic cooling | 830-660°C<br>915 130°C$^{\Delta}$ | 11kbar$^{\Delta}$ | ca. QFM* |
| Cessation of Fe-Mg exchange involving cpx | ca. 550°C* | - | - |
| Retrogression by introduced fluids | 530-320°C* | - | Unbuffered† |

Table 1.2 Estimate of the conditions of Scourian metamorphism.

| | P (kbar) | T (°C) | |
|---|---|---|---|
| O'Hara 1967 | 17 | 1000 | Pyroxene parageneses |
| Bowdidge 1969 | 17 | 1000 | " |
| Muecke 1969 | 7-9 | 700-800 | |
| *Wood 1975,1977 | 13 | 825 | 2 pyroxene temperature; cpx-plg-qtz pressures |
| O'Hara 1977<br>O'Hara and Yarwood 1978 | 15 | 1250±100 | Feldspar and pyroxene parageneses melting relations, garnet stability in basic rocks |
| Pride in Pride and Muecke 1980 | 11 | 900 | 2 pyroxene temperature and garnet stability in basic rocks |
| Rollinson 1980b | 11 | 915±130 | Plagioclase - scapolite temperatures, cpx-plg-qtz pressures |
| Savage and Sills 1980 | 12-15 | 1000±100 | Estimate of pre-reequilibration compositions |

* South Harris, may not be Scourian.

Table 1.3 O'Hara (1977) model of the evolution of the Scourie complex.

| | P(kbar)* | T(°C)* | Date* |
|---|---|---|---|
| (i) Formation of supracrustal series | 0 | 0 | > 2.8Gyr |
| (ii) Partial melting and dehydration during prograde amphibolite facies metamorphism. | 8 | 550 | |
| (iii) Drier melts produced at granulite facies. | 12 | 900 | |
| (iv) Further, dry melting at peak of metamorphism. | 15 | 1250 | ca.2.8Gyr |
| (v) Breakdown of magnesian garnet due to collapse of crustal geotherms, followed by regrowth of garnet at lower temperatures and pressures. | 12.5 | 800 | ca.2.6Gyr |
| (vi) Inverian deformation. | 8 | 500 | ca.2.3Gyr |
| (vii) Intrusion of Scourie dykes into relatively hot country rock. | 6 | 450 | 2.25Gyr |
| (viii) Laxfordian event. | 6.5 | 500 | 1.89Gyr |
| (ix) Steady recovery to the surface prior to the deposition of Torridonian sediments. | 0 | 0 | 1.0Gyr |

* These values are order of magnitude estimates.

partial melting was important), followed by a slow recovery to the Earth's surface prior to the deposition of the Torridonian sediments. The whole sequence of events was couched only in broad P - T terms, and O'Hara and Yarwood (1978) started to quantify the model, placing emphasis on estimating the peak conditions.

Minimum pressures for the metamorphism were estimated at 12kbar from experiments on rocks described by O'Hara (1961a) as transition gneisses. These contain symplectites of plagioclase, spinel and orthopyroxene, commonly with garnet present, and occasionaly with small quantities of clinopyroxene. Garnet also forms cores to the symplectites in some rocks. These mineralogies and textures have been interpreted (O'Hara and Yarwood, 1978; Savage and Sills, 1980) as showing the symplectites to have been magnesium - rich garnets which have broken down by the reaction

Mg rich garnet = Mg poor garnet + hypersthene + calcic plagioclase + aluminous spinel + trace augite.

O'Hara and Yarwood also describe the regrowth of garnet on a smaller scale between crystals of the symplectite, indicating a re-crossing of the reaction P-T conditions.

Minimum temperatures for the peak conditions were estimated by O'Hara and Yarwood (op. cit.) on the basis of the composition of 0.1mm (001) pigeonite lamellae exsolved from augite in an iron rich quartz - two pyroxene - magnetite rock. Comparison with the 1

atmosphere data of Ross et al (1973) suggested an equilibration temperature in excess of 1050°C.
High temperature feldspars were reported from granitic material by O'Hara (1965) and O'Hara and Yarwood; rare intergrown mesoperthite and antiperthite suggested temperatures in excess of 1200°C, although dry melting of the rock begins at about this temperature. O'Hara and Yarwood therefore consider this rock to be an approximately in situ partial melt, and interpret the temperatures (and pressures needed to raise the solidus to these levels) as indicating that the complex as a whole was under these conditions. In contrast, Rollinson and Windley (1980b) considered that these rocks are of igneous origin, resulting from the fractional crystallisation of tonalitic liquids (with lower liquidus temperatures) and that the temperatures do not reflect the general P -T regime, but localised igneous activity. The conditions proposed by O'Hara and Yarwood for the peak of metamorphism did not agree with the cation exchange geothermometers and geobarometers available at the time. The reasons for this are complex; the calibrations then in use are inaccurate, and reequilibration has undoubtedly occured during cooling (e.g. exsolution,garnet destabilisation, see Chapters 3,4,5) giving rise to closure effects (Dodson, 1976) and probably cation ordering as well.
This thesis examines some of the evidence put forward by O'Hara and Yarwood in greater detail ,

Chapters 2, 3, 4 and 5 provide new data on the conditions at the peak of Scourian metamorphism, with reference to both the general petrology and to specific rocks. Particular attention is paid to rocks of coarser than average grain size (>5mm) as such material records the earliest, highest grade conditions. The ironstone discussed in chapter 3 and the intergrowths discussed in chapter 4 additionally throw some light on the early history of the complex. Chapter 6 contains an update of the petrography and metamorphic petrogenesis of the Scourie dyke swarm. Chapter 7 presents a discussion on the role of partial melting as the cause of the observed geochemistry of the Scourie complex, in particular the part played by water is discussed. In chapter 8, alternative ways of generating the high observed metamorphic temperatures have been investigated, and a tectonic thickening model involving partial melting is presented. The final chapter contains a synopsis of the possible evolution of the Scourie complex in the light of the data of this thesis and other workers.

# Chapter 2 The Granulite facies at Scourie

## 2.1 Introduction

It has long been recognised that the rocks of the Scourie complex are metamorphic rocks containing the assemblage qtz-plg-opx-cpx in silica saturated lithologies (Peach et al., 1907). Sutton and Watson (1951) were the first workers to place the Scourian complex in the Granulite facies. The position of these rocks within the granulite facies is uncertain; Miyashiro (1973) puts the rocks into the 'low pressure part of the medium pressure subfacies', whereas other authors have simply suggested P-T conditions for the equilibration of these rocks.

Much of this uncertainty is undoubtedly due to the poor understanding of the sub-division of the granulite facies. Many authors have followed de Waard (1965) in using the production of garnet in quartz-saturated rocks, modelled by the reaction

Opx + Ca-rich plg = Qtz + cpx + Na-rich plag + Py-rich gnt

to subdivide granulites into pyroxene and garnet bearing assemblages. On the other hand, O'Hara (1967a) divided the quartz-free spinel lherzolite facies (= granulite facies) into Seilandite (low pressure) and Ariegite (high pressure) subfacies using the reaction

Opx + cpx +plg + spn = Py-gr-gnt

The formation of garnet granulites has been investigated (in rocks of specific composition) as an intermediate stage in the gabbro-eclogite transition by various authors (see Wyllie, 1971 for a review).

## 2.2 Petrogenetic grids

In an attempt to clarify the uncertainty, in particular the relationship of quartz-bearing and quartz-free garnet forming reactions and the relationship of the granulite facies to neighbouring facies, a theoretical analysis of possible reactions in CMAS has been performed. Both anhydrous and hydrous grids have been constructed; the reactions are prefixed by A and H respectively.

### 2.2.1 Anhydrous grid

In this section, amphibole-free assemblages are considered. The possible reactions between qtz, plg, cpx, opx, gnt, spn, kya and olv have been determined using the program REACTION (Finger and Burt, 1973). This program allows known mineralogical incompatibilities to be defined, hence reducing the number of reactions calculated. In this case, assemblages containing qtz + olv, qtz+spn and plg + olv + gnt have been excluded from the analysis. On the basis of the experimental determinations of Jenkins and Newton (1979) and Hansen (1981), the composition of garnet used in these calculations was 0.15 grossular, 0.85 pyrope (c.f. Obata and Thompson, 1981;Jenkins, 1981). The reactions

calculated are given in table 2.1.

The grid produced (fig 2.1) is similar to that of Obata and Thompson (op cit.) although they have produced an incorrect reaction for the production of garnet (their no. 13) for the garnet composition that they quote. This grid contains assemblages and reactions, especially at lower temperatures, which are undoubtedly metastable with respect to other anhydrous assemblages containing, for example, sapphirine and cordierite, and also with regard to hydrous amphibole and chlorite bearing assemblages.

### 2.2.2 Amphibole-bearing grid

A second analysis, of amphibole bearing assemblages, has also been performed. To simplify the analysis, only clinopyroxene bearing assemblages were considered, and it was assumed that either amphibole or a vapour phase was present. The amphibole composition used was intermediate between tremolite and tschermakite, as suggested on the basis of experimental evidence by Jenkins (1981). This amphibole is strictly suitable only for olivine saturated assemblages, but it is unlikely that the amphibole stable in quartz bearing assemblages will be of a composition sufficiently different to change the nature of the reactions considered.

The same mineral incompatibilities as before were used in the construction of this grid. The reactions are presented in table 2.2, and the relevant part of the grid in figs. 2.2 and 2.3. Fig. 2.3 shows two alternative configurations for one particular region; although they

Table 2.1 Reactions in the water-free system using a calcium - bearing garnet.

| | |
|---|---|
| A1 | opx + spn = kya + olv |
| A2 | cpx + kya = plg + opx |
| A3 | cpx + kya + olv = gnt + spn |
| A4 | cpx + opx + spn = gnt + olv |
| A5 | cpx + opx + kya = gnt + spn |
| A6 | cpx + opx + kya + olv = gnt |
| A7 | plg + opx + kya + spn = gnt |
| A8 | cpx + kya + spn = plg + olv |
| A9 | cpx + kya + spn = plg + gnt |
| A10 | cpx + opx + spn = plg + olv |
| A11 | cpx + gnt = plg + spn + opx |
| A12 | qtz + gnt = cpx + opx + kya |
| A13 | qtz + gnt = plg + opx + kya |
| A14 | qtz + plg + gnt = cpx + kya |
| A15 | qtz + cpx + gnt = plg + opx |

Fig. 2.1 Schreinemakers web of possible reactions in the system $CaO - MgO - Al_2O_3 - SiO_2$ . Compatibilty diagrams are for Cpx bearing assemblages. See section 2.2.1 for details.

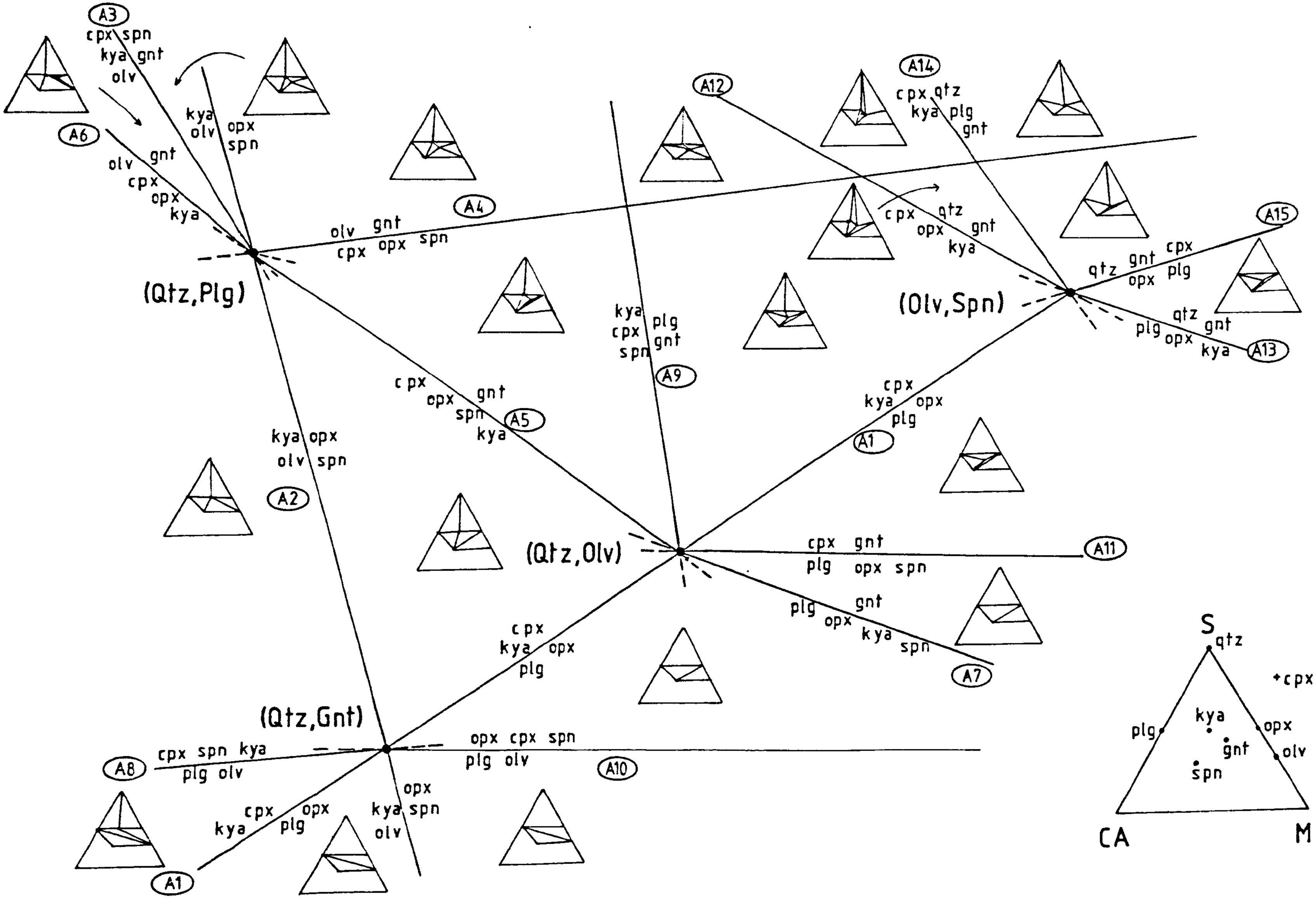
A3
cpx spn
kya gnt
olv
A6
olv gnt
cpx
opx
kya
kya
olv opx
spn
A4
olv gnt
cpx opx spn
(Qtz,Plg)
A12
A14
cpx qtz
kya plg
gnt
cpx qtz
opx gnt
kya
A15
qtz gnt cpx
opx plg
(Olv,Spn)
qtz gnt
plg opx kya
A13
kya plg
cpx gnt
spn
A9
cpx
opx gnt
spn
kya
A5
cpx
kya opx
plg
A1
kya opx
olv spn
A2
(Qtz,Olv)
cpx gnt
plg opx spn
A11
plg gnt
opx kya spn
A7
cpx
kya opx
plg
(Qtz,Gnt)
cpx spn kya
plg olv
A8
opx cpx spn
plg olv
A10
cpx
kya
opx
plg
opx
kya spn
olv
A1
S
qtz
+cpx
kya
plg
opx
gnt
olv
spn
CA
M

Table 2.2 Reactions in the system CA-M-S-H O with a Calcium - bearing garnet and a mixed tremolite - tschermakite amphibole (see text for discussion).

H1 gnt + olv = spn + amp
H2 opx + kya = gnt + amp
H3 opx + gnt = spn + amp
H4 plg + opx = gnt + amp
H5 qtz + gnt = plg + amp
H6 kya = plg + opx
H7 kya + olv = spn + amp
H8 gnt = kya + olv + amp
H9 gnt = spn + kya + amp
H10 gnt + spn = kya + olv
H11 opx + kya = olv + amp
H12 opx + spn = olv + amp
H13 opx + kya = spn + amp
H14 opx + spn = kya + amp
H15 opx + gnt = olv + amp
H16 opx + gnt = kya + olv
H17 opx + spn = gnt + olv
H18 gnt = opx + spn + kya
H19 kya = plg + olv + amp
H20 plg + olv = spn + amp
H21 kya = plg + spn + amp
H22 spn + kya = plg + olv
H23 kya = plg + gnt + amp
H24 gnt = plg + spn + amp
H25 plg + gnt = spn + kya
H26 plg + opx = olv + amp
H27 plg + opx = spn + amp
H28 opx + spn = plg + olv
H29 gnt = plg + opx + spn
H30 qtz + gnt = kya + amp
H31 qtz + opx + kya = amp
H32 qtz + opx + gnt = amp
H33 qtz + gnt = opx + kya
H34 qtz + kya = plg + amp
H35 qtz + plg + gnt = kya
H36 qtz + plg + opx = amp
H37 plg + opx = qtz + gnt

Fig. 2.2 Schreinemakers Web of possible reactions involving phases projected from Cpx onto CaO. $Al_2O_3$ - MgO - $SiO_2$. Details of the area between ( olv,spn,opx), ( olv, spn,plg ), ( olv,spn,amp ), ( olv,spn,gt ) and ( olv, spn,qtz ) is given in Fig. 2.3 . See section 2.2.2 for details.

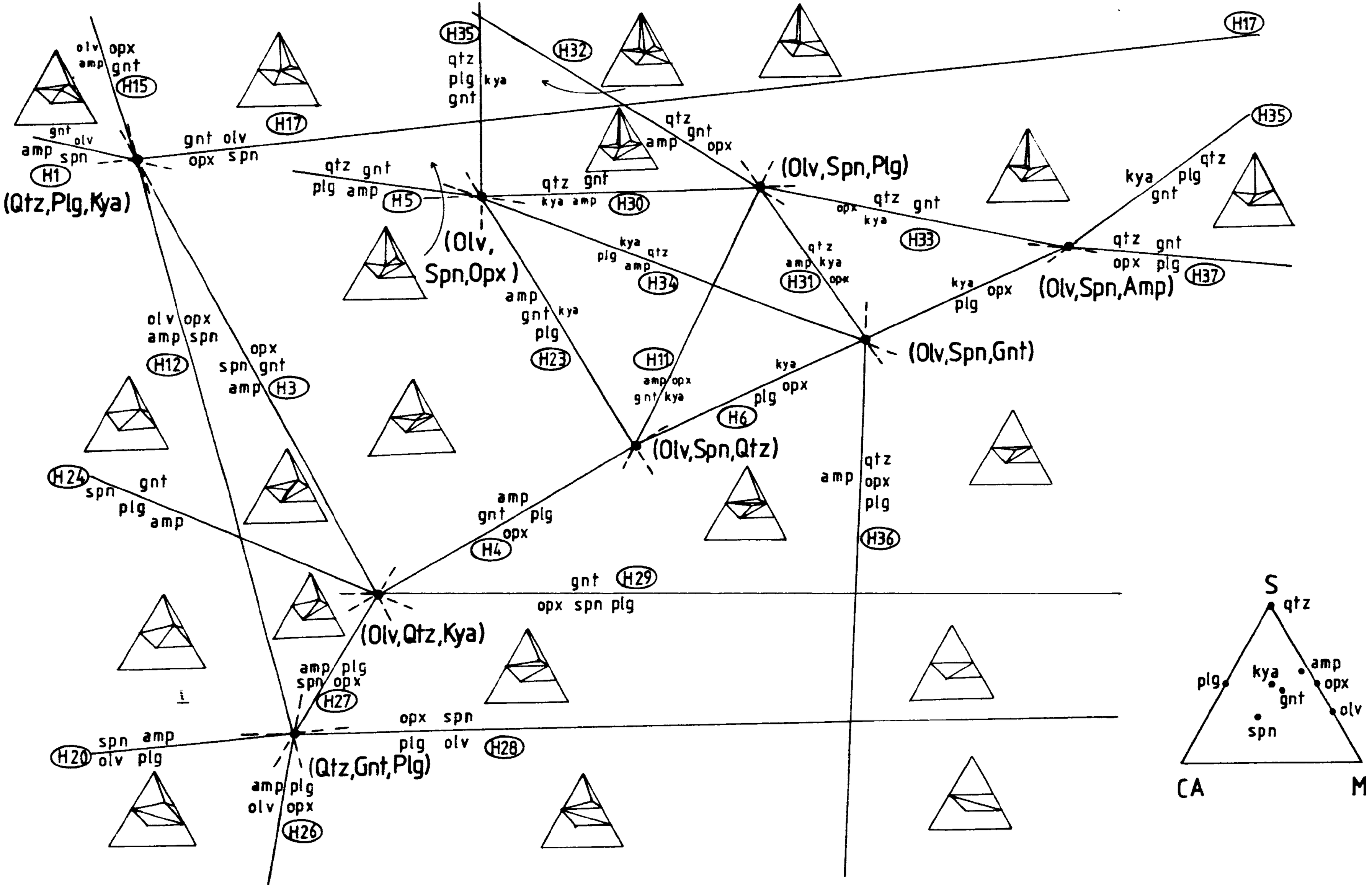
olv opx amp gnt
H15
gnt olv amp spn
H1
(Qtz,Plg,Kya)
gnt olv opx spn
H17
H35
qtz plg gnt kya
H32
qtz gnt plg amp
H5
qtz gnt amp
qtz gnt kya amp
H30
(Olv, Spn,Opx)
(Olv,Spn,Plg)
H17
H35
kya plg qtz gnt
qtz gnt opx kya
H33
kya qtz plg amp
H34
qtz amp kya opx
H31
qtz gnt opx plg
H37
(Olv,Spn,Amp)
kya opx plg
(Olv,Spn,Gnt)
olv opx amp spn
H12
opx spn gnt amp
H3
amp gnt kya plg
H23
H11
amp opx gnt kya
kya opx plg
H6
(Olv,Spn,Qtz)
H24
spn gnt plg amp
amp gnt plg opx
H4
amp qtz opx plg
H36
gnt H29
opx spn plg
(Olv,Qtz,Kya)
amp plg spn opx
H27
opx spn plg olv
H28
spn amp olv plg
H20
(Qtz,Gnt,Plg)
amp plg olv opx
H26
S
qtz
plg
kya
amp
opx
gnt
olv
spn
CA
M

Fig. 2.3 Detail of Fig. 2.2 showing two possible arrangements at the low - pressure end of reaction H37. See text for discussion.

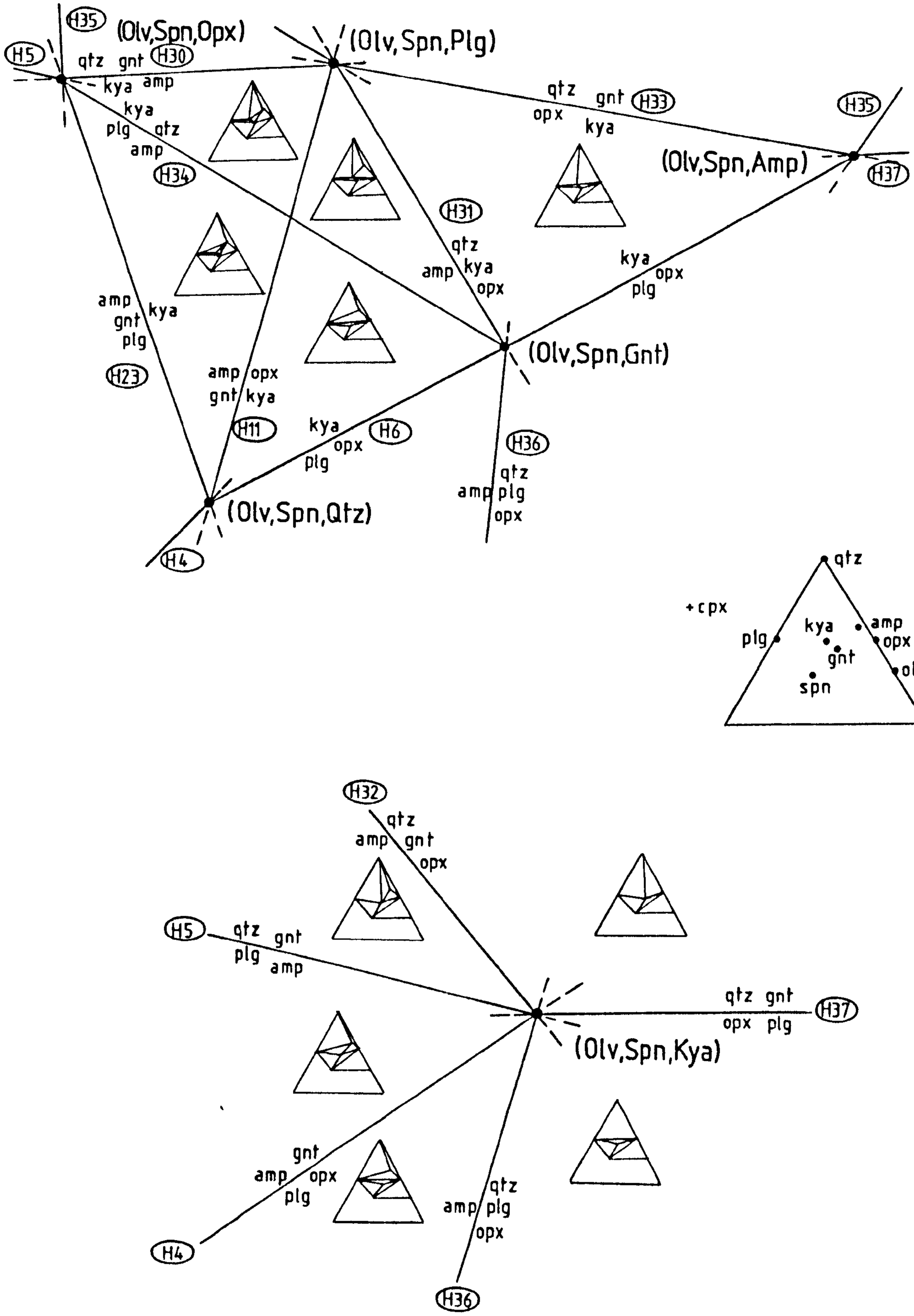
(Olv,Spn,Opx)
(Olv, Spn,Plg)
(Olv,Spn,Amp)
(Olv,Spn,Gnt)
(Olv,Spn,Qtz)
(Olv,Spn,Kya)
H5
H35
H30
H34
H31
H33
H37
H23
H11
H6
H36
H4
H32
qtz gnt opx kya plg amp
+cpx
qtz
plg
kya
amp
opx
gnt
olv
spn

are markedly different, this is of little consequence when the grid is put into P-T space (see fig. 2.4). Again, the grid is similar to that of Obata and Thompson (1981, figs.3 and 4) and Jenkins (1981, fig 7). It does not consider chlorite (which is not found as a granulite facies mineral), but it does consider assemblages of a wider range of silica contents, and also kyanite bearing assemblages.

The grid has been placed approximately in P-T space using the experimental data of Boyd (1959); Herzberg (1972, 1975); Hensen (1976); Oba (1978); Jenkins (1981), Hansen (1981) and O'Neill (1981) (fig 2.3).

Reaction H28 (separating plagioclase and spinel lherzolites) is the low pressure boundary of the granulite facies (O'Hara, 1967a; Turner, 1981). It separates granulites from pyroxene hornfels facies rocks, although Miyashiro (1973) implies it separates low and medium pressure granulites. Essentially 'igneous' assemblages are retained in basic and quartz-bearing rocks to higher presure. Reaction H35 is the low-pressure boundary of the eclogite facies in olivine-free rocks, while H17 (the spinel to garnet lherzolite reaction) marks the change to eclogitic assemblages in peridotites. The two reactions producing garnet, H29 and H37 plot quite close together, although this may be an artefact of the differing experimental techniques of Hansen (op.cit.) and Herzberg (1975). Hansen used NaCl pressure cells, whereas Herzberg used cells of talc/BN, which are subject

Fig. 2.4 P - T grid of the relevant reactions of Fig. 2.2 indicating the limits of the granulite facies as defined in the system $CaO - MgO - Al_2O_3 - SiO_2$. See section 2.2.2 for details of data sources.

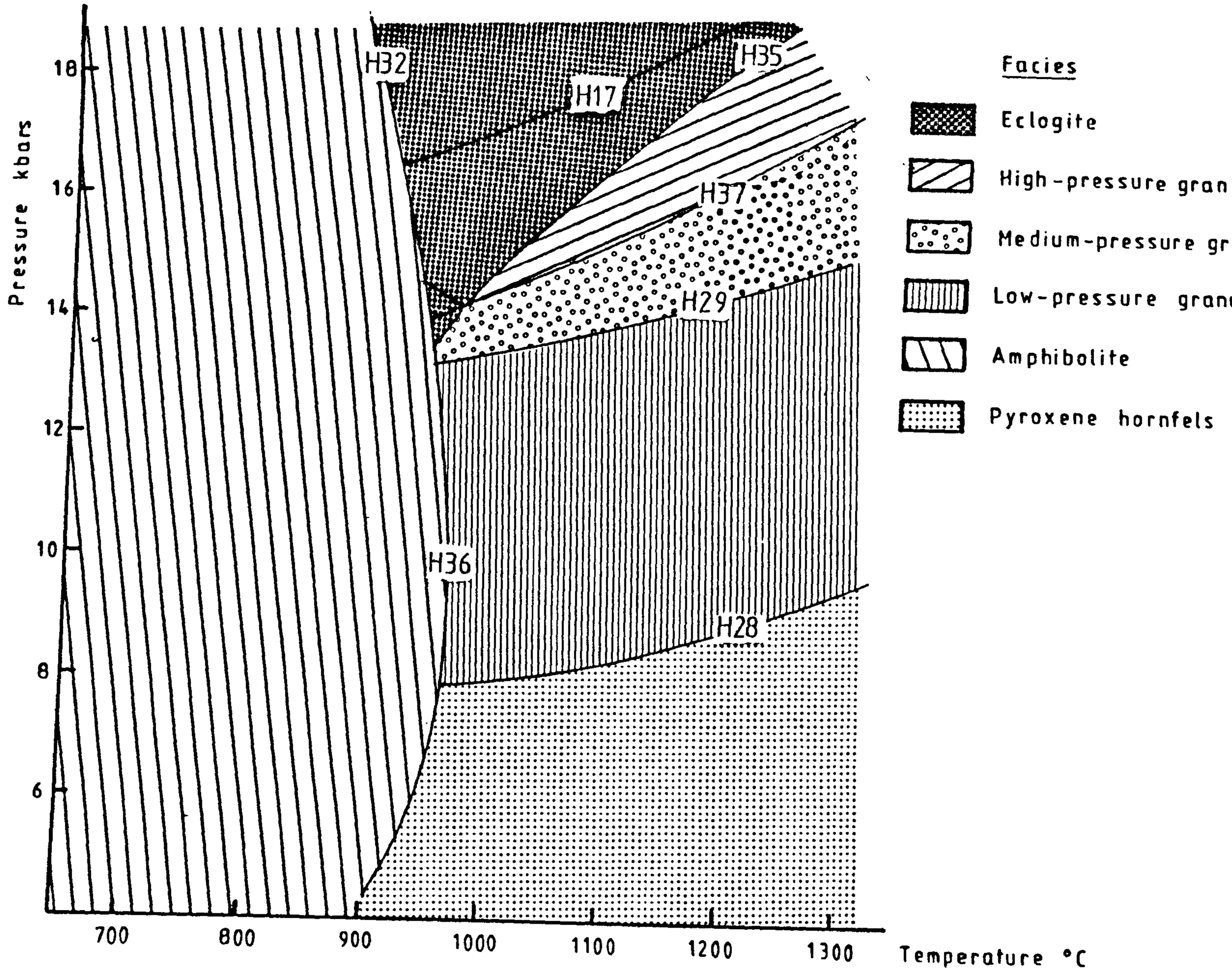
Pressure kbars
18
16
14
12
10
8
6
H32
H17
H35
H37
H29
H36
H28
700
800
900
1000
1100
1200
1300
Temperature °C
Facies
Eclogite
High-pressure granulite
Medium-pressure granulite
Low-pressure granulite
Amphibolite
Pyroxene hornfels

to greater uncertainty in pressure (see Chapter 5). It is suggested that these two garnet producing reactions may be used to subdivide the granulite facies into low, medium and high pressure subfacies. It must be borne in mind that the resulting grid is strictly applicable only to the system $CaO-MgO-Al_2O_3-SiO_2$ when containing excess water, so extrapolation to natural rocks will be complicated by the effects of iron, $CO_2$ and partial melting.

## 2.3 Application to rocks

Two additional components are likely to be important in relating the grid derived above to real rocks: Fe is important because marked Fe/(Fe + Mg) partitioning occurs between the phases of interest; Na is important because it will stabilise amphibole to higher pressures (compare Oba (1978) and Holloway (1973)). The activity of water will also affect the position of all reactions involving amphibole. Effects involving the CMAS exchange vectors $CaMg^{-1}$ and $Al^2Mg^{-1}Si^{-1}$ are likely to be small at temperatures of interest (below 1100 °C) for all reactions except those involving solid phases only.

The effect of these three important variables will now be discussed with respect to the parageneses displayed by the Scourie rocks.

### 2.3.1 Granulite facies assemblages at Scourie.

Table 2.3 contains a list of the important mineral parageneses in rocks of the Scourie complex. The table shows that the rocks of the Scourie complex fit in

Table 2.3b Representative mineral analyses from some of the assemblages of table 2.3a.

78001:

| | CPX1D | OPX1D | PLG2D | CPX4 | OPX1 | PLG2 |
|---|---|---|---|---|---|---|
| $SiO_2$ | 51.04 | 52.07 | 58.67 | 52.01 | 52.20 | 58.35 |
| $TiO_2$ | 0.30 | n.d. | n.a. | 0.23 | 0.14 | n.a. |
| $Al_2O_3$ | 3.02 | 1.98 | 25.68 | 2.54 | 1.57 | 26.01 |
| FeO | 10.84 | 24.52 | 0.12 | 10.20 | 25.49 | 0.77 |
| MnO | 0.35 | 0.85 | n.a. | 0.27 | 0.95 | n.d. |
| MgO | 12.45 | 20.76 | n.d. | 12.72 | 20.55 | n.a. |
| CaO | 21.23 | 0.43 | 7.63 | 21.54 | 0.61 | 8.29 |
| $Na_2O$ | 0.73 | n.d. | 6.82 | n.d. | n.d. | 6.95 |
| $K_2O$ | n.a. | n.a. | 0.30 | n.a. | n.a. | 0.34 |
| | 99.96 | 100.61 | 99.22 | 94.57 | 101.57 | 100.71 |

All analyses by EDS; CPX1D, OPX1D and PLG2D with beam defocussed to 30 μm.

Table 2.3b continued

78027

| | GNT1 (core) | GNT2 (rim) | CPX1 (rim) | CPX2 (core) | OPX3 (rim) | OPX4 (core) | PLG1 (rim) | PLG2 (core) |
|---|---|---|---|---|---|---|---|---|
| $SiO_2$ | 37.56 | 37.81 | 53.42 | 52.24 | 51.33 | 51.72 | 55.85 | 56.06 |
| $TiO_2$ | 0.10 | 0.09 | 0.52 | 0.10 | 0.04 | 0.06 | 0.01 | n.d. |
| $Al_2O_3$ | 20.86 | 21.08 | 1.54 | 1.57 | 0.84 | 0.88 | 27.60 | 27.66 |
| $Cr_2O_3$ | 0.01 | 0.03 | 0.01 | n.d. | n.d. | 0.02 | n.d. | n.d. |
| FeO | 28.19 | 28.01 | 8.02 | 8.53 | 26.14 | 26.33 | n.d. | 0.06 |
| MnO | 1.78 | 1.55 | 0.07 | 0.15 | 0.36 | 0.34 | 0.02 | 0.02 |
| MgO | 5.11 | 4.86 | 13.47 | 13.34 | 19.30 | 20.10 | 0.07 | 0.01 |
| CaO | 6.41 | 6.79 | 22.69 | 22.33 | 0.49 | 0.54 | 10.48 | 10.11 |
| $Na_2O$ | 0.03 | 0.03 | 0.86 | 0.68 | 0.01 | 0.03 | 6.26 | 5.85 |
| $K_2O$ | n.d. | n.d. | 0.43 | n.d. | n.d. | n.d. | 0.16 | 0.13 |
| | 100.14 | 100.25 | 100.73 | 98.94 | 98.52 | 100.02 | 100.45 | 99.90 |

All analyses by MWDS.

45,575 see Table 5.1

Table 2.3b continued

78042

| | OPX1 | OPX2 | AMP1 | AMP2 | CPX4 | CPX5 | OLV4 | SPN1 |
|---|---|---|---|---|---|---|---|---|
| $SiO_2$ | 53.88 | 53.75 | 42.20 | 41.79 | 50.70 | 51.64 | 39.62 | 0.08 |
| $TiO_2$ | 0.04 | 0.06 | 1.04 | 1.26 | 0.20 | 0.22 | n.d. | n.d. |
| $Al_2O_3$ | 3.10 | 3.86 | 13.73 | 14.31 | 3.73 | 3.55 | 0.01 | 57.74 |
| $Cr_2O_3$ | 0.07 | 0.12 | 0.26 | 0.31 | 0.22 | 0.27 | n.d. | 4.66 |
| FeO | 11.55 | 11.61 | 7.19 | 7.28 | 4.32 | 4.22 | 14.57 | 16.92 |
| MnO | 0.29 | 0.30 | 0.09 | 0.07 | 0.14 | 0.13 | 0.28 | 0.29 |
| MgO | 30.20 | 29.12 | 15.80 | 15.85 | 16.06 | 15.03 | 44.73 | 15.60 |
| CaO | 0.33 | 0.47 | 12.25 | 12.22 | 22.90 | 24.14 | n.d. | n.d. |
| $Na_2O$ | 0.01 | 0.01 | 2.50 | 2.58 | 0.28 | 0.22 | n.d. | 4.16($Fe_2O_3$) |
| $K_2O$ | n.d. | n.d. | 0.96 | 0.90 | n.d. | n.d. | n.d. | n.d. |
| | 99.47 | 99.30 | 96.02 | 96.57 | 98.55 | 99.42 | 99.21 | 99.40 |

All analyses by MWDS.

general into the medium pressure division of the granulite facies as defined above and this suggests that equlibrium assemblages (as opposed to compositions) have been recovered. However, several of the assemblages listed do not fit strictly into this region. In the case of ultrabasic rocks such as 79028 and 78042 it is probable that the amphibole is stabilised to higher temperatures than possible in CMAS because of its sodium bearing (pargasitic) nature.

Other rocks, such as 78027/8, also contain five phases; in this case the garnet + quartz assemblage has been stabilised by the iron rich nature of the garnet in this rock, which lowers the pressure of the garnet producing reaction as iron partitions strongly into garnet with respect to pyroxenes. The effect of iron on reaction H29 is likely to be less marked as both garnet and spinel, which appear on opposite sides of the reaction, tend to be enriched in iron with respect to the bulk composition.

The effect of water on the position of the equilibria can be visualised if one invariant point (say (olv,spn,kya) is considered (fig 2.5). At all values of $X_{H_2O}$, the invariant point must lie on the metastable extension of the reaction [amp] which is independent of variations in $P_{H_2O}$. The invariant point will slide to lower temperatures as $X_{H_2O}$ is reduced, so amphibole will react out at lower temperatures. In addition the stability of amphibole is influenced by the the presence

Fig. 2.5 The effect of reducing $P_{H_2O}$ on the invariant point ( olv, spn, kya ).
$P^{A}_{H_2O} > P^{B}_{H_2O} > P^{C}_{H_2O}$

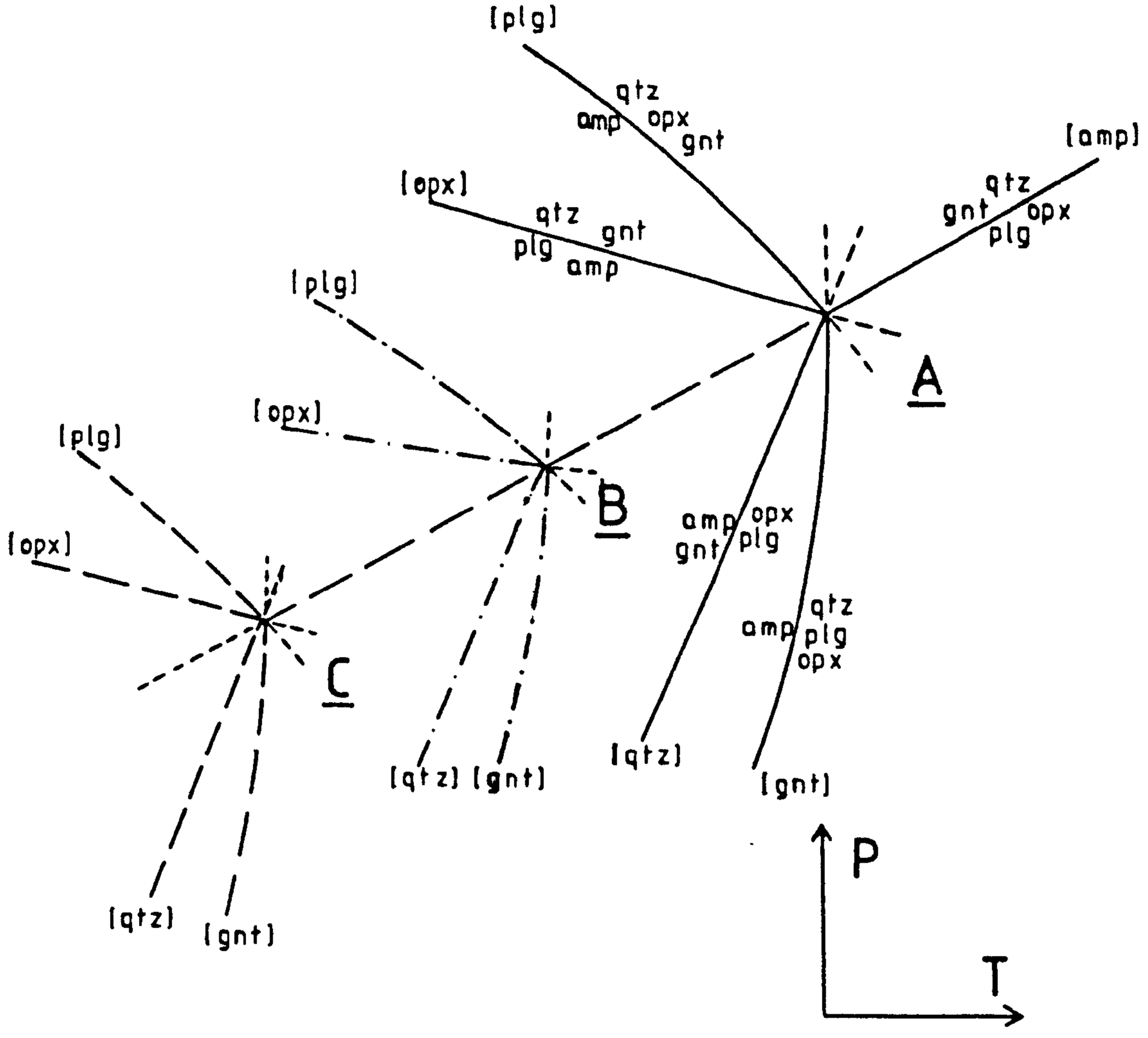
[plg]
qtz
amp
opx
gnt
[amp]
qtz
gnt
opx
plg
[opx]
qtz
gnt
plg
amp
[plg]
A
[opx]
[plg]
B
[opx]
amp
opx
gnt
plg
C
qtz
amp
plg
opx
[qtz]
[qtz]
[gnt]
[gnt]
P
T

or absence of a hydrous melt. Holloway (1973), among others, has shown that the presence of a melt containing more water than the coexisting amphibole leads to a breakdown reaction which increases in temperature as $X_{H_2O}$ decreases. The maximum stablity of pargasite in the presence of a melt and vapour occurs when $X_{H_2O} = 0.45$. With this bulk volatile composition the maximum thermal stability of amphibole is increased by more than 50°C with respect to its stability with pure water. These effects must be balanced against the increased thermal stability of amphibole due to the addition of sodium.

These considerations of the stability of amphibole in the Scourie rocks may be summed up as follows: amphibole is stable in the ultrabasic rocks owing to their high Mg/(Mg + Fe) values. Water activity is hard to gauge: there is no evidence for the presence of a melt in these rocks, although liquid - vapour fluid inclusions are rarely present, suggesting that a free vapour phase may have existed ( at the peak of metamorphism ?). Other considerations, including detailed analysis of the amphibole-bearing assemblage (section 2.4.5) and of possible melting behaviour (cf Eggler, 1978) suggest that the ultrabasic rock may have been in a 'zone of invariant vapour composition' (ZIVC) and hence unlikely to contain a melt under the P-T conditions at Scourie. The maximum possible temperature of equilibration for these rocks is therefore likely to be within 50°C of the amphibole breakdown curve plotted on fig. 2.4.

A meaningful absolute P-T estimate is impossible to produce from this CMAS based grid due to the effects of additional components outlined above. The next section contains the neccessary treatment to provide this estimate.

## 2.4 P-T estimates for the Scourie area

Previous P-T estimates for the peak conditions of metamorphism at Scourie have been reviewed earlier (1.2.5). This section contains P-T estmates based on new mineral data; further details of equilibration conditions of rocks of more specific interest are given in Chapters 3, 4 and 5, where discussion of those lithologies is presented.

### 2.4.1 Re-equilibration and the closure problem

It has previously been shown that in slowly cooled, deep-seated rocks, re-equilibration of mineral assemblages such as opx-gnt, cpx-gnt and opx-cpx occurs, rendering the P-T estimates obtained unsuitable for use as indicators of anything other than the minimum possible peak conditions (Fraser and Lawless,1978;O'Hara and Yarwood,1978;Harte,Jackson and Macintyre, 1981).

Harte et al (op.cit.) showed that a clinopyroxene crystal 5mm in diameter may be re-equilibrated (at least with respect to $Ca^{2+}$) within 10 Myr at temperatures greater than 850°C. Many rocks will have re-equilibrated completely down to this temperature over the time scale applicable to rocks of the Scourie complex. Only coarser grained rocks will perhaps preserve (in grain cores)

compositions equilibrated at higher temperatures. Several such rocks are described in subsequent chapters: this section is concerned with 'ordinary' rocks which are, in the light of the above discussion, likely to give cooling or blocking temperatures below which diffusion ceased for elements involved in the reaction under consideration. The work of Humphries and Cliff (1982) on the Sm-Nd dating of Scourian mineral assemblages supports this conclusion. As different elements have different diffusion coefficients in the same mineral, they will cease effective movement at different temperatures. For example, tschermaks exchange ($Mg^{-1}Si^{-1}$ AlAl) will probably cease at higher temperatures than $CaMg^{-1}$ exchange, due to the charge balance induced ordering constraints, so the $CaMg^{-1}$ exchange will continue to lower temperatures in minerals with metastable aluminium contents. This is likely to invalidate calculated equilibration temperatures for minerals involving complex solid-solution (eg clinopyroxenes, amphiboles), although at present the magnitude of such inaccuracies is unknown.

Data on the diffusion coefficients of different species within the minerals of interest (eg garnet, pyroxene) are very limited (Freer, 1981), but the data available suggests that Al does diffuse less readily than Ca in pyroxenes, and hence equilibria involving Al exchange will probably give a better indication of equilibrium conditions than those involving Ca.

Despite these problems, some purpose can be served

in calculating the apparent equilibration conditions for the rocks at Scourie as a guide to minimum peak conditions.

2.4.2 Two pyroxene temperatures.

2.4.2.1 Wells (1977) method

The most commonly used geothermometer for high-grade rocks is that based on the two pyroxene miscibility gap. The most widely used version at present is probably that of Wells (1977). He used an ideal solution mixing model for the pyroxenes, together with an empirical correction for the Fe/ Fe+Mg value of the system. A more extensive data set, including some for the effects of Al on the miscibility gap is now available (Perkins and Newton, 1981), and it is now clear that the ideal model for pyroxene solid solution is incorrect (Powell, 1978; Holland et al, 1979; Lindsley et al, 1981). In spite of this, the Wells (op cit.) equation adequately represents the pyroxenes in the CMAS system, and does contain a correction for the iron content of the pyroxenes, considered adequate by some authors (Perkins and Newton, op cit.) . Comparison of calculated temperatures with run conditions for the Ca-Mg-Fe pyroxene data set of Mori (1978) show that eqn.5 of Wells tends to overestimate equilibrium conditions of pyroxenes with Fe/Fe+Mg of about 0.5 by 70 -100 °C. It seems appropriate, therefore, to use this equation only for iron-poor bulk compositions. The main group of rocks under this heading are the ultramafics and some of the basics; many of the

basic rocks have no 'primary' orthopyroxene.

The results obtained are, as expected, in the range 700-900°C (c.f. Rollinson, 1981) for both basic and ultrabasic lithologies (see table 2.4). Somewhat surprisingly, the core-core equilibration temperatures are lower than the rim-rim temperatures. Rollinson (op.cit.) also noted this in some cases. The most likely cause of this is exsolution; evidence presented in Chapter 4 indicates that this is present on a sub-microscopic scale as well as in optically detectable lamellae.

2.4.2.2 Powell (1978) method

Powell (1978) has proposed a two-pyroxene thermometer based on the reaction

$$CaMgSi_2O_6 + Mg_2Si_2O_6 = Mg_2Si_2O_6 + CaMgSi_2O_6$$

cpx opx cpx opx

after demonstrating the undue sensitivity of the type of formulation used by Wells (op cit.) to small differences in composition of the phases. Powell's thermometer, like that of Wells (op cit.) also has a correction for the iron content of the pyroxenes; this again does not satisfactorially represent the data of Mori (1978) for pyroxenes with Fe/Fe+Mg of about 0.5. It gives larger discrepancies between calculated and observed run conditions than Wells' formulation. It is again appropriate, therefore to use this geothermometer for iron-poor rocks only. Temperature estimates for basic and

Table 2.4 Two pyroxene temperatures. (°C)

| | | Wells (1977) | Powell (1978) |
|---|---|---|---|
| 78042 | Cores | 777±50 | 754±42 |
| | Rims | 927±28 | 769±19 |
| 45,475/1 | Cores | 885±20 | 812±20 |
| | Rims | 881±23 | 767±20 |

Errors calculated using 2% relative uncertainty in analysed wt%.

ultrabasic rocks range from 700 to 850°C (table 2.4).

2.4.3 Garnet-clinopyroxene temperatures.

Garnet-clinopyroxene thermometers, based on the Fe - Mg exchange reaction

$$\tfrac{1}{3}Fe_3Al_2Si_3O_{12} + CaMgSi_2O_6 = \tfrac{1}{3}Mg_3Al_2Si_3O_{12} + CaFeSi_2O_6$$

have been formulated by Ganguly (1979), Saxena (1979) and Ellis and Green(1979). The equations derived are all applicable to a wide range of bulk compositions in terms of Fe/Fe+Mg values.

The experimental data upon which the calibration of these thermometers is based is almost solely at high temperatures. Ellis and Green (op cit) do have some lower temperature data, the fit of their calibration to this data is not especially good (see their fig.3, 1000°C data). With the caveat that the data may be unreliable at lower temperatures, calculated temperatures are presented in table 2.5.

The difference in calculated temperatures between lithologies could be due to several factors: the smaller grain size of 78027, the small amount of observable retrogression in 78027, or the faster diffusion in Fe rich garnets (Duckworth and Freer, 1981). The small amount of low-temperature data used in calibrating the thermometers is the probable cause of the differences between the garnet-clinopyroxene thermometers.

2.4.4 Pressure estimates.

Reliable geobarometers are scarce; alumina solubility in orthopyroxene coexisting with garnet is

Table 2.5 Typical garnet - clinopyroxene equilibration temperatures (°c).

| | | Ganguly | Saxena | Ellis & Green |
|---|---|---|---|---|
| 78047 (Garnetiferous basic) | core | 1004±13 | 997±14 | 930±15 |
| | rim | 935±11 | 920±13 | 837±14 |
| 78027 (metasediment) | core | 815± 9 | 790±10 | 840±12 |
| | rim | 738±8 | 703±10 | 750±10 |

Errors calculated assuming 2% error on Wt% analysed only.

still not a reliable method (O'Hara and Yarwood,1978). Two potentially useful methods are considered here: the plagioclase - clinopyroxene -quartz assemblage and the orthopyroxene plus plagioclase reaction

2.4.4.1 Plagioclase-clinopyroxene-quartz barometer.

The equilibrium

$$CaAl_2Si_2O_8 = CaAl_2SiO_6 + SiO_2 \qquad 2.1$$

Anorthite CaTs pyroxene Quartz

has been studies by Wood (1979). Wood also gives apparent activity coefficients for diopside-hedenbergite-CaTs clinopyroxenes, which allows the reaction to be used as a barometer for a range of bulk compositions. However, mole fractions of CaTs in granulite facies pyroxenes are small and errors consequently large.

Equation 4 of Wood (op.cit.) can be expressed in the form

$$G_{(P,T)} = 0 = 23220 + 12.57T + P\Delta V$$

using the volume change for the reaction calculated from the data given by Wood (op cit.) and Robie et al (1978). This equation can then be used to calculate equilibration pressures as a function of temperature using the equation

$$P = 1/\Delta V \left(23220 + 12.57T + RT\ln\left(X_{CaTs}^{cpx}\,\gamma_{CaTs}^{cpx} \;/A_{an,id}^{plg}\,\gamma_{an}^{plg}\right)\right)$$

where $\Delta V$ is the volume change for the reaction calculated from the partial molar volume of cpx(ss) ,interpolated from the data of Wood (1979).

$X_{CaTs}^{cpx}$ is the equivalent mole fraction of CaTs calculated using Newton-Raphson iteration to solve

equations 10 and 12 of Wood (op cit).

$\gamma^{cpx}_{CaTs}$ is the apparant activity coefficient of CaTs (Wood, op cit.)

$A^{plg}_{an,id}$ is the ideal activity of anorthite in plagioclase, calculated using model 2 of Kerrick and Darken (1975)

$\gamma^{plg}_{an}$ is the activity coefficient of Anorthite calculated using the sub- regular model and data of Newton et al (1980).

In spite of the uncertainties involved in these calculations, the equilibration pressures for two markedly different lithologies are dissimilar (table 2.6).

Reaction 2.1 has also been studied by Gasparik and Lindsley (1981) who used a PbO fluxing technique in experiments to grow larger crystals faster than is otherwise possible. They examined relations in the Di-CaTs-CaEs system, although they did not reverse pyroxene compositions with respect to CaEs contents, and hence obtained no mixing parameters for it. This is of no consequence for the pyroxenes studied here as $X^{cpx}_{CaEs}$ =0 Gasparik and Lindsley (op cit.) expressed the non-ideality of CaTs-Di solid solutions with a sub-regular model for ordered mixing. The data can be used, therefore, if the apparant mole fracton of CaTs, calculated as above is used for the natural clinopyroxenes, as this assumes ordered molecular mixing. Pressure calculated using these equations give higher equilibration pressures (table 2.6). These pressure estimates are probably less

Table 2.6 Typical cpx-plg-qtz equilibration pressures.

| | Wood | | Gasparik and Lindsley | |
|---|---|---|---|---|
| | 1000°C | 800°C | 1000°C | 800°C |
| 78001 (acid gneiss) | | | | |
| cores | 13.4±0.3 | 12.7±0.3 | 21.8±0.3 | 22.1±0.3 |
| rims | 12.1±0.6 | 11.7±0.5 | 20.4±0.6 | 21.0±0.5 |
| 78027 (metasediment) | | | | |
| cores | 7.7±0.5 | 8.1±0.4 | 15.7±0.5 | 17.5±0.4 |
| rims | 6.2±0.7 | 6.8±0.8 | 15.2±0.6 | 17.1±0.8 |

Errors calculated assuming 2% error in analysed wt% only.

reliable than those obtained using Wood (op cit.) equations as it is necessary to assume that $W_{CaFe}$ in clinopyroxene is zero , and additionally it is not known what ordered model for clinopyroxene Gasparik and Lindsley used.

2.4.4.2 Garnet + quartz assemblage

As mentioned in section 2.3.2, several rocks (which may be metasedimentary; see Chapter 9) contain the assemblage gnt + qtz + opx + cpx +plg, due to the high iron contents of the bulk rock. This assemblage has great potential for equilibrium thermodyamic calculation of equilibration conditions as it is of relatively low variance. However, as it is iron rich, most of the available geothermometers and geobarometers are unsuitable due to the lack of data on Fe-Mg interactions. Clinopyroxene -garnet equlibration temperatures for 78027 range up to 830°C (see section 2.4.4 for discussion). The full assemblage is in equilibrium; the five minerals are occasionally seen in close contact. These phases are related by the reaction

$$CaAl_2Si_2O_8 + 2Mg_2Si_2O_6 = Mg_3Al_2Si_3O_{12} + CaMgSi_2O_6 + SiO_2$$

An En Pyr Di

which is relatively sensitive to pressure. This reaction has been used as a barometer by several authors (Wood, 1975; Newton, 1978; Wells, 1979), and has most recently been experimentally determined by Hansen (1981). Using his equation and activity - composition models of various

authors, (see table2.7), equilibration pressures of 14.1 kbar(800°C) to 15.9 kbar(1000°C) are obtained for core-core compositions.

### 2.4.5 Amphibole-bearing rocks and $P_{H_2O}$

The only rocks containing amphibole from the earliest stages of metamorphism are the ultrabasics. These include assemblages such as olv-cpx-opx-amp-spn-mgt. As mentioned in section 2.4.3, two pyroxene equilibration temperatures for these rocks are in the 700-900°C range, and represent cooling temperatures rather than the peak of metamorphism.

There is no suitable equilibrium for estimating the equilibration pressure of these rocks, but their spinel lherzolite mineralogy constrains them to have equilibrated at pressures between a minimum of 6 kbar (inversion to plagioclase lherzolite assemblages) and a maximum of about 16 kbar, based on the data of O'Neill (1981) for the spinel to garnet lherzolite reaction. If the pressure and temperature of equilibration of the assemblage can be estimated, the activity of water in the vapour phase may be calculated using the equilibrium

$$Ca_2Mg_5Si_8O_{22}(OH)_2 + Mg_2SiO_4 = 2CaMgSi_2O_6 + 2.5Mg_2Si_2O_6 + H_2O$$

Tremolite Fo Di En

which buffers $A_{H_2O}$. Using the modified Fisher-Zen approximation of Holland (1981), relatively simple expressions for $A_{H_2O}$ at various pressures and temperatures may be derived.

Table 2.7 Activity - composition relations used in sections 2.4.4.2 and 5.4.2.

Garnet

$$RT\ln \gamma_{py}^{gnt} = W_{CaMg}X_{Ca}^2 + W_{FeMg}X_{Fe}^2 + (W_{CaMg} + W_{FeMg} - W_{CaFe})X_{Ca}X_{Fe} + \Delta V_{py}P$$

where

$W_{CaMg} = 15980 - 6.28T$ (a)
$W_{FeMg} = 840J$ (b)
$W_{CaFe} = 0J$ (c)
$\Delta V$ (d)

(a) based on Newton and Haselton (1981), modified to fit 1000°C data of Jenkins and Newton (1979) and O'Neill and Wood (1979).
(b) O'Neill and Wood (1979) and Wood and Kleppa (1981).
(c) Cressey et al.(1978) cf. Newton and Haselton (1981).
(d) from expressions of Newton and Haselton (1981).

Plagioclase

$$A_{an}^{plg} = A_{an}^{id,plg}\gamma_{an}^{plg}$$

$A_{an}^{plg} = 0.25(X_{Ca}(1+X_{Ca})^2)$ after Kerrick and Darken (1978)

$RT\ln\gamma_{an}^{plg} = X_{ab}^{plg}(W_{an} + 2(W_{ab} - W_{an})X_{an}^{plg})$

$W_{an} = 8473$ J
$W_{ab} = 28225$ J
after Newton et al. (1980)

Orthopyroxene, clinopyroxene

Ideal mixing.

The basic equation for dehydration reactions is

$$\Delta G_{(P,T)} \simeq \Delta H_{(1,297)} - T\Delta S_{(297)} + \Delta V\ (P-1) + n(p+qT) + nRT\ln f H_2O$$

where n=no. of moles of water librated by the reaction

p,q are coefficients of a function F(Cp)=p+qT used to represent the effects of changes in Cp with temperature and

$RT\ln f H_2O$ is represented by a quadratic in T, as tabulated by Holland (1981)

The data used for this reaction are given in table 2.8

For impure phases we can also write

$$G_{(P,T)} = -RT\ln K$$

where K is the equilibrium constant for the reaction, given by

$$K = A_{di}^{cpx}\ A_{en}^{opx}\ A_{H_2O}^{vap} /\ A_{tr}^{amp}\ A_{fo}^{olv}$$

where $A_{H_2O}$ here is the activity of water relative to a (P,T) standard state.

The activity composition models used for the phases are give in table 2.8. Amphiboles are strongly non-ideal, and quantitative data are sparse. Exsolution is well documented between hornblende or tremolite and cummingtonite (Ross et al,1969). This is due mainly to non-ideal mixing of Ca and Mg on B site (M4). Some short range order involving Al and Si as in sodic pyroxenes is also possible. The only available set of data is that of Powell (1975), who calculated interaction parameters from coexisting natural cummingtonites and hornblendes from rhyolites. These figures are not considered reliable (R

Table 2.8 Data used in 2.4.5 for the modified Fisher - Zen approximation for the reaction -

$$Ca_2Mg_5Si_8O_{22}(OH)_2 + Mg_2SiO_4 = 2\,CaMgSi_2O_6 + 2.5Mg_2Si_2O_6 + H_2O$$

| | |
|---|---|
| $\Delta H$ | = 128720 J |
| $\Delta S$ | = 162.27 J K |
| $\Delta v$ | = - 1.733 J bar |
| p | = - 2784 J mol |
| q | = 5.68 J K mol |

$RT\ln f_{H_2O}$ from polynomial of Holland (1981)

Activity of tremolite calculated from

$$A_{tr}^{id,} = X_{vac\ A}\ (X_{Ca})^2 \cdot (X_{Mg\ M1,2,3})^5 \cdot (X_{Si,T2})^4 (X_{Si,T1})^4$$

Activities of fo,di,en calculated assuming ideal mixing on sites.

Powell, oral comm.), but they will have the effect of raising tremolite activity by up to two orders of magnitude. Such activity coefficients and their effect on tremolite activity are of the order suggested by Phillips (1981) to account for discrepancies in $A_{H_2O}$ calculated from metapelites and metabasics from Broken Hill in Australia.

Calculated values of $A_{H_2O}$ for a variety of pressures and temperatures are given in table 2.9. It is possible that the minerals of these rocks equilibrated with a hydrous vapour phase , albeit containing some diluent, probably $CO_2$.

## 2.5 Discussion

Most of the rocks of the Scourie complex record equilibration temperatures of about 800-850 °C, and pressures of 10-15 kbar. Consideration of both cation and isotope exchange kinetics (Harte et al, 1981; Humphries and Cliff, 1982) suggests that recorded conditions are those of the cessation of diffusion, not the highest grades experienced. Other, coarser-grained rocks, discussed in the following three chapters, contain minerals which retain evidence of higher-grade conditions. Many of these larger crystals are compositionally zoned, unlike those from most of the Scourie rocks.

Table 2.9 Values of $A_{H_2O}$ calculated using the equations of section 2.4.5.

| P | 10 kbar | 8 kbar | 6 kbar |
|---|---|---|---|
| T | | | |
| 1000°C | 0.0047±0.0018 | 0.0041±0.0016 | 0.0035±0.0013 |
| 800°C | 0.028 ±0.011 | 0.026±0.010 | 0.023±0.008 |
| 700°C | 0.088±0.035 | 0.082 ±0.033 | 0.073 ±0.029 |

If $\gamma_{tr}^{amp} = 10\pm2$ , $\gamma_{sp}^{spn} = \gamma_{fo}^{olv} = \gamma_{en}^{opx} = 1\pm0.1$ and P=8kbar T=800°C , $A_{H_2O}=0.22\pm0.13$

" $\gamma_{tr}^{amp} = 20\pm4$ , " " " " " " " $A_{H_2O}=0.43\pm0.25$

# Chapter 3 Scourie Bay Ironstone

## 3.1 Introduction

The Scourie Bay ironstone, mentioned in chapter 1, has a two - fold importance for the geology of the Scourie complex. It is of such a composition that, unlike many rocks of the Scourian, its original metasedimentary nature is beyond reasonable doubt ( see section 3.4.2). In addition, it contains unequivocal evidence of high - grade metamorphic conditions and evidence of re - equilibration during the return of the rock to the surface.

## 3.2 General description

The ironstone is found as a prominent rib of rock set in basic gneisses in the first inlet west of the pier on the north side of Scourie Bay (see fig 1.2). It is traceable only for a short distance due to poor exposure, and its northern end may be boudinaged. The main exposure of the ironstone forms a layer 30cm thick and shows reaction zones with the adjacent basic gneiss at its margins. The outermost zone of the layer is 1cm thick and consists of abundant red garnet and quartz, in which the garnet contains both euhedral and vermicular inclusions of quartz. This zone is followed by a 0.5cm thick zone of magnetite crystals. Inside this, the ironstone is quartz rich, but rapidly becomes richer in pyroxenes and magnetite. The bulk of the layer is composed of quartz

(ca. 30% by volume), magnetite (ca. 20%) and clino- and ortho- pyroxenes (ca. 50% total pyroxene). Minor quantities of garnet are present. Magnetite crystals, which are rimmed by a thin layer of garnet when at the edge of the layer, are clustered in small lenses parallel to the regional foliation, which is also defined by pods rich in quartz. The pyroxenes are variable in appearance: some are highly exsolved, others consist of separate grains intergrown to sugest an origin by exsolution and later coarsening while others occur as apparently unconnected separate grains. In places, fibrous amphibole is present either as an overgrowth on, or replacing the pyroxenes.

## 3.3 Mineralogy

### 3.3.1 Minor minerals.

Quartz grains in the ironstone have an average size of 0.5 to 1.0mm; some are strained and show sub - grain structures. Magnetite is present as grains and aggregates of variable size (aggregates range up to about 10 x 1 mm). Very narrow lamellae of an aluminous material are present in some magnetites and may be altered exsolution bodies of hercynitic spinel. The only readily detectable minor components of this magnetite are aluminium and manganese, present at about 0.5 wt% $Al_2O_3$ and 0.2 % MnO respectively. Pyrrhotite is present in concentrations up to 1% in some sections. It is frequently partially replaced by marcasite. Pyrite and chalcopyrite also occur in trace amounts.

### 3.3.2 Garnet

Garnets of two different compositions are present in the rock: a lower manganese garnet within the outermost zone of the layer, and a high manganese garnet within the layer as a rim to magnetite grains (see table 3.1). In all cases, aluminium is insufficient to fill the $R^{3+}$ site, and up to 9mol% (in the case of the high manganese garnet) of the site must be filled with $Fe^{3+}$ to maintain stoichiometry. Much of the garnet in the magnetite-rich layer contains many vermicular quartz inclusions, giving rise to spongy garnets with up to 30% quartz inclusions (see fig. 3.1)

### 3.3.3 Pyroxenes

The earliest formed pyroxenes detectable in the rock are present in the centre of the layer and originally had a grain size of 0.5 - 1.0 mm. Two types of early pyroxene may be distinguished in thin section: one shows some exsolution and is now pleochroic from pale red to pale green, the other is pale green and complexly exsolved; three sets of lamellae are optically visible. Probe analyses, performed using a defocussed beam and combined on the basis of relative areas for grains in which more than one distinct probeable area is present, show that the first of these pyroxenes had a pigeonitic bulk composition, the second was a low - calcium ferroaugite (see table 3.1 and fig 3.2). The exsolution history of these pyroxenes is chronicled in fig 3.3. Within the pigeonite there occurs a single set of clinopyroxene

Table 3.1 Analyses of garnets and pyroxenes from, the Scourie bay ironstone ( 45, 517 ).

| | GT1 | GT2 | P1(d) | P2(d) | OP | C1(s) |
|---|---|---|---|---|---|---|
| $SiO_2$ | 37.94 | 37.10 | 50.52 | 50.20 | 50.28 | 51.72 |
| $Al_2O_3$ | 20.57 | 18.89 | 0.67 | 0.32 | 0.56 | 0.58 |
| FeO | 29.44 | 21.71 | 28.26 | 30.49 | 31.33 | 25.46 |
| $Fe_2O_3$ | 1.22 | 2.91 | - | - | - | - |
| MnO | 3.36 | 9.88 | 3.95 | 4.32 | 4.82 | 3.10 |
| MgO | 2.17 | 1.68 | 11.92 | 11.60 | 12.70 | 9.66 |
| CaO | 6.76 | 7.53 | 5.10 | 3.88 | 0.77 | 9.30 |
| $Na_2O$ | - | - | - | - | - | 0.63 |
| Total | 101.46 | 99.70 | 100.42 | 100.81 | 100.46 | 100.45 |

| | C1(a) | C2(a) | Cc(d) | Pc(d) | Ccc | Occ |
|---|---|---|---|---|---|---|
| $SiO_2$ | 50.96 | 49.68 | 49.63 | 49.94 | 51.87 | 49.45 |
| $Al_2O_3$ | 0.65 | 0.71 | 0.74 | 0.55 | 0.81 | 0.50 |
| FeO | 26.81 | 25.97 | 25.26 | 29.59 | 15.93 | 32.84 |
| $Fe_2O_3$ | - | - | - | - | - | - |
| MnO | 3.04 | 3.33 | 3.14 | 4.27 | 1.95 | 4.65 |
| MgO | 10.60 | 10.82 | 10.61 | 11.96 | 9.56 | 11.84 |
| CaO | 7.40 | 8.69 | 9.68 | 3.65 | 20.45 | 0.77 |
| $Na_2O$ | - | - | - | - | - | - |
| Total | 99.46 | 99.26 | 99.06 | 99.96 | 100.57 | 100.05 |

(d) signifies a defocussed beam EDS analysis.
(a) an average analysis, compiled by area weighting of defocussed beam EDS analyses.
(s) a mechanical scan MWDS analysis.
$Fe_2O_3$ in garnet calculated by assuming a formula of the form $R_8O_{12}$.

See fig. 3.3 for key

Fig. 3.1 Garnet with many vermicular quartz inclusions, from the marginal zone of the Scourie bay ironstone ( 45,517 ). ( plane polarised light ).

Scale bar is 0.5mm.

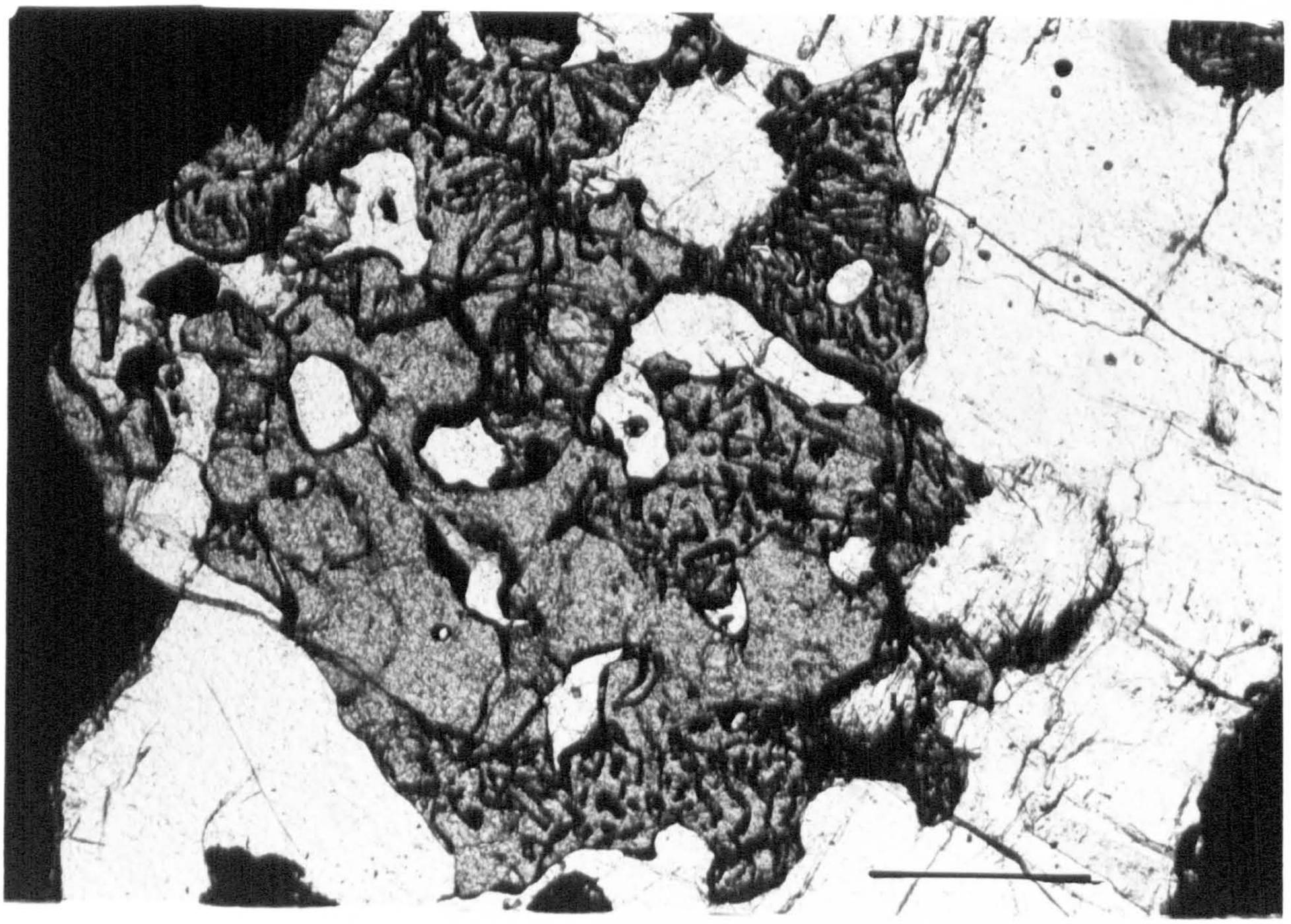

Fig. 3.2 Composition of pyroxenes from the Scourie Bay ironstone, neglecting Mn and Al. See Fig. 3.3 for key.

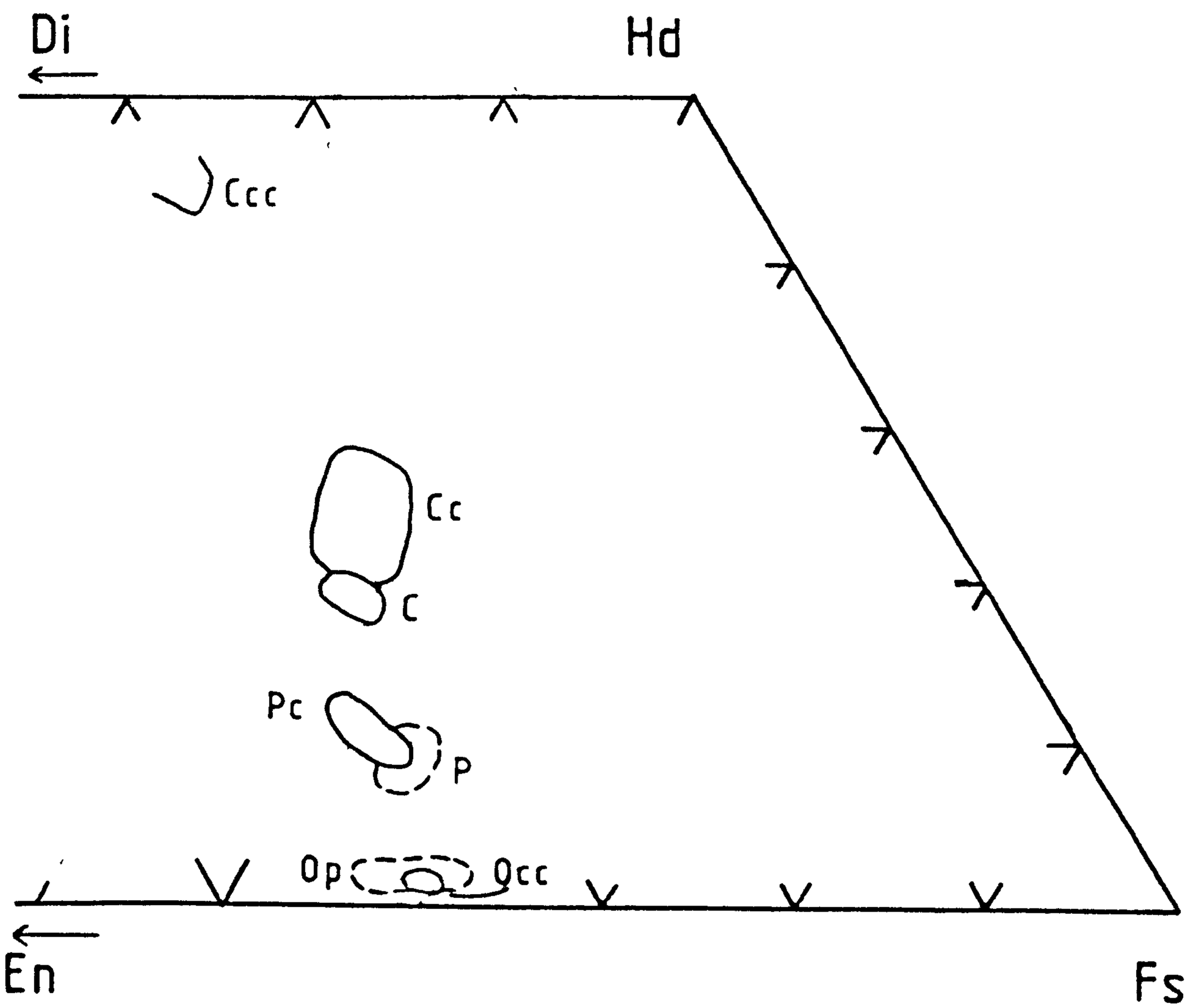
Di
Hd
Ccc
Cc
C
Pc
P
Op
Occ
En
Fs

Fig.3.3 Flow chart of exsolution within pyroxenes from the ironstone. Pc indicates pigeonite from clinopyroxene , Cpc clinopyroxene from pigeonite , and that pigeonite from clinopyroxene, etc. Asterisk indicates probed phase.

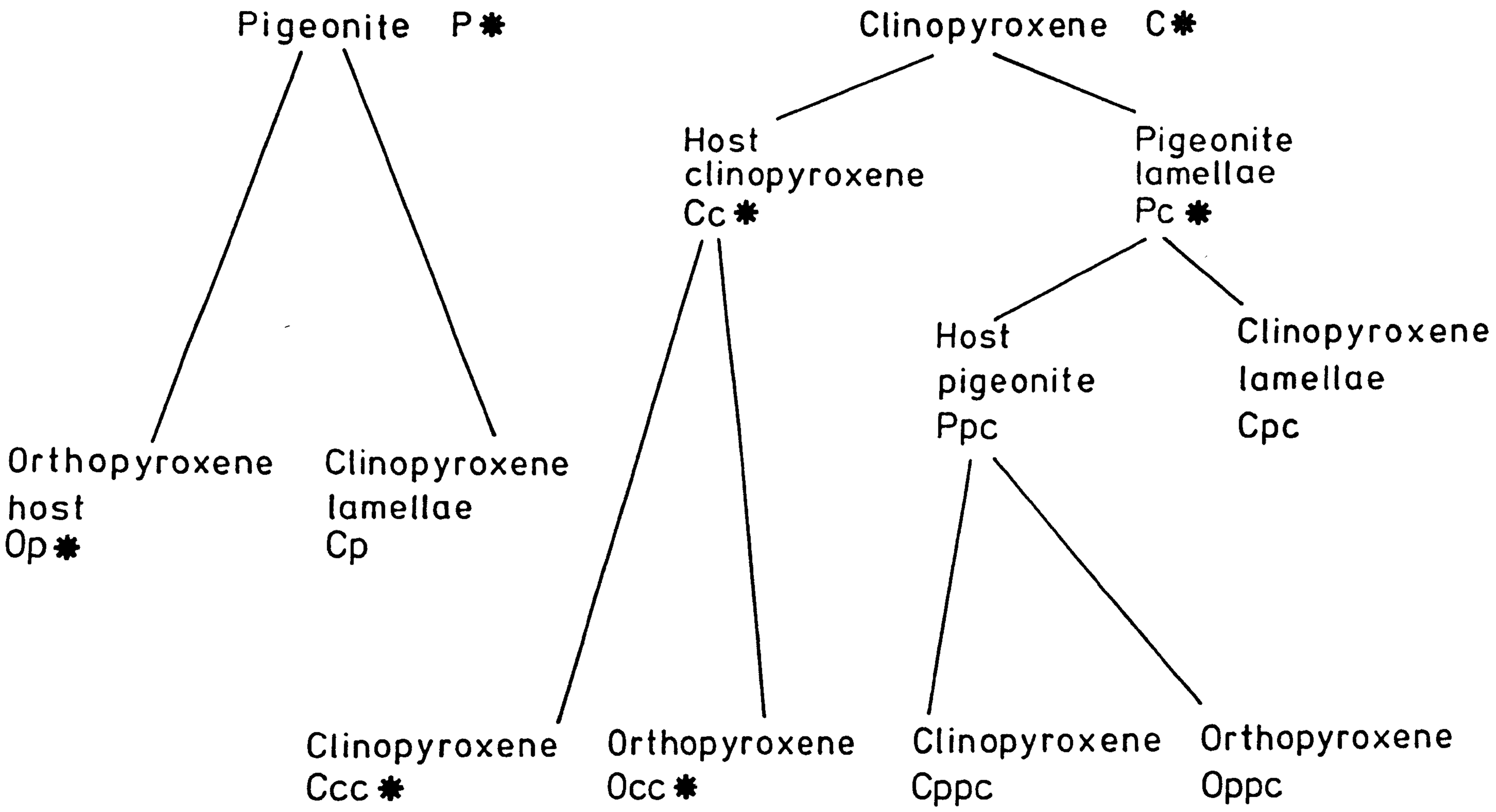
Pigeonite P*
Orthopyroxene host Op*
Clinopyroxene lamellae Cp
Clinopyroxene C*
Host clinopyroxene Cc*
Pigeonite lamellae Pc*
Clinopyroxene Ccc*
Orthopyroxene Occ*
Host pigeonite Ppc
Clinopyroxene lamellae Cpc
Clinopyroxene Cppc
Orthopyroxene Oppc

lamellae (Cp), which are parallel to (100) and 1-2μm thick. Exsolution within the low calcium ferroaugite occurred in two crystallographic directions: early pigeonitic lamellae are apparently usually parallel to (001) , although they are in places in approximately the (100) direction. The clinopyroxene (Cpc) lamellae within these pigeonite lamellae are again approximately on (001); the obtuse angle between them and (100) is greater in this case (fig 3.4), owing to diferential changes in lattice parameters (Robinson et al,1977). Subsequently, the clinopyroxene host has exsolved orthopyroxene (Occ) parallel to (100) and the pigeonite lamellae have inverted to orthopyroxene (Oppc) with the exsolution of clinopyroxene (Cppc) parallel to (100) (see fig. 3.4). The early lamellae of pigeonite (Pc) within the clinopyroxene are about 150μm across; the later lamellae (Cpc,Cppc,Oppc) are generally ca. 2μm wide but in some instances more. Fig. 3.4 shows the three generations of lamellae present in the ferroaugite. Those phases coarse enough to be probed are indicated in fig. 3.3, and the compositions given in table 3.1 and fig 3.2. In addition, all the pyroxenes contain small, oriented bodies of magnetite, especially near grain boundaries.

Pyroxene-pyroxene grain boundaries are also marked by small grains of magnetite and quartz, and it therefore appears that oxidation has accompanied cooling and exsolution. This is manifested on fig 3.2 as a shift in the tie lines towards the Ca - Mg join with decreasing

Fig. 3.4 Photomicrograph of the sub-calcic ferroaugite in the ironstone. The host augite and (001) pigeonite with small (001) augite lamellae are both cut by (100) lamellae of hypersthene. (Crossed Polars).

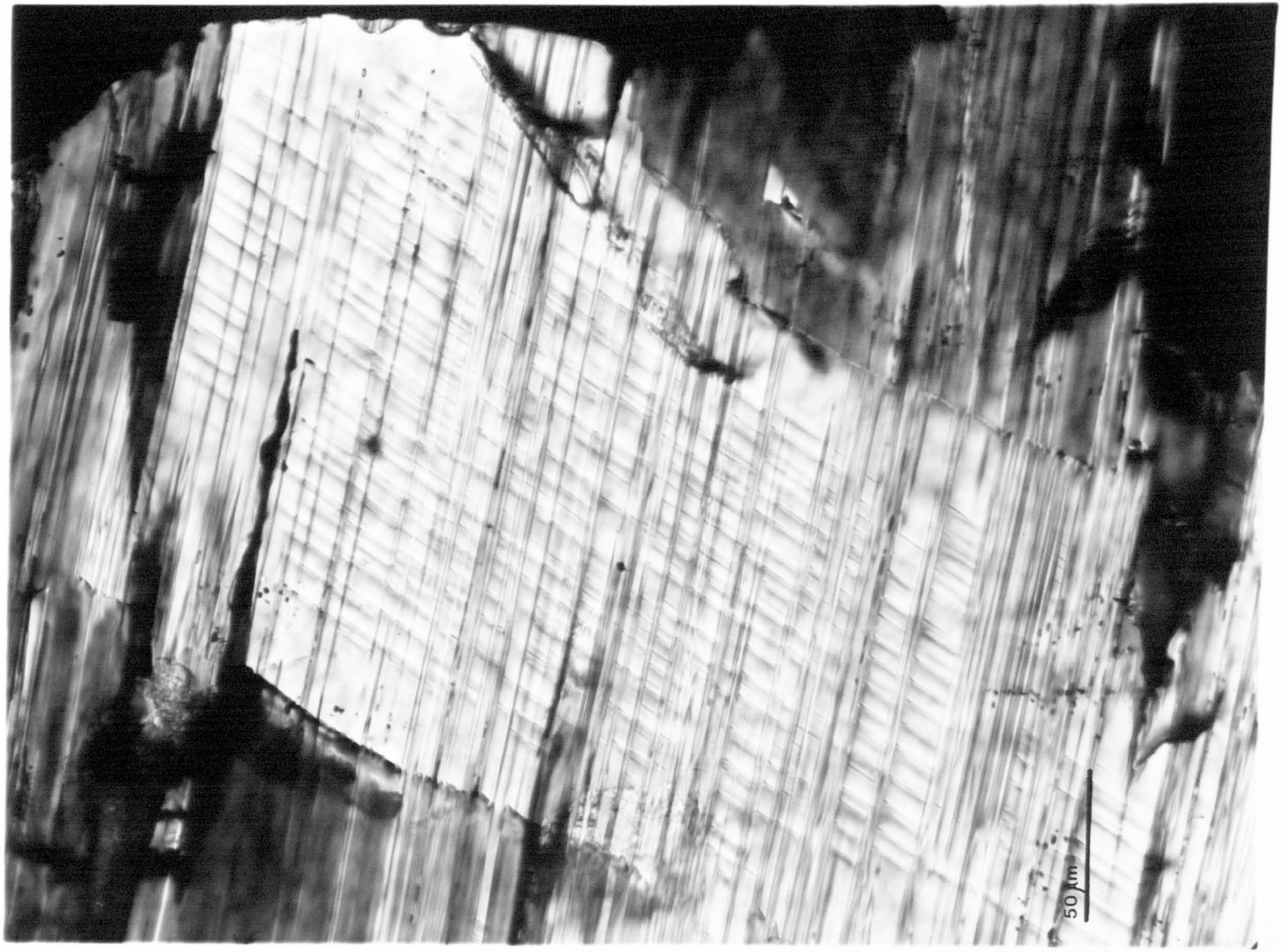
50 µm

temperature.

## 3.4 Discussion

### 3.4.1 Pyroxene paragenesis and equilibration conditions

Pigeonite has been fairly widely reported from metamorphic rocks (e.g. Bonnichsen, 1969), but always from shallow, contact metamorphic aureoles. In rocks with higher Fe/Fe+Mg values than those reported here, equilibration conditions have been estimated as 800C and 2-4kbar on the basis of pyroxene compositions.

The experimental data of Lindsley et al (1974) and Mori (1978) on subsolidus pyroxene assemblages in the system CaO-MgO-FeO-$SiO_2$ enables the data presented above to be interpreted reasonably accurately. The Scourie pyroxenes are very poor in Al and Ti, but contain substantial quantities of Mn, so a close comparison with the experimental data may be possible if Mn is treated correctly. If Mn is not added to any other component (fig. 3.5) a minimum temperature of 1050°C for the stable coexistence of the Scourie pyroxenes is obtained by linear interpolation of the experimental data. The wollastonite contents of the Scourie pyroxenes are lower than those determined experimentally for the three phase assemblage. Data at lower pressure (up to 5Kbar, Ross and Huebner, 1975) show that the wollastonite content of pigeonite decreases with decreasing pressure. However, other rocks in the Scourie district indicate that the pressure at the peak of metamorphism must have exceeded 10kbar (O'Hara and Yarwood, 1978; Chapter 5). Ignoring the

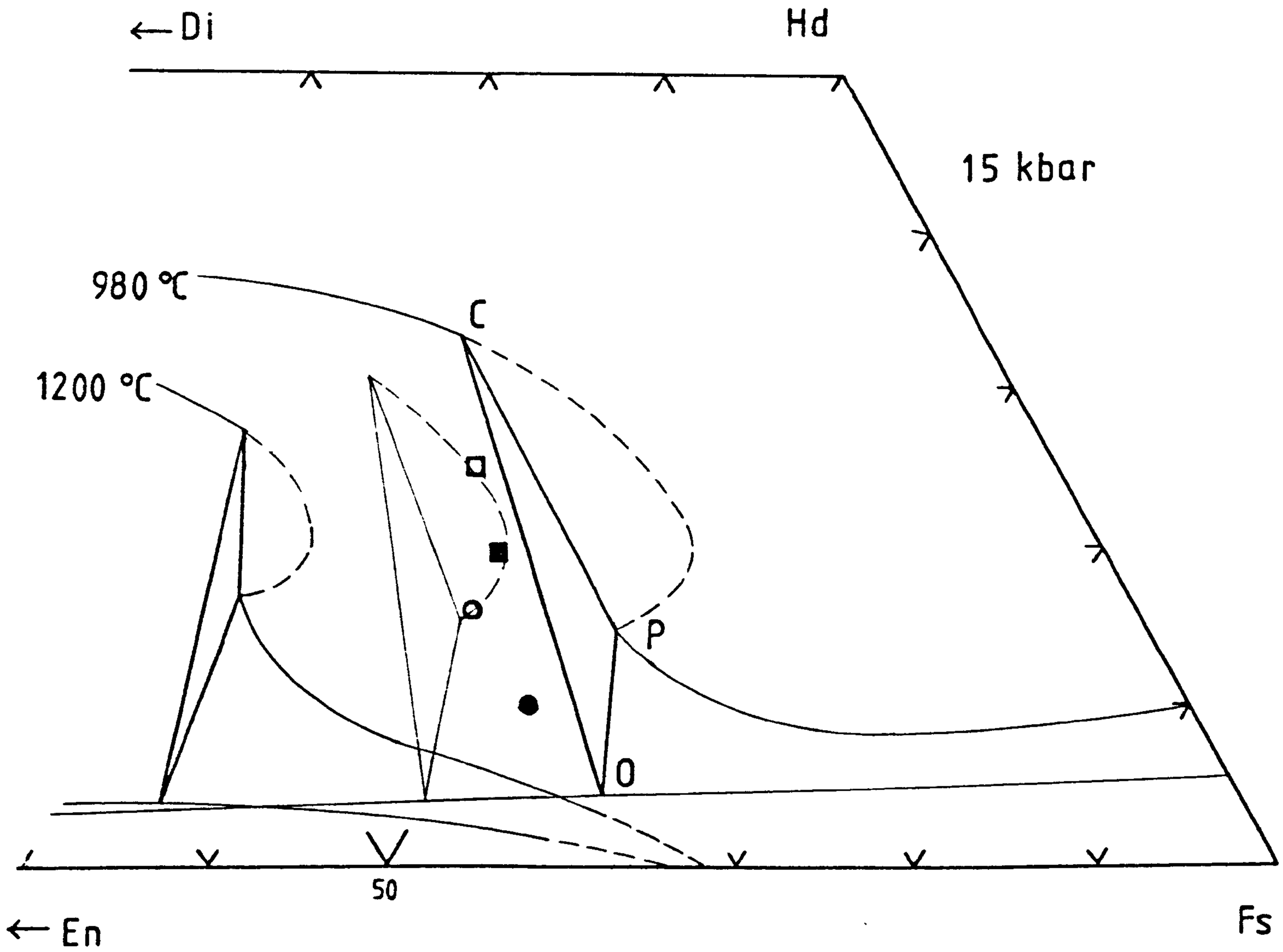
← Di
Hd
15 kbar
980 °C
C
1200 °C
P
O
50
← En
Fs

Mn content of pyroxenes therfore leads to incorrect results. Both Lindh (1974) and Bostwick (1976) conclude from data upon natural pyroxenes that manganese competes with calcium for the M2 site. If the Scourie pyroxenes are recalculated on this basis (ie in terms of (Ca + $Mn)_2Si_2O_6$ - $Fe_2Si_2O_6$ - $Mg_2Si_2O_6$ ) and then compared with the experimental data (open symbols, fig. 3.5), the natural pyroxenes plot much closer to the experimental compositions. Experimental data on the effect of manganese upon pyroxene stability is sparse (Lindsley et al 1974b, Bostwick, 1976), but indicates that for Fe/(Fe+Mg) values of 0.75, the addition of 5mol% rhodonite to the system depresses the lower stability limit of pigeonite by 50°C. In the light of this, it may be concluded that the Scourie pyroxenes equilibrated at a temperature in excess of 1000°C.

The composition of the lower temperature pyroxenes now present (eg Ccc and Occ) suggests a very low equilibration temperature of ca. 600°C: the effect of manganese (8mol% rhodonite in orthopyroxene, 3mol% in clinopyroxene ) at these temperatures is completely unknown. Estimates of exsolution temperatures are impossible to make accurately anyway, due to the unknown magnitude of strain and ordering effects upon the solvus in pyroxenes. The bulk composition of these pyroxenes, as noted above, is more magnesian than the earlier pyroxenes, due to oxidation of iron during cooling of the rock.

### 3.4.2 Metasedimentary origin

The bulk composition of the Scourie ironstone (analyses 1 - 3, table 3.2) shows that the rock is at least 85% $SiO_2$ and $Fe_2O_3$, the remainder being largely MgO and CaO. No real alternative to a metasedimentary ironstone can be envisaged, without invoking large scale, localised metasomatism. These analyses compare closely with those of McGregor and Mason (1977) and Gole and Klein (1980) (see table 3.2) for early and late Archaean ironstones in west Greenland and the Yilgarn Block of Western Australia respectively. In the Yilgarn occurence, the ironstones occur as 5 -20m layers within amphibolite facies metabasic schists of volcanic origin, together with minor pelitic horizons. In the west Greenland occurrence, the ironstone is one of several metasedimentary rock types that occurs, together with layered basic rocks, as amphibolite facies inclusions within the Amitsoq gneiss. The thicknesses of the ironstone layers here reach up to 20m, but most are 'much thinner'. The geological setting of these two examples is similar to the Scourie ironstone described here, and all three examples show similarities with the Algoma and Lake Superior types of iron formation described by Gross and McLeod (1980). However, the grade of metamorphism is higher than that of the association described by Gross and MacLeod (op cit), and in the Scourian case, rock compositions may have been modified by partial melting. A fuller discussion of the geological setting is given in

Table 3.2. Whole-rock analyses of Scourie bay and other ironstones.

| | 1 | 2 | 3 | 4 | 5 | 6 | 7 |
|---|---|---|---|---|---|---|---|
| $SiO_2$ | 50.77 | 54.54 | 65.34 | 51.35 | 62.78 | 57.39 | 50.90 |
| $TiO_2$ | 0.04 | 0.02 | 0.01 | 0.05 | n.d. | 0.08 | 0.08 |
| $Al_2O_3$ | 1.06 | 0.59 | 0.37 | 1.03 | 0.06 | 5.00 | 0.33 |
| $Cr_2O_3$ | n.a. | n.a. | n.a. | n.a. | n.a. | 0.01 | n.d. |
| $Fe_2O_3$ | 35.73 | 33.77 | 26.82 | 36.72 | 16.61 | - | - |
| FeO | - | - | - | - | 14.68 | 30.1 | 41.4 |
| MnO | 1.12 | 1.17 | 0.79 | 0.93 | 0.31 | 0.15 | 0.13 |
| MgO | 3.91 | 3.66 | 2.42 | 3.25 | 0.97 | 2.40 | 2.97 |
| CaO | 6.23 | 5.06 | 3.70 | 5.31 | 3.65 | 1.95 | 1.38 |
| $Na_2O$ | n.d. | n.d. | n.d. | n.d. | 0.05 | 0.09 | 0.13 |
| $K_2O$ | n.d. | n.d. | n.d. | n.d. | 0.01 | 0.03 | 0.26 |
| $P_2O_5$ | 0.24 | 0.10 | 0.09 | 0.21 | 0.11 | 0.11 | 0.08 |
| $H_2O$ | - | - | - | - | 0.22 | - | - |
| LOI | -0.37 | -0.25 | -0.07 | -0.75 | - | - | - |
| | 99.10 | 99.91 | 99.54 | 98.85 | 99.45 | 97.31 | 97.70 |

1 Scourie Bay Ironstone 45, 577 Edinburgh XRF.

2 Scourie Bay Ironstone 78401/1 Edinburgh XRF.

3 Scourie Bay Ironstone 78402/2 Edinburgh XRF.

4 Scourie Bay Ironstone 77002 Edinburgh XRF.

5 Ironstone, Gole and Klein (1981) analysis 2.

6 Ironstone, McGregor and Mason (1977) analysis 119217.

7 Ironstone, McGrefor and mason (1977) analysis 119233.

Chapter 9.

# Chapter 4 Garnet-clinopyroxene intergrowths

## 4.1 Introduction

The granulite facies mineralogy (grain size 0.5 to 1 cm) is the earliest stage in the evolution of the Scourie complex generally visible. Rarely, earlier intrafolial folds of lithological banding can be seen, with an axial planar granulite facies fabric (eg Cleit Mhor GR NC141442). Within several of the basic/ultrabasic masses, most notably those on the north side of Scourie Bay (but also at Geodh Eanruig and as far north as Gorm Loch), sub- to euhedral- intergrowths composed largely of garnet and clinopyroxene are found (fig. 4.1). The intergrowths are interpreted as relics of a mineralogy pre-dating the main granulite facies stage in the history of the complex for reasons discussed below.

## 4.2 Petrography

The intergrowths are generally most abundant in particular basic horizons of the basic/ultrabasic masses, and are sparsely distributed throughout much of the basic rock of these associations.

### 4.2.1 Intergrowth petrography

In thin section, it can be seen that while garnet and clinopyroxene make up the bulk of the intergrowths, plagioclase and ilmenite are also present in significant quantities (table 4.1). Rounded to subrounded clinopyroxene crystals (usually rimmed to varying degrees

Fig. 4.1 Garnet clinopyroxene intergrowths set in basic gneisses in the first inlet west of the pier on the north side of Scourie bay.

Note the crudely euhedral outline of the intergrowths and the coarse grain-size of their minerals.

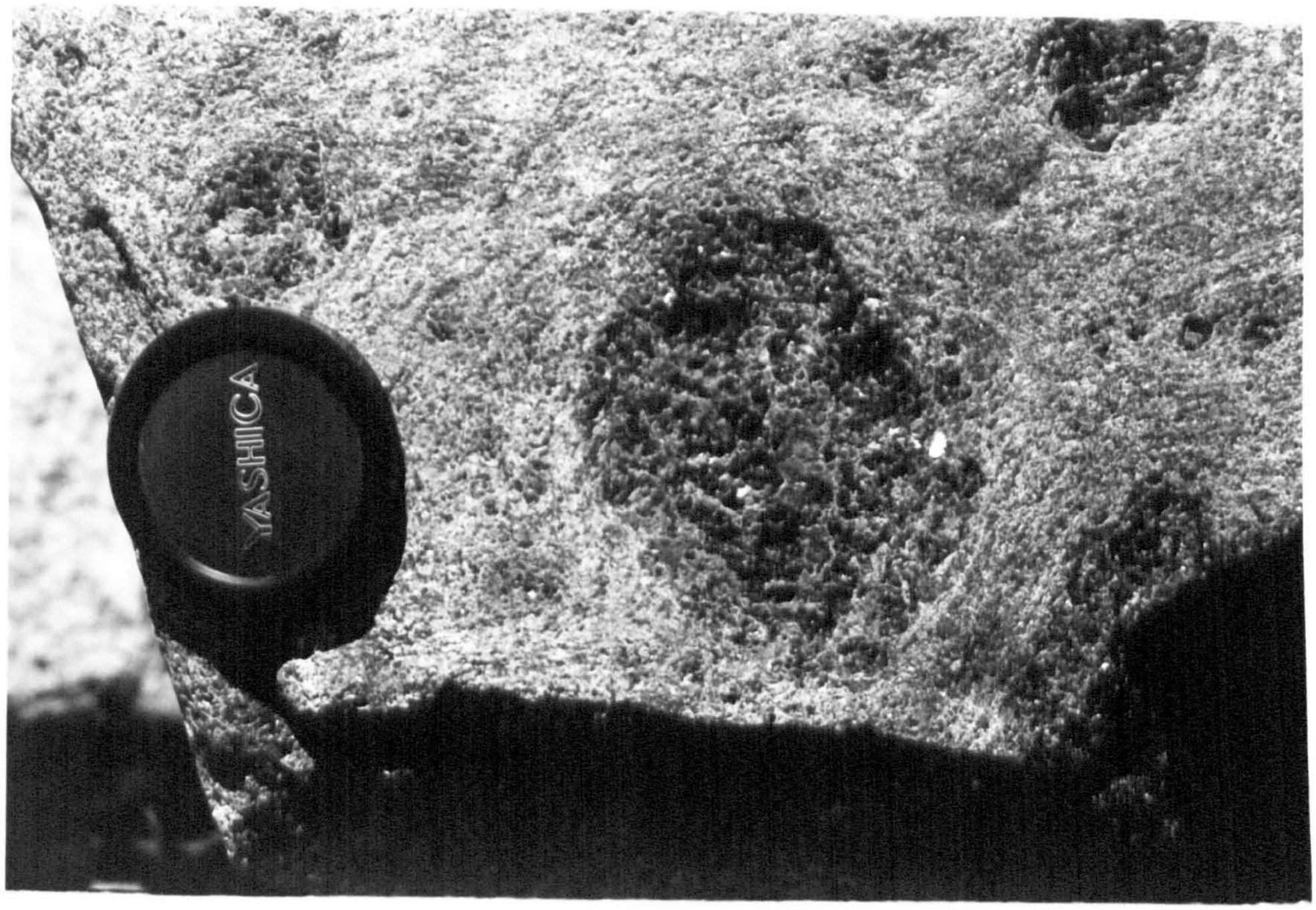
YASHICA

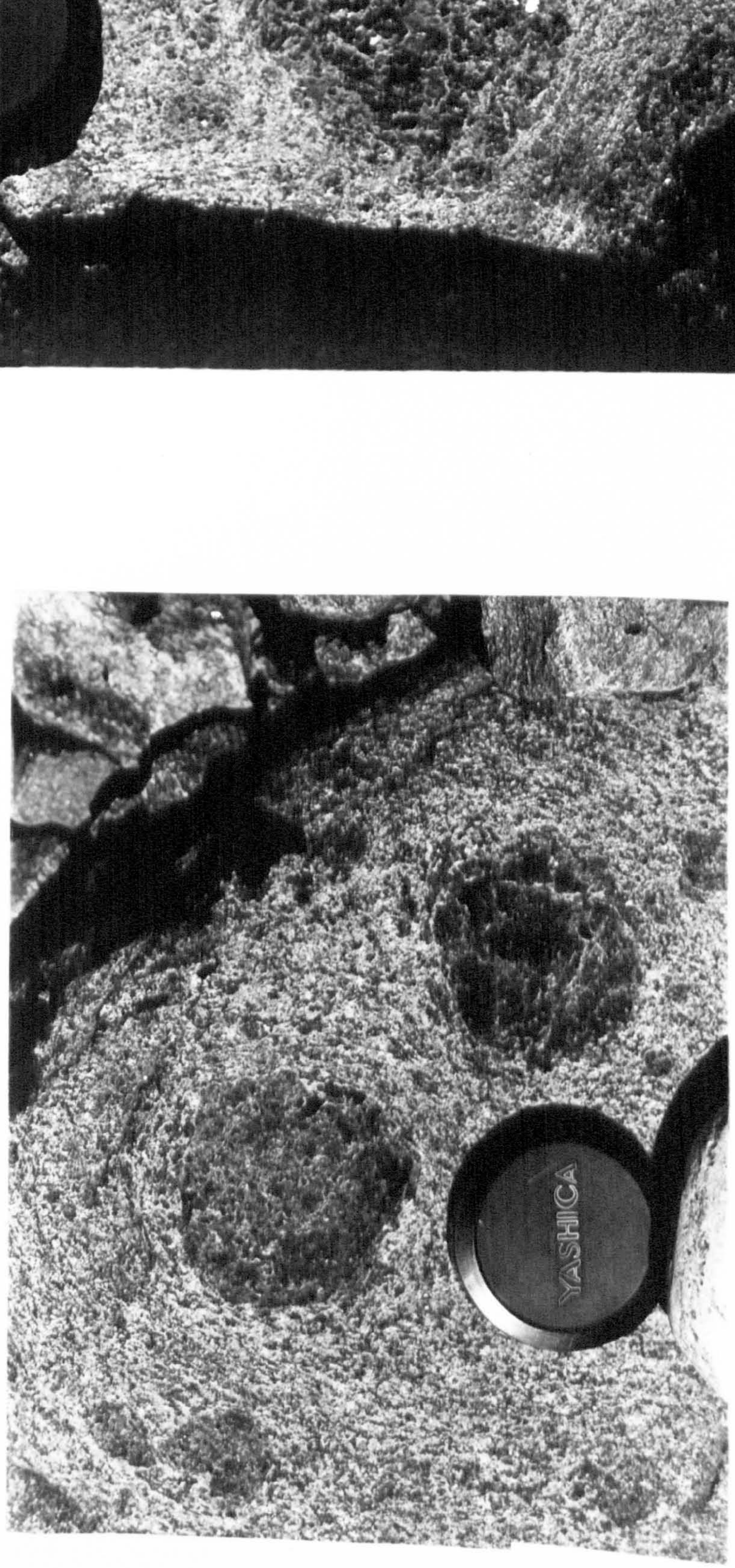
YASHICA

Table 4.1 Point - count of garnet - clinopyroxene intergrowth 45,472 (600 points ).

| | |
|---|---|
| Garnet | 63% |
| Clinopyroxene | 31% |
| Plagioclase | 5% |
| Ore | 1% |
| Biotite | trace |

by plagioclase) occur within the garnet. (fig 4.2). There is a crude prefered orientation of clinopyroxene crystals as determined from cleavage orientation. As well as forming the bulk of the intergrowth, garnet also occurs rimming ore crystals.

4.2.1.1 Clinopyroxene exsolution

Exsolution lamellae of three types are visible in the fresh clinopyroxene of the intergrowths (figs. 4.3 and 4.4) and can also be seen in the coarse marginal clinopyroxene. Lamellae of hypersthene are abundant parallel to the strong (100) parting. Between the hypersthene lamellae, and possibly nucleating at the augite-hypersthene interface, are a set of fine (1-2$\mu$m) lamellae at about 13 - 14° to (100). By analogy with the lamellae described by Robinson et al. (1971,77) and Jaffe et al.(1975) they are thought to be of pigeonite (or clinohypersthene). Abundant very fine (<1$\mu$m) lamellations parallel to (010) are visible in optic axis sections of the host clinopyroxene. These are likely to be of clinoamphibole, as lamellae of amphibole have been described on (010) of clinopyroxene by Yamaguchi et al. (1978) among others.

To allow more complete description of the lamellae, they have been examined by TEM at the Chemistry dept, UCW, Aberystwyth (Drs. ES Davies and JO Williams , pers comm 1981), and selected area diffraction patterns and lattice images have been obtained. A selection of them is reproduced here by permission of Dr. ES Davies. These

Fig. 4.2 Clinopyroxene crystals with a partial rim of plagioclase, set in garnet. From garnet-clinopyroxene intergrowth, north of Scourie bay ( 45,572).
(plane polarised light ).

Scale bar is 0.5mm.

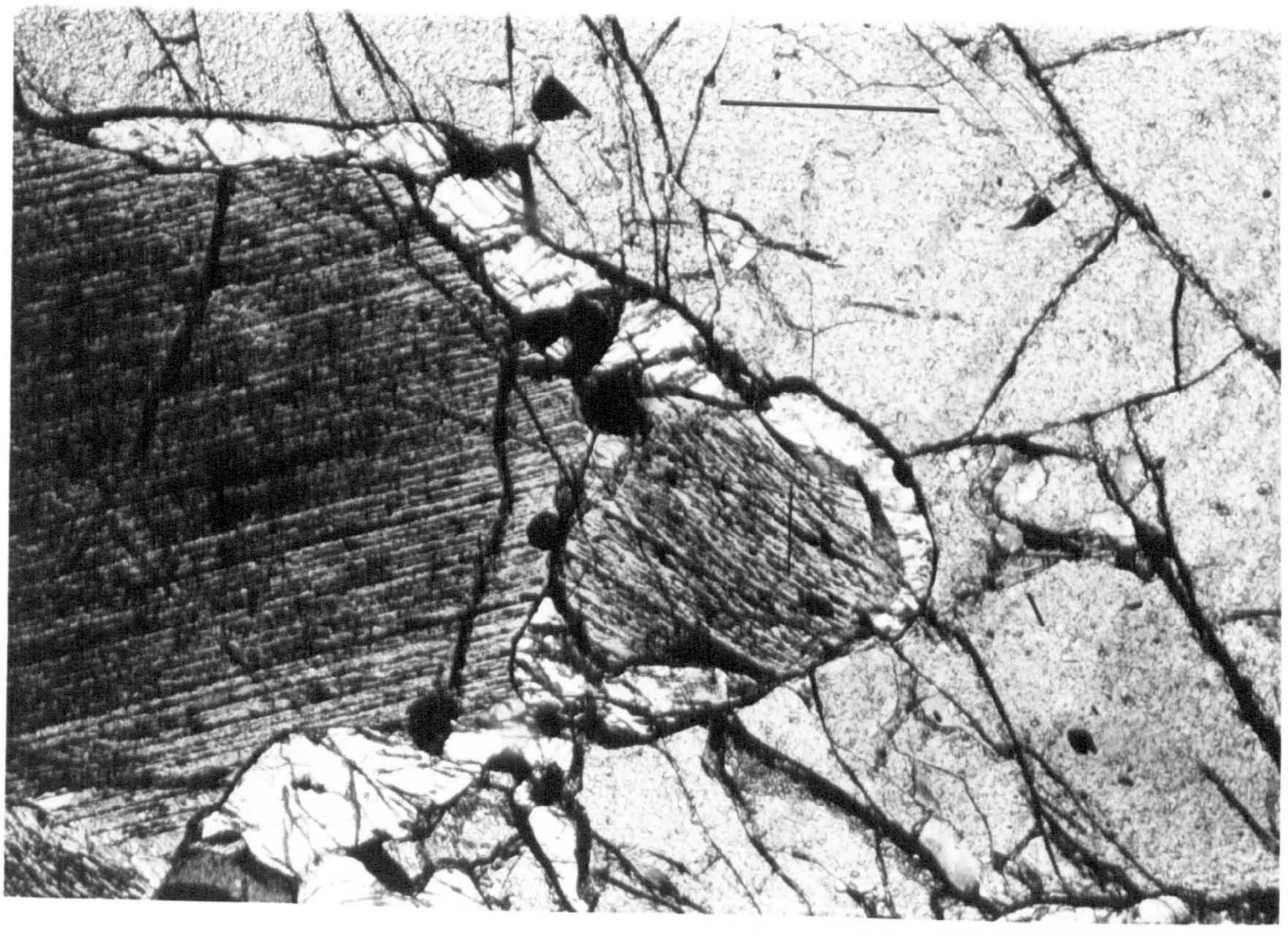

reveal that the (100) hypersthene lamellae are strained, coherent and have rational boundaries (figs. 4.5, 4.6, 4.10 and 4.11). The finer lamellae close to (100) are indeed of pigeonitic structure. They have coherent but irrational boundaries (c.f. (001) pigeonite described by Copley et al., 1974). Small ledges are present along the margins of the lamellae, and they contain (100) stacking faults (c.f. (001) pigeonites of Robinson et al.,1977) (figs 4.7, 4.8). The (010) lamellations proved to be regions in which one or more amphibole chains have been formed (by crystallographic shear, Chisolm, 1973) from the clinopyroxene matrix (figs. 4.9, 4.10 and 4.11).

Compositional data are not available for any of the exsolved phases, but the hypersthene lamellae are presumably very calcium poor, and the pigeonite presumably has less than 10 atom% calcium. The amphibole lamellae may be very significant; if they are stoichiometric amphiboles ($A_{0-1}B_2C_5T_8O_{22}(OH)_2$) then they represent a source/sink for water in these rocks.

The presence of such stuctural defects may modify the thermodynamic properties of the pyroxenes, and it would be interesting to know if they are commonly present in metamorphic pyroxenes. Similarly, the presence of such defects in clinopyroxenes crystallised synthetically in solid-media experiments using water as a flux (e.g. Danckwerth and Newton, 1978; Jenkins and Newton, 1979; Perkins and Newton, 1980) may affect their thermodynamic properties and limit their application to natural rocks.

Fig. 4.3 Optical micrograph along the b - axis of augite from garnet-clinopyroxene intergrowth showing lamellae of hypersthene parallel to (100) and lamellae of pigeonite at an angle to (100).
(plane polarised light).

Fig. 4.4 Optical micrograph along the c - axis of augite from garnet-clinopyroxene intergrowth showing lamellae of hypersthene parallel to (100) and of amphibole parallel to (010). The small lensoid bodies parallel to (100) in the top centre are probably of pigeonite.
(plane polarised light).

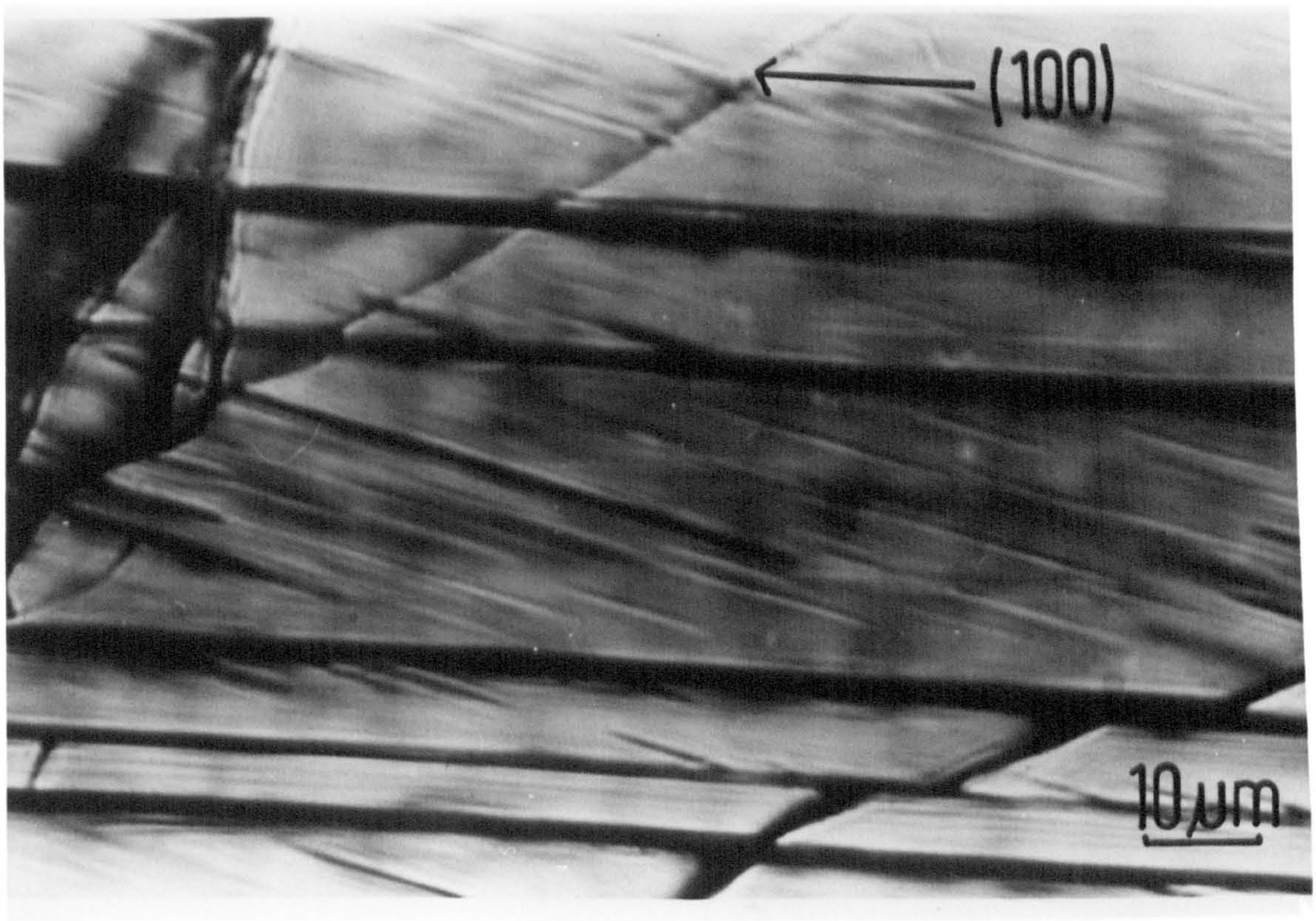
(100)
10 μm

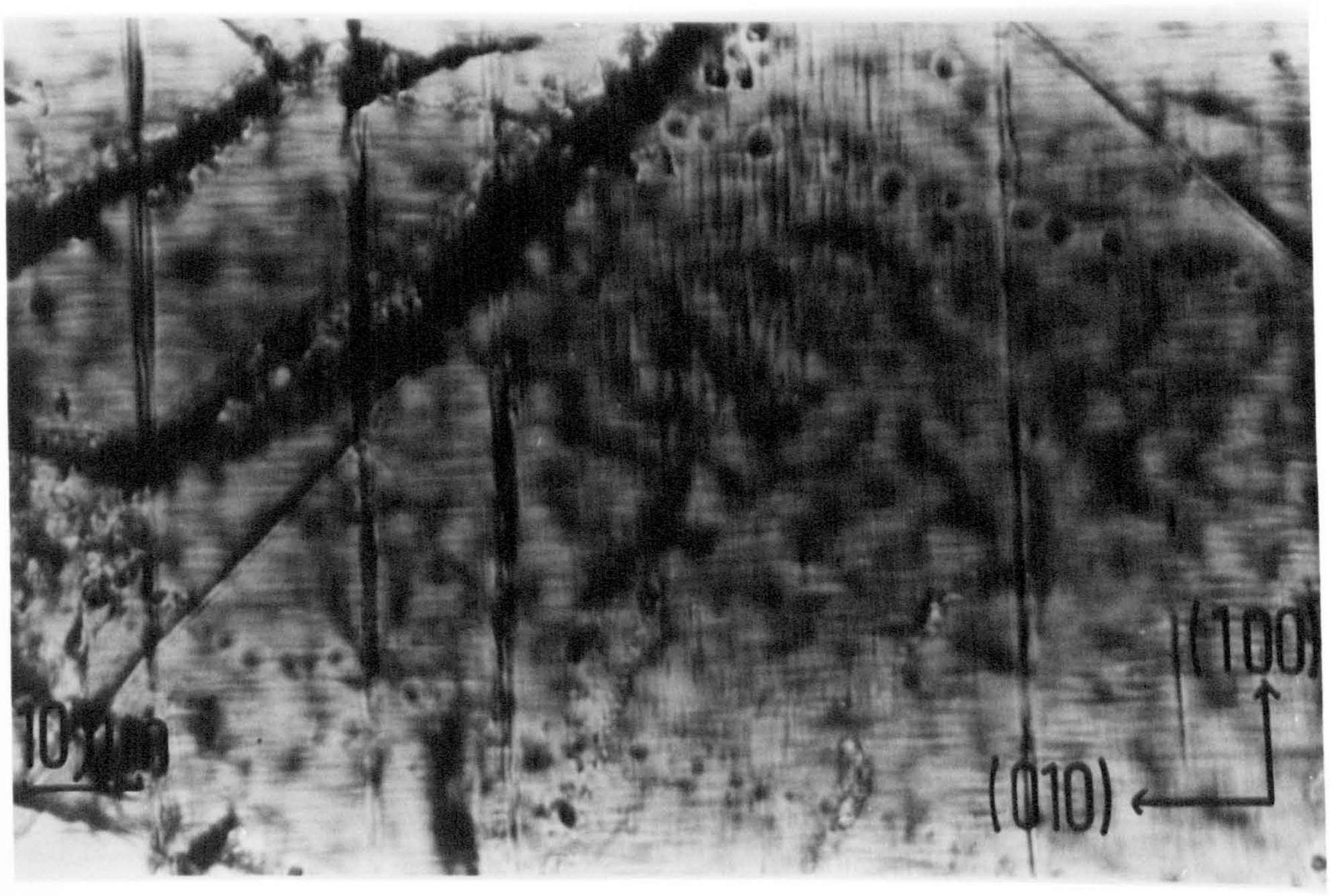
10 μm
(100)
(010)

Fig. 4.5 Electron micrograph along the b - axis of the boundary (AB) between hypersthene (top) and augite (bottom).

Fig. 4.6 Lattice image of the hypersthene - augite interface showing the thin, discontinuous area of pigeonite along the contact.

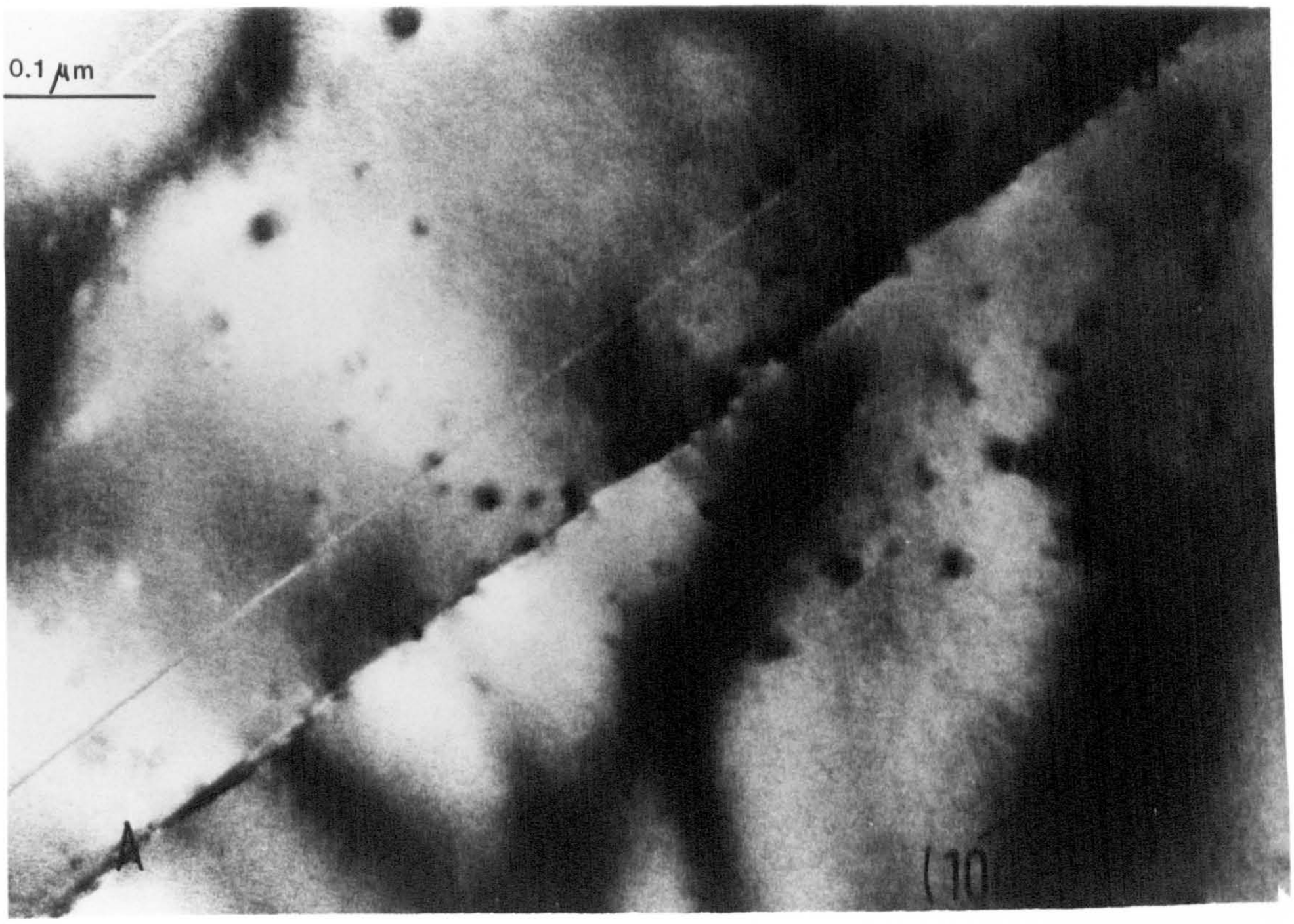
0.1 μm
A
(10)

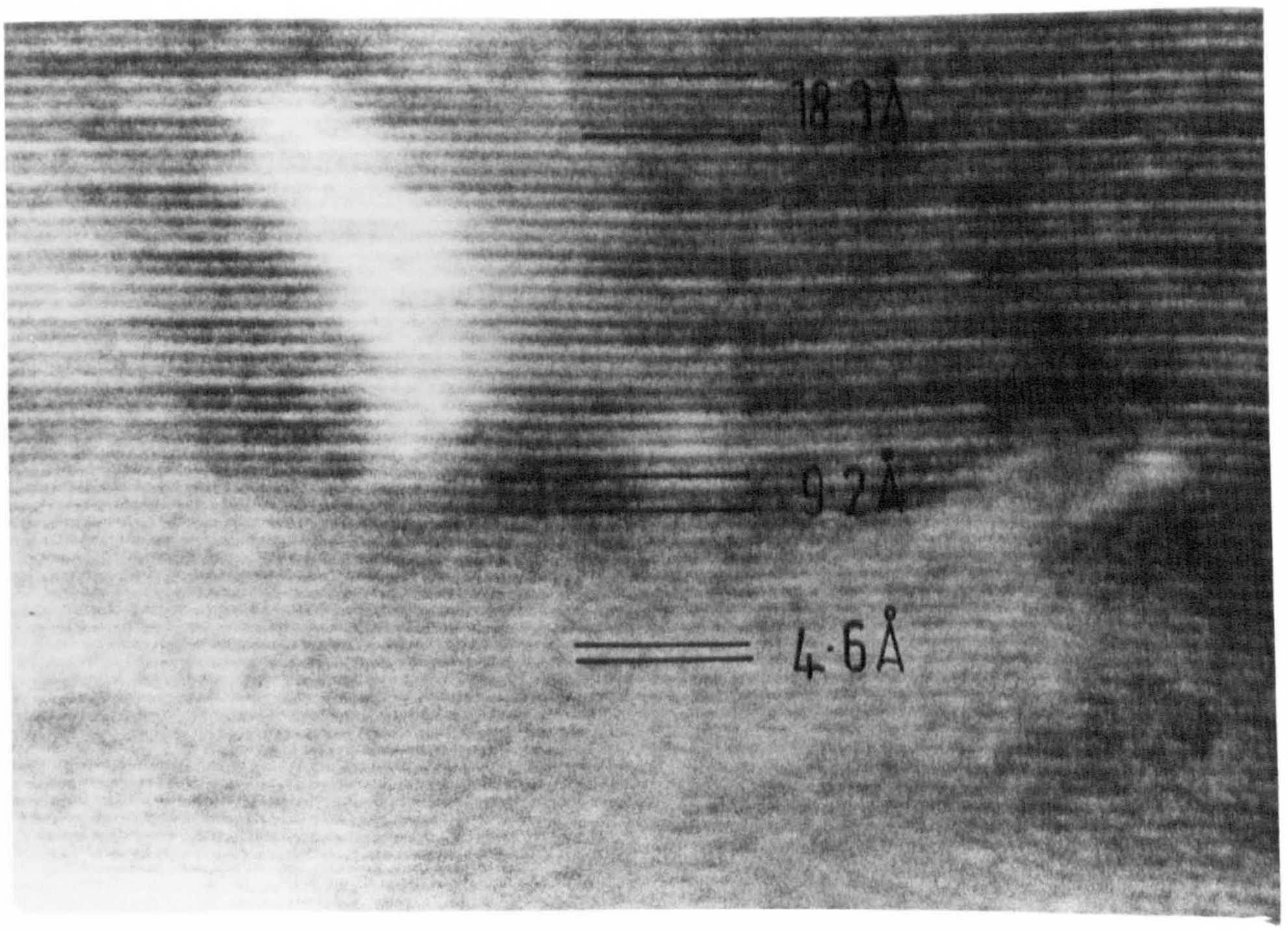
18·9Å
9·2Å
4·6Å

Fig.4.7 B axis lattice image of a strained lamellae of pigeonite (centre) in an augite matrix. Notice that the interface, although at an angle of ca. 12° to (100), is perfectly coherent.

Fig.4.8 B axis electron micrograph of pigeonite lamella in augite showing (100) stacking faults in the pigeonite, terminating in steps at the interface.

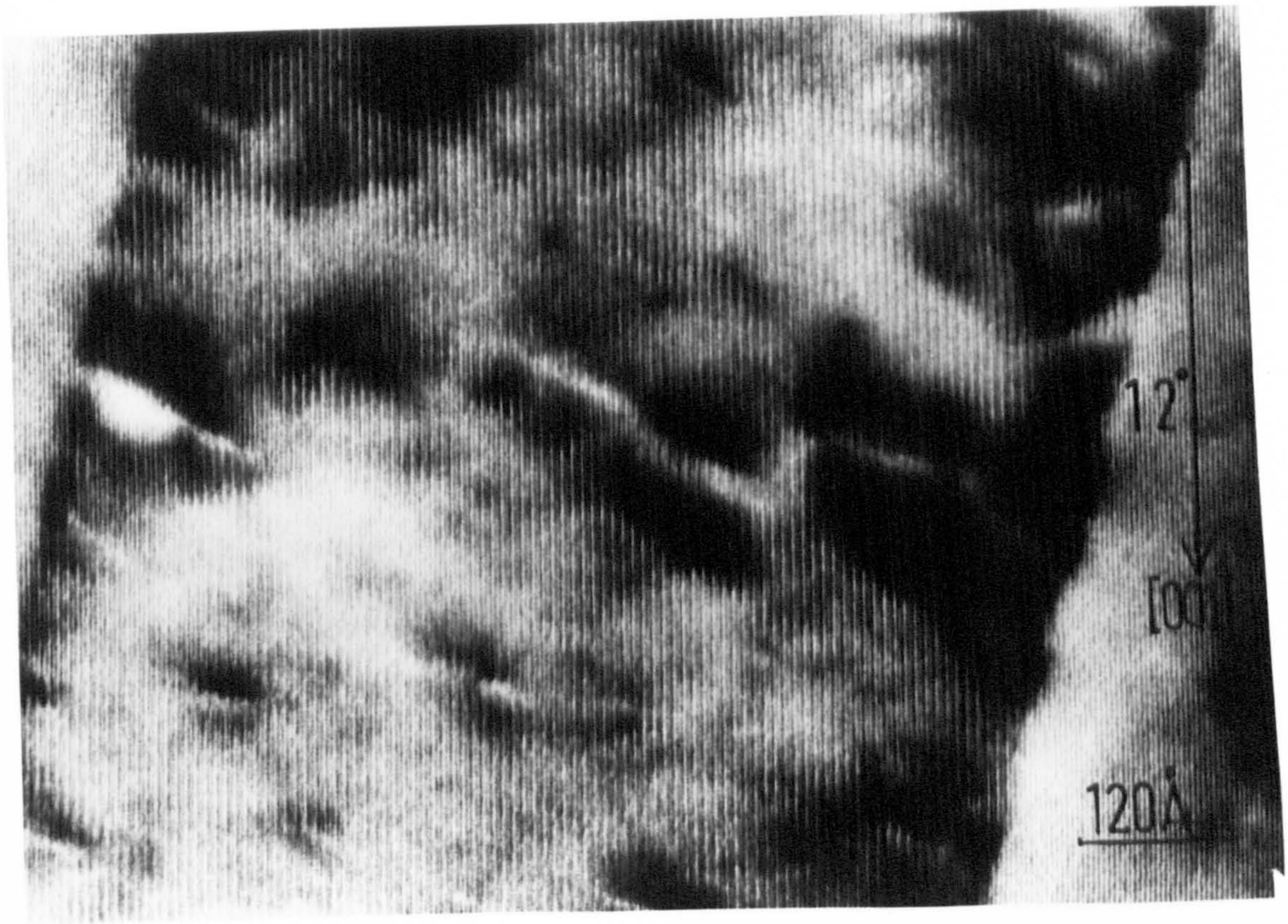
12°
[001]
120Å


(100)
800Å

Fig. 4.9 A - axis lattice image of two and four chain lamellae ( A and B ) of amphibole in augite matrix, together with a schematic model showing the relationship of the image to the mineral structure.

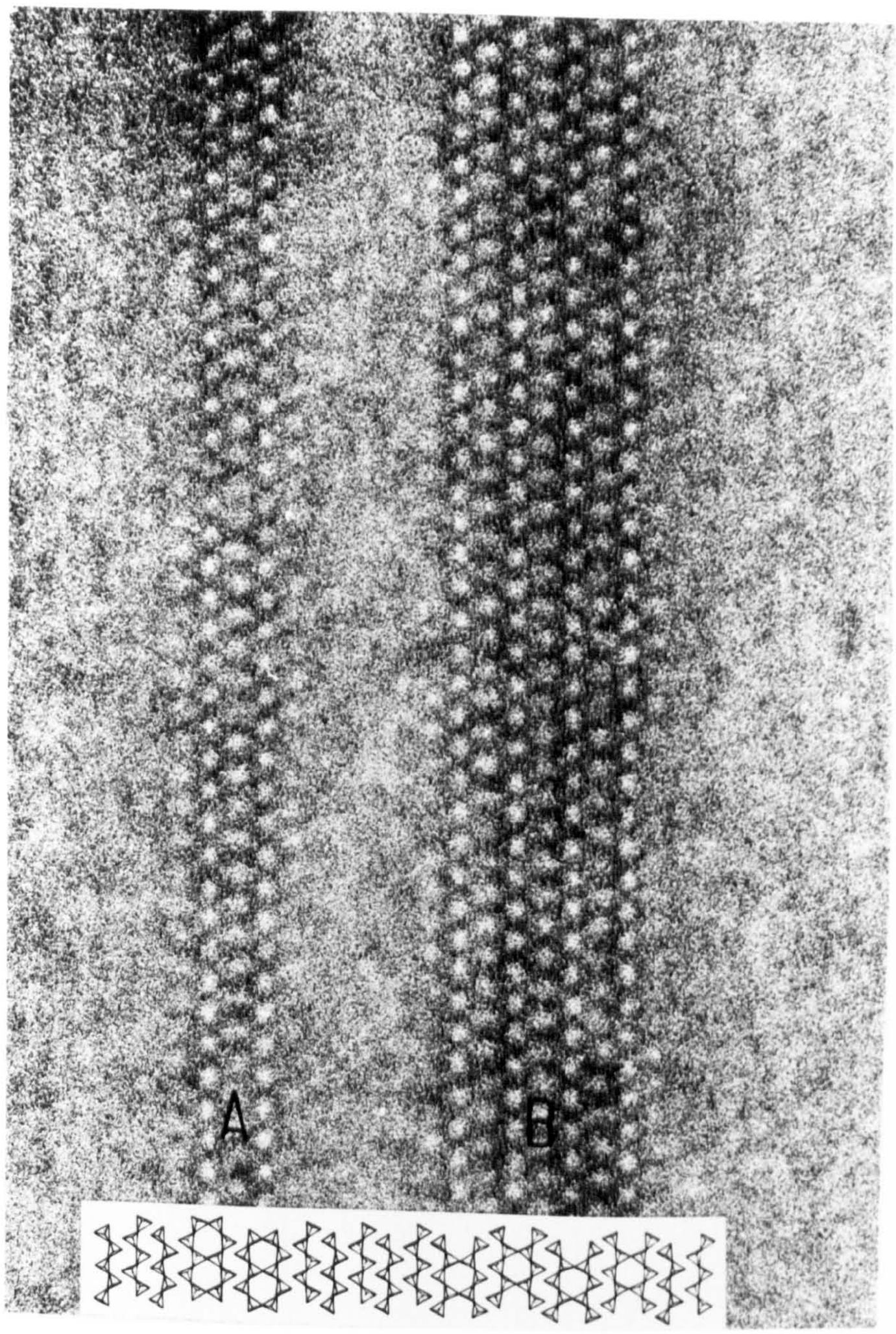
A
B

Fig 4.10 Electron micrograph along c axis of augite (A) with (100) lamellae of hypersthene (H) and (010) lamellae of amphibole (Am).

Fig. 4.11 High resolution lattice image of the junction of amphibole (Am) and hypersthene (H) lamellae in augite (A) matrix viewed along the **c** axis .

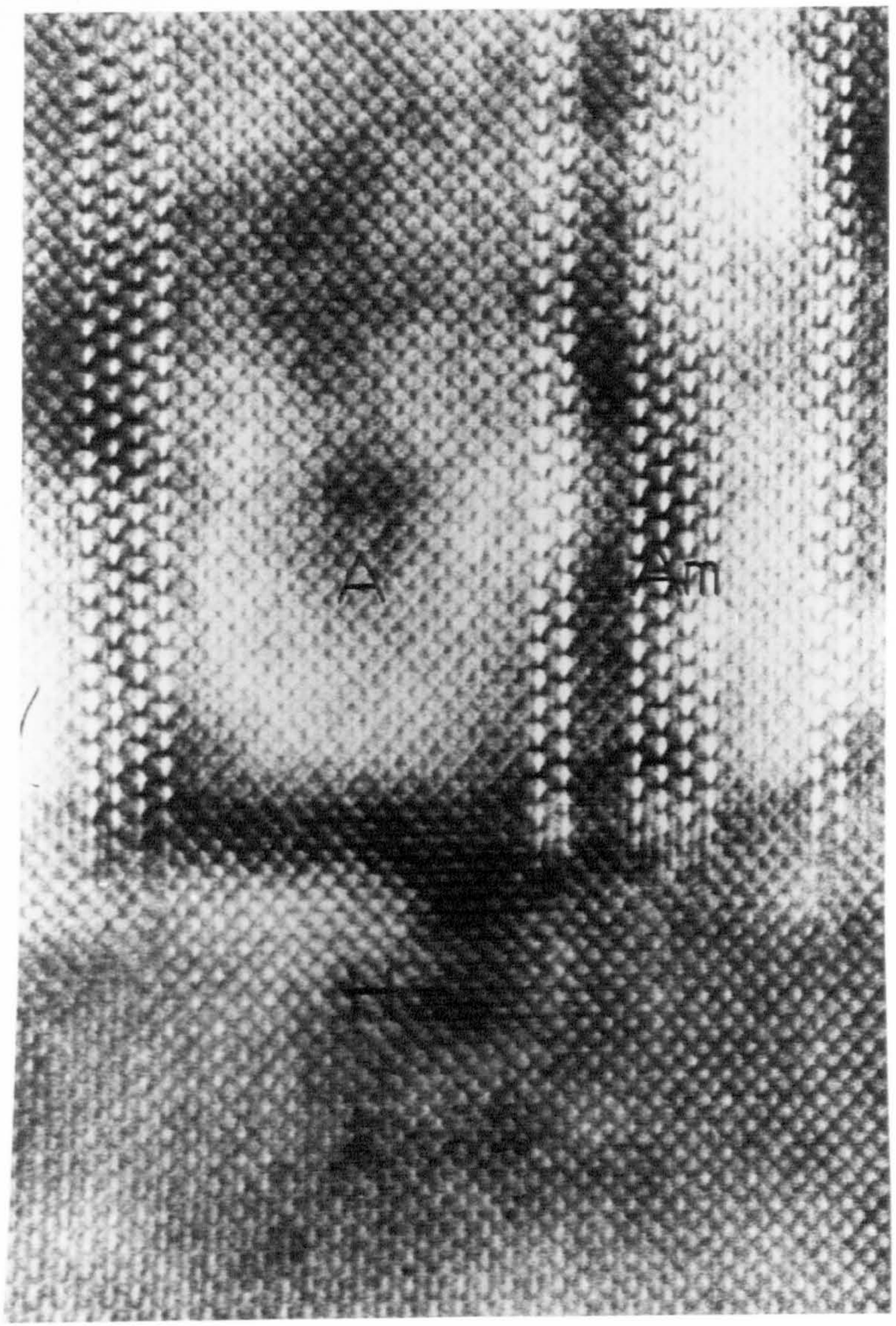
A
Am

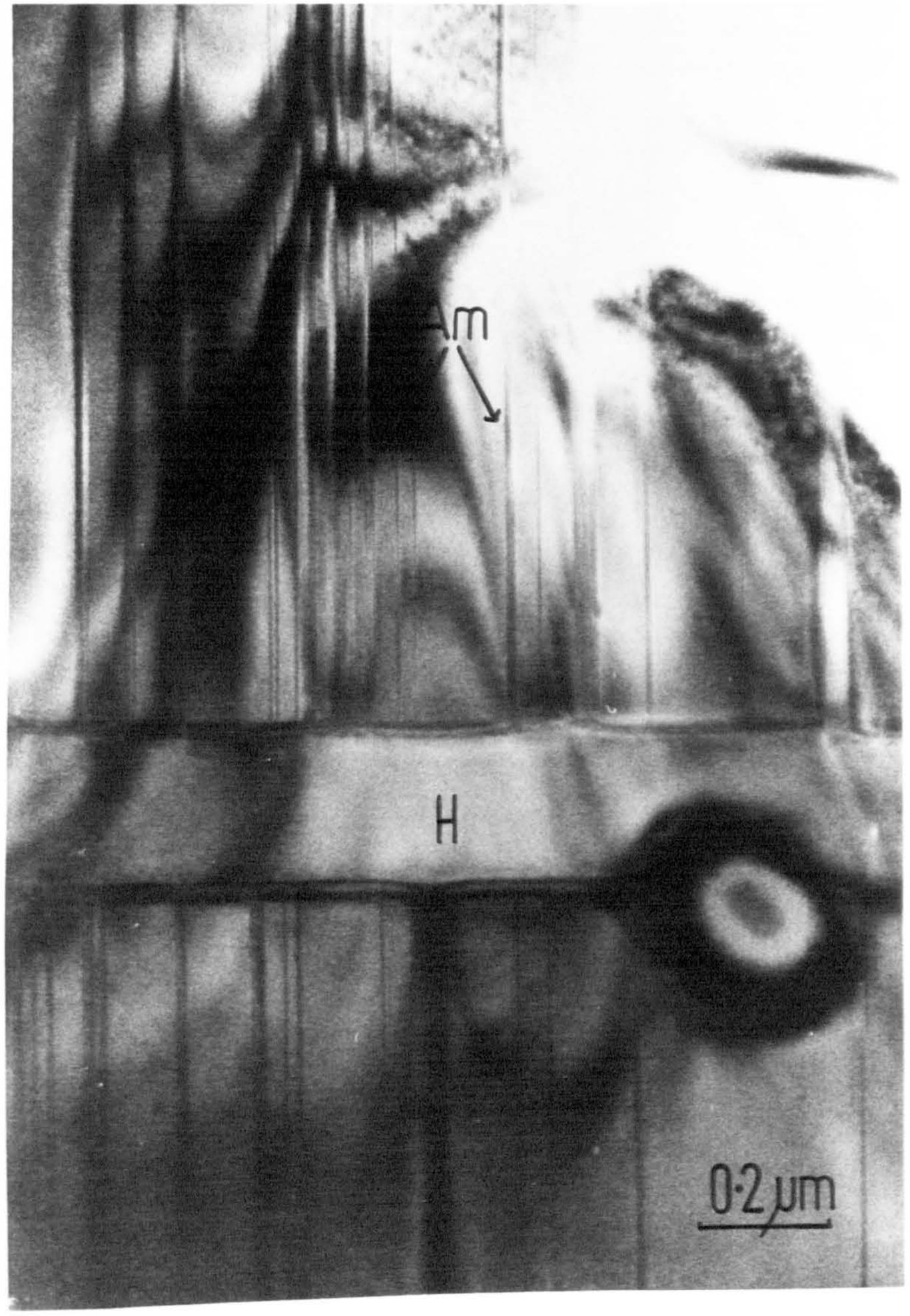
Am
H
0·2 µm

### 4.2.2 Matrix petrography

The matrix is composed of an approximately equigranular aggregate of clinopyroxene and optically zoned plagioclase, with occasional small garnet crystals. Large unaltered clinopyroxene crystals, which are close to the intergrowths and freshest, contain one or more generations of exsolution lamellae, the most prominent of which are (100) hypersthene lamellae (see section 4.2.1.1).

## 4.3 Mineral chemistry

### 4.3.1 Intergrowth

Representative analyses are presented in table 4.2. All minerals are zoned, and are treated in turn below.

#### 4.3.1.1 Garnet

Garnet has rims of composition Alm 56.1 Pyr 23.5 Gro 17.3 and cores of composition Alm 49.8 Pyr 27.5 Gro 21.0. Garnet rimming ore minerals are richer in almandine and grossular and poorer in pyrope than all other garnet.

#### 4.3.1.2 Clinopyroxene

Clinopyroxene crystals are strongly zoned; in the same core to rim transition, $Al_2O_3$ ranges from 7.1% (core) to ca. 4.0% (rim), $Na_2O$ goes from 0.65% to 0.3%, $TiO_2$ from 1.0% to 0.4% and Fe/Fe + Mg (atom) from 0.32 to 0.37.

#### 4.3.1.3 Plagioclase

Matrix plagioclase averages An50, both in grain cores and next to clinopyroxenes. The one analysis of a plagioclase rim next to a garnet is An39.6.

Table 4.2 Analyses of minerals from garnet - clinopyroxene intergrowth ( 45,572 ).

| | CPX204D | GT202D | CPX103 | GT107 | CPX203 | GT203 |
|---|---|---|---|---|---|---|
| $SiO_2$ | 48.26 | 39.55 | 49.42 | 39.77 | 49.91 | 39.30 |
| $TiO_2$ | 0.73 | nd | 0.71 | nd | 0.75 | nd |
| $Al_2O_3$ | 6.41 | 21.71 | 5.94 | 21.83 | 6.26 | 21.81 |
| $Cr_2O_3$ | nd | nd | nd | nd | 0.17 | nd |
| FeO | 11.97 | 24.96 | 10.33 | 24.00 | 10.34 | 24.55 |
| MnO | 0.20 | 1.03 | 0.13 | 0.86 | 0.14 | 1.00 |
| MgO | 10.71 | 7.39 | 11.43 | 7.39 | 10.92 | 7.18 |
| CaO | 20.22 | 7.46 | 21.53 | 7.87 | 21.62 | 7.29 |
| $Na_2O$ | 0.79 | na | 0.56 | na | 0.89 | na |
| | 99.29 | 102.10 | 100.05 | 101.72 | 101.89 | 101.13 |

CPX204D and GT202D :EDS analyses with beam defocused to 30$\mu$m.
All other analyses EDS.

### 4.3.2 Matrix

The matrix plagioclase is zoned: the range is at least An37 (core) to An47 (rim). Antiperthitic texture is present. Clinopyroxenes are zoned with cores richer in Fe, Mn and Al and poorer in Mg and Ca than the rims (see table 4.3.).

### 4.4.1 Major elements

Both intergrowths and matrices have been analysed, four of each by ICPS (Induction coupled plasma spectroscopy) at Kings College, London (Walsh and Howie, 1980) and one of each by XRF (Edinburgh). Results are presented in table 4.4.

The fit of the intergrowth analyses to pyroxene, garnet and amphibole structural formulae has been checked: in no instance is the fit very good assuming standard site occupancies, although the fit with the amphibole formula is the best. It is also possible to obtain a match with a mixture of clinopyroxene and garnet as seen in the mode.

The suggestion that the intergrowths were originally amphibole recieves support from analyses of Fe-Al rich amphiboles reported by Doolan et al (1978). They examined material from Massachusetts which has a very similar bulk composition to the Scourie intergrowths (table 4.4). Furthermore, amphiboles with higher Fe/Fe+Mg than matrix have been reported by Ujike (1980) in dykes from Japan, and by Helz (1973, 1976) during the partial melting of basalts with $P_{H_2O} = P_{Tot}$ .

Table 4.3 Minerals in the matrix to the intergrowth ( 45,572 ).

| | CPX5 core | CPX 6 rim | CPX3 core | CPX2 rim |
|---|---|---|---|---|
| $SiO_2$ | 49.57 | 51.21 | 49.39 | 50.13 |
| $TiO_2$ | 0.53 | 0.53 | 0.69 | 0.67 |
| $Al_2O_3$ | 4.66 | 4.35 | 5.14 | 4.65 |
| $Cr_2O_3$ | 0.19 | 0.20 | nd | nd |
| FeO | 12.80 | 9.90 | 11.16 | 10.66 |
| MnO | 0.22 | 0.14 | 0.13 | 0.19 |
| MgO | 11.67 | 12.16 | 11.02 | 11.83 |
| CaO | 19.57 | 22.28 | 20.65 | 21.38 |
| $Na_2O$ | 0.24 | 0.66 | 0.39 | 0.57 |
| | 99.45 | 101.66 | 98.57 | 100.08 |

Analyses by EDS.

Table 4.4 Major element analyses of garnet - clinopyroxene intergrowths.

| | 1 | 2 | 3 | 4 | 5 | 6 | 7 | 8 |
|---|---|---|---|---|---|---|---|---|
| $SiO_2$ | 40.02 | 40.2 | 43.2 | 41.4 | 42.1 | 36.91 | 42.34 | 40.12 |
| $TiO_2$ | 0.76 | 0.62 | 0.70 | 0.79 | 0.60 | 0.19 | 0.21 | 0.80 |
| $Al_2O_3$ | 15.94 | 17.47 | 16.26 | 16.37 | 17.57 | 20.46 | 16.31 | 18.68 |
| $Fe_2O_3$ | 23.45 | 23.29 | 19.36 | 21.99 | 21.59 | - | - | 5.43 |
| FeO | - | - | - | - | - | 19.29 | 18.11 | 13.20 |
| MnO | 0.60 | 0.57 | 0.40 | 0.49 | 0.46 | 0.23 | 0.17 | 0.29 |
| MgO | 7.10 | 7.16 | 7.53 | 7.55 | 7.57 | 4.50 | 7.53 | 6.36 |
| CaO | 10.30 | 10.10 | 11.22 | 10.66 | 9.73 | 9.98 | 11.00 | 11.10 |
| $Na_2O$ | 0.49 | 0.61 | 1.12 | 0.79 | 0.86 | 1.28 | 1.14 | 1.29 |
| $K_2O$ | 0.01 | 0.07 | 0.08 | 0.05 | 0.07 | 0.35 | 0.31 | 0.58 |
| $P_2O_5$ | 0.04 | 0.10 | 0.10 | 0.11 | 0.88 | na | na | tr |
| $H_2O$ | na | na | na | na | na | na | na | 2.56 |
| LOI | -0.36 | 0.20 | 0.60 | 0.1 | 0.4 | na | na | na |
| | 98.35 | 100.39 | 99.57 | 100.30 | 101.03 | 93.19 | 97.12 | 100.41 |

1 Intergrowth 78590I , Edinburgh XRF analysis
2 " 78209I/1, ICPS analysis
3 " 78209I/2, " "
4 " 77040I , " "
5 " 78535I , " "
6 Amphibole analysis 3 - 1, Doolan et al 1978
7 " " 2 - 1, "
8 " " , Deer, Howie and Zussman Vol 2

The CIPW norms of the matrix analyses show that it is basaltic, with between 4.5 and 7.5% total olivine in the norm.(table 4.5).

4.4.2 REE

Four intergrowth and four matrix specimens were analysed for REE by ICPS at Kings (Walsh et al., 1981). The data are presented in table 4.6, and normalised to chondrite in fig 4.12. The matrices show patterns at about 10x chondrite ,with slight HREE depletion, whilst the intergrowths show rather steeper HREE enriched patterns averaging 10x chondrite.

The critical data come from the intergrowth - matrix partition patterns (fig 4.13). These show that for elements lighter than Eu, the intergrowth is depleted relative to the matrix (down to intergrowth/matrix values of 0.3), whereas the heavier REE are enriched in the intergrowth by factors of up to 10. Furthermore, the patterns show that the intergrowths are all depleted in Eu with respect to the matrix.

Comparison with natural mineral - matrix partitioning data is not easy due to the abnormal bulk compositions involved, but reveals that the patterns obtained here are shallower than garnet/matrix pairs, especially iron rich compositions (Irving and Frey, 1978, fig 4.14). Natural samples also have greater extremes of depletion and enrichment for light and heavy elements respectively. When the data are compared with natural clinopyroxene - matrix pairs (Cullers et al.,1973; fig

Table 4.5 Analyses and norms of matrices to intergrowths.

| | 1 | 2 | 3 | 4 |
|---|---|---|---|---|
| $SiO_2$ | 49.89 | 48.93 | 50.39 | 49.90 |
| $TiO_2$ | 0.82 | 0.84 | 0.78 | 0.83 |
| $Al_2O_3$ | 17.34 | 17.00 | 16.57 | 17.39 |
| $Fe_2O_3$ | 1.94 | 2.20 | 1.98 | 2.01 |
| FeO | 6.99 | 7.89 | 7.11 | 7.21 |
| MnO | 0.12 | 0.13 | 0.12 | 0.12 |
| MgO | 5.93 | 5.66 | 5.90 | 5.58 |
| CaO | 12.79 | 13.01 | 13.09 | 12.27 |
| $Na_2O$ | 3.19 | 2.83 | 3.18 | 3.22 |
| $K_2O$ | 0.32 | 0.30 | 0.23 | 0.37 |
| $P_2O_5$ | 1.01 | 0.81 | 0.61 | 0.61 |
| LOI | 0.09 | 0.09 | 0.08 | 0.09 |
| | 99.89 | 99.69 | 100.04 | 99.52 |
| Or | 1.9 | 1.8 | 1.4 | 2.2 |
| Ab | 27.0 | 24.0 | 26.9 | 27.3 |
| An | 32.1 | 32.8 | 30.3 | 31.9 |
| Di | 12.3 | 12.7 | 15.6 | 12.4 |
| Hd | 8.1 | 9.1 | 9.6 | 8.1 |
| En | 4.1 | 3.6 | 2.7 | 2.9 |
| Fs | 3.1 | 2.9 | 1.9 | 2.2 |
| Fo | 2.6 | 3.2 | 3.4 | 3.7 |
| Fa | 2.1 | 2.9 | 2.6 | 3.1 |
| Mag | 2.8 | 3.2 | 2.9 | 2.9 |
| Ilm | 1.6 | 1.6 | 1.5 | 1.6 |
| Ap | 1.9 | 1.9 | 1.4 | 1.4 |
| Water | 0.09 | 0.01 | 0.03 | 0.09 |

Analyses recalculated assuming 20% of iron is ferric.

1 78209M/1
2 78209M/2
3 77040M
4 78535M

Table 4.6 REE analyses of gt - cpx intergrowths and matrices.

| | 78029I/1 | 78029I/2 | 77040I | 78535I | 78029 M/1 | 78029M/2 | 77040M | 78535M |
|---|---|---|---|---|---|---|---|---|
| La | 1.4 | 2.2 | 0.7 | 2.5 | 4.5 | 3.2 | 2.4 | 4.0 |
| Ce | 4.7 | 8.1 | 3.8 | 7.2 | 9.8 | 8.9 | 6.6 | 9.2 |
| Pr | 0.5 | 1.1 | 0.6 | 0.9 | 1.2 | 1.2 | 0.9 | 1.2 |
| Nd | 3.1 | 6.6 | 3.2 | 4.4 | 6.1 | 6.1 | 5.4 | 5.9 |
| Sm | 2.0 | 2.6 | 1.8 | 2.2 | 1.8 | 2.1 | 1.7 | 1.8 |
| Eu | 0.69 | 0.82 | 0.64 | 0.76 | 0.68 | 0.73 | 0.64 | 0.66 |
| Gd | 4.0 | 3.8 | 3.4 | 3.6 | 1.8 | 2.1 | 1.7 | 1.9 |
| Dy | 8.59 | 6.6 | 6.12 | 7.69 | 1.9 | 2.24 | 1.7o | 1.81 |
| Yb | 7.24 | 4.91 | 4.2 | 6.09 | 0.8 | 1.07 | 0.68 | 0.81 |
| Lu | 1.15 | 0.76 | 0.65 | 0.97 | 0.13 | 0.18 | 0.11 | 0.13 |

Fig. 4.12a Chondrite-normalised REE data for four intergrowths.

Fig. 4.12b Chondrite-normalised REE data for four matrix specimens.

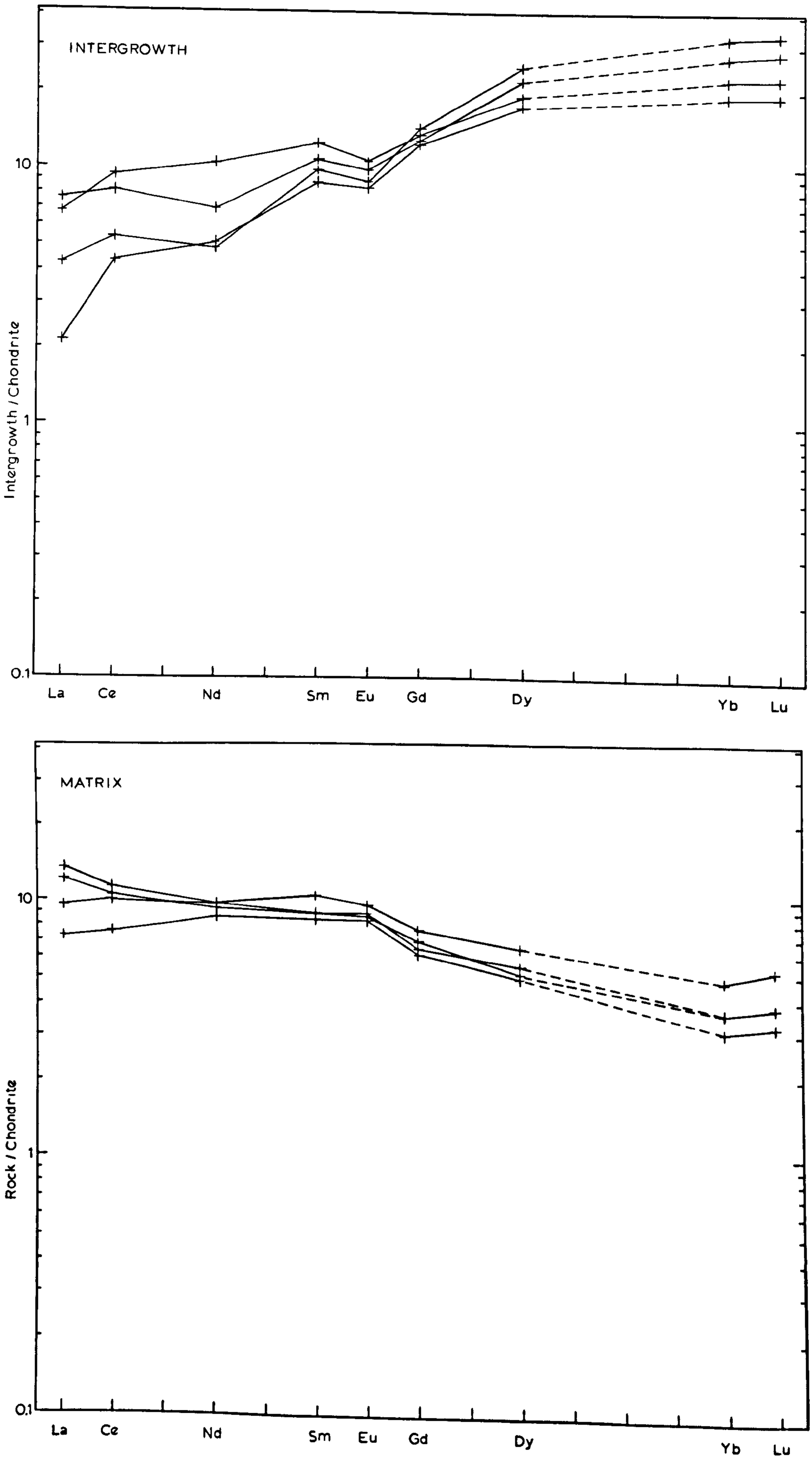
INTERGROWTH
10
1
0.1
Intergrowth / Chondrite
La
Ce
Nd
Sm
Eu
Gd
Dy
Yb
Lu
MATRIX
10
1
0.1
Rock / Chondrite
La
Ce
Nd
Sm
Eu
Gd
Dy
Yb
Lu

Fig. 4.13 Intergrowth/matrix REE partition coefficients for four intergrowth-matrix sample pairs.

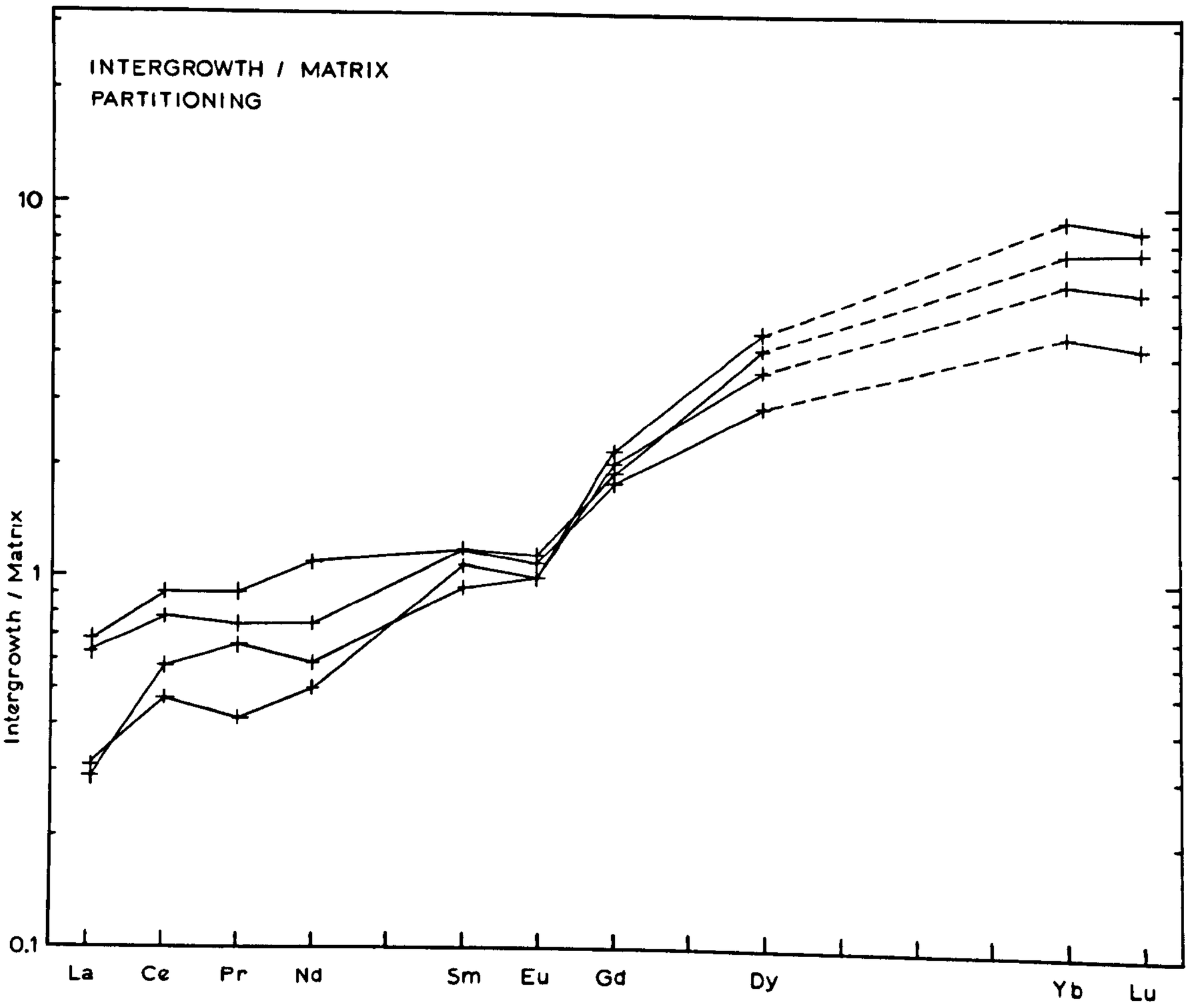
INTERGROWTH / MATRIX
PARTITIONING
10
1
0.1
Intergrowth / Matrix
La
Ce
Pr
Nd
Sm
Eu
Gd
Dy
Yb
Lu

Fig. 4.14 A comparision of intergrowth/matrix partitioning with natural garnet/rock data.

Fig. 4.15 A comparision of intergrowth/matrix partitioning with natural clinopyroxene/rock data.

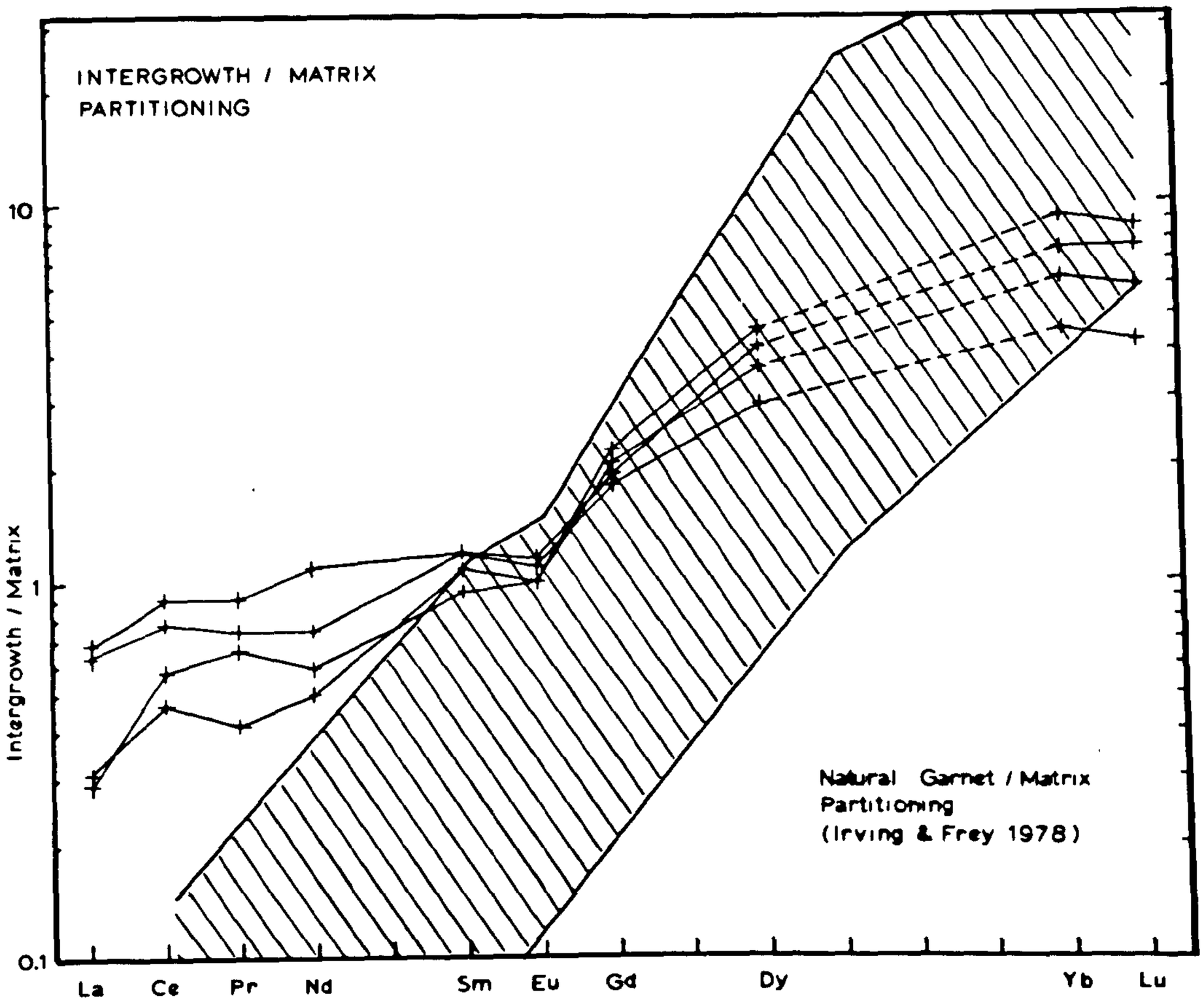
INTERGROWTH / MATRIX
PARTITIONING
10
1
0.1
Intergrowth / Matrix
Natural Garnet / Matrix
Partitioning
(Irving & Frey 1978)
La
Ce
Pr
Nd
Sm
Eu
Gd
Dy
Yb
Lu

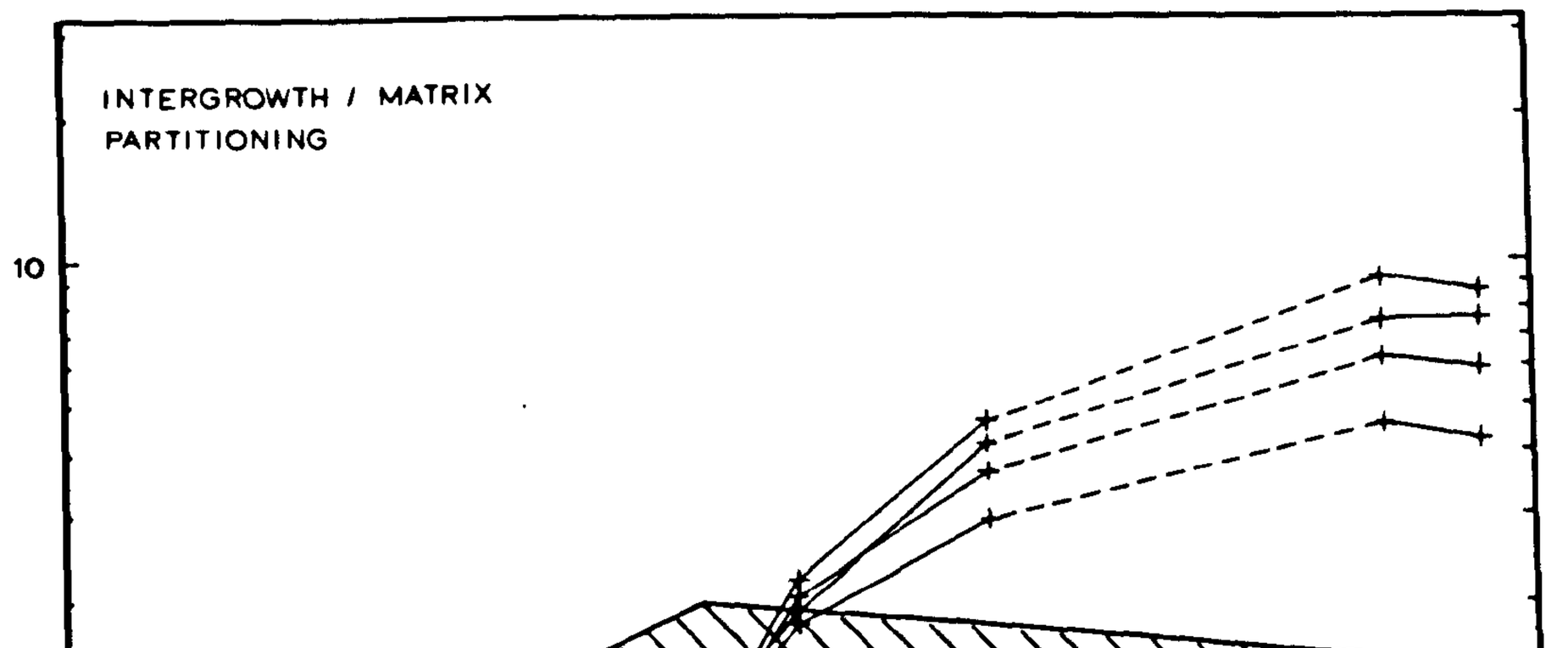
INTERGROWTH / MATRIX
PARTITIONING
10
1
0.1
Intergrowth / Matrix
Natural Clinopyroxene / Matrix
Partitioning (Cullers et al 1973)
La
Ce
Pr
Nd
Sm
Eu
Gd
Dy
Yb
Lu

4.15), it can be seen that the natural clinopyroxenes (which have much lower aluminium contents than the intergrowths) have kinked patterns with much smaller HREE enrichments. Comparison with natural amphibole data (compiled from Arth and Barker,1976; Nicholls and Harris,1980 ) as in fig 4.16. shows the best fit of the three. More specific comparison with individual natural and synthetic partition curves from Arth and Barker (1976) and Nicholls and Harris (1980) (fig. 4.17) shows a reasonably close fit. The only other model capable of fitting the major element data, a mixture of garnet and clinopyroxene, does not give a good fit; the patterns obtained are too steep (fig 4.17). It must be borne in mind, however, that comparisons are between somewhat dissimilar clinopyroxenes and garnets, especially in terms of Al content.

## 4.5 History of intergrowths

The chemical data have been shown to favour the intergrowths as initially representing amphibole crystals.The suggestion that they have been a discrete phase for a considerable period of time is supported by Sm/Nd work performed by Humphries and Cliff (1982). They showed that while the intergrowth and matrix give identical 2.42±0.03 Gyr ages, the intergrowth has a high initial $^{147}Nd/^{143}Nd$ ratio, which, with its Sm/Nd ratio, implies that it separated from the matrix about 2.6 ±0.12Gyr.

The actual age of formation of these amphiboles is

Fig. 4.16 A comparision of intergrowth/ matrix partitioning with natural amphibole/matrix data from Arth and Barker (1976) and Nicholls Harris (1980).

Fig. 4.17 Specific natural and synthetic amphibole and garnet/clinopyroxene mixture partitioning data compared to intergrowth/matrix patterns.

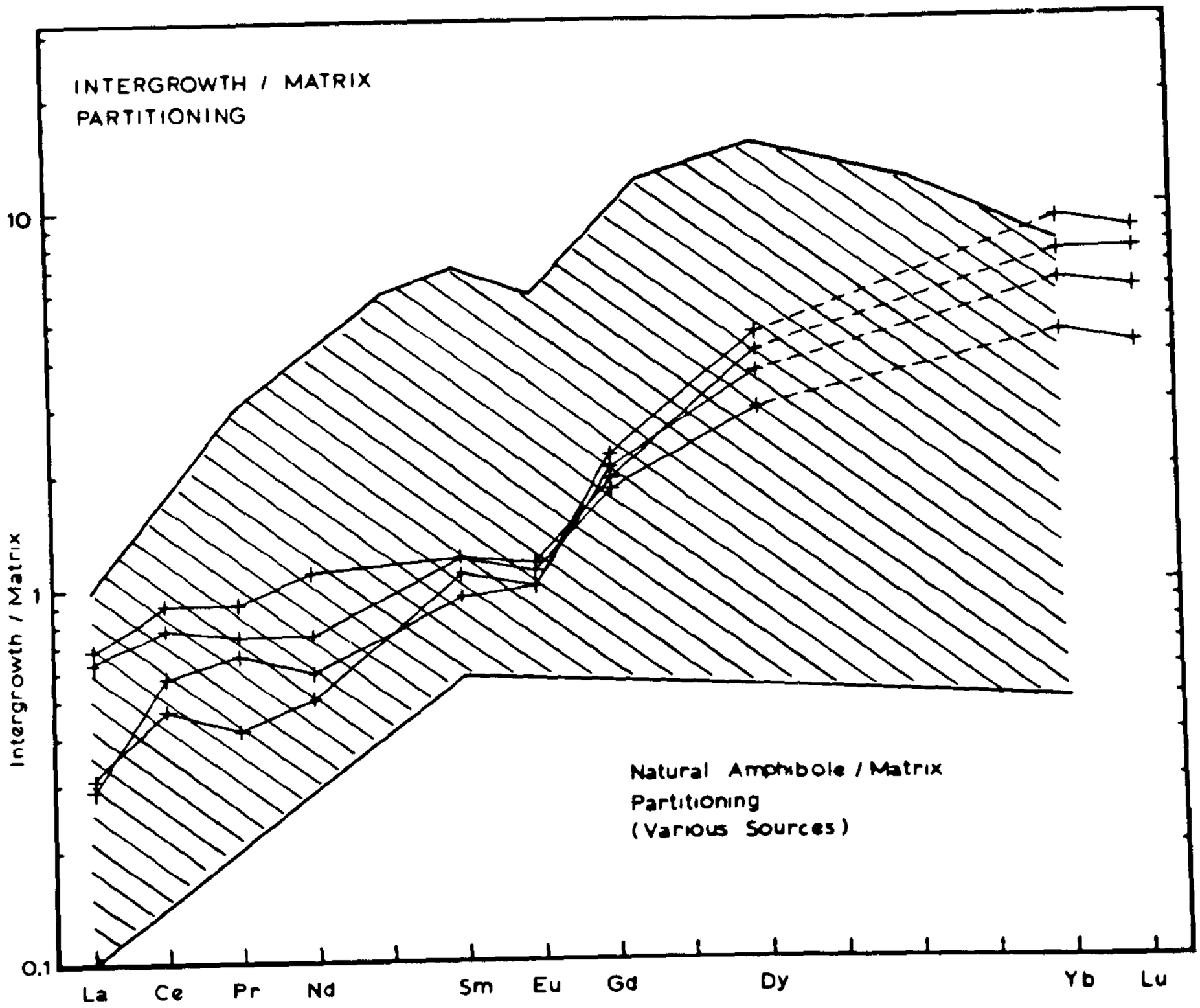
INTERGROWTH / MATRIX
PARTITIONING
10
1
0.1
Intergrowth / Matrix
Natural Amphibole / Matrix
Partitioning
(Various Sources)
La
Ce
Pr
Nd
Sm
Eu
Gd
Dy
Yb
Lu

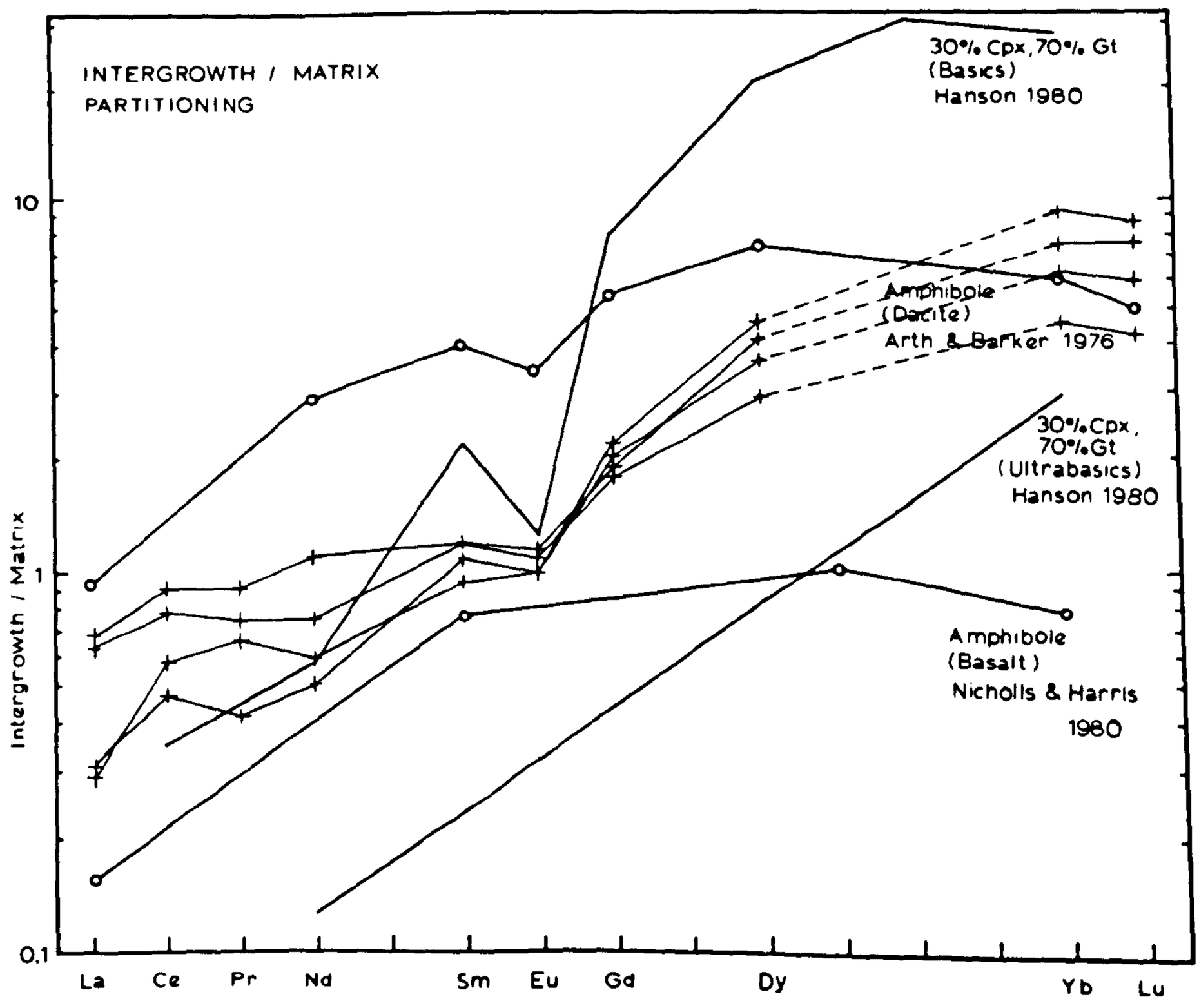
INTERGROWTH / MATRIX
PARTITIONING
30% Cpx, 70% Gt
(Basics)
Hanson 1980
Amphibole
(Dacite)
Arth & Barker 1976
30%Cpx,
70%Gt
(Ultrabasics)
Hanson 1980
Amphibole
(Basalt)
Nicholls & Harris
1980
10
1
0.1
Intergrowth / Matrix
La
Ce
Pr
Nd
Sm
Eu
Gd
Dy
Yb
Lu

unknown, although it is unlikely that they are igneous as amphibole crystals of this size would sink through a magma rapidly, and there is no field evidence of any gravitational accumulation of intergrowths.

The present mineralogy of the intergrowths could be attained under a variety of P- T conditions as amphiboles break down to gt+cpx±plg under a range of conditions; it is probable that the pressure would have been greater than 10kbar (fig 4.18) although garnet was generated in experimental charges at $P_{H_2O}=P_{Tot}=8$kbar (see table 4.7). This breakdown of amphibole would in consequence have released whatever anions were present, and these need not have been solely or mainly water. The presence of a vapour could have aided the growth of the large marginal clinopyroxene crystals now present,and could also have facilitated partial melting within the basic rocks (chapter 7).

The resulting garnet and clinopyroxene crystals were presumably homogenous, but subsequent reequilibration has lead to zoning and the formation of plagioclase rims to the clinopyroxene. Garnet-clinopyroxene equilibration temperature calculated using any of the three current formulations (see section 2.4.3) are about 1000°C ± 15°C for core-core compositions, and about 810°C ± 20°C for rim-rim analyses. The garnet rimming ore minerals equilibrated with local clinopyroxene at less than 800°C. The clinopyroxene-plagioclase zoning relationship suggests a higher pressure, lower temperature, or a

Fig. 4.18 Amphibole - out and garnet - in curves for basic and intermediate rocks with variable $X_{H_2O}$. Data from Allen and Boettcher (1978) and Lambert and Wyllie (1972).

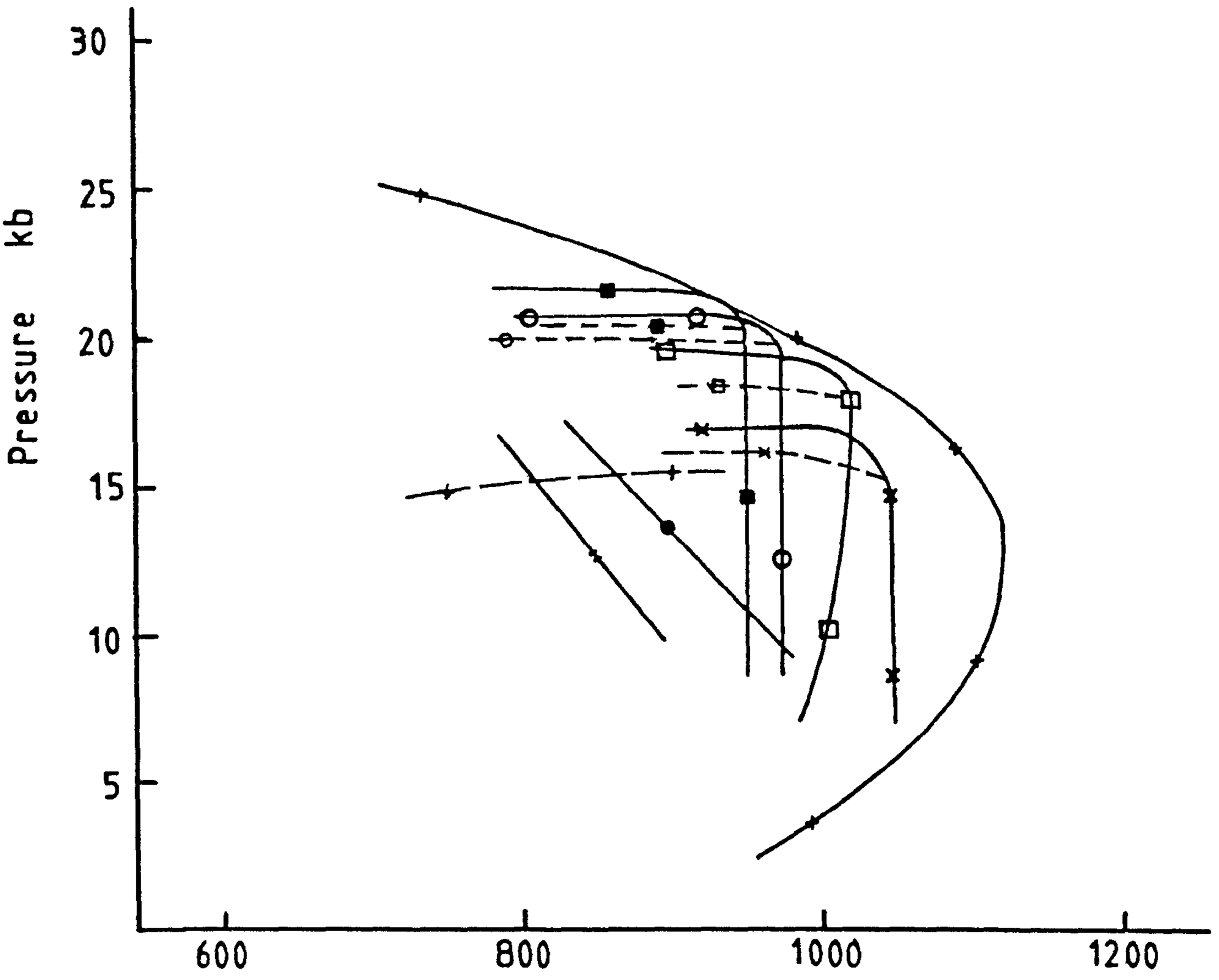


Amp out  Gnt in

—+—  —+— Lambert & Wyllie, gabbro

—□—  —□— Allen & Boettcher, basalt. $X^{V}_{H_2O}$ =0.75

—×—  —×— " " =0.5

—■—  — —■— " andesite. $X^{V}_{H_2O}$ =1.0

—○—  — —○— " " 0.75

—●— " " 0.5

—|— " " 0.25

combination of the two for rim material.

## 4.6 Experiments

A set of reconnaissance experiments attempting to verify the suggestion that the intergrowths were originally amphibole have been performed. Experiments were conducted in internally heated vessels of the type described by Ford (1972).

About 100mg of sample was packed into silver-palladium capsules together with 5 or 10mg of water or 10mg of silver oxalate (to provide an $H_2O$-$CO_2$ mixed vapour phase). Run details are given in table 4.7. Charges W,6 &F generated large quantities of amphibole, together with magnetite in significant quantities. Probe analyses (table 4.8) show that the amphibole contains up to 15.7% $Al_2O_3$ and has Fe/(Fe+Mg) of up to 0.5. Oxygen fugacities in the experiments were somewhat above the QFM oxygen buffer, and had they been controlled at lower values, amphiboles poorer in $Fe^{3+}$ and richer in $Fe^{2+}$ (and presumably $Al^{3+}$ too) would have been formed.

In so far as they go, the experiments support the conclusions presented in section 4.5

The experimental amphiboles (table 4.5) compare well in composition with the intergrowths (table 4.4) except for a few elements. Experimental amphiboles are higher in $TiO_2$, MgO, $Na_2O$ and $K_2O$ and lower in $Al_2O_3$ and $FeO^{Tot}$ than the intergrowths. These differences are probably largely due to the relatively high activity of oxygen in the experimental charges, as evinced by the magnetite found in the optical mounts of the charges.

Table 4.7 Details of experiments.

| | | | |
|---|---|---|---|
| Run 3/557 | 1000°C | 10 kbar | |
| Capsule | A | 10% $H_2O$ | No loss |
| | F | 5% $H_2O$ | Lost 20% $H_2O$ (during quenching ?) |
| | Z | 10% Oxalic acid | Lost all volatiles |
| Run 3/560 | 900°C | 8 kbar | |
| Capsule | 6 | 5% $H_2O$ | Lost 20% $H_2O$ (during quenching ?) |
| | N | 2% $H_2O$ | Lost 50% $H_2O$ (during quenching ?) |
| | 2 | 10% Oxalic acid | Lost 12% (during quenching ?) |
| Run 3/651 | 1000°C | 8 kbar | |
| Capsule | W | 5% $H_2O$ | No loss |
| | O | 3% $H_2O$ | No loss |
| | Y | 10% Oxalic acid | Lost 20% vapour (during quenching ?) |
| Run 3/562 | 800°C | 8 kbar | |
| Capsule | H | 4% $H_2O$ | No loss |
| | E | 2% $H_2O$ | Lost 50 % vapour |
| | S | 17% Oxalic acid | No loss |

Run products ( Optical and XRD determination ).

A Gnt, cpx, mag, amp, glass
Z Gnt, cpx, mag, amp, glass
F Gnt, cpx, mag, amp, glass
6 Gnt, amp, mag, glass
W Amp, mag
Y Amp, mag
H Amp, mag
E Amp, mag
S Amp, mag

Sample consisted of a separated intergrowth TEMA mill and hand-ground to >5 $\mu$m.

Table 4.8 Analyses of experimental amphiboles.

| | AMF/3 | AMF/8 | AM6/20 | AM6/22 | AMN/9 | AMW/57 | AM /72 |
|---|---|---|---|---|---|---|---|
| $SiO_2$ | 41.41 | 40.85 | 41.16 | 43.21 | 45.65 | 42.04 | 43.96 |
| $TiO_2$ | 1.12 | 1.03 | 1.16 | 0.81 | 1.08 | 0.66 | 0.55 |
| $Al_2O_3$ | 14.62 | 15.03 | 14.23 | 12.33 | 11.79 | 15.70 | 14.49 |
| FeO | 13.02 | 12.83 | 13.0 | 12.74 | 14.52 | 14.61 | 16.29 |
| MnO | 0.30 | 0.27 | 0.59 | 0.66 | 0.37 | 0.65 | 0.51 |
| MgO | 12.74 | 13.28 | 11.78 | 13.97 | 10.46 | 11.37 | 8.90 |
| CaO | 11.53 | 11.08 | 10.55 | 10.64 | 12.65 | 10.13 | 12.86 |
| $Na_2O$ | 1.87 | 2.05 | 0.99 | 0.93 | 0.97 | 1.03 | 0.30 |
| $K_2O$ | 0.07 | 0.10 | 0.04 | 0.04 | 0.07 | 0.02 | n.d. |
| | 96.71 | 96.50 | 95.82 | 95.33 | 97.61 | 96.21 | 97.86 |

Analyses by AWDS.

# Chapter 5 Garnet Granulites.

## 5.1 Introduction

The pressure of metamorphism is notoriously difficult to estimate - in many cases useful geobarometers are scarce, and many of those available are very sensitive to variations in composition. As mentioned earlier (Chapter 1), the presence in the Scourie complex of magnesian garnets breaking down under post-peak-metamorphic conditions allows a minimum estimate of the peak-metamorphic pressure to be made. This will not necessarily correspond to the highest pressure to which the rocks have been subjected if they have undergone the type of recovery path suggested by England and Richardson (1977) involving heating during the early stages of depressurisation.

The garnets in the basic rocks at Scourie are breaking down by the reaction

$$Gt + Cpx = Opx + Sp + An \qquad 5.1$$

which can be modelled in CMAS by the simplified reaction

$$CaMg_5Al_4Si_6O_{24} = 2Mg_2Si_2O_6 + MgAl_2O_4 + CaAl_2Si_2O_8 \qquad 5.2$$

Pyr-gross En Sp An

This particular reaction has been experimentally investigated by Kushiro and Yoder (1966) and Herzberg (1975). It has been discussed in the context of the Scourie rocks by O'Hara and Yarwood (1978) and Savage and Sills (1980). O'Hara and Yarwood (op.cit.) suggested that

the reaction probably occured at about 12kbar at 1150 C on the basis of reconnaissance experiments on hand-picked mineral separates. Savage and Sills (op cit.) estimated the pressure of the reaction at 10-15kbar on the basis of equations of Wood (1974), using the Al content of orthopyroxene in equilibrium with garnet as a barometer.

It is possible to use the experimental data of Herzberg and Kushiro and Yoder and thermochemical data of Newton and coworkers to provide an additional estimate of the pressure of the reaction. Firstly, a description of the Scourie rocks is given to put the calculations into perspective.

## 5.2 Field Occurence

The reaction assemblage under consideration occurs in the transition rocks at the contact of basic and ultrabasic rocks; these rocks have the highest Mg/Mg+Fe values of any olivine-free Scourie rock. All specimens studied are from Geodh Eanruig (fig 1.2).

The garnets in these rocks are surrounded by plagioclase bearing rims of varying widths. A crude correlation of this feature with garnet Fe/Fe+Mg is apparent, with Fe rich garnets having better developed rims. Some of the rims have a vermicular texture, whereas others are partially or completely recrystallised to more stable, equigranular crystal morphologies (fig 5.1).

## 5.3 Petrography

The mineralogy of these basic gneisses can be discussed on the basis of a three-stage model for its

Fig. 5.1(a) Recrystallised symplectite from garnet-granulite. Garnet has regrown in an equigranular matrix of (now altered) plagioclase, orthopyroxene and spinel ( 77063 ). From Geodh Eanruig. (crossed polars).

Fig. 5.1(b) Vermicular symplectite of orthopyroxene, plagioclase and spinel. Garnet (left) has started to regrow, partially engulfing the symplectite. Clinopyroxene matrix visible to the right and bottom. (78016B). From Geodh Eanruig. (plane polarised light).

Scale bars are 0.5mm.

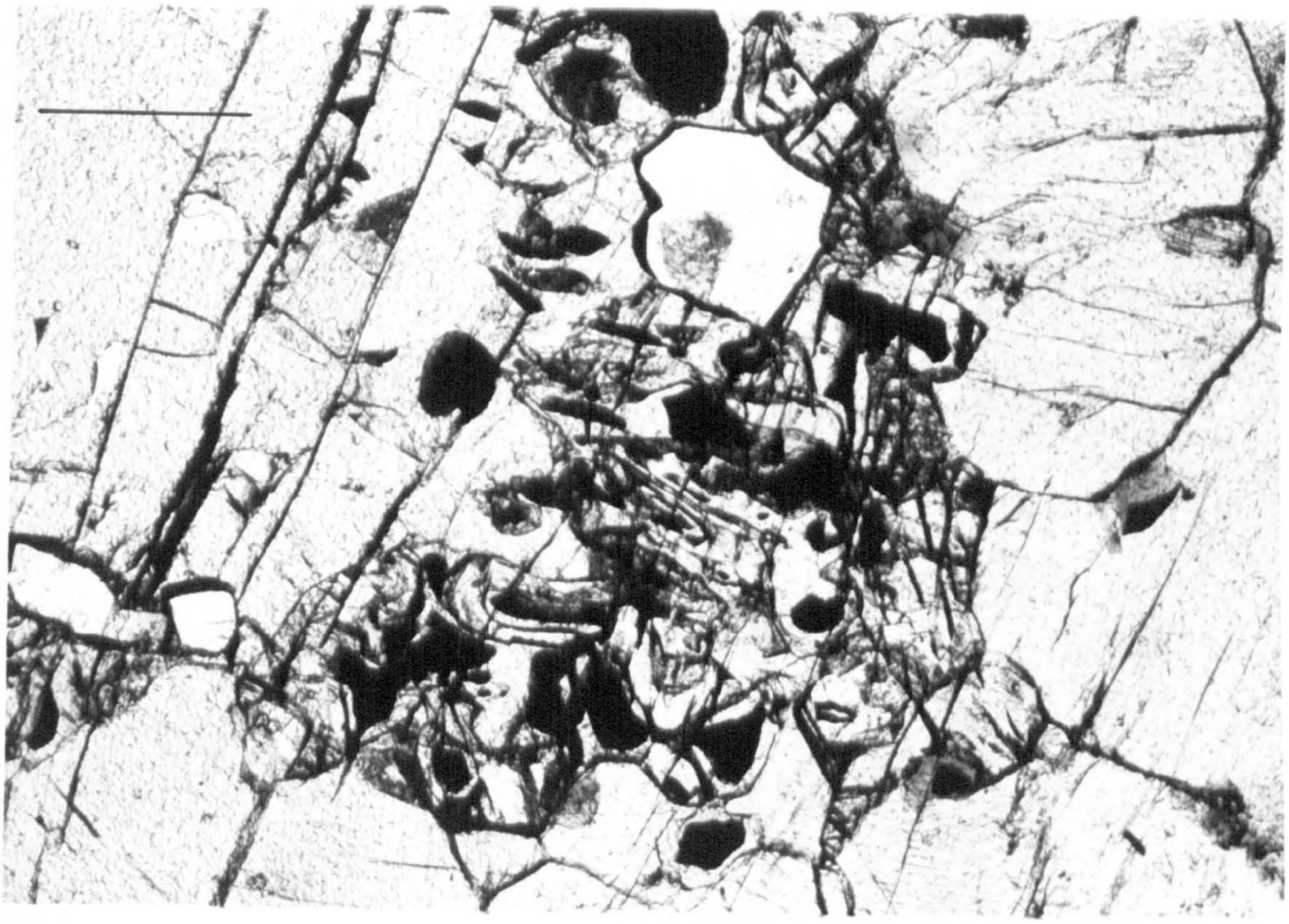

development (O'Hara and Yarwood,1978; Savage and Sills; 1980).

5.3.1 Stage 1

The earliest stage of mineral development preserved consists of a coarse mosaic (ca. 1cm) of garnet and clinopyroxene crystals together with occasional orthopyroxene. The clinopyroxenes record a long sequence of exsolution events difficult to relate temporally to the breakdown of the garnets. Lamellae of orthopyroxene, ilmenite and plagioclase are present (fig 5.2). The first is present in considerable quantities, the last is present only in a few places. In addition to these, there are preserved much finer lamellae of amphibole and pigeonite asdescribed in section 4.2.1.1. The preservation of these lamellae depends on the subsequent history of the rock, with altered specimens containing no small-scale exsolution products.

The composition of the cores of large garnet and clinopyroxene is given in table 5.1.

5.3.2 Stage 2

At some stage during the recovery of the rocks, the garnet became unstable and reaction 5.1 occured, so the garnet became rimmed with vermicular intergrowth of orthpyroxene, spinel and plagioclase (fig 5.1) The extent to which this occurred depended on the bulk composition (especially Fe/Fe+Mg; see Savage and Sills,1980) of the system. Magnesium-rich garnets are completely replaced by breakdown products, whereas more Fe-rich garnets,

Fig. 5.2 Large crystal of clinopyroxene with exsolved bodies of orthopyroxene (grey), plagioclase and ilmenite (45,575). From Geodh Eanruig.
(plane polarised light).

Fig. 5.3 Stage 1 garnet (top centre) with stage 2 breakdown minerals (centre) and stage 3 regrown garnet with a euhedral crystal form (below and left of centre).

Stage 1 garnet (top) with stage 2 breakdown minerals plagioclase, spinel and orthopyroxene and stage 3 regrown garnet with a euhedral outline (below and left of centre) ( 78016B ). From Geodh Eanruig.
(plane polarised light).

Scale bars are 0.5mm.

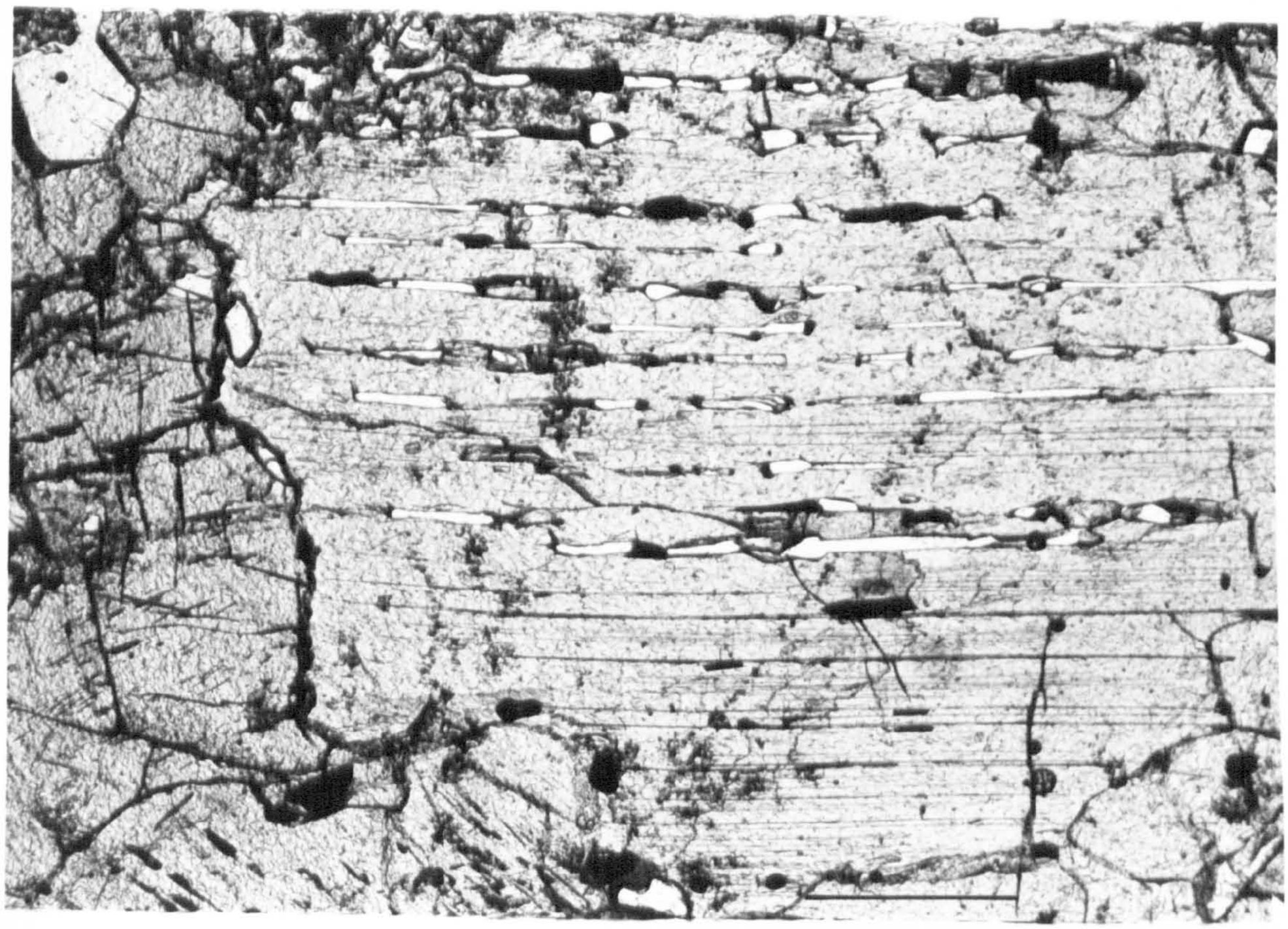

Table 5.1 Stage 1 minerals, garnet granulites ( 78016B ).

| | CPX6 | CPX4 | GNT7 | GNT1 |
|---|---|---|---|---|
| $SiO_2$ | 48.71 | 48.20 | 39.54 | 39.86 |
| $TiO_2$ | 0.79 | 0.83 | 0.13 | 0.12 |
| $Al_2O_3$ | 6.82 | 6.82 | 21.82 | 22.10 |
| $Cr_2O_3$ | 0.06 | 0.04 | 0.05 | 0.06 |
| FeO | 7.59 | 7.82 | 21.49 | 21.57 |
| MnO | 0.19 | 0.20 | 0.97 | 0.88 |
| MgO | 11.90 | 11.93 | 10.56 | 10.29 |
| CaO | 21.50 | 22.07 | 6.08 | 6.17 |
| $Na_2O$ | 1.28 | 1.02 | 0.02 | 0.02 |
| | 98.84 | 98.93 | 100.66 | 100.07 |

Analyses by MWDS

collected further from the basic/ultrabasic contact contain garnets surrounded by much smaller rims.

The real reaction occurring must have involved clinopyroxene as the plagioclase is significantly sodium-bearing, and clinopyroxene is the only phase containing measurable quantities of sodium. Corroboration of this is provided by the recrystallisation of clinopyroxene next to the coronas, and by the compositional gradient in these crystals.

5.3.3 Stage 3

O'Hara and Yarwood (1978) suggested that, subsequent to stage two, garnet regrew, resulting from a recrossing of the reaction in P-T space. They cited the presence of garnet along all phase boundaries within the coronas as evidence. The presence of this apparently later garnet was neither figured nor mentioned by Savage and Sills (1980).

The material of O'Hara and Yarwood (op.cit.) and additional material, also from Geodh Eanruig, has been examined in an attempt to decide whether the garnet is a new growth, or whether it is from an arrested stage of the breakdown of the original garnet. Specimen 10038 of O'Hara and Yarwood contains large amounts of garnet along the grain boundaries between spinel, orthopyroxene and plagioclase, and this garnet has good crystal faces developed in places, indicating that it has grown at the expense of the other minerals. Material richer in iron (eg 78016,78047) contains many garnets which have

inclusions of spinel and orthopyroxene near their rims, implying that the garnet has grown, engulfing the pre-existing symplectite (fig 5.3). Once again, the form of the garnets suggests that it has grown at the expense of the symplectite. Analytical data shows that the garnet in the rims of the large crystals contains up to 5mol% more iron end member than the core garnet, and that the corona phases are also zoned (table 5.2).

The evidence presented here supports the contention of O'Hara and Yarwood (op cit.) that garnet has regrown at a late stage in the evolution of these rocks. That this garnet is richer in iron than the early garnet suggests that lower pressures were prevalent. Likely conditions of the garnet regrowth are discussed further in section 5.4.2.

## 5.4 Estimation of P-T conditions of garnet breakdown

Experiments have been performed on the CMAS reaction by Kushiro and Yoder (1966) and Herzberg (1975). Reconnaissance experiments on the reaction in these rocks were conducted by O'Hara and Yarwood (1978),. These suggested that the reaction proceeds at about 12kbar and 1125 C. To enable consideration of the significance of the reaction in detail, it is necessary to know the effects of varying temperature and bulk composition on the location of the reaction in P,T space. To this end, thermodynamic data for the reaction are needed.

### 5.4.1 Extraction of thermodynamic data for the reaction

It is posible to estimate $\Delta H_{(1,970)}$ for the reaction

Table 5.2 Stage 3 minerals from garnet granulites ( Geodh Eanruig ).

| | GNT4 | GNT5 | GNT9 | OPX2 core | OPX3 rim | CPX1 | SPN1 | PLG1 | PLG3 |
|---|---|---|---|---|---|---|---|---|---|
| $SiO_2$ | 39.20 | 39.51 | 39.97 | 52.06 | 53.46 | 51.23 | n.d. | 51.63 | 50.36 |
| $TiO_2$ | 0.02 | 0.06 | 0.08 | 0.12 | 0.07 | 0.70 | 0.02 | n.d. | n.d. |
| $Al_2O_3$ | 21.39 | 22.11 | 21.75 | 3.22 | 2.65 | 4.34 | 58.41 | 30.77 | 29.85 |
| $Cr_2O_3$ | n.d. | n.d. | n.d. | tr | 0.03 | 0.02 | 0.42 | n.d. | n.d. |
| $Fe_2O_3$* | - | - | - | - | - | - | 4.85 | - | - |
| FeO tot | 23.93 | 24.37 | 23.57 | 18.27 | 17.53 | 5.89 | 21.63 | n.d. | 0.54 |
| MnO | 0.74 | 0.80 | 0.79 | 0.19 | 0.76 | 0.68 | 0.06 | n.d. | n.d. |
| MgO | 9.10 | 8.69 | 9.04 | 25.31 | 26.34 | 13.88 | 12.28 | n.d. | 0.02 |
| CaO | 5.88 | 6.00 | 6.33 | 0.39 | 0.27 | 22.79 | 0.01 | 13.38 | 13.40 |
| $Na_2O$ | 0.05 | tr | 0.02 | 0.06 | 0.05 | 0.92 | n.d. | 4.09 | 3.95 |
| $K_2O$ | n.d. | n.d. | n.d. | n.d. | n.d. | n.d. | n.d. | 0.11 | 0.03 |
| | 100.31 | 101.54 | 101.55 | 99.62 | 101.16 | 99.77 | 97.68 | 99.98 | 97.85 |

* calculated assuming stoichiometry.

Analyses by MWDS.

from the thermochemical data of Charlu et al., 1978; Newton et al., 1978; Newton et al., 1979 and Newton et al, 1980. The following equation can then be used to retrieve data from the experimental points (using a 1bar, 970K standard state):

$$\Delta G_{(P,T)} = (\Delta H_{(1,970)} + (P-1)\Delta V + \int_{970}^{T} CpdT ) - T(\Delta S_{(970)} + \int_{970}^{T} Cp/TdT ) + RT\ln K$$

if compressibilities and thermal expansion are neglected. This equation may be rearranged to give

$$\Delta H_{(1,970)} - T\Delta S_{(970)} = - (P-1)\Delta V - RT\ln K - \int_{970}^{T} CpdT + T\int_{970}^{T} Cp/TdT \quad 5.3$$

The volume change of the reaction may be estimated from the molar volume data for spinel, plagioclase and orthopyroxene tabulated in Robie et al (1978); the term for garnet was calculated using partial molar volumes of pyrope and grossular, (weighted by the reaction coefficients) from the polynomial expressions given by Newton and Haselton (1981). This was done to allow the use of 1bar activities for garnet in the retrieval equation. The heat capacity integrals were evaluated using the four-term polynomials of Holland (1981) for garnet, enstatite and anorthite, and the four-term polymomial of spinel from Robie et.al. (1978). AB Thompson (quoted in Jenkins and Newton,1979) has shown that the heat capacities of mix-garnets can be satisfactorially modelled as linear combinations of the heat capacities of end-members in the temperature range of interest.

K was calculated using enstatite compositions from

Hansen (1981) for the Opx + An reaction for want of more suitable data. $A_{en}^{opx}$ was calculated using the regular solution parameter for Ca-Mg interactions on M2 assumed by Lindsley et al (1981). $A_{M5C}^{gnt}$ was set to one so that A in systems other than CMAS needs to be calculated as $A_{M5C}^{gnt}(rock)/A_{M5C}^{gnt}(CMAS)$. The composition of garnet remains constant within experimental limits in CMAS experiments; it is here assumed to be Xgr=0.167 Xpy=0.833.

Fig. 5.4 shows the experimental data of Herzberg and Kushiro and Yoder, and the line fitted to the data by eye. After values for the right hand side of equation 5.3 had been calculated, a linear regression of the data was calculated. This was constrained by a value of $H_{(1,970)}$ calculated from the calorimetric data of Charlu et al., 1975; Newton et al., 1977; Newton et al., 1979 and Newton et al., 1980. As this calculation yields a result subject to considerable error, the point calculated from the experiments were given double weighting in the linear regression. The calculated value for $\Delta H_{(1,970)}$ is 34300$\pm$800J, $\Delta S_{(970)}$ is -20.0$\pm$0.6JK.

5.4.2 Application to rocks

Calculation of equilibration pressures for the Scourie rocks follows the reverse of the procedure above. Values of $A_{M5C,rock}^{gnt}$ were calculated using the mixing parameters in table 2.7 and normalised with the values of $A_{M5C,CMAS}^{gnt}$. $A_{an}^{plg}$ was calculated with the model of Newton et al.(1980), $A_{en}^{opx}$ as above. Values of $\int CpdT$ and $\int Cp/TdT$ were used to yield $\Delta H_{(1,970)}$ and $\Delta S_{(970)}$. Calculated

Fig. 5.4 Experimental data of Kushiro and Yoder (1968) and Herzberg (1978) for the reaction

$$gnt = opx + spn + plg$$

in the system $CaO - MgO - Al_2O_3 - SiO_2$. The line is the fit to the data used to extract thermodynamic data.

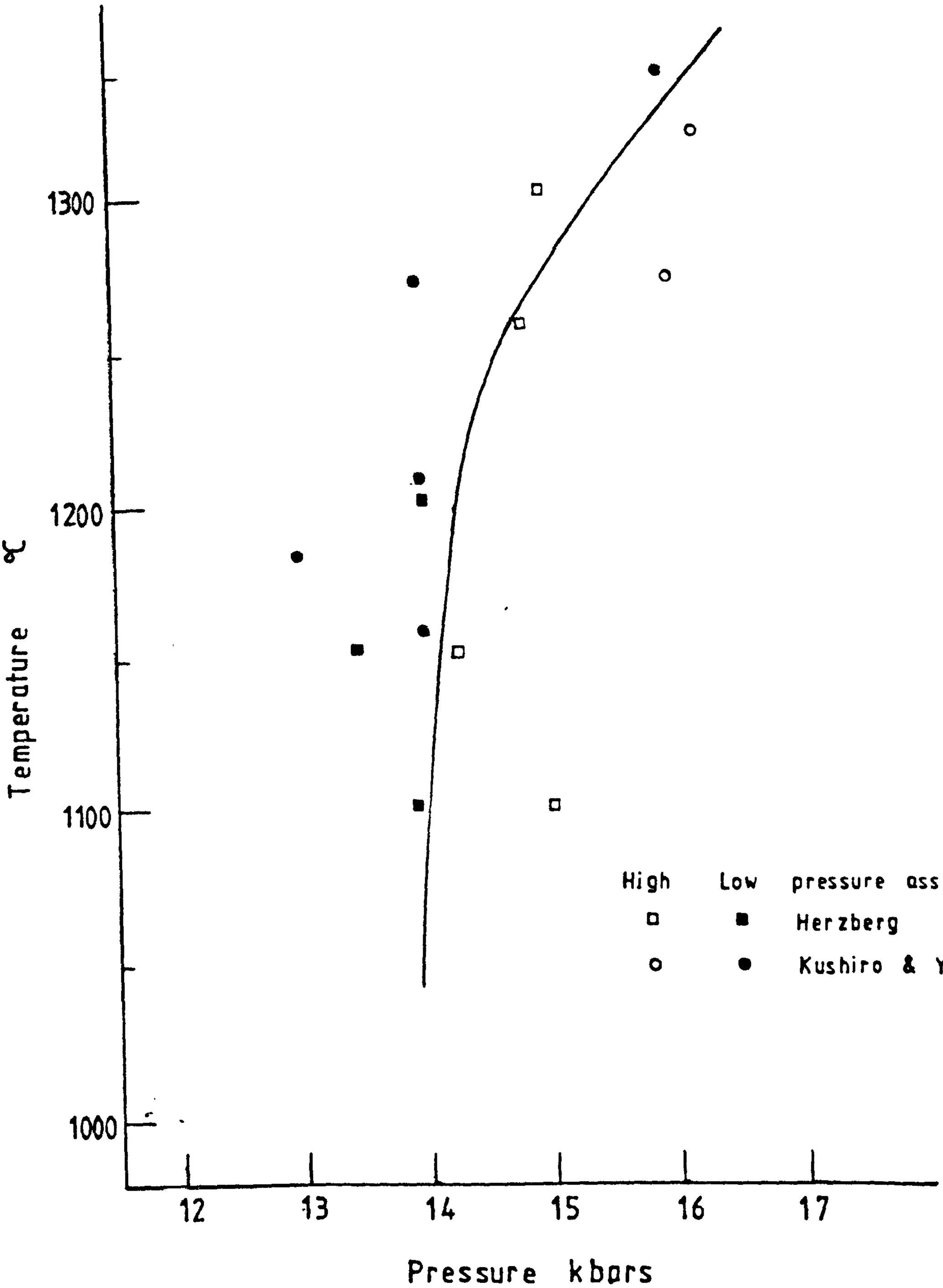
1300
1200
1100
1000
Temperature °C
12
13
14
15
16
17
Pressure kbars
High pressure assemblage
Low pressure assemblage
Herzberg
Kushiro & Yoder

pressures for 78047 are 14.9±0.9 kbar (1000°C) and 13.7±0.8 kbar (800°C) for core compositions and 12.3±0.9 kbar (1000°C) and 11.7±0.9 kbar (800°C) for rim compositions. A possible P-T-t path is suggested on fig 5.5. A warning must be sounded here: the experimental data used as calibration here was all collected in solid-media cells made of material other than NaCl, which is effectively frictionless. Comparison of the data of Jackson (1981) and Hansen (1981) for the reaction Opx + An = Py + Di + Qz at 1200°C show that the former, using Talc/ pyrex cells, reversed the reaction about 2kbar higher than the latter, who used NaCl assemblies. The size of the friction correction necessary will decrese with decreasing pressure (see Herzberg and O'Hara, 1972) so an overestimate of about 1kbar is likely in the pressures used above. It is likely that the calculated pressures are overestimated by the same margin.

Previous workers P-T estimates were discussed in section 1.2.5. In general the estimates have clustered at about 900 C and 11kbar. Estimates of granulite facies conditions from other granulite facies terrains also cluster at similar temperatures. In this thesis, P-T estimates on the basis of 'point' microprobe analyses of small (<1mm) grains found in many common rocks give conditions similar to those presented by other workers (e.g. Rollinson, 1981). However, the material investigated in Chapters 3, 4 and 5 is coarser grained (>5mm) and grain cores retain evidence of higher grade conditions.

The maximum estimated temperatures and pressures have been obtained from the cores of grains analysed using the microprobe with the beam defocussed to ca. 30 m, to give an average including all exsolution lamellae. Peak temperatures estimated from coarse grain cores range up to just over 1000 C, whereas rim temperatures are about 800-820 C. Pressures were in excess of 14kbar. It should be stressed that these are the highest recorded conditions and reequilibration may have eradicated evidence of earlier, higher temperatures.

Fig. 5.5 Calculated equilibration pressures for 78047. Also indcated is a possible P - T - t path, the form of which may be related to the tectonic history of the rocks (see Chapter 9).

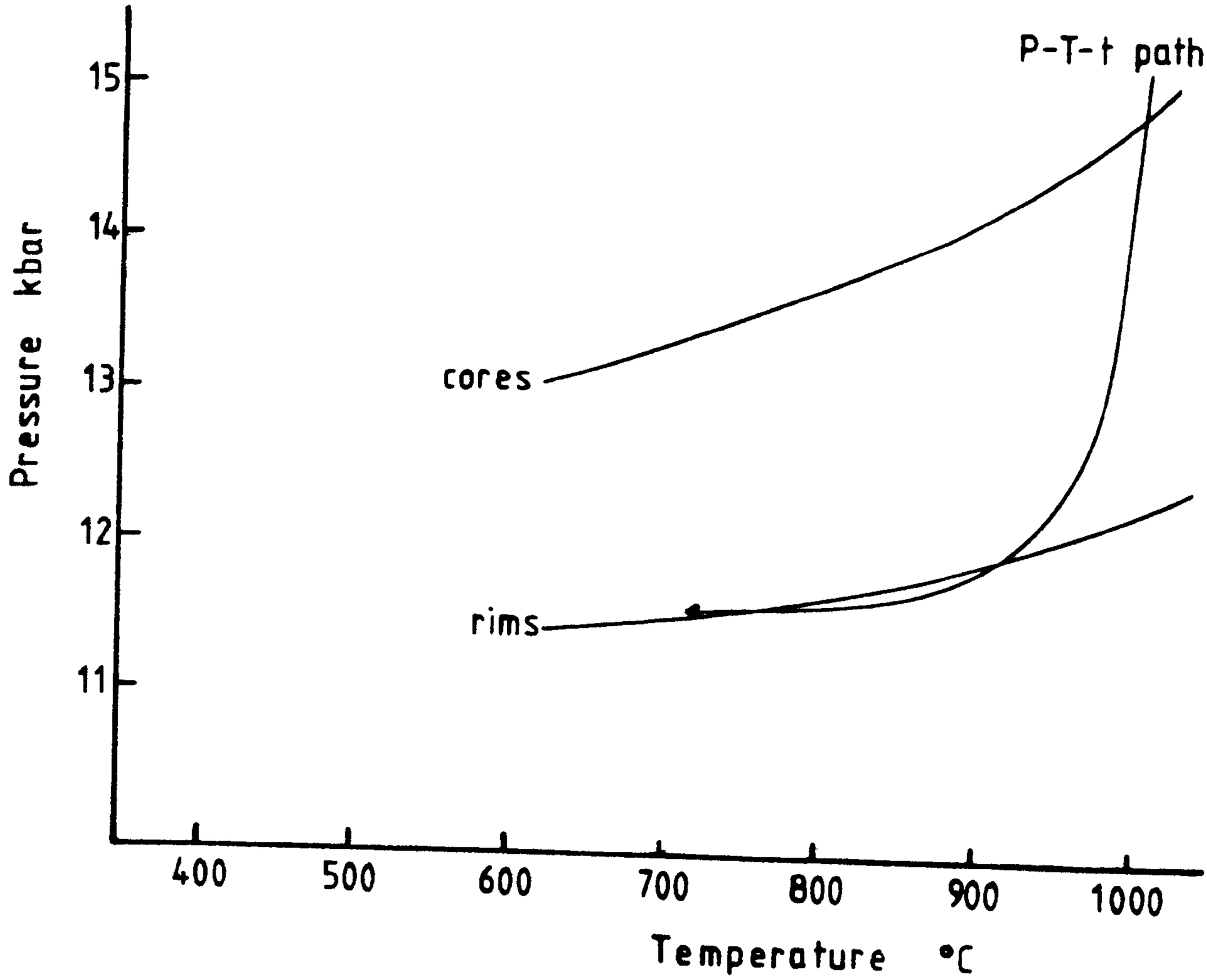
P-T-t path
cores
rims
Pressure kbar
15
14
13
12
11
400
500
600
700
800
900
1000
Temperature °C

# Chapter 6 Scourie dykes.

## 6.1 Introduction

The Scourie dyke swarm is part of a much larger group of dykes, stretching from Labrador, through Greenland to NW Scotland. The dykes in the Scourie area have been examined in detail by O'Hara (1961a, 1962) who described both the litholgical range of dykes present and the post-emplacement changes seen within the most common dykes, the dolerites. Tarney (1963, 1973) has described the dykes of the Assynt area in detail, and Weaver and Tarney (1981a,b) have investigated the geochemistry of dyke swarm as a whole.

The most common dykes in the area around Scourie are quartz-dolerites. These vary widely in size, ranging from the narrow veins at Geodh Eanruig (ca. 15cm) to the much larger dykes, such as the Scourie dyke (first described by Teall in 1885) , which are about 30m across. These dykes are very variable, both mineralogically and texturally. They range from almost unaltered igneous rocks, with plagioclase and subcalcic pyroxenes (both of which are zoned) and ilmenite, through amphibolites of various types to hornblende schists within shear zones (Teall, 1885; O'Hara, 1961a) . In addition, dykes of ultrabasic and noritic composition occur, together with rare 'primary' amphibolites.

In the context of this thesis, the most important

aspect of these dykes is the variation in post-solidification mineralogy which is found (O'Hara, 1961a; Tarney, 1973). In the marginal zones of the dolerites, especially at Scourie, amphibolite facies mineral assemblages have developed during the cooling of the dykes, giving rise to garnet-amphibolite parageneses. These have been interpreted as indicating that the dykes were intruded into crust under amphibolite facies conditions, and that the fine-grained or glassy chills of the dykes recrystallised to mineral assemblages stable under ambient conditions (O'Hara, 1961b). The temperature was estimated by O'Hara (1977) as 450°C on the basis of the compositions of clinopyroxene- garnet, two feldspar and ilmenite-magnetite assemblages in the groundmass (O'Hara, oral comm., 1982). The pressure estimate of 6kbar is largely speculative, and in an attempt to confirm this and to commence a study of mineral compositions in these rocks, probe analyses have been obtained from a number of specimens.

## 6.2 Petrography and mineralogy

The various forms of dolerite found around Scourie are described here, under the names used by O'Hara, 1961a.

### 6.2.1 One pyroxene dolerite

The freshest material sampled is from the small dyke on the northern side of Scourie Bay, which possibly cuts the Scourie dyke itself. This material was investigated optically and chemically by O'Hara (1961a). It consists

dominantly of twinned and zoned clinopyroxene and zoned plagioclase, both of which are clouded by inclusions. O'Hara (op.cit.) reports the results of X-ray examination of similar clinopyroxenes revealing them to be composed of intergrown augite and pigeonite. Also present are skeletal plates of ilmenite (intergrown with subordinate magnetite), long prisms of apatite, occasional quartz and rare chalcopyrite. A small amount of amphibole present is a late phase, replacing clinopyroxene. The rock has an igneous texture with sub- to euhedral tablets of plagioclase and intersertal clinopyroxene (fig 6.1).

6.2.1.1 Mineral chemistry

A preliminary study of mineral chemistry and zoning has been performed, revealing a more complex picture than hitherto suspected (O'Hara, 1961a). The pyroxenes contain concentric zones of inclusions, making interpretation of the probe data difficult. It is nonetheless clear that a marked range of Fe/Fe+Mg values is present in these pyroxenes as well as variations in the wollastonite content (fig. 6.3; table 6.1). It appears probable that pigeonite is also present as crystals or zones of sufficient size to be analysed, as well as a sub-microscopic exsolution product (O'Hara, 1961a).

The variation in pyroxene composition shown in fig. 6.2 has undoubtedly been controlled by igneous processes, although both metamorphic reequilibration, amphibole formation and the exsolution-oxidation production of pyroxene and ores has occured, obscuring the details of

Fig. 6.1 One pyroxene dolerite from east of Poll Eorna showing zoned clinopyroxenes with slightly amphibolised margins and euhedral tablets of plagioclase. ( 79008 )
(plane polarised light).

Fig. 6.2 Amphibolite from the Scourie dyke at Poll Eorna. Plagioclase and amphibole with relic pyroxene cores forms the bulk of the rock. (79010)
(plane polarised light).

Scale bars are 0.5mm.

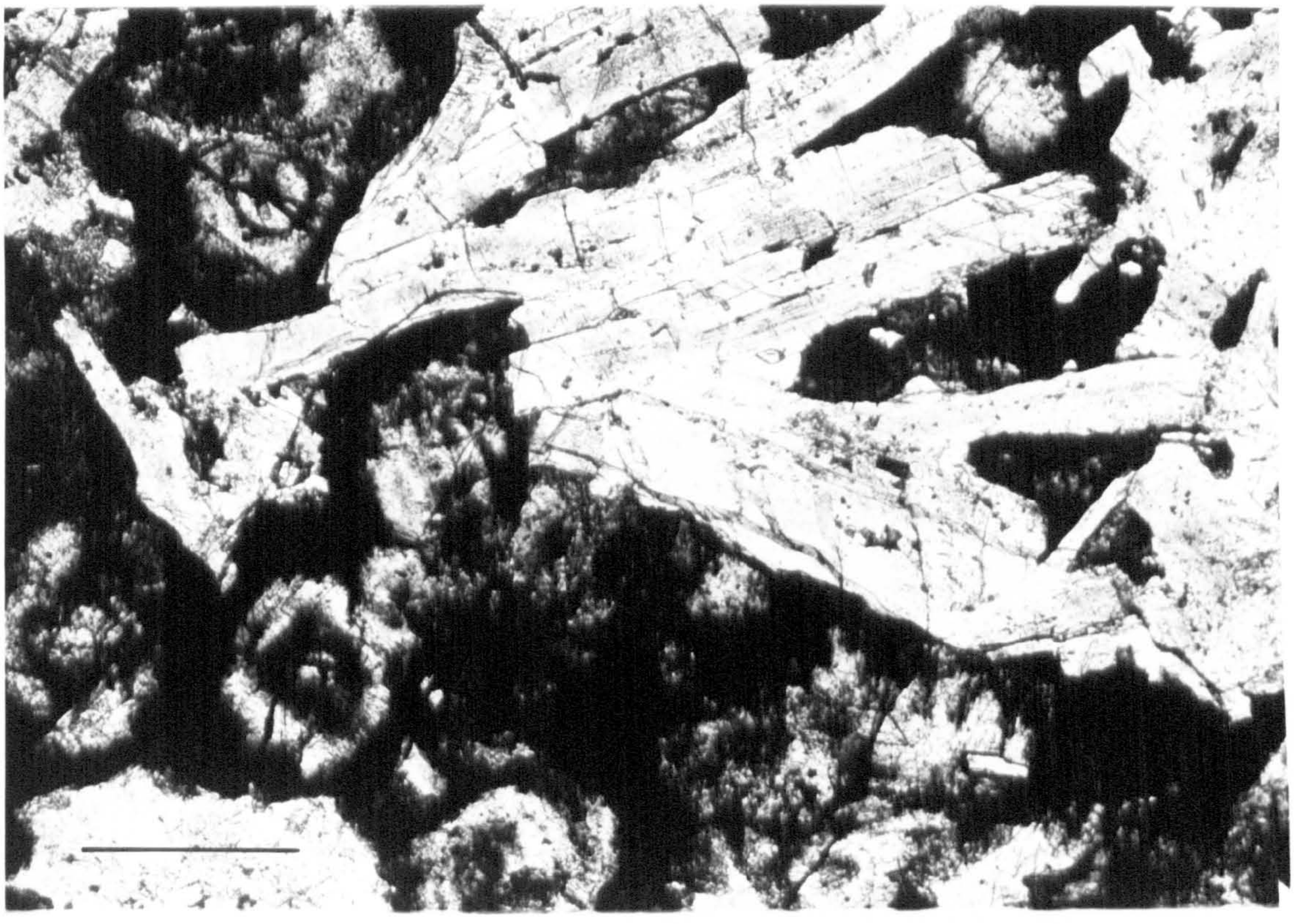

Fig. 6.3 Analyses of representative zoned clinopyroxenes from the one pyroxene dolerite plotted in the pyroxene quadrilateral.

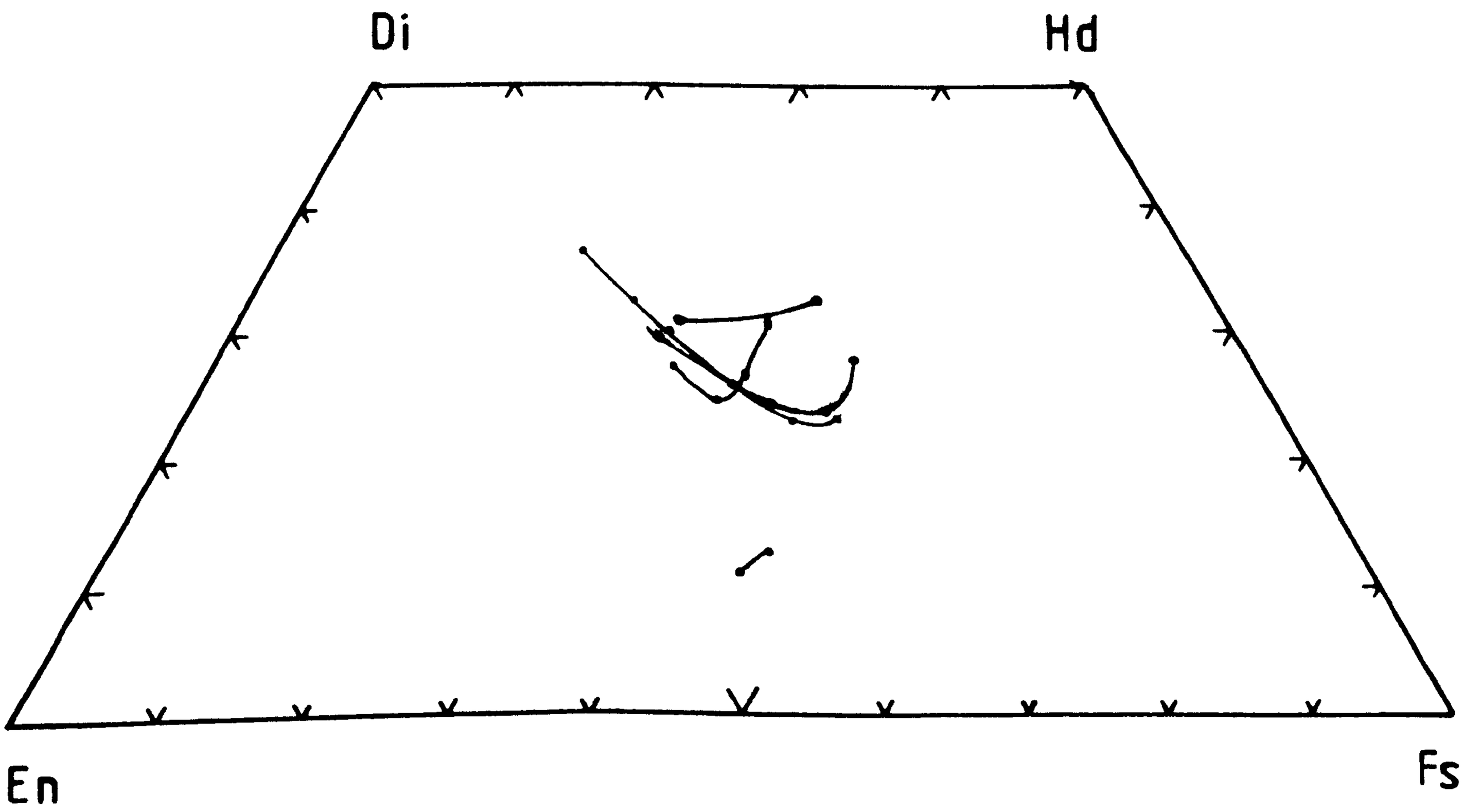
Di
Hd
En
Fs

Table 6.1 Pyroxenes from one pyroxene dolerite dyke, Poll Eorna (79008)

| | PX1 | PX14A | PX16 | PX18 |
|---|---|---|---|---|
| $SiO_2$ | 50.33 | 49.54 | 51.04 | 49.52 |
| $TiO_2$ | 0.36 | 0.81 | 0.34 | 0.52 |
| $Al_2O_3$ | 2.43 | 3.61 | 1.94 | 2.84 |
| FeO | 20.58 | 16.91 | 25.17 | 21.94 |
| MnO | 0.42 | 0.33 | 0.48 | 0.41 |
| MgO | 14.21 | 13.11 | 15.29 | 12.73 |
| CaO | 11.58 | 15.08 | 6.35 | 11.70 |
| $Na_2O$ | 0.28 | 0.33 | 0.16 | 0.28 |
| $K_2O$ | 0.01 | 0.02 | 0.07 | 0.01 |
| | 100.20 | 99.74 | 100.84 | 99.95 |

Analyses by MWDS.

that trend.

The range of plagioclase zoning found, from An63 (core) to An36 (rim) is identical to that reported by O'Hara (1961a).

### 6.2.2 Two pyroxene dolerite

No rocks that could be classified as such were collected during this study.

### 6.2.3 Amphibolite

Many of the dykes around Scourie are composed of coarse-grained plagioclase and hornblende. Crystals of the latter are frequently 'sieved' with small quartz inclusions. Quartz, both as inclusions and separate crystals, is abundant, and apatite is also present. Occasionally, relict crystals of clinopyroxene are present as cores to amphiboles, which are present as polycrystalline pseudomorphs after the original pyroxene (fig. 6.2). Ilmenite is present, intimately associated with magnetite. The ilmenite/magnetite ratio is rather lower than in the one pyroxene dolerite. Chalcopyrite is again present in small amounts.

#### 6.2.3.1 Mineral chemistry

Representative amphibole analyses are given in table 6.2. They are ferrotschermakite and ferroan pargasite according to the nomenclature of Leake (1978). Plagioclase is less zoned than in unaltered material and is at least as sodic as An30.

### 6.2.4 Hornblende schist

The Scourie dykes are converted to hornblende

Table 6.2 Amphiboles from amphibolite of the Scourie dyke at Poll Eorna (78010)

| | AMP2 | AMP3 |
|---|---|---|
| $SiO_2$ | 40.00 | 40.32 |
| $TiO_2$ | 1.42 | 1.01 |
| $Al_2O_3$ | 14.01 | 12.81 |
| $FeO^{Tot}$ | 21.62 | 21.78 |
| MnO | 0.14 | 0.21 |
| MgO | 6.59 | 7.10 |
| CaO | 11.23 | 11.34 |
| $Na_2O$ | 1.81 | 1.16 |
| $K_2O$ | 1.70 | 1.48 |
| Cl | n.d. | 0.09 |
| | 98.52 | 97.30 |

Amphiboles coexist with plagioclase $An_{39}$

Analyses by EDS.

schists where the dykes are cut by Laxfordian shear zones, as described by Teall in 1885. These schists are composed of a totally recrystallised aggregate of hornblende, zoned but untwinned plagioclase and opaque. A foliation is defined by thin (0.5mm) segregations of plagioclase about 1cm long, and by an alignement of amphibole crystals.

### 6.2.4.1 Mineral chemistry

Plagioclase ranges from An27 to An20. Amphiboles (analyses in table 6.3) are ferroan pargasite according to the nomenclature of Leake (1978).

### 6.2.5 Garnet-bearing amphibolites

The garnet-bearing dyke rocks at Scourie may be divided into two groups, those which contain garnet in a fine-grained, marginal facies, and those with a coarser grained, igneous texture.

### 6.2.5.1 Marginal garnet amphibolites

In rocks from the margins of the Scourie dyke at Poll Eorna, and from the small, fine-grained dykes on northern Cleit Mhor, garnet is present as 0.5 - 1cm aggregates of small (ca. 40 m) crystals (O'Hara, 1961a). They occur together with fine-grained (40 - 100μm) plagioclase, amphibole and magnetite and ilmenite (magnetite dominant). In the Cleit Mhor dykelets there are also phenocrysts of plagioclase and clinopyroxene present, both of which are frequently bent. The shape of the garnet clots varies across the dyke, with rounded clots found in general in the centre. In the marginal

Table 6.3. Amphiboles from hornblende schist from the Scourie dyke at Creag a'Mhail (78015)

| | AMP4 | AMP2A |
|---|---|---|
| $SiO_2$ | 42.13 | 41.57 |
| $TiO_2$ | 0.80 | 0.63 |
| $Al_2O_3$ | 12.19 | 12.44 |
| $FeO^{Tot}$ | 20.65 | 22.55 |
| MnO | 0.45 | n.d. |
| MgO | 8.02 | 7.49 |
| CaO | 11.64 | 11.75 |
| $Na_2O$ | 1.33 | 1.32 |
| $K_2O$ | 0.89 | 0.85 |
| | 98.10 | 98.60 |

Amphiboles coexist with plagioclase ca. $An_{27}$

region of the dyke, the clusters of garnet become elongated, and as the contact with the country rock is approached, the axial ratio of the clusters increases and the angle between the long axes of the clusters and the contact decreases (figs. 6.4,6.5) and amphibole average about 40μm across, whereas phenocrysts range up to 1mm.

### 6.2.5.2 Garnet-bearing dolerites

Coarser grained garnet bearing rocks are found in the centre of some dykes. The southernmost Cleit Mhor dyke contains garnet throughout in rocks with a blastophitic texture (fig. 6.6). The original clinopyroxene of the rock has been largely pseudomorphed by amphibole. Poikiloblasts of garnet up to 2cm in diameter, containing inclusions of quartz and apatite occur throughout the rock. Ilmenite and haematite are present.

### 6.2.5.3 Mineral chemistry

Probe data have been obtained only for the northernmost of the Cleit Mhor dykelets. Representative analyses are presented in table 6.4. The garnet is about 60% almandine; some iron must be trivalent to fill the octahedral sites. Some relic pyroxenes when probed appear to be pigeonitic (analysis 4, table 6.4). The magnesian nature of the pyroxenes when compared with clinopyroxene analyses from other dykes gave rise to a possibility that this dyke is more magnesian than average; this is refuted by whole rock analyses (table 6.5).

Fig 6.4 The northern of the Cleit Mhor dykes. Small cpx phenocrysts (black) and garnet aggregates (mid - grey) are visible in the upper photograph. The lower view (a close-up of the lower contact in the top photograph) shows the change in axial ratio and orientation of the garnet aggregates near the contact. The fabric developed indicates that simple shear has shaped the garnet aggregates.

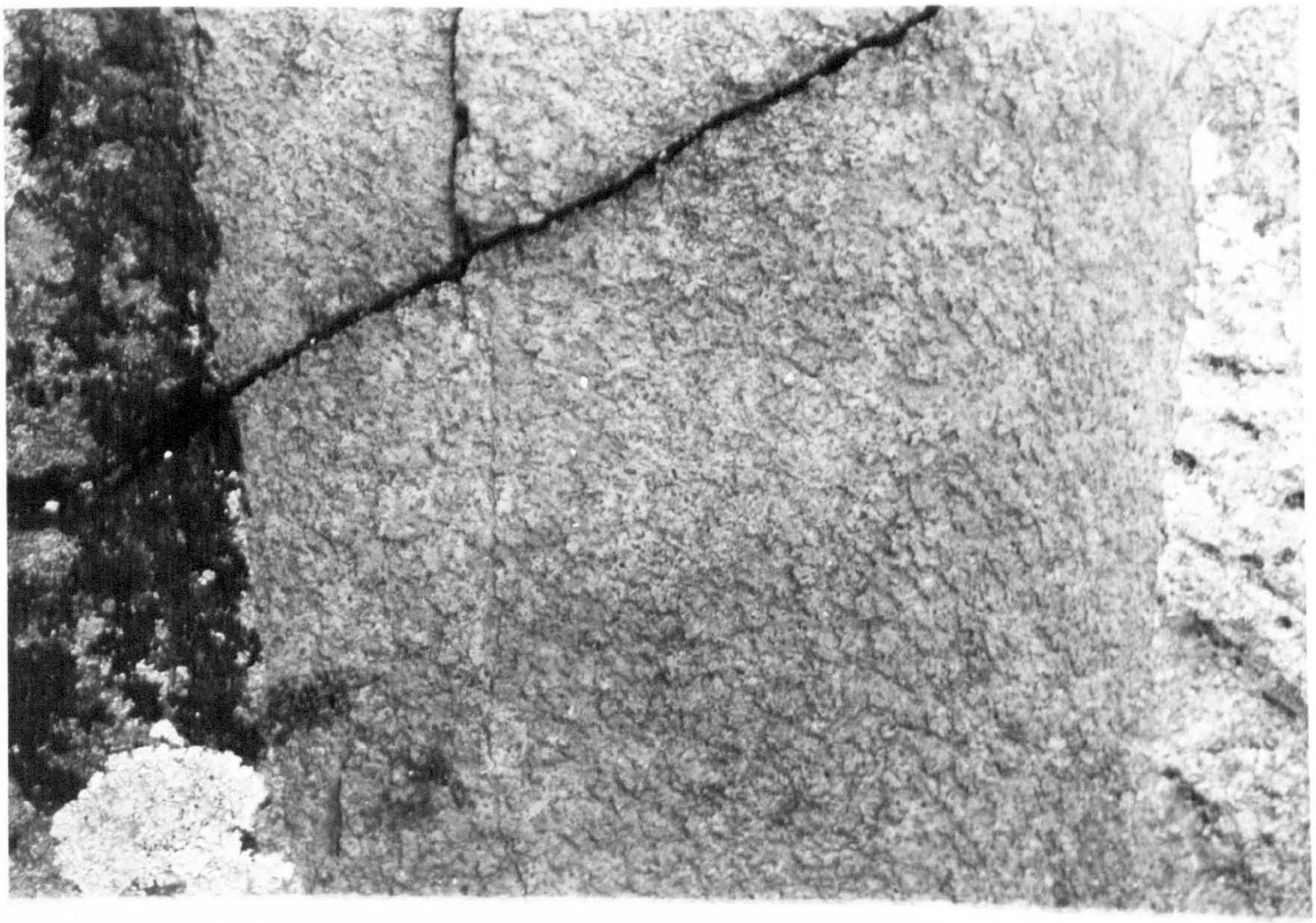

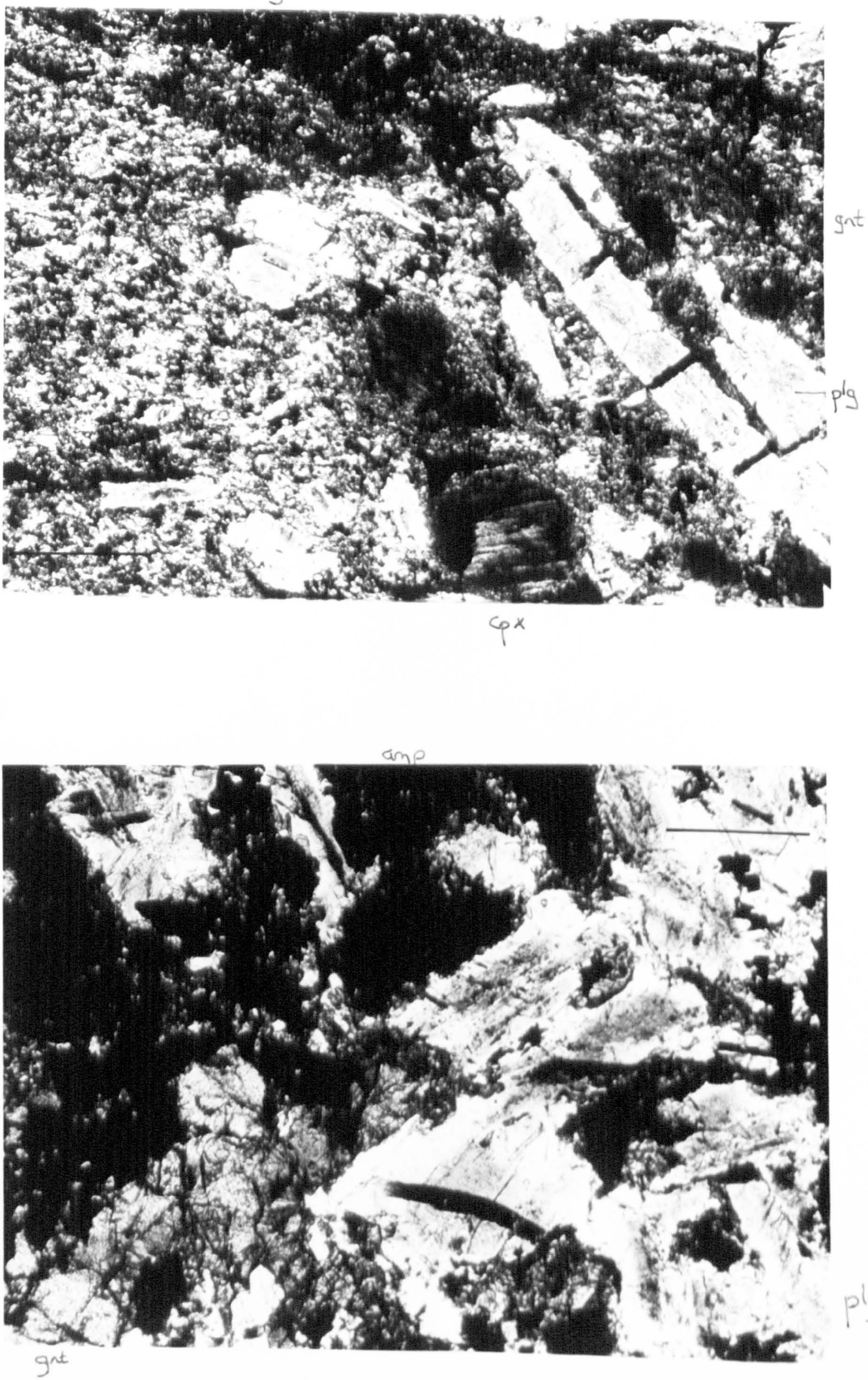
grt
grt
plg
cpx
amp
amp
plg
grt

Table 6.4 Minerals from the northern garnet amphibolite dyke, Cleit Mhor dyke (78003)

| | GT3 | PL5 (core) | PL6 (rim) | CPX6 | CPX2D |
|---|---|---|---|---|---|
| $SiO_2$ | 41.67 | 53.32 | 57.89 | 49.02 | 48.96 |
| $TiO_2$ | 0.67 | 0.32 | 0.06 | 1.17 | 0.80 |
| $Al_2O_3$ | 18.03 | 27.94 | 24.28 | 4.76 | 3.77 |
| $FeO^{Tot}$ | 26.63 | 0.31 | 0.85 | 13.34 | 14.94 |
| MnO | n.d. | n.d. | n.d. | 0.44 | n.d. |
| MgO | 4.10 | 0.03 | 0.02 | 13.29 | 14.09 |
| CaO | 8.67 | 11.42 | 8.20 | 16.41 | 16.01 |
| $Na_2O$ | n.d. | 5.07 | 7.19 | 0.74 | 1.00 |
| $K_2O$ | n.d. | 0.16 | 0.38 | n.d. | n.d. |
| | 99.77 | 98.57 | 98.87 | 99.17 | 99.57 |

All analysed by MWDS except CPX2D analysed by EDS with beam defocussed to 30 μm.

Table 6.5 Whole-rock analyses of Scourie dykes

| | 1 | 2 | 3 | 4 | 5 | 6 | 7 |
|---|---|---|---|---|---|---|---|
| $SiO_2$ | 49.74 | 49.75 | 48.58 | 48.23 | 48.9 | 49.9 | 49.8 |
| $TiO_2$ | 2.77 | 2.60 | 2.43 | 2.96 | 1.9 | 2.66 | 3.00 |
| $Al_2O_3$ | 12.14 | 11.94 | 13.48 | 13.22 | 12.6 | 11.2 | 12.9 |
| $Fe_2O_3$ | 18.48 | 18.14 | 2.62 | 4.56 | 4.5 | 16.17 | 17.17 |
| FeO | - | - | 14.07 | 12.62 | 10.9 | - | - |
| MnO | 0.27 | 0.26 | 0.22 | 0.30 | 0.24 | 0.26 | 0.23 |
| MgO | 4.25 | 4.64 | 5.11 | 5.20 | 6.4 | 5.07 | 4.40 |
| CaO | 8.43 | 8.92 | 9.48 | 8.61 | 9.7 | 7.76 | 8.74 |
| $Na_2O$ | 1.71 | 1.89 | 2.40 | 1.97 | 2.5 | 2.29 | 2.93 |
| $K_2O$ | 1.00 | 0.93 | 0.75 | 0.96 | 0.56 | 1.14 | 0.81 |
| $P_2O_5$ | 0.36 | 0.33 | 0.23 | 0.04 | 0.18 | 0.42 | 0.20 |
| $H_2O$ | n.a. | n.a. | 0.79 | 1.65 | 1.2 | n.a. | n.a. |
| LOI | 0.70 | 0.03 | n.a. | n.a. | n.a. | n.a. | n.a. |
| | 99.85 | 99.43 | 100.16 | 100.31 | 100.20 | 96.87 | 100.18 |

Where only $Fe_2O_3$ is quoted, all iron was measured as ferric.

1 Edinburgh XRF analysis, northern Cleit Mhor dyke (78003).

2 Edinburgh XRF analysis, northern Cleit Mhor dyke (S7A, collector E. Stolper).

3 O'Hara (1961a) analysis 1.

4 O Hara (1961a) analysis 4.

5 Burns (1966) average 34 samples, Scourie zone.

6 Weaver and Tarney (1981) Poll Eorna, L636.

7 Weaver and Tarney (1981) Assynt, 916.

## 6.3 Discussion

It is now generally accepted (following O'Hara, 1961a) that the Scourie dykes were emplaced into hot crust at depth (see for example Dickinson and Watson, 1976), leading to the development of garnet-amphibolite assemblages in parts of the dykes that recrystallised. The assemblages in the northern Cleit Mhor dykelet are likely to have developed by the devitrification of the initially chilled margin, whilst the elongation of the garnet clusters was due either to the magma having been subject to shear near the margins during emplacement, or to continued plastic deformation of the glass during devitrification. These two models are opposite endmembers of a continuum of processes.

A model of this family should also be applicable to the margins of the Scourie dyke on the north side of Scourie Bay, whereas the development of garnet at the expense of a pre-existing gabbroic texture was probably facilitated by the continued outflow of heat from the still crystallising and cooling dyke core, as suggested by O'Hara (1961a).

The garnet forming reaction may be modelled in CMAS as

Pigeonite+Anorthite = Quartz+Hornblende+Ca-Mg garnet

The ambient conditions prevalent when these dykes were emplaced may be estimated by the use of several geothermometers and barometers. Garnet- clinopyroxene

temperatures for the northernmost Cleit Mhor dyke are about 1000°C; the clinopyroxene here is a metastable sub-calcic augite and temperatures calculated have little meaning. In the more recrystallised rocks about 0.5m in from the contact of the Scourie dyke at Poll Eorna, clinopyroxene is present as recrystallised, calcium-rich relics. Garnet-clinopyroxene equilibration temperatures here are in the range 650-725°C. The pyroxenes from this rock plot on the 600°C isotherm within the pyroxene quadrilateral as suggested by Ross and Huebner (1975). An approximate minimum temperature is given by the lower stability limit of almandine at the QFM oxygen buffer, which is ca. 550°C (Hsu, 1968). These temperatures are higher than those of O'Hara (1977) as he examined fine-grained groundmass minerals, whereas coarser-grained material has been analysed here.

The ambient pressure is still very difficult to constrain although some information is obtainable from ultrabasic dykes at Scourie, Badcall and Assynt, where they are later than the dolerites. The ultrabasic veins at Badcall, together with the Assynt dykes contain olivine and calcic plagiolase (O'Hara, 1962; Tarney, 1973). The coexistence of these two minerals limits the pressure to less than 8.5 - 9 kbar (Herzberg, 1972). A minimum pressure is even less easy to estimate: amphibole-plagioclase-quartz assemblages are potentially very useful for assessing conditions of recrystallisation, but as yet only preliminary data are

available (Best, 1978), and mixing parameters are far too imprecise for use at low temperatures.

# Chapter 7 Geochemical evolution of the Scourie complex.

## 7.1 Introduction.

Many analyses of Lewisian rocks have been performed (Sheraton, 1970, Sheraton, Skinner and Tarney, 1973; Tarney, 1976; Tarney, Weaver and Drury, 1979; Rollinson and Windley, 1980a,b; Weaver and Tarney, 1980; Pride and Muecke, 1980).These workers have come to diverse conclusions about the processes that have controlled the geochemistry of the gneisses. Two aspects of the petrogenesis have been considered in detail:

(A) the origin of the marked depletion in incompatible elements, such as K,Rb,U

(B) the ultimate origin of the complex

Three hypotheses have been put forward to explain (A).These are:

(Ai) The removal of incompatibles by a mantle derived fluid (Drury, 1973; Tarney and Windley, 1977; Hamilton et al., 1979; Rollinson and Windley, 1980b)

(Aii) The expulsion of the residual liquid of an igneous fractionation process (Holland and Lambert, 1975)

(Aiii) The removal of a partial melt from the precursor to the present Scourie complex during metamorphism (Fyfe, 1973; O'Hara and Yarwood, 1978; Pride and Muecke, 1980; Weaver and Tarney, 1980 in

part)

Hypotheses for the initial origin of the Scourian complex can be grouped together under four headings:

(Bi) A sequence of sediments or volcaniclastics (Sutton and Watson, 1951; Pride and Muecke, 1980)

(Bii) Calc-alkaline volcanics (Sheraton, 1970; Bowes, 1978)

(Biii) Calc-alkaline plutonic igneous rocks generated by deep melting/ fractionation (Tarney, 1976; Tarney and Windley, 1977; Weaver and Tarney, 1980; Rollinson and Windley, 1980b), with generation of trondhjemites by in situ fractional crystallisation (Rollinson and Windley, 1980b)

Obviously if process (Aiii) led to the depletion in incompatible elements, it becomes extremely difficult to examine the various possible origins of the Scourie complex. The cause of the depletion must first be correctly resolved before any attempt can be made to determine the original nature of the rocks. Model (Ai) has to some extent been erected because of supposed failings of model (Aiii); model (Aii) is closely related to model (Aiii), the difference depending on the timing of emplacement of the source rocks relative to the peak of metamorphism.

A re-evaluation of the available evidence below reveals that, far from being unsatisfactory, hypothesis (Aiii) is in fact better suited to the data than the others. It also has the attraction of not requiring the

action of ill-defined ichors of unknown origin.

## 7.2 Original hydration

Crucial for an anatectic model for depletion is evidence of the originally hydrous nature of the Scourie complex, as $H_2O$ bearing rocks commence melting at much lower temperatures than anhydrous rocks (fig 7.1; see Wyllie, 1971). It is necessary to ascertain the degree of hydration of both acidic and basic rocks, as both have the potential to melt under the high-grade conditions recorded at Scourie (fig 7.1).

The only rocks from which unequivocal evidence of the activity of water can be obtained are the amphibole-bearing, ultrabasic rocks which contain the water-buffering assemblage amp-olv-cpx-opx (see section 2.4.5). However, it is unlikely that these rocks have melted (Eggler, 1978, fig ) so an attempt to generalise from these rocks to those of interest must be made. As discussed in section 2.4. , the evaluation of $A_{H_2O}$ for these rocks is fraught with difficulty, revolving around the small amount of data on amphibole mixing parameters, which are crucial to quantitative calculation using the $H_2O$ buffer outlined above. It nonetheless seems possible that $A_{H_2O}$ was of the order of 0.2 or higher within these ultrabasic rocks. These ultrabasic rocks, which are intimately associated both with basic rocks and with metasediments, probably originated as high-level intrusions (Davies, 1974) or as komatiite-type lavas (see Chapter 9). They must have been hydrated subsequent to

Fig. 7.1 Melting relations of various rocks as a function of $SiO_2$ content at 10 kbar with 2% $H_2O$. After Wyllie (1977).

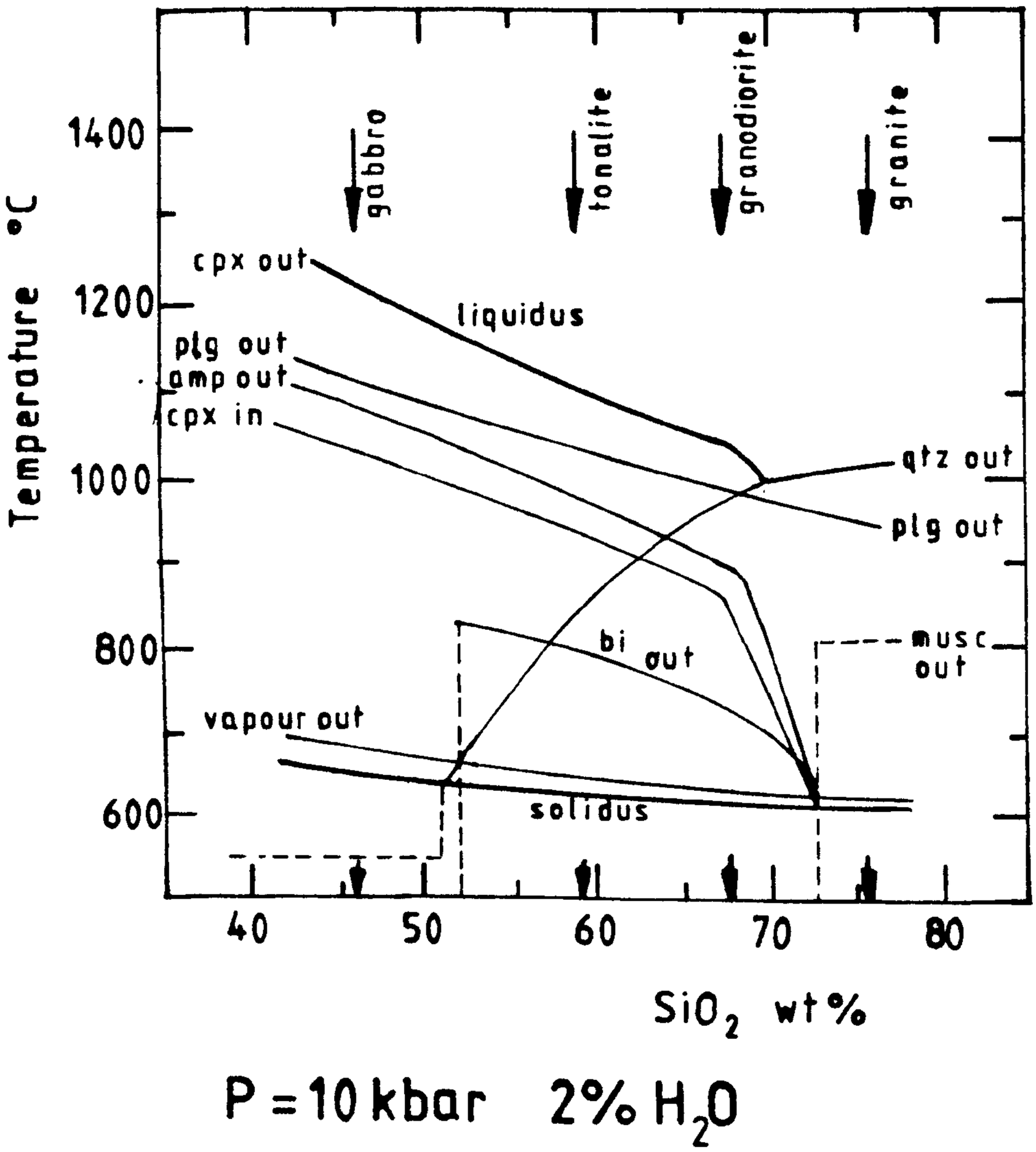
Temperature °C
1400
1200
1000
800
600
gabbro
tonalite
granodiorite
granite
cpx out
liquidus
plg out
amp out
cpx in
qtz out
plg out
bi out
musc out
vapour out
solidus
40
50
60
70
80
SiO2 wt%
P = 10 kbar
2% H2O

their initial emplacement, and as the basic rocks would require less water to hydrate them due to their lower maximum potential amphibole content, they were presumably also amphibole bearing at an early stage in their history.

The origin of the acid gneisses that form the bulk of the Scourie complex is still not settled: many authors consider them to be recrystallised plutonic rocks, whereas others postulate a metasedimentary origin (see section 7.1). If these rocks did originate as metasediments, they would have been hydrous: if they were igneous they may have been hydrous or anhydrous, depending on original mineralogy and degree of alteration. Rollinson and Windley (1980b) and Weaver and Tarney (1980) both suggest that amphibole was an important phase in the tonalites that they regard as precurssors to the acid gneisses. If amphibole was a supersolidus phase when the rocks crystallised, $A_{H_2O}$ must have been greater than ca. 0.3 (Eggler and Burnham, 1973, fig 4), and any trapped fluid inclusions will have had a similar composition. Subsequent reheating of the rocks would lead to melting at temperatures of 930 - 960°C at pressures between 4 and 10kbar, assuming that $A_{H_2O}$ remained internally buffered or otherwise free from externally imposed change. If an externally buffered fluid was flushed through the rocks, imposing a lower $A_{H_2O}$ on them, amphibole would break down prior to melting, releasing $H_2O$ from the system. The fluid would

need to have $A_{H_2O}$ less than 0.1 to prevent melting at 1000°C (Eggler and Burnham, 1973, fig 4).

Evidence from other high-grade terrains suggests that internal buffering of the fluid phase is important in amphibolite-granulite transition zones. Amp-cpx-opx bearing assemblages are widespread in Greenland (Bridgewater et al, 1974,; Wells, 1979) and the granulites around Broken Hill, Southern Australia, also contain $A_{H_2O}$ buffering assemblages (Phillips, 1980) . The highest-grade rocks of these regions contain no remaining hydrous phase.

These mineral assemblages may be interpreted in terms of an analysis of the phase relations in the system CMAS, involving the phases qtz, plg, opx, amp and liq in a projection from cpx onto the plane MS-AS-S. Fig 7.2 is a $T-X_{CO_2}$ section of the resulting reactions; its form may be compared with fig 4 of Eggler and Burnham (1973) and fig 5b of Wyllie (1979). The slope of the reactions [opx] and [plg] on fig 7.2 will depend on total pressure, as this affects the partitioning of water between liquid and supercritical fluid. Eggler (1978) states that vapour fractionation (the distribution of water between silicate magma and vapour) is most marked at low pressure and small degrees of partial melting, so both reactions have been drawn with a positive slope, implying the presence of vapour on the opposite side of the reaction from liquid.

A rock composed of qtz-plg-amp, such as X (fig 7.2)

Fig. 7.2 Theoretical analyses of melting relations in the clinopyroxene saturated part of the system $SiO_2-Al_2O_3.SiO_2-MgO.SiO_2-H_2O$
The dashed line indicates the path of composition X if the activity of water is externally controlled. Solid line indicates the path of composition X if the activity of water is internally controlled Heavy dashes indicate the path if there is insufficient of one phase to allow the buffering to continue to the invariant point. Note how when the composition buffers the composition of the fluid internally, $X_{H_2O}$ first increases until the melting curve is reached , and then decreases again as $H_2O$ rich liquid is formed in increasing quantities.

[qtz] opx + plg = liq + amp

[liq] qtz + amp = plg + opx

[plg] qtz + amp = liq +opx

[amp] qtz + plg + opx = liq

[opx] qtz + amp + plg = liq

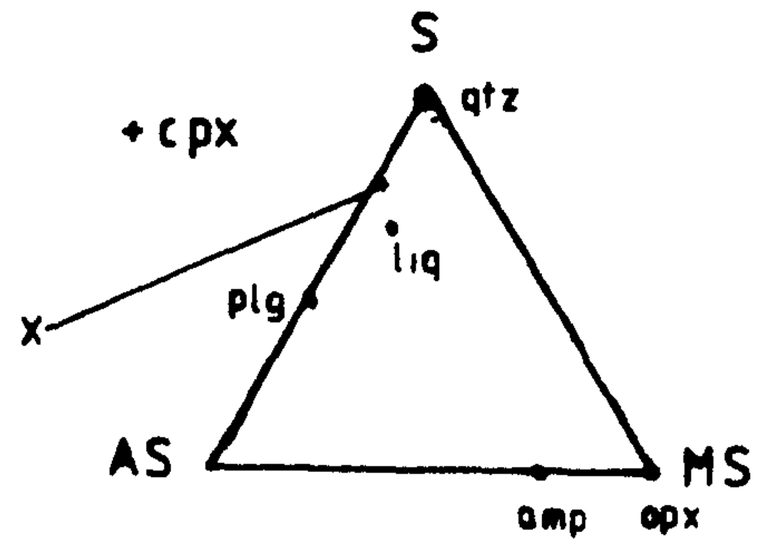


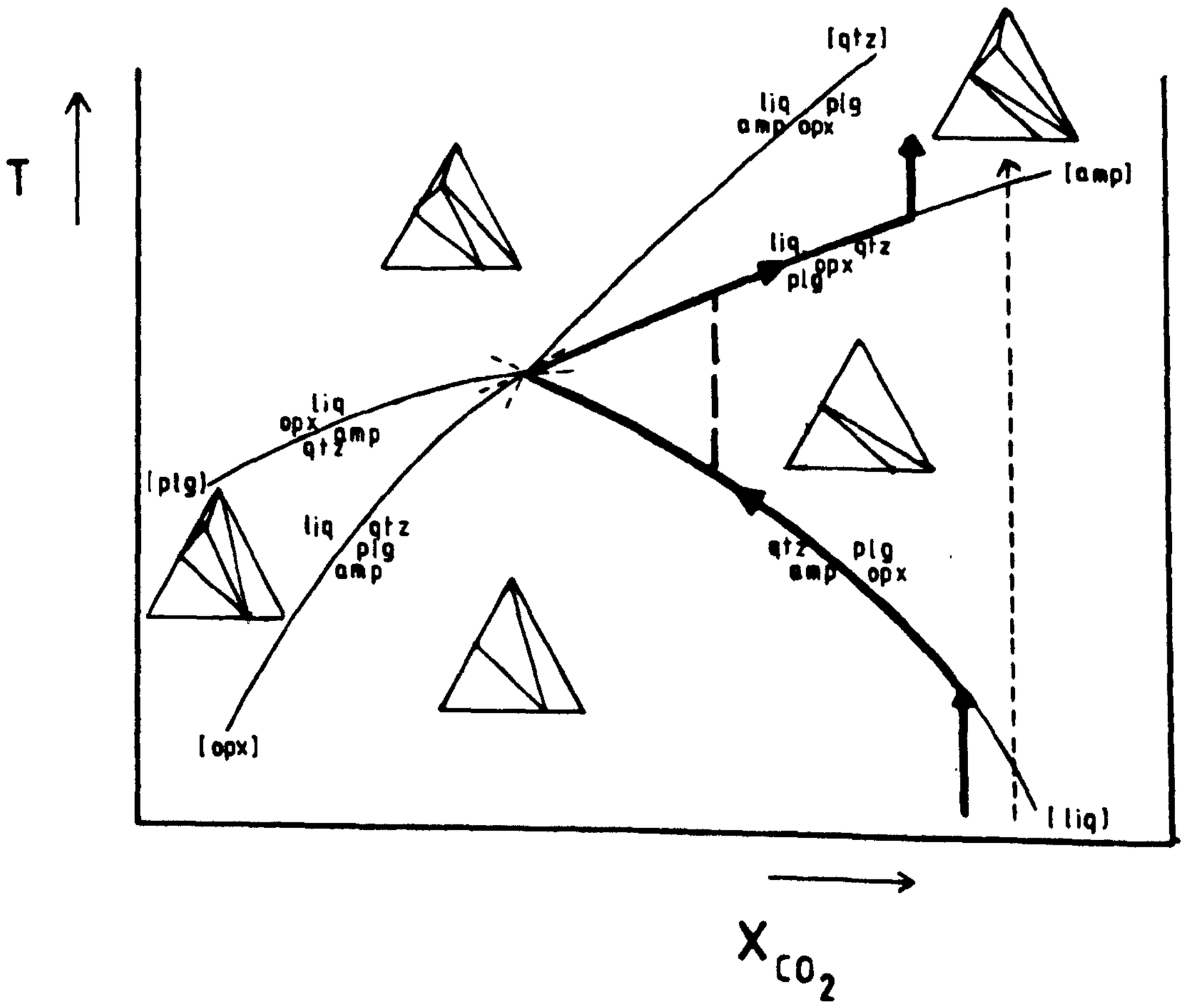

will, if heated from low temperatures, evolve along a path such as the heavy lines on the figure if the fluid is internally buffered. In doing so, it will successively display water-bearing vapour saturated, buffered and (apparently) unbuffered assemblages, the latter arising upon escape of the melt.

With the figured geometry, any internally buffered rock will either start to melt with the breakdown of amphibole, driving the fluid composition towards $CO_2$, or it will first encounter the amphibole breakdown curve, which will cause enrichment in the vapour in water until the invariant point is reached, when melting will commence.

In conclusion, the available petrological evidence points to the Scourie complex originally being hydrated, and hence having undergone partial melting because of the inferred P-T conditions.

## 7.3 Nature of melts of the original complex.

It has been known for some time that the solidus curves of hydrated rocks are similar for a wide range of compositions (fig 7.1; Wyllie, 1977).This is also true for partially hydrated rocks (those with no free vapour phase). This is due to two factors: the broadly similar nature of initial melts produced (quartzo-feldspathic), and to the similarity of the melting curves of the main mafic mineral, amphibole, over a range of compositions. This means that rocks as diverse as hornblende gabbros, tonalites, granodiorites and granites will be partially

molten under similar conditions. Initial melt compositions will vary depending on the mineralogy of the source rock.

7.3.1. Mineralogy of source rocks.

Obviously there was initially a diverse mineralogy in the Scourie complex. A problem arises in assessing the nature of the original feldspar(s) present prior to granulite facies metamorphism - most of the rocks now have a single, antiperthitc plagioclase. It is likely that rocks like the 'tonalitic' gneisses originally contained two feldspars prior to granulite facies recrystallisation. The effect on initial melt compositions of a single, ternary feldspar is difficult to judge as experiments are usually conducted under water saturated conditions for kinetic reasons, and they therefore do not usually attain the temperatures neccessary for the development of a notable degree of solid solution. It is reasonable to assume that, at least in the early stages of evolution, the most abundant rocks in the Scourie complex had the assemblage qtz-plg-ksp-amp +zircon+apatite, and that the more basic rocks were amp-plg+qtz.

7.3.2 Melt compositions.

The compositions of melts from the qtz-plg-ksp- amp assemblage will be close to the three phase eutectic (or the two phase minimum at lower $P_{H_2O}$ ) in the system qtz-or-ab-$H_2O$.As there is likely to have been little ksp in the starting composition, equilibrium melts would tend

to migrate along the qz-ab cotectic if much melting occured. Alternatively, if fractional melting was operative, melting would cease after the last ksp disappeared until the qtz-ab(-amp) cotectic was reached. A summary of pertinent data is given in fig 7.5 Data on the melting of hb-plag + qz is limited to that presented by Helz (1973,1976) for $P_{H_2O} = P_{Tot} = 5$kb and Holloway and Burnham (1972) for $P_{H_2O} < P_{Tot} = 5$ and 7kb. A compilation of these data is provided in fig 7.3

7.4 Comparison of likely melts with rocks of the Scourie complex.

It has previously been suggested (Sheraton et al., 1973; Weaver and Tarney,1980) that the "microcline pegmatites" of Assynt represent remelts of Scourian tonalitic gneisses.It further seems likely that the larger granite sheets of Rollinson and Windley (1980b) were also generated by this mechanism (fig.7.5). Granitic segregations are also present throughout the 'tonalitic' gneisses, and are rather more common than published statements suggest (Rollinson and Windley, 1980;Savage and Sills, 1980). It has been tentatively suggested (Weaver and Tarney, 1980) that the anorthosites of the Scourian may be the result of wet partial melting of amphibolite facies basic rocks. The evidence here is also substantial, although the experimental partial melts are slightly richer in orthoclase than the Scourian trondhjemites. This is due to the lower potassium content of the postulated source when compared to the

Fig. 7.3 A comparision of the data of Holloway and Burnham (1972) and Helz (1976) on the wet melting of basalt with the composition of Scourie trondhjemites from Rollinson and Windley (1980b).

Arrows on the liquid evolution path point down temperature. Also indicated are the compositions of starting materials used in the experiments and the compositions of the presumed parental material to the trondhjemites, early Scourian basic rocks ( from O'Hara, 1961b and Tarney 1980 ).

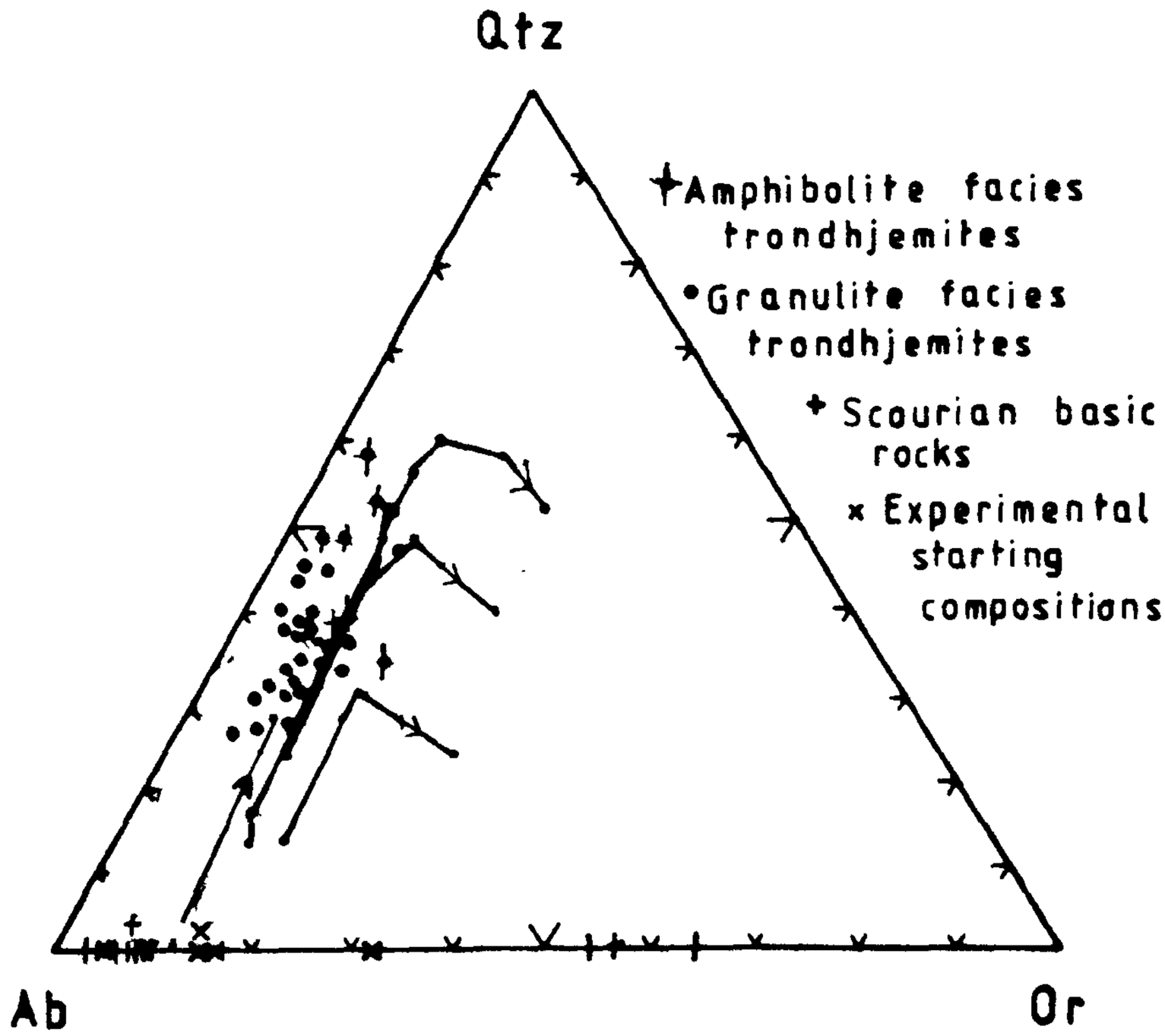
Qtz
Amphibolite facies trondhjemites
Granulite facies trondhjemites
Scourian basic rocks
Experimental starting compositions
Ab
Or

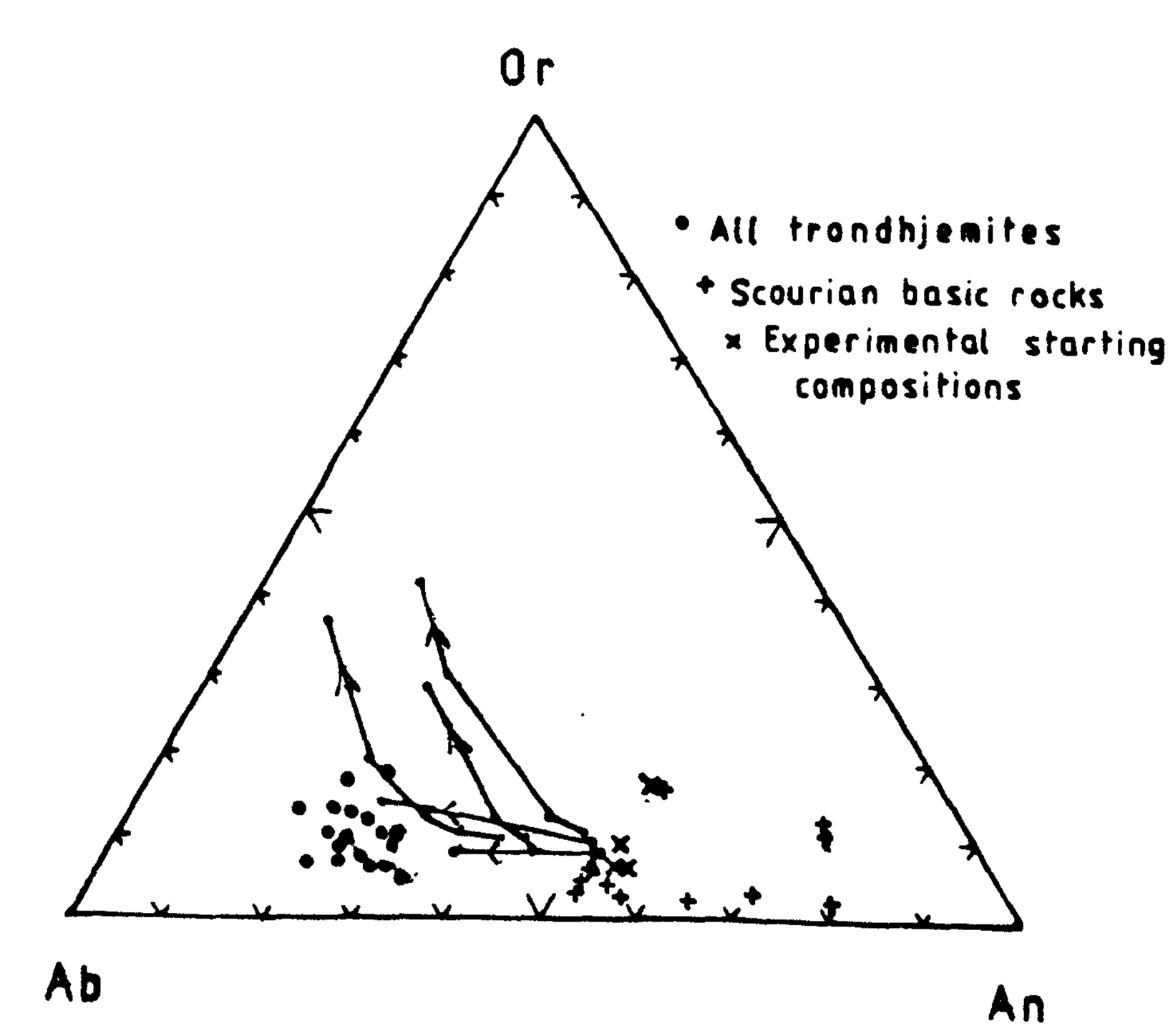
Or
All trondhjemites
Scourian basic rocks
Experimental starting compositions
Ab
An

experimental starting materials. The composition of Scourian trondhjemites also plots very close to the low-temperature melts of hb-plag-qz assemblage (fig 7.3) The basic rocks of the Scourie complex do contain feldspar-rich segregations of a composition close to that of likely melts of the basic rocks (fig 7.4).

## 7.5 Arguments against partial melting of the Scourie complex.

In the the past, an apparently formidable range of problems, mostly related to minor or trace element considerations, have been used to discount partial melting within the Scourie complex.They are listed and then discussed.

1) $(Ce/Y)_N$ vs. $Y_N$ plots show that too large a range in geochemical parameters is present within the granites to be explained by anatexis.(Rollinson and Windley, 1980b)

2) Positive Eu anomalies are present within the trondhjemites, and the REE pattern of the anorthosites is virtually identical to that of extracted plagioclase,(Tarney, Weaver and Drury, 1979; Weaver and Tarney, 1980)

3) Compositions of possible partial melts are remote from the Qtz-Ab-Or minimum melt (Tarney, Weaver and Drury, 1979; Rollinson and Windley, 1980b

4) Potassic pegmatites have a depleted nature (Tarney, 1976; Rollinson and Windley, 1980a)

Fig.7.4 Coarse - grained clinopyroxene - plagioclase schlierens in garnetiferous basic rocks from Geodh Eanruig. These are thought to be recrystallised partial melt segregations generated during the wet-melting of the basic rocks.

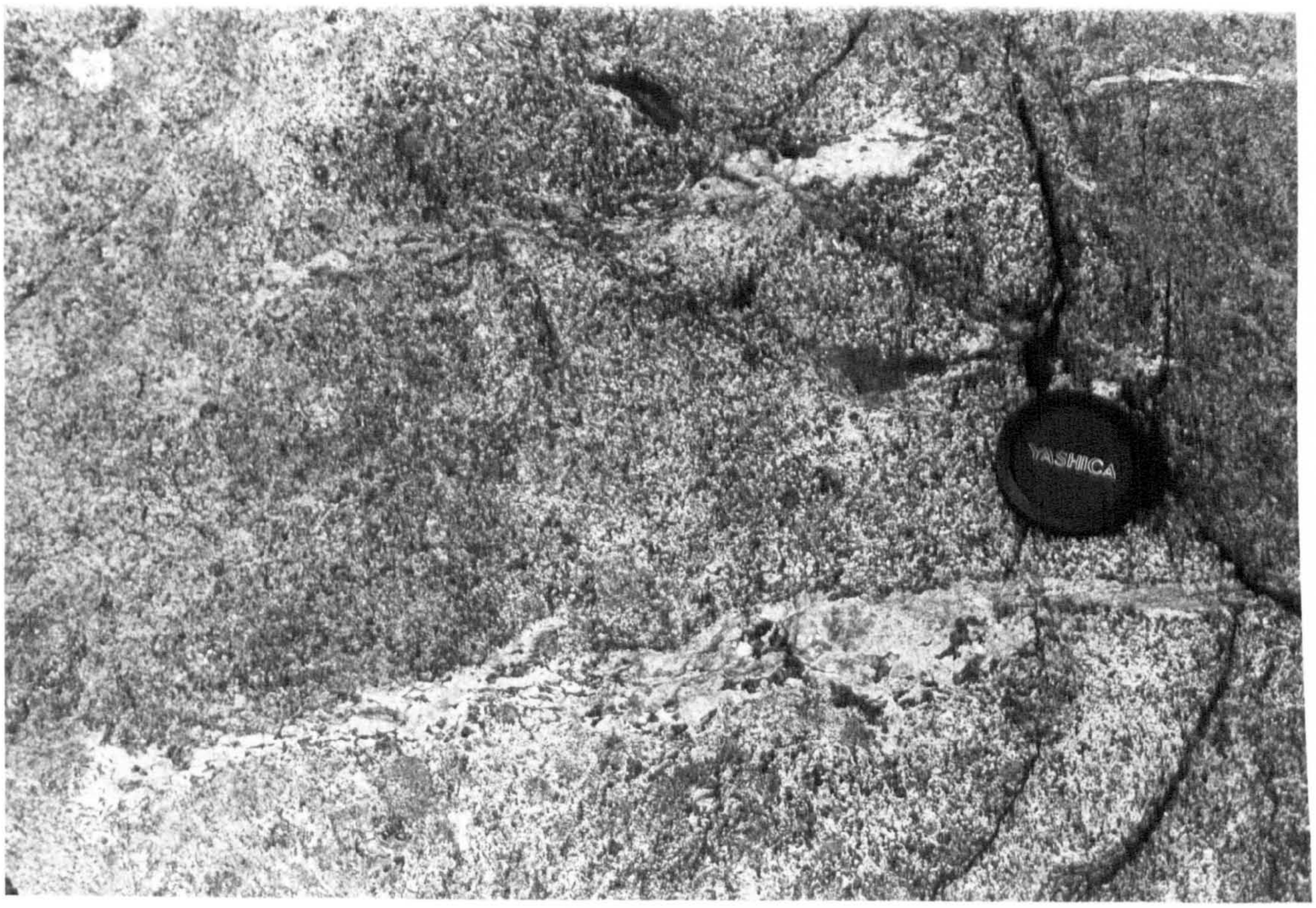
YASHICA

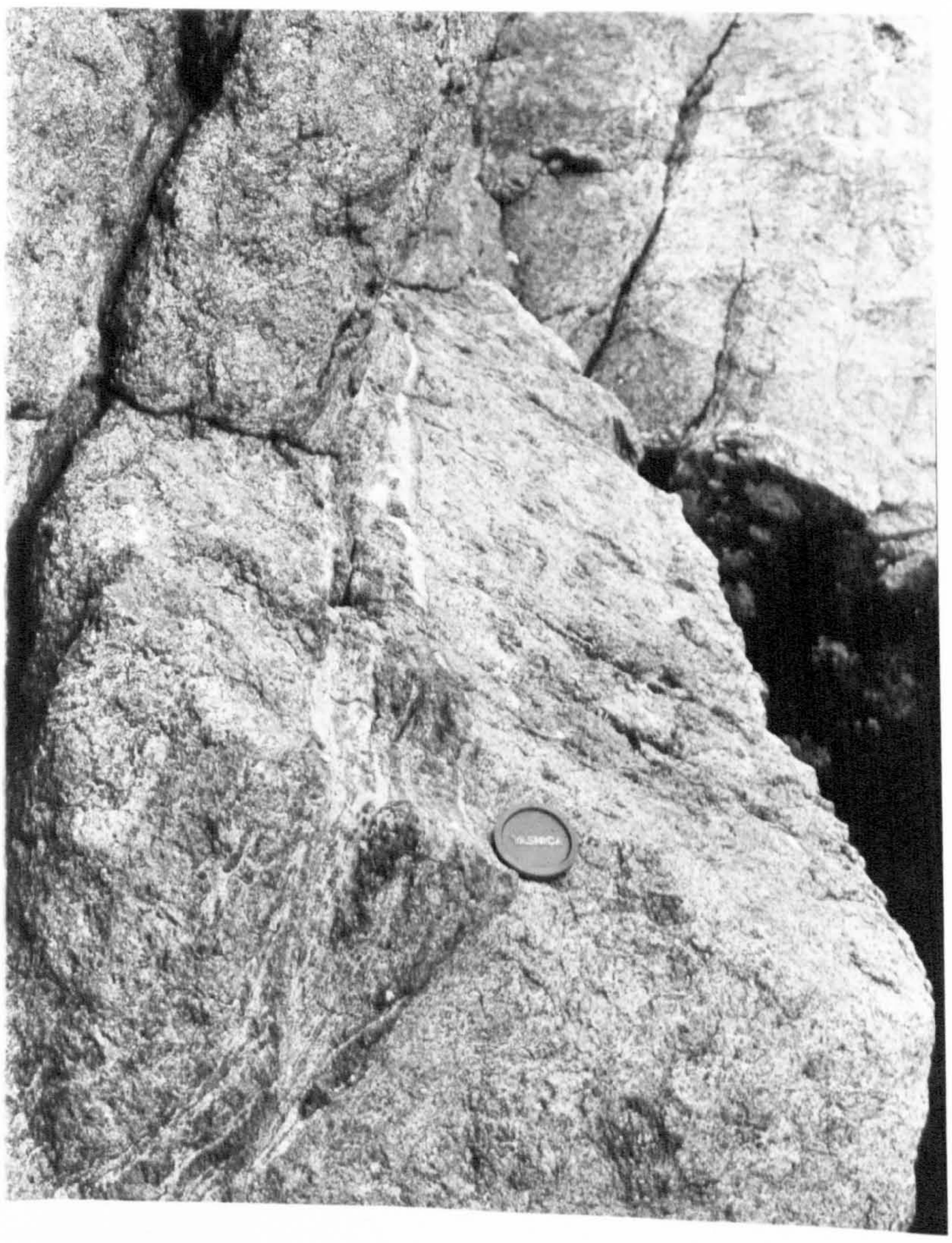
YASHICA

5) Granulite facies residua left after the extraction of a partial melt should be depleted in Ba with respect to their original composition (Tarney, 1976; Tarney and Windley, 1977)

6) Sr is too enriched in trondhjemites for them to be melts of tonalites (Rollinson and Windley, 1980b)

7) Sm/Nd systematics allow dating of the origin of the Lewisian complex as a whole indicating that a melt,which would upset REE partitioning,has not been extracted.(Hamilton et al,1979)

8) Fluid inclusions and phase equilibria considerations show that the fluid present duing metamorphism was $CO_2$ rich ($X_{H_2O} < 0.8$), and this would have increased the solidi of the rocks concerned above metamorphic temperatures.

The strength of these arguments will be discussed in the same order of listing.

1) The spread in $(Ce/Y)_N$ in the granites may be explained by the possible range in bulk composition of the parental tonalites, which will affect the bulk distribution coefficients. The presence of apatite and zircon (ca. 0.5% and 0.06% respectively, based on the analyses of Rollinson and Windley, 1980) will have a marked effect on the Ce/Y value of derived

partial melts. Zircon in particular has a very marked affinity for HREE and analogues, especially Y (Hanson, 1980; Deer, Howie and Zussman, 1962). In any case, the tonalite:granite partitioning need not vary markedly if high Y, low (Ce/Y) tonalites are parental to granites of similar characteristics.

The very high Ce/Y values of the trondhjemites are probably due to equilibration with a residue containing garnet, such as the basic gneisses now seen throughout the Scourie complex.

2) It is highly likely that, at the temperatures attained in the Scourie complex, all of the plagioclase will have melted out of the basic source of the trondhjemites and anorthosites, giving positive Eu anomalies in the liquids.

3) The liquid compositions are likely to be remote from the minimum in the Qtz-Ab-Or system, as many of them were never in equilibrium with the three phases; those likely to have been formed in equilibrium with qtz, ab and or (the granites) are not remote from the minimum (see fig 7.5).

4) Most of the granites are enriched relative to the tonalites (see Rollinson and Windley, 1980b, figs 5 and 6). As it seems probable that

Fig. 7.5 The composition of Scourie granites and granodiorites compared with experimental phase boundaries in the system qtz - ab - or . Most points fall between $P_{H_2O}$= 1 and 5 kbar curves when plotted in the An free system. Data from Rollinson and Windley (1980b) and Wyllie (1977).

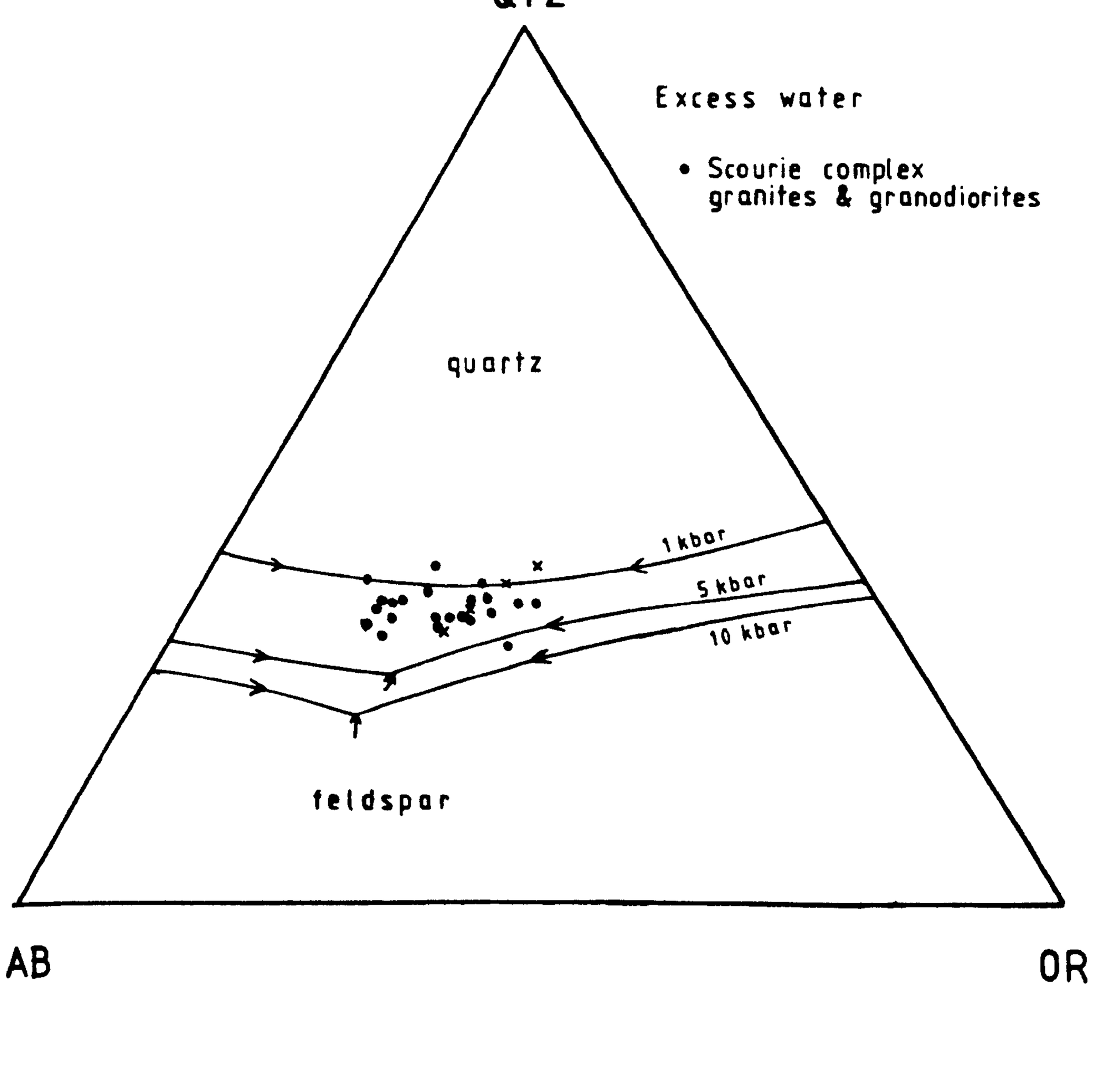
QTZ
Excess water
• Scourie complex
granites & granodiorites
quartz
1 kbar
5 kbar
10 kbar
feldspar
AB
OR

the trondhjemites were formed by partial melting of basic rocks, this criticism is not relevant. It seems likely that the basics will have a lower Sr content than the trondhjemites, for two reasons: plagioclase may not have been a significant residual phase, and the melting may have been fractional.

5) At the temperatures of melting likely to have been attained in the Scourie complex, distribution coefficients for plagioclase (the dominant residual phase) are greater than unity resulting in the liquid being poorer in Ba than the residue (Drake and Weill, 1975)

6) It is suggested here (section 7.4) that the trondhjemites are partial melts of the basic rocks, not the tonalites, and as is expected, the Sr contents of the trondhjemites are higher than those of the basic rocks, as the Sr of the basics will have been present dominantly in plagioclase, most or all of which melted during the generation of the trondhjemites.

7) The Sm/Nd values of the extracted liquids are very close to that of the source and so not likely to have disturbed Sm/Nd systematics. The nature of the actual event dated by Hamilton et al., 1979 is not clear however, as it appears that HREE in particular have been mobile to some degree during metamorphism, notably to

give rise to HREE enrichment in garnet-bearing basics (Weaver and Tarney, 1980).

8) The $CO_2$-rich nature of fluids recorded is probably due to several processes:the depletion of the complex in water by the escape of water-bearing melt (see section 7.2 and Eggler, 1978), and the depletion of residual fluid in water by the retrograde formation of hydrous minerals such as amphibole (Fry, oral comm.,1980) Also potentially important at the high temperature involved is the diffusion of hydrogen ions away from the inclusions, through the host mineral (Hollister and Burruss, 1976).

The arguments discussed above, based upon minor and trace elements, can thus be refuted by a closer examination of the details. The preferred model is one in which the observed geochemical characteristics of the Scourian complex are due to partial melting of the rocks during and after their passage through the amphibolite-granulite transition.

# Chapter 8 Thermal models

## 8.1 Introduction

Using numerical thermal models, it is possible to examine the potential causes of the metamorphism of the Scourie complex and to discover if any constraints can be put on the tectono-thermal history of these rocks. At this stage, any conclusions are necessarily speculative as the timing and conditions of various events are still poorly constrained, due both to the small data base and to the cooling/closure problem discussed in section 2.4.1.

Several workers have examined various aspects of the thermal structure of the Earth's crust during the Archaean; eg Bickle (1978); England (1978) and Wells (1980,1981). Each examined different aspects and stressed different styles of model. Bickle (op cit.) concluded that as geotherms estimated from metamorphic conditions recorded by Archaean crustal rocks are not dissimilar from those recorded in recent orogenic belts such as the Alps, the palpably greater heat production during the Archaean must have been dispersed by more active plate creation and destruction processes. Wells (op cit.) criticises this work on the basis that in his model, involving the emplacement of large volumes of tonalitic magma into a (thin) pre-existing crustal pile, metamorphic conditions recorded are controlled by the

large amounts of heat released by the crystallisation of the magmas. He further concludes that the metamorphic conditions bear no relation to the heat flowing into the crust from the mantle so it is impossible to constrain this 'mantle heat flow'. In a penetrating short analysis, England (op cit) puts the general case that in the Archaean, as in the Phanerozoic, recorded metamorphic conditions were due to transient events giving rise to hotter geotherms than those for the crust in a state of thermal equilibrium.

In this chapter, the possible thermal evolution of the Scourie complex rocks is examined. The heat flow equation has been approximated using an implicit finite difference technique (see appendices 2 and 3). There are two main potential heat sources for the metamorphism at Scourie (which are not necessarily mutually exclusive) - internal (radiogenic) heat, possibly magnified by tectonic thickening (cf England and Richardson, 1977; England, 1978) and external heat, as added heat in the form of magma bodies or enhanced mantle heat flow (cf Oxburgh and Turcotte, 1972, England and Richardson, 1977, Wells, 1980). The effects of shear heating are not considered, as they are likely to be short-lived, and at the temperatures of interest will be small owing to the low shear strength of rocks at high temperatures (Graham and England, 1976; Barton and England, 1979). The effects of reactions within the rocks (other than partial melting) have also been ignored as the possible

dehydration reactions (the only reactions with enthalpy changes large enough to be significant) will have been very limited in extent due to the low potential hydrous mineral content of the rocks, at least at the stage of interest here.

## 8.2 Enhanced heat flow models

The work of Wells (1980,1981) has shown that the emplacement of large bodies of tonalitic magma into the crust can give rise to granulite facies conditions. The thermal equilibration times for such processes are generally about 50my (England, 1979, Wells, 1980) so metamorphism should follow very soon after emplacement of the igneous rocks. On the basis of Pb-Pb and Sm-Nd studies, Moorbath et al (1969) and Hamilton et al (1979) have concluded that the Lewisian was derived from the mantle at about 2.9 Gyr. The metamorphic growth of zircon (a mineral capable of retaining evidence of a pre-magmatic history) has been dated at 2.68 Gyr by Pidgeon and Bowes (1972), and Chapman and Moorbath (1977) give a Pb-Pb age of 2.68±0.06 Gyr for the metamorphism. A similar age for a period of mineral growth is given by the Sm-Nd mineral studies of Humphries and Cliff (1982). These ages suggest a period of >200 Myr between intrusion of igneous rocks and metamorphism, rendering a model for the metamorphism based on the latent heat of tonalitic magmas unlikely.

This conclusion is likely to be valid for most possible heat flows into the base of the crust. As Wells

(1980) states, varying this heat flow will affect the absolute temperatures attained, especially at long times after emplacement, and it is conceivable that heat flow was of the order of 50 mW $m^{-2}$, sufficient to give rise to steady-state conditions of 1000 °C at 50km, as observed at Scourie. However, post-emplacement erosion is likely to have been significant in the Cordilleran tectonic setting envisaged by Wells (op cit.) and this will reduce the maximum temperature attained at depth if the erosion starts before thermal equilibrium is achieved. Evidence from the Andes (Pitcher, 1979, p645) suggests that erosion keeps pace with intrusion in a Cordilleran setting, rendering a static equilibrium unlikely.

A redemption for the magmatism-based model for the Scourian metamorphism would be possible if it could be shown that near-surface emplacement of tonalitic magma and accompanying burial of underlying material had occurred over an extended time period (of the order of 150-200 Myr). However, there is no evidence from the Lewisian of large-scale igneous activity over time-spans as long as this, so the enhanced heat flow model must be set aside.

## 8.3 Tectonic thickening models

If enhanced heat flow models are unsatisfactory, a tectonic thickening / erosion model must be considered as the causal mechanism of Scourian metamorphism. There is evidence (discussed in Chapter 9) for tectonism of the the Scourie complex during the early Scourian. For such

models, there is far too little geological data to construct a model even purporting to be defensible, although the general plausibility of such models may be demonstrable if some constraints can be placed on the input parameters required. Table 8.1 lists those input parameters.

Bulk rock properties, such as conductivity, heat capacity and density are readily determined. A minimum estimate of internal heat generation during the Archaean can be derived from present-day contents of U, Th and K; heat production is likely to have been higher due to the subsequent loss of incompatible radiogenic elements (eg K, U) during partial melting. (see below). Heat flowing from lower levels ('mantle heat flow'), erosion and a maximum estimate of internal heat generation are very important, and difficult to evaluate. Initial conditions are also important.

### 8.3.1 Mantle heat flow

Mantle heat flow is impossible to estimate accurately; Bickle (1978) indeed used the metamorphic conditions to constrain it! At the present day, it has a value of about 30 mW $m^{-2}$. During the Archaean it must have been higher, but not necessarily greatly so as convection (and plate generation and destruction processes) will have been more rapid due to the marked decrease in mantle viscosity with increased temperature. Bickle (op cit.) suggests a maximum value of 50 mW $m^{-2}$ for Greenland, Wells (1980) estimates an upper limit of 60mW $m^{-2}$

Heat flows of 60 mW $m^{-2}$ give rise to steady-state temperatures at 40km of ca. 860°C with internal heat production due only to the radiogenic elements now present (see section 8.4.2). The evidence (eg Moorbath et al, 1969) suggests that at the time under consideration (before the Scourian metamorphism), radiogenic elements were present in greater abundance, so heat production and hence temperatures would have been higher. The upper limit to internal heat production (see section 8.3.2) gives rise to steady state temperatures of 960°C at 40km in an 80km crustal pile. Such temperatures inevitably would have given rise to the partial melting of even dry acid rocks at slightly greater depths (Huang and Wyllie, 1975). England (1979) shows that heat flows as high as 90 mw $m^{-2}$ are plausible, but as they would give rise to even more extensive melting (temperatures of 1250°C are attained at 40km depth in a 40km crust, with the lower internal heat geneation figures), a value of 50 mW $m^{-2}$ has been adapted here.

Two assumptions are implicit in reaching these conclusions: that thermal equilibrium was attained and that the crust was at least 40km thick at this time. The two are related as the thickness of crustal material involved will affect thermal equilibration times. If the crust was about 40km thick in total, only limited melting at most would occur, and the underlying mantle would remain solid at such temperatures. The maximum thickness of stable crust can therefore be estimated as 40km at

these times (2.8 Gyr), and the mantle heat flow estimated at ca. 50 mW $m^{-2}$ .

### 8.3.2 Internal heat generation

As mentioned above, internal heat generation may be estimated by taking the present-day abundances of heat-generating elements (Th, U and K), recalculating the abundances of the radiogenic isotopes at say 2.8 Gyr, and then calculating the power released by that amount of isotopes. The value calculated (0.2 $\mu$W $m^{-3}$ =0.5hgu) is rather lower than values calculated for other Archaean rocks (eg England, 1978) due to the extremely low U and Th content of the Scourie rocks. This value is a minimum as heat-generating elements, notably U and Th have been removed from the rocks. Wells (1980) adapted a formula for heat production based upon the model of Hawkesworth (1974) in which heat production decreases exponentially with depth according to the formula

$$A(\text{heat production}) = 2.6\exp(-x/20) \quad \mu W\ m^{-3} \qquad 8.1$$

where x is depth in km. It is probably coincidental that this formula gives a heat production of 0.21 $\mu$W $m^{-3}$ at 50km, which corresponds closely with the 0.2 $\mu$W $m^{-3}$ for the Scourie rocks which are estimated to have equilibrated at 50km.

### 8.3.3 Erosion

The geochronological data of Humphries and Cliff (1982), combined with other geochronological data, suggests that the early cooling of the complex was slow

(>100 Myr for ca. 500°C temperature drop), and this suggests modest erosion rates. An approximate lower limit to the amount of erosion may be made by noting the difference in pressure of the granulite facies metamorphism and the intrusion of the Scourie dykes. The former may be estimated as 14 kbar, the later as 6 kbar, corresponding to a difference in depth of about 24km. This uplift occured between about 2.68 Gyr and 2.39 Gyr (Pidgeon and Bowes, 1972; Chapman, 1979), corresponding to a uniform uplift rate of 0.08 km $Myr^{-1}$ ($\equiv$mm $yr^{-1}$). As this is a minimum estimate, a value of 0.1 km $Myr^{-1}$ has been used in these calculations.

### 8.3.4 Other input parameters

The effects of partial melting have been included in the models, as it is likely to have occurred both at the depth of interest and deeper. It tends to lengthen the response time of a section of crust to change, and to decrease the maximum temperatures attained by 20-50°C. The effects are not larger because the transfer of latent heat occurs over a 200-400°C melting range (see appendices 2 and 3), and the amount of heat evolved is small relative to that flowing through the crust from below over the time scale involved.

Initial thermal profiles used were sawtooth profiles with the upper and lower portions in equilibrium with either a constant internal heat generation, or with the distribution of heat generation given by equation 8.1. Sawtooth profiles were used as the duration of the

tectonic event causing thickening is likely to have been considerably shorter than thermal equilibration times. Movement rates of 10 cm $yr^{-1}$ correspond to total translations of 100km in 10 Myr. The timing and nature of the postulated tectonic thickening cannot be accurately constrained. The timing has been left undefined, as the feasibility of a tectonic model for the metamorphism is to be demonstrated, not its accuracy. The effects of varying the thickness of the overthrust block are considered in the following section. Estimates of geologically constrained parameters such as these are impossible to make accurately due to the unknown effects of later deformation.

It has been assumed that erosion commenced immediately after tectonism, as any 'eclogite anchor' (Richardson and England, 1979) will have lasted for >10 Myr, giving rise to only small additional heating.

### 8.3.5 Results

Two groups of models have been used, one with a heat generation of 0.2 $\mu W\ m^{-3}$, distributed uniformly, and the other with heat generation distributed according to equation 8.1. The results are presented graphically in figs. 8.1 and 8.2. The models with constant internal heat production all reach a peak temperature of $1000 \pm 25\ ^{\circ}C$ at $50 \pm 4$ km, with the exception of (iv) which has to heat up from much lower temperatures at depth. This model is the one most likely to form an 'eclogite anchor' (Richardson and England, 1979) and hence to have a static period of

Table 8.1 Thermal model parameters.

Distance step = 1 km

Time step = 1 Myr

$\rho$ = 2.8 $gcm^{-3}$ = 2800 $kgm^{-3}$

c = $0.76 + 4.6 + 10^{-4}T \times 1.4 \times 10^{4} / T^{2}$ $Jg^{-1}K^{-1}$

(temperature in K)

K = 2.9 $Wm^{-1}K^{-1}$*

Internal heat generation;

(1) 0.2 $\mu Wm^{-3}$

(2) $2.6\exp(-x/20)$ $\mu Wm^{-3}$

(x, depth in km)

Erosion rate = 0.1 $mmyr^{-1}$ ($\equiv$ km $Myr^{-1}$)

* the use of a heat dependent conductivity ( cf. England and Richardson 1977 ) has a negligible effect upon the results.

Partial melting model parameters (cf Wells, 1980)

Liquidus $T_L$ = 1000 + 2.0 x depth(km) °C

Solidus $T_S$ = 800 + 2.5 x depth(km) °C

Latent heat of fusion = 335 $Jg^{-1}$ ( $kJkg^{-1}$)

Fig. 8.1 Themal profiles generated during the recovery of an overthrust terrain uniform internal heat generation of $0.2 \mu W\ m^{-3}$ . Initial profile (a) has a 20km thick upper thrust slice and a 60 or 70km lower unit; initial profile (b) has 40km thick upper and lower units.

Profile (i) is the result of thermal relaxation of initial profile (a) without melting. Profiles (ii) and (iii) result if melting occurs during the relaxation of 80 and 90km thick forms of initial profile (a) respectively. Profile (iv) is the result of thermal relaxation of initial profile (b) if melting occurs. See text and table 8.1 for details of other parameters.

Profiles (i)-(iii) all attain maximum temperatures of ca. 1000 C at between 45 and 50km depth.

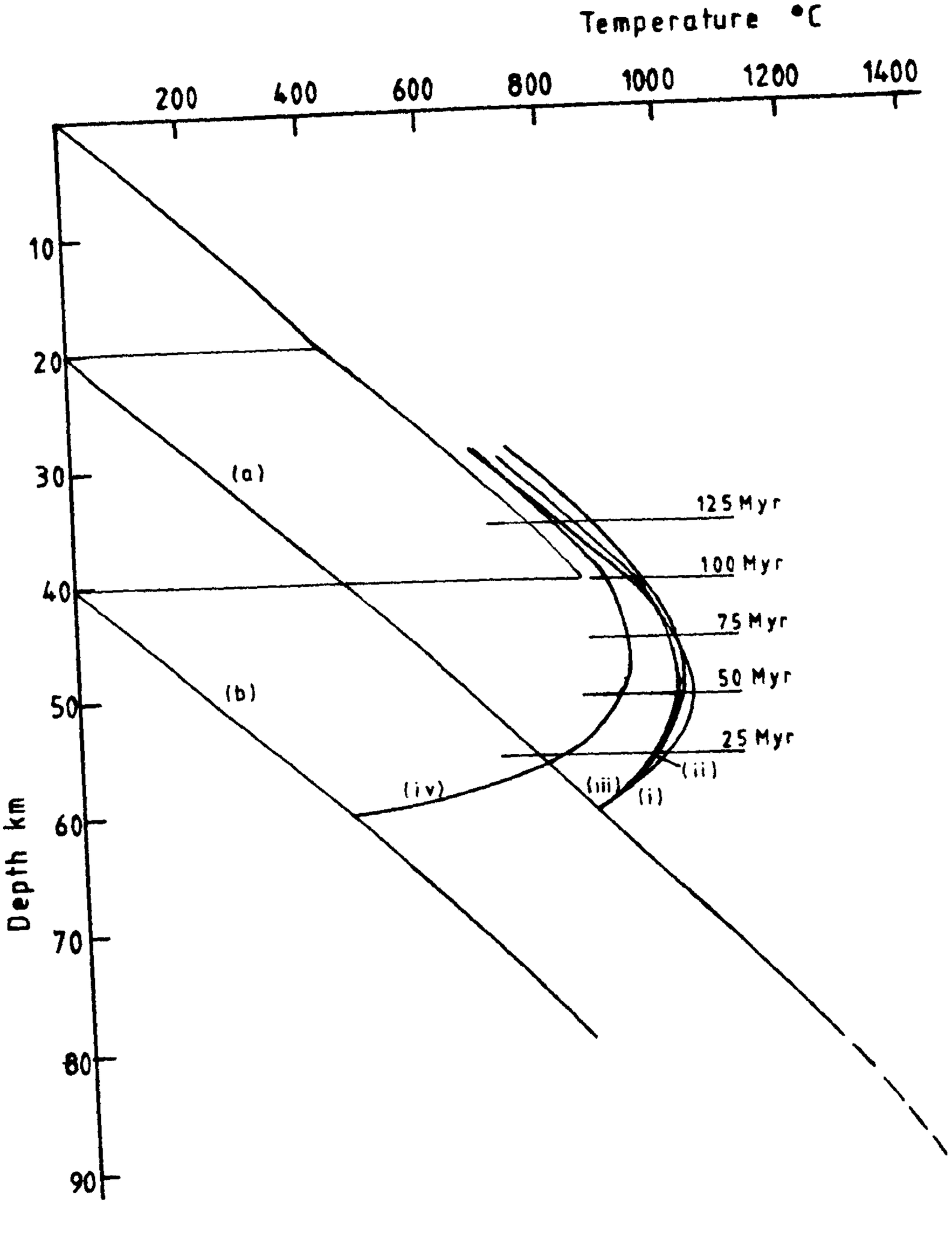
Temperature °C
200
400
600
800
1000
1200
1400
10
20
30
40
50
60
70
80
90
Depth km
(a)
(b)
125 Myr
100 Myr
75 Myr
50 Myr
25 Myr
(i)
(ii)
(iii)
(iv)

Fig. 8.2 Thermal profiles generated during the recovery of an overthrust terrain with an internal heat generation given by equation 8.1. Initial profile (a) has a upper nappe 20km thick with a 60km lower unit whereas initial profile (b) has upper and lower units both of 40km.

Profiles (i) and (ii) are the result of thermal relaxation of initial profile (a) if melting does not or does occur respectively. Profile (iii) is the result of thermal relaxation of initial profile (b) if melting does occur.

Profile (iii) is hotter than (i) and (ii) and (i) - (iv) of Fig. 8.1 as there is a much larger amount of internal heat production at depth than in the other models.

See text and table 8.1 for details of other parameters. Further discussion is presented in section 8.3.5.

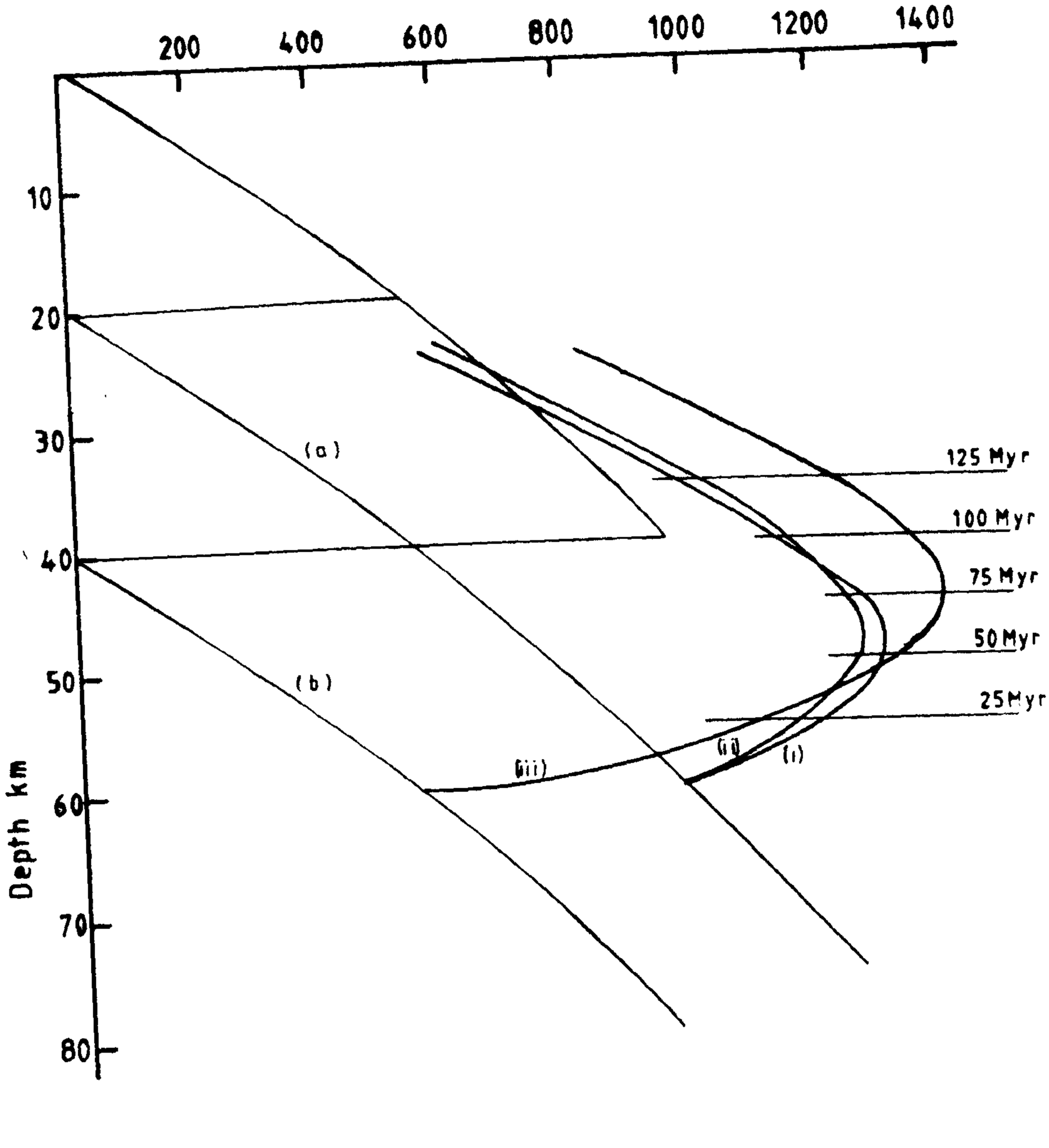
Temperature °C
200
400
600
800
1000
1200
1400
10
20
30
40
50
60
70
80
Depth km
(a)
(b)
125 Myr
100 Myr
75 Myr
50 Myr
25 Myr
(i)
(ii)
(iii)

pre-erosive warming.

In the case of the models with internal heat production given by equation 8.1 models (i) and (ii) reach peak temperatures of 1250±40 °C at ca. 48 km while model (iii) reaches a peak temperature of about 1375 °C at about 45 km. These models are all hotter than (i)-(iv) of fig. 8.1 above as they have greater internal heat generation; model (iii) is the hottest as it has much more heat generation at depth where it remains effective for longest.

It should be noted that when melting occurs at depth the melt, and hence both heat and incompatible heat-generating elements will be transported upwards at a comparatively rapid rate, leading to the dispersion of energy faster than indicated by the purely conductive models used here. Maximum temperatures are therefore likly to be between those indicated for the models presented in fig. 8.2 and those of fig. 8.1 which has only the heat generation observed to remain in the rocks. The models also show that the rocks of the Scourie complex could readily have remained at temperatures in excess of 900 °C for a period of 125±25 Myr, allowing diffusive re-equilibration to occur on a large scale (see section 2.4.1).

This chapter has attempted to quantify the unquantifiable, an obviously diffucult task! It has been possible to show that a tectonic thickening model for the metamorphism of the Archaean continental crust is

feasible. Discrimination between this model and a magmatic heat model (c.f. Wells, 1980) is possible with good geochronological data. In the case of the Lewisian, there is no evidence of igneous activity less than 200Myr before the metamorphism. This is too long before the Scourian metamorphism to be causal, so a tectonic thickening model is preferred as the mechanism of raising the temperature and pressure.

# Chapter 9 Geological evolution of the Scourie complex

## 9.1 Introduction

In this concluding chapter, various aspects of the geology of the Scourie complex touched on and discussed in earlier sections are drawn together. A model for the evolution of these rocks has been constructed, using data and ideas from this thesis and other workers.

## 9.2 Early Scourian history

The earliest history of the Scourie rocks is uncertain; evidence presented in Chapter 7 indicates that partial melting has occurred, rendering straightforward interpretation of the geochemistry of the rocks difficult. Several aspects of the geology are clear. Some constituents of the complex are of definite igneous origin - the basic/ultrabasic masses seen on Scouriemore, the north side of Scourie Bay, and at lower grade south of Loch Laxford are the best examples. Other rocks are of clearly sedimentary derivation - the brown schists of Beach et al. (1974), the Scourie Bay ironstone (Chapter 3) and rocks such as 78027/8, from the north side of Scourie Bay, which are found in close association with basic/ultrabasic masses in the Scourie region. Rocks such as 78027/8 are composed of qtz (58%), gnt (23%), plg (3%), cpx (3%), opx (4%) and opaques (9%). The latter comprise magnetite, ilmenite (as separate grains and as lamellar and granular exsolution products), pyrite,

pyrrhotite and chalcopyrite. These rocks are thought to be metamorphosed impure sandstones; their occurence as layers up to 30cm thick at Geodh Eanruig and the north side of Scourie Bay, intimately associated with the basic-ultrabasic masses suggests a supracrustal origin for these meta-igneous rocks.

Other aspects of the geology remain unclear - the origin of the grey gneisses (the tonalites of many authors) which form the bulk of the complex is uncertain, as they are likely to have undergone the greatest degree of partial melting and hence to have the least certain bulk composition. An additional uncertainty is the environment within which the basic/ultrabasic rocks were formed. It has been suggested in the past by several workers (eg Bowes et al.,1964; Davies,1974) that these rocks were originaly plutonic intrusives, but it is equally possible that they were extrusive. Features described as cumulate textures by Davies (op.cit.) (grain-size and mineralogical layering, 'cumulus' texture) also occur in komatiitic lava flows (Arndt, 1977). The range of rock-types present can be matched by those found in greenstone belts (Nisbet et al., 1977), with the possible exception of the iron-rich garnetiferous ultramafics from Scourie, which contain up to 25% $FeO_{Tot}$ (O'Hara, 1961b, analysis UA12). Compositions such as this are also unlikely to be of plutonic origin, and their chemistry probably originated by limited metasomatism during garnet growth as suggested on the basis of REE data by Weaver and Tarney (1981).

Comparison of the rocks and structures of the basic-ultrabasic masses of the Scourie complex with greenstone belts of southern Zimbabwe and north-eastern Botswana described by Coward et al. (1976) reveals a series of similarities. Ultrabasic rocks of extrusive and/or hypabyssal origin are found at the base of the pile in both cases (Davies, 1974; Coward et al., op. cit.), overlain by variable quantities of basic and acid igneous rocks and metasediments of various types, including ironstones, quartzites, metapelites and meta-carbonate rocks in the Scourie complex (Chapters 3, 9 and Bowdidge, 1969) in the Scourie complex and ironstones, quartzites, shales, limestones and greywackes in southern Africa (Coward et al., op. cit.). Both areas underwent early, flat-lying imbrication, which appears to have been more intense and at greater depths in the rocks of the Scourie complex.

## 9.3 Scourian metamorphism

It has been shown in Chapter 2 that it is not possible to estimate the peak conditions during metamorphism due to re-equilibration during cooling. The thermal modelling of Chapter 8 shows that temperatures will have exceeded 900°C for about 100 Myr. Using the relationship $x \simeq Dt^2$ (Freer, 1981), an upper limit of $8 \times 10^{-21} m^2 s^{-1}$ can be placed on the diffusion coefficient for two pyroxene and garnet-clinopyroxene equlibration. This falls at the lower end of the experimentally determined range (Duckworth and Freer, 1981), suuporting the case

made in Chapter 2 for re-equlibration during cooling. However, temperatures in excess of 1000°C were attained and pressures were greater than 14 kbar at the climax of metamorphism. Evidence of partial melting is present in the form of the present-day chemistries of the rocks, and also as (now occasional) in situ partial melt features. Partial melting is also suggested from a consideration of the activity of water in the complex (Chapter 7).

Thermal considerations, outlined in Chapter 8, make it likely that the energy for the Scourian metamorphism did not come from the cooling of the igneous component of the Scourie complex, so a tectonic enhancement of internal heat generation has been invoked as the causal process. The rocks of the Scourie complex contain evidence, presented by Davies (1976) and Coward et al.(1980) for the repetition of the sequence within 'supracrustal' belts by thrusting. In addition, early mineral fabrics are defined by aggregates of quartz, feldspar and pyroxenes (Bowes, 1978; Coward et al., 1980). This deformation may have been of a 'thin-skinned' nature, similar to the repetition of very similar lithological sequences in Botswana and Zimbabwe (Coward et al., 1976) . In support of this suggestion, it may be noted that no large scale (>10km) repetitions of sequence are apparant in the Scourie complex.

These early ($D_1$) repetitions of the sequence have been deformed by large flat-lying $F_2$ fold structures (Davies, 1976; Coward et.al.,1980). Coward et al.

(op.cit.) suggest that fresh pyroxene did not grow during this deformation, and that amphibolite facies assemblages developed at this time in the eastern portion of the outcrop of the Scourie complex. Davies (1976) considers that granulite facies metamorphism was actively proceeding during and after this folding episode. It is not clear which of these deformation episodes was the causal one for the main metamorphism, but if $D_1$ was thin-skinned as suggested, $D_2$ must have given rise to the necessary crustal thickening and the suggestion of Coward et al (op.cit.) that metamorphic conditions were not of granulite facies rejected.

Davies (1978) discusses a curvature of the $F_2$ fold trends and relates it to dextral shear movement on the structure that later became the Laxford front. Approximate integration of his shear-strain versus distance plot suggests strains of ca. 15km during the 'early Scourian', corresponding to vertical displacements of about 13km as the linear element of the fabric dips at about 40°. Although the errors here are inestimable (and probably large) this estimate compares well with the pressue range involved in the garnet breakdown and regrowth discussed in Chapter 5.

## 9.4 Late Scourian deformation

Two late Scourian deformation events have been recognised by Coward et al. (1980). They have given rise to upright folds with axial planes trending NE-SW ($F_3$) and NW-SE ($F_4$). Close to the Laxford front, $F_4$ folds

tighten and rotate into parallelism with the Laxford front, adapting a sheath fold morphology (Coward et al., op cit.). This reorientation has been ascribed to end Scourian (Davies, 1978) and early Laxfordian (Beach et al., 1974) shear on the Laxford front.

## 9.5 Scourie dyke emplacement

The emplacement of the Scourie dykes has been dated at 2.39±0.02 Gyr by Chapman (1979). These dykes were emplaced into country rocks at elevated temperatures (ca. 600 °C) at depths of about 15km (O'Hara, 1961a, Tarney, 1963, 1973, Chapter 6). Emplacement may have been in a region of simple shear, giving rise to margin parallel fabrics seen, for example at Rubh A'Tiompain.

## 9.6 Laxfordian events

Various lines of evidence suggest that in the early Laxfordian, rocks of the Scourie complex were emplaced northwards over rocks of the Laxford complex. Beach (1974) favours a thrust, whereas Coward (1974) suggests a ductile shear zone of considerable but unspecified thickness. Such tectonic thickening may have been the cause of melting of the 'fertile' amphibolite facies gneisses of the Laxfordian complex, giving rise to the zone of granite sheets north of Loch Laxford.

As suggested by Graham (in Coward, 1974), the gravitational instability of dense granulite overlying less dense granites and amphibolites is the probable cause of the later, south-side down sense of movement recorded both at the Laxford front and by other

Laxfordian shear zones cutting across the Scourie complex (Beach et.al., 1974, Beach, 1974).

A shear zone cutting metasedimentary rocks ca. 1.5km NW of Scourie, and presumably of Laxfordian age, has been studied by Beach (1973). He concluded that the deformation occured at 600±50°C and 6±1.5 kbar. This estimate must be viewed with some care, as no account was taken of the effect of minor components, notably zinc, on staurolite stability. Analysed staurolite contains 4.2 wt% ZnO, and as staurolite is the only phase in the rock to contain zinc, the postulated staurolite producing reactions (nos. 6 and 7 in fig.1 of Beach, op cit.) will be at lower temperatures than plotted. A revised P,T estimate would be 590±90°C, 5±2kbar. Temperatures are likely to have been raised during the development of these mineral assemblages in the vicinity of the shear zones by the passage of considerable volumes of supercritical water up the shear zones (Beach, 1976). There is no evidence in the Scourie area with which to test the suggestion of O'Hara (1977) that there was a regional increase in temperature during the Laxfordian event. If the tectonic thickening models of Beach (1974) or Coward (1974) are correct it is probable that the Laxfordian recrystallisation event was a prograde one over significant areas.

## Appendix 1 Error analysis.

The techniques of error analysis are well known in scientific circles (eg Bevington, 1973), but until recently have been sparingly applied to petrology. The treatment used in this work is due entirly to Dr Roger Powell of Leeds University.

In petrology, it is frequently neccessary to calculate, for example, the ideal-mixing activity of tremolite as a function of the weight % of the various elements present:

$$X_{Trem.} = f(W_{SiO_2}, W_{Al_2O_3}, W_{FeO}, W_{MgO}, W_{CaO}, \ldots) \qquad A1.1$$

We can generalise this to:

$$y = f(x_1, x_2, x_3, \ldots x_n) \qquad A1.2$$

Assuming that the errors in $x_1, x_2, \ldots$ are uncorrelated (in problems of the nature considered here, this is usually all that can be done), we can write :

$$\sigma_y^2 = \sum_i^n \left(\frac{\partial y}{\partial x_i}\right) \sigma_{x_i}^2 \qquad A1.3$$

By expressing algebraically the formula for recalculating a mineral analysis to atoms, it is possible to generalise the expressions given by Powell (1978), pp126-7 to yield:

$$\sigma_k^2 = \sum_{i(i \neq k)} \left[ \left( -\frac{F^2 NO_i W_k}{N \; MW_i MW_k} \cdot NM_k \right)^2 \sigma_{W_k}^2 \right] + \sigma_{W_k}^2 \left( \frac{F}{MW_k} - \frac{W_k}{MW_k^2} \frac{F^2}{N} \right)^2 \qquad A1.4$$

where $\sigma_k^2$ is the error in the calculated number of atoms, F is the factor for calculating the number of oxygens associated with a given weight % of element, N is the number of oxygens in the formula unit of the mineral, $NO_i$ and $NM_i$ are the number of oxygens and metals per oxygen

in the formula unit of the oxide, $MW_i$ is the molar weight of the oxide, $W_i$ the weight % of oxide and $\sigma^2_{W_i}$ the proportional error in $W_i$ (about 0.02 for a probe analysis).

This approach can be generalised to calculate the effect of a given $\sigma^2_{W_i}$ on the activity of tremolite, for example, if the expression for calculating the activity from the weight % may be partially differentiated with respect to all of the input parameters. This process is tedious and prone to error itself, and specific analysis is needed for all activities, etc. calculated.

Assuming a computer is used to calculate the mineral analysis, it is far easier to calculate the errors in activity (illustrated by $X_{Trem}$ below) as follows:

(a) Use a subroutine to calculate $X_{Trem}$ from the $W_i$ values

(b) Use another subroutine to calculate $\frac{\partial X_{Trem}}{\partial W_i}$, using a finite difference approximation of the partial differential:

$$\frac{\partial X_{Trem}}{\partial W_i} = \frac{X_{Trem}(W_i + \Delta) - X_{Trem}(W_i - \Delta)}{\Delta} \qquad \text{A1.5}$$

where $\Delta$, the finite difference parameter is small (ca. 0.0001 in this case). $\sigma^2_{Trem}$ can then be calculated using A1.3

Whilst using this technique increases the computing time per analysis, it is easy to calculate the effect of errors in input parameters upon activities or any other complex

expression. For example, the uncertainty in calculated equilibration temperature caused by uncertainty in analyses, thermodynamic data and pressure may be simply computed without recourse to involved partial differentiation. Sample programs are presented in appendix 3.

# Appendix 2 Heat flow modelling

## A2.1 The heat conduction equation

It is an observed fact that in a system transfering heat by conduction

$$\frac{q}{a} = \frac{\partial T}{\partial X}$$

where q is the rate of transfer of heat and a is the cross-sectional area of the body in question. If a constant of proportionality K (conductivity) is now introduced, the observed relationship becomes:

$$q = -Ka\frac{\partial T}{\partial X} \qquad \text{A2.1}$$

The minus sign is present because heat is conducted down the temperature gradient, from a high temperature region into one of lower tempeature. If a 1-D system (ie one in which there is a temperature difference only in one direction) is now considered, such as that illustrated in fig A2.1, an energy balance equation may be constructed :

Energy conducted into LH face, $q_x$ (i) + heat generated within the element, $q_{gen}$ (ii) = change in internal energy, $q_{int}$ (iii) + energy conducted out from RH face, $q_{x+\partial X}$ (iv)

where (iii) is due to the change in temperature of the element. Now

(i) $q_x = -Ka\,\partial T/\partial x$

(ii) $q_{gen} = \dot{q}a\partial X$

(iii) $q_{int} = \rho c\frac{\partial T}{\partial t}\partial X$

(iv) $q_{x+\partial X} = -Ka\frac{\partial T}{\partial x}) = -a\left(K\frac{\partial T}{\partial X} + \frac{\partial}{\partial X}K\frac{\partial T}{\partial x}.\partial x\right)$

Fig. A2.1 One dimentional heat conduction; a block of material, containing an element of thickness dX and a cross-sectional area a , through which heat is being conducted in one direction. The heat flow at the left-hand face is $q_X$ , that at the right-hand face $q_{X+dX}$ . Heat is produced internally in the element at a rate $q_{gen}$ .

Fig. A2.2 A graph of $f(x,y)$ at $y = y_o$, showing the use of forward, reverse and central differences ( AB, BC and AC respectively ) to approximate $\partial f(x,y_o) / \partial X$. (See section A2.2 for details.)

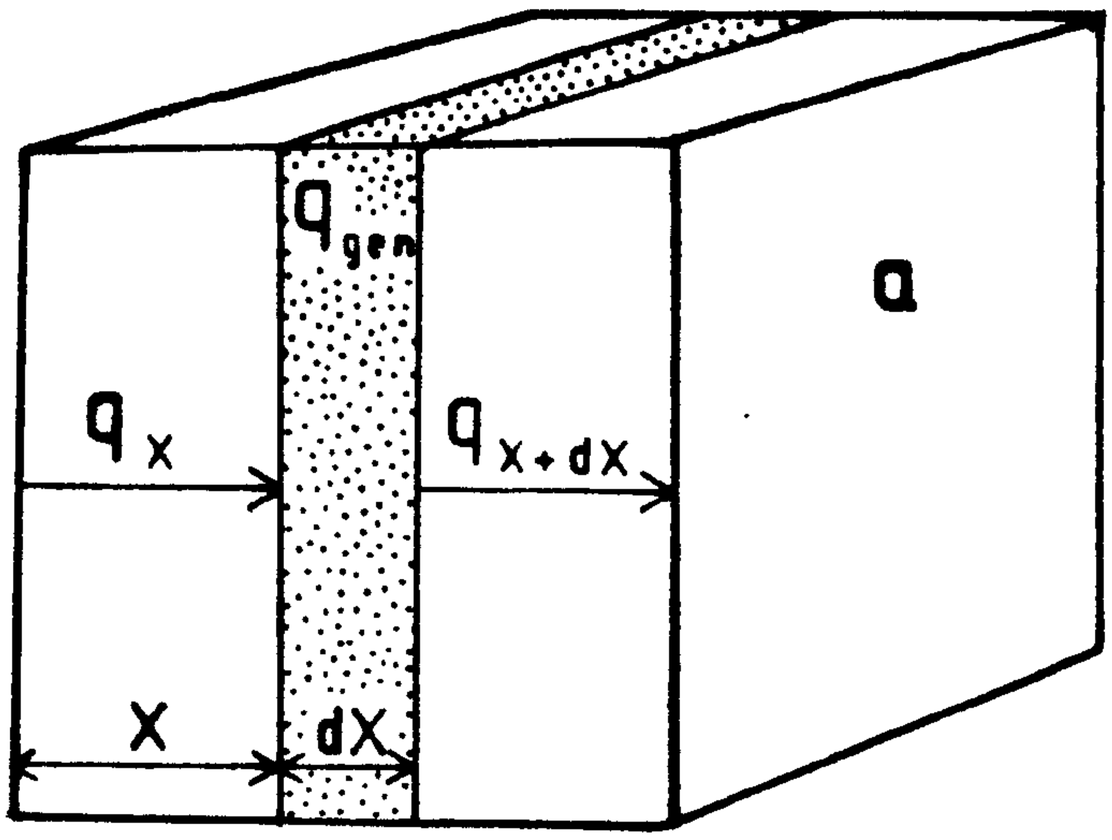
$q_{gen}$
q
$q_x$
$q_{x+dx}$
x
dx


Y
$\partial f(x, y_0)/\partial x$
$f(x+\delta x, y_0)$
$f(x, y_0)$
$f(x-\delta x, y_0)$
$f(x, y_0)$
A
B
C
$x-\delta x$
x
$x+\delta x$
X

The last term follows because

$$\frac{\partial T}{\partial x}\Big)_{x+\partial x} = \frac{\partial T}{\partial x} \; \partial x \frac{\partial}{\partial x}\left(\frac{\partial T}{\partial x}\right).\partial x$$

Substituting these terms into the energy balance equation above yields

$$K a\frac{\partial T}{\partial x} + \dot{q} a \partial x = C a \frac{\partial T}{\partial t} \partial x \quad a\left(K\frac{\partial T}{\partial x} + \frac{\partial}{\partial x}\left(K \frac{\partial T}{\partial x}\right).\partial x\right)$$

Collecting terms and eliminating, gives

$$x\left(K\frac{\partial T}{\partial x}\right) + \dot{q} = \rho C \frac{\partial T}{\partial t}$$

If K is independant of X, this reduces to

$$K\frac{\partial^2 T}{\partial x^2} + \dot{q} = \rho C \frac{\partial T}{\partial t}$$

This equation describes the change in temperature with time of the element of material under consideration. This equation may be integrated , yielding an analytical solution for the temperature distribution throughout the body, providing that the starting and boundary conditions are suitably defined. The starting conditions are defined by describing the temperature distribution at some fixed but arbitary time, and the boundary conditions by fixing the temperature at the edge of the body for 'all time' or by fixing the heat flow there for 'all time' (the derivative boundary condition). The results of integrations for certain boundary and starting conditions are presented by Carslaw and Jaeger (1959).

In many situations, including those in geology, simple starting and boundary conditions are unrealistic, and it is not possible to integrate the partial differential equation for the more realistic situations that arise. Numerical methods of solution are a

well-known method for such situations. The finite difference technique has been particularly succesful in geological contexts (eg England and Richardson, 1977; Graham and England, 1976; Richardson and England, 1979; Wells, 1980)

## A2.2 Finite difference methods

The finite difference technique can be used to approximate partial differentials and thus to solve partial differential equations. Finite difference methods are approximate in the sense that the derivatives at point are approximated by difference quotients over a small interval, ie $\partial\phi/\partial X$ is replaced by $(\phi(x+\delta_x)-(\phi(X))/\delta X$.

Consider a function of X and Y, f(X,Y) at a constant value of Y ($=Y_o$) (see fig A2.2)

$$\frac{\partial F(X, Y_o)}{\partial X} \qquad \frac{AB}{\delta X} \qquad \frac{BC}{\delta X} \qquad \frac{AC}{\delta X}$$

Or, in terms of differences

$$\frac{\partial F(X,Y_o)}{\partial X} \simeq \frac{F(X+\delta X, Y_o) - F(X, Y_o)}{\delta X} \quad \text{forward difference}$$

$$\simeq \frac{F(X, Y_o) - F(X-\delta X, Y_o)}{\delta X} \quad \text{backward difference}$$

$$\simeq \frac{F(X+\delta X, Y_o) - F(X-\delta X, Y_o)}{2\,\delta X} \quad \text{central difference}$$

If, as is usually the case, F(X,Y)/ X is to be calculated at a series of points, it is convenient to construct a grid of points or nodes with a constant spacing in the X and Y directions. These nodes each bear an integer label (fig A2.3). In terms of the heat flow equation, or temperature is considered as a function of distance and time, so i=0 corresponds to the earth's surface and increasing i to increasing depth. Each

Fig. A2.3 The division of 2 - D space into a series of nodes (not necessarilly equispaced ) at which values of f(x,y) may be calculated using finite - difference approximations.

Fig. A2.4 The movement of the lower boundary of a finite - difference grid between time steps j = 1 and j = 2 . The boundary has moved a distance $\Delta S$, so when j = 2 the distance between the two lower nodes is $\Delta X - \Delta S$.

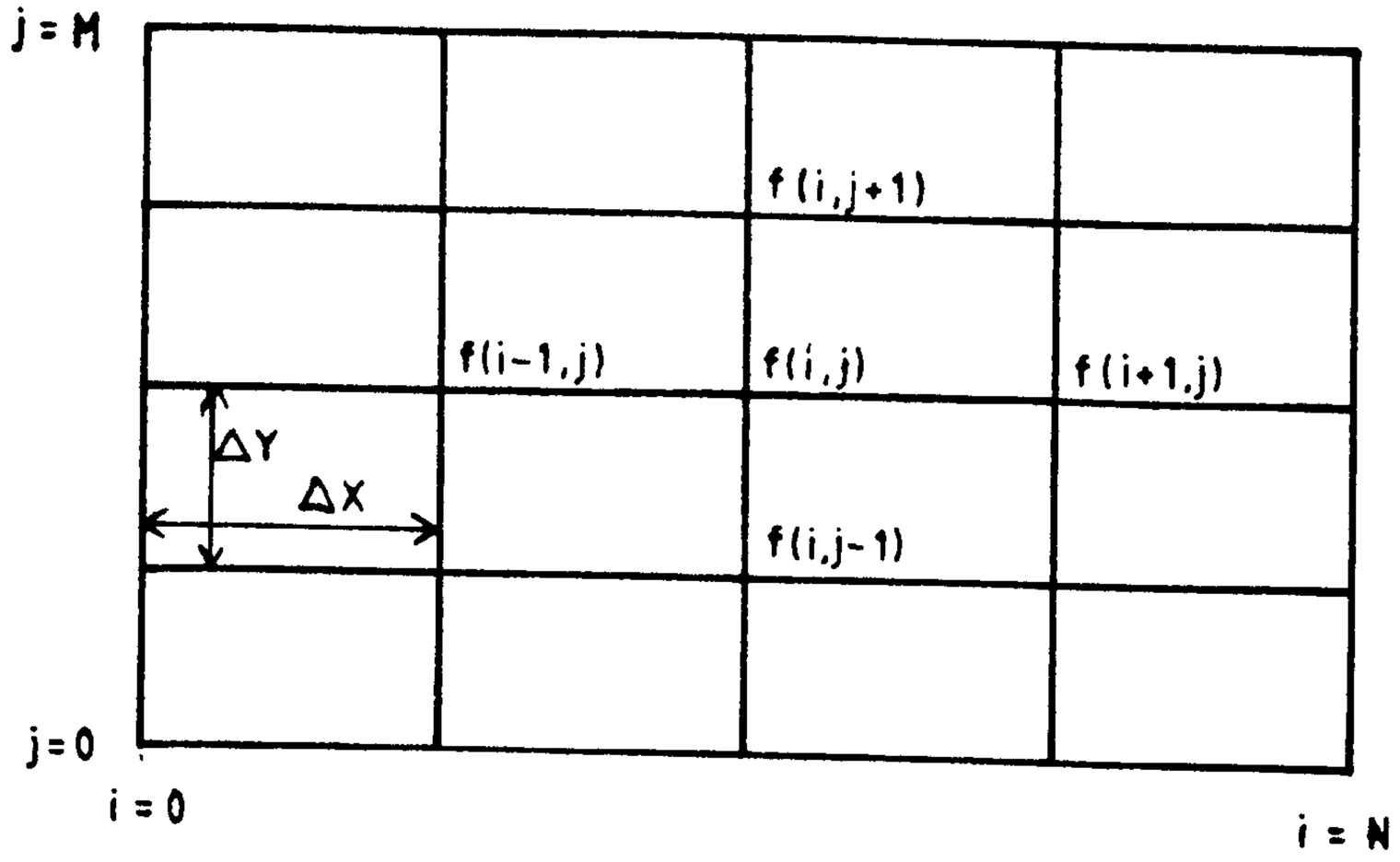
j = M
f(i,j+1)
f(i-1,j)
f(i,j)
f(i+1,j)
ΔY
ΔX
f(i,j-1)
j=0
i = 0
i = N

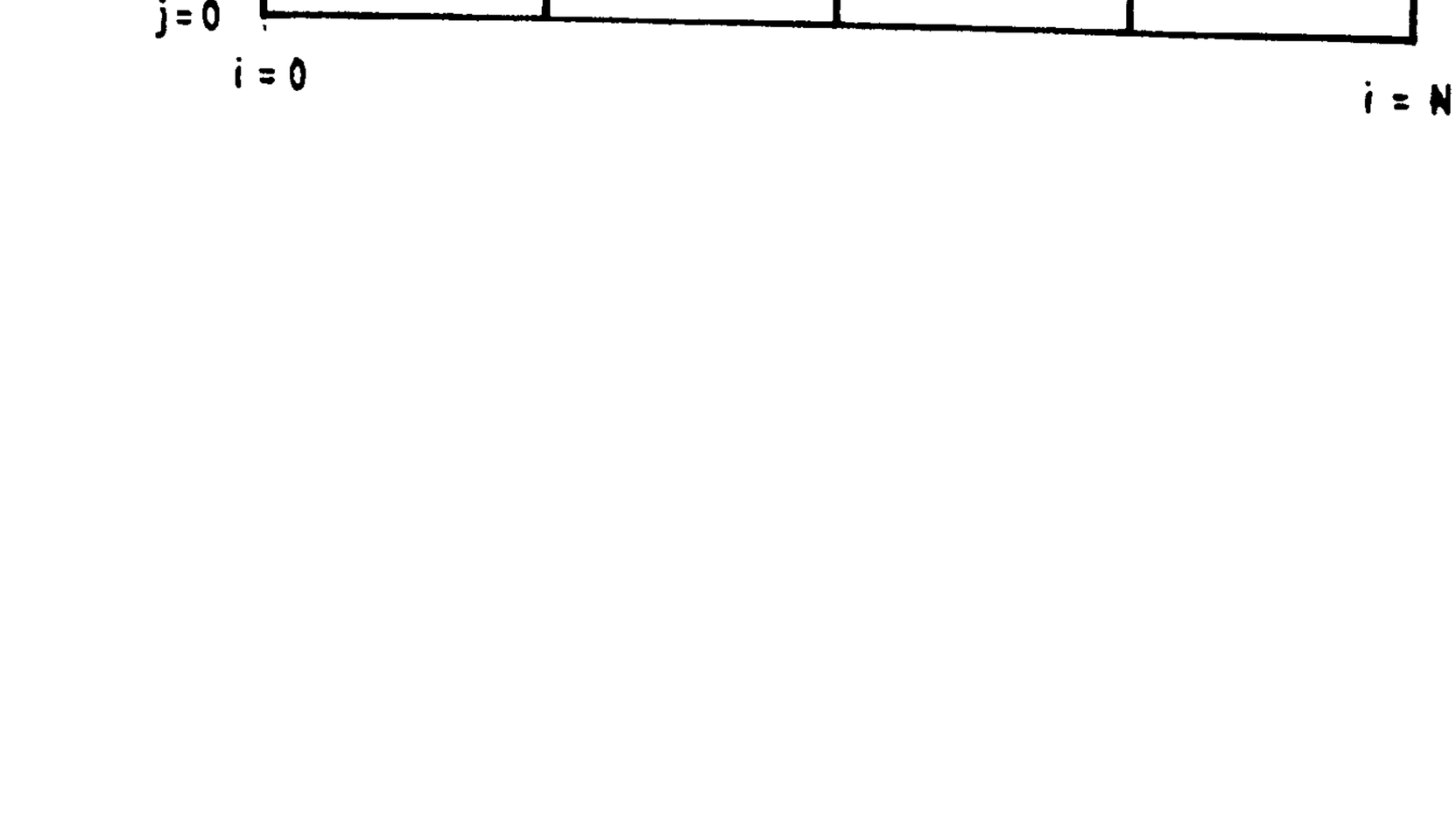
j = 1
N-3
N-2
N-1
N
Δx
Δx
j = 2
Δx
Δx-Δs
Δs

increment in j corresponds to an increment of time. Now:

$$\frac{\partial f(X,Y)}{\partial X} \simeq \frac{f(i+1,j) - f(i,j)}{\delta X} \qquad \text{A2.2}$$

Higher derivatives may also be approximated by higher differences. To obtain $\partial^2 f/\partial X^2$ the forward difference for the second derivative is taken, using backward differences for the first derivatives (to avoid a bias in the second derivative). Thus:

$$\frac{\partial^2 F}{\partial X^2} = \left(\frac{\partial F(i+1,j)}{\partial X} - \frac{\partial F(i,j)}{\partial X}\right)\Big/\delta X = \frac{1}{\delta X}\left(\frac{F(i+1,j)-F(i,j)}{\delta X} - \frac{F(i,j)-F(i-1,j)}{\delta X}\right)$$

$$= \frac{1}{\delta X^2}\left(F(i+1,j) - 2F(i,j) + F(i-1,j)\right)$$

and similarly:

$$\frac{\partial^2 F}{\partial Y^2} = \frac{1}{\delta y^2}\left(F(i,j+1) - 2F(i,j) + F(i,j-1)\right)$$

## A2.2.1 Application

These finite difference approximations are used by substituting them into the partial differential equation to be solved. In time dependant equations, such as those resulting from the analysis of heat flow and diffusion problems, the solution at times greater than zero may be obtained directly from a given set of starting and boundary conditions. If time is varying along f the j lines of the grid, then the initial or starting conditions are given along the j=0 line and the boundary conditions along the i=1 and i=n lines for all j. A method that yields f(i,j) directly from the difference equations is said to be explicit, whereas one that requires the solution of a set of simultaneous equations over the whole grid is said to be implicit. One widely used implicit method is that due to Crank and Nicholson (1949). A discussion of the use of finite difference

methods in the solution of differential equations is given by Smith (1978).

Consider, for example, the solution of the partial differential equation:

$$K\frac{\partial^2 T}{\partial t^2} = \rho C\frac{\partial T}{\partial t}$$

where K is thermal conductivity, $\rho$ density, C heat capacity, T temperature and t time. The differential equation can be replaced with a difference equation by making the following substitutions:

$$\frac{\partial^2 T}{\partial X^2} = \frac{1}{\Delta X^2}\left(T(i+1,j) - 2T(i,j) + T(i-1,j)\right)$$

$$\frac{\partial T}{\partial t} = \frac{1}{\Delta t}\left(T(i,j+1) - T(i,j)\right)$$

Hence:

$$\frac{K}{\Delta X^2}\left(T(i+1,j) - 2T(i,j) + T(i-1,j)\right) = \rho C\frac{\left(T(i,j+1) - T(i,j)\right)}{\Delta t}$$

which can be re-arranged to give $T(i,j+1)$ as the subject solution:

$$T(i,j+1) = RT(i+1,j) + (1-2R)T(i,j) + RT(i-1,j) \qquad \text{where} \quad R = \frac{K\Delta T}{\rho C\Delta X^2} \qquad \text{A2.4}$$

One of these equations must be constructed for each grid point, after substituting in the boundary conditions for $T(i,j)$ and $T(n,j)$.

$$\begin{aligned} T(2,j+1) &= RT(3,j) + (1-2R)T(2,j) + RT(1,j) \\ T(3,j+1) &= RT(4,j) + (1-2R)T(3,j) + RT(2,j) \\ &\vdots \\ T(N-1,j+1) &= RT(N,j) + (1-2R)T(N-1,j) + RT(N-2,j) \end{aligned}$$

For stable solutions, R must be less than 0.5, otherwise errors oscillating on either side of the actual solution grow with increasing time.

Equations of this form may be used to examine the heating of an area of country rock by an intrusion at one end of

the grid. One of the boundary coditions is a fixed temperature, that of the intrusion, the other is the (constant) temperature of the country rock outside the region of influence of the intrusion. As R needs to be small to maintain stable solutions, large amounts of computation may be needed to study long-term thermal effects.

A2.3 Crank-Nicholson methods

The rather restrictive criterion that R must be less than 0.5 for stable solutions may be avoided by using the Crank-Nicholson method. It may still be wise to keep R reasonably small for accurate solutions. In the Crank-Nicholson method, partial differentials are replaced by the averages of them at the begining and end of each time step, corresponding to the value of that derivative at the centre of that time step. This is done because the expression use to replace $\partial T/\partial t$ may be regarded as a central difference about $J=J+\frac{1}{2}$. Therefore, the equation:

$$\kappa \frac{\partial^2 T}{\partial X^2} = \rho c \frac{\partial T}{\partial t}$$

may be approximated by:

$$\frac{K}{2}\left( \frac{T(i+1,j)-2T(i,j)+T(i-1,j)}{\Delta X^2} + \frac{T(i+1,j+1)-2T(i,j+1)+T(i-1,j+1)}{\Delta X^2} \right) = \rho c \left( \frac{T(i,j+1)-T(i,j)}{\Delta t} \right)$$

Central diff. at $t=j$ ; $t=j+1$ ; $t=j/2$

When this is rearranged, the Crank-Nicholson formula is obtained:

$$-RT(i+1,j+1)+(2+2R)T(i,j+1)-RT(i-1,j+1) = RT(i+1,j)+(2-2R)T(i,j)+RT(i-1,j) \qquad \text{A2.5}$$

As can be seen, $T(i,j+1)$ is not given directly. The equations

must be constructed for all the grid points and then solved simultaneously, giving all the unknown temperatures at J+1.

$$-RT(3,j+1)+(2+2R)T(2,j+1)-RT(1,j+1)=RT(3,j)+(2-2R)T(2,j)+RT(1,j)$$
$$-RT(4,j+1)+(2+2R)T(3,j+1)-RT(2,j+1)=RT(4,j)+(2-2R)T(3,j)+RT(2,j)$$
$$\vdots$$
$$-RT(N,j+1)+(2+2R)T(N-1,j+1)-RT(N-2,j+1)=RT(N,j)+(2-2R)T(N-1,j)+RT(N-2,j)$$

As the system is tridiagonal, Gaussian elimination offers the best method of solution in terms of storage and speed (Gerald, 1978)

A2.3.1 Boundary conditions

In geological problems imvolving the temperature distribution down through the crust, the upper boundary of the crustal pile is usually taken as 0 °C, and the lower boundary is treated as having a constant heat flow. Therefore

$$F = -K\partial T/\partial X \qquad \text{A2.6}$$

where F is the heat flux in or out. Using a fictitious point, NP at NX+1 yields:

$$\frac{\partial T}{\partial X} = \frac{T(NP)-T(NX-1)}{2\Delta X}$$

Hence the temperature of the fictitious point may be obtained:

$$T(NP) = \frac{F}{K}2\Delta X + T(NX-1)$$

Equations of this form can then be substituted in to an equation of the form of A2.4 or A2.5 at depth NX

A2.3.2 The effects of erosion

Erosion must be accounted for in the heat flow equation by the addition of a term $U\partial X/\partial T$ to allow for the convection of heat within the material, where U is the velocity of the material in the direction of

increasing X (Carslaw and Jaeger, 1959, 388).

The finite difference representation of this is obviously simple, using the Crank-Nicholson representation of the partial differential. An additional factor to be considered is that the lower boundary of the material is now moving. This may be modelled by moving the boundary past the grid (see fig.A2.4).

Using a derivative boundary condition like A2.6 gives

$$\frac{\partial T}{\partial X} = \frac{T(NP) - T}{2\Delta X - \Delta S} = \frac{-F}{K}$$

and hence $T(NP)$ may be found rearrangement:

$$T(NP) = -\frac{F}{K}(2\Delta X - \Delta S) + T(NX-1)$$

which may be calcualted for the J and J+1 th steps, and substituted into an equation of the form of A2.4 or A2.5 for the NX point.

A2.3.4 Latent heat of crystallisation

Latent heat of crystallisation may also be accounted for, as shown by Wells (1980). A term $L \rho \partial V/\partial t$ where L is the latent heat of fusion and $\partial V/\partial t$ is the derivative of the volume fraction of melt crystallised with respect to time . Assuming that the volume of crystals varies linearly with temperature between the liquidus and solidus:

$$V = bT + a$$

where a is a constant and b is given by $b = 1/(T_l - T_s)$ where $T_l$ is the liquidus temperature and $T_s$ the solidus

temperature. Under these circumstances

$$\frac{\partial V}{\partial T} = \frac{1}{T_l - T_s} \cdot \frac{\partial T}{\partial t} \qquad \text{while} \quad T_l > T > T_s \qquad \text{A2.7}$$

which can be used in writing a finite differnce representation of the now modified heat flow equation.

## A2.4 Generalised heat flow equation

The program listed in appendix 3 solves the generalised heat flow equation

$$\rho C \frac{\partial T}{\partial t} = K \frac{\partial^2 T}{\partial X^2} + \dot{q} + U \frac{\partial T}{\partial x} \quad L\rho \frac{\partial V}{\partial t} \qquad \text{A2.8}$$

with a fixed upper boundary temperature of 0°C and a constant flux, optionally moving lower boundary. It reproduces the analytical solution of Carslaw and Jaeger (1959,p388) (for a region moving with velocity U, a linear initial temperature gradient and uniform heat generation throughout) to within a few % over 100 Myr (using T=1.0 Myr and X=1.0 km). Reduction of T to 0.25 Myr has a small (>0.5%) effect on the results. This is the nearest to geologically reasonable situation that has been solved by integration. The program may also be used for a layered crust, but care is advised as the treatment of discontinuities in changes of K,etc with X may be inaccurate in detail.

# Appendix 3 Computer programmes

Included in this appendix are three programmes written in FORTRAN and running on the Honeywell 6080 at UCW Aberystwyth. They are

(a) The MIN package for recasting mineral analyses and calculating the activities of end-members and the errors in those activities.

(b) PERROR, as an example of determining the error in calculated quantity (in this case the pressure given by the barometer of Chapter 6).

(c) HEATFLOW, a programme to solve the generalsed heat-flow equation summarised in section A2.4. This programme was written in 1977 and is in cgs units, although parameters are quoted in SI units in Chapter 8. It is simple to convert the programme to run in SI units.

```
C MIN package
C  This package of routines will recalcualte a mineral anlysis to atoms,
Cand determibe the errors on those atom proportions, assuming  a2% error
C for each element in the analysis. The programme will also calcualte
C the amount of various end-members, using the approach presented in
C appandix 1. The end-members calculted are governed by the name
C of the analysis.
C                                                    AC Barnocoat
C                                                     March 1979
C                                                    Last revised April 1982
C
      DIMENSION IEL(90),WTPC(90),NAME(20),CPROP(90),OXMOL(90),TITLE(30)
     1,SIG(90),ERRACT(10),ERRLA(10),PCERR(10),PCERLA(10),ACTI(10),
     2 ACTLN(10)
       EXTERNAL GTACT,FSPACT,OLACT,PXACT,AMACT,SPACT
      COMMON/MINDAT/MINNAM(2,25),NOXMIN(25),MINCAT(25)/OXDATA/MOLWT(90)
     1,NOXOX(90),CATPOX(90),OXNAM(2,90),NAMION(90)
      DATA TITLE/30*' '/
      IN=5
      IOUT=6
      READ(IN,50) (TITLE(I),I=1,30)
   50 FORMAT(30A1)
      WRITE (IOUT,61)
      WRITE(IOUT,62)
      WRITE(IOUT,60) TITLE
      WRITE(IOUT,62)
      WRITE(IOUT,61)
   60 FORMAT(1X,'*',T4,30A1,T41,'*')
   61 FORMAT(1X,'****************************************')
   62 FORMAT(1X,'*',T41,'*')
   10 DO 5 I=1,90
         IEL(I)=0
    5 CONTINUE
      IFLAG=0
      WRITE(6,20)
   20 FORMAT(/,1X,'************************************************'
     1,'************************************************')
C
C Read in and rocess the analysis
C
      CALL ANALIN(IN,NAME,IEL,WTPC,MORE,NEL)
      WRITE(IOUT,40)
   40 FORMAT(/)
      CALL MINID(NAME,MINNUM)
      IF(MINNUM.EQ.0) GOTO 30
      IF (MINNUM.EQ.6 .OR. MINNUM.EQ.8) NEL=NEL+1
   70 CALL RECAST(IEL,WTPC,NEL,MINNUM,CPROP,TOTWT,TOTCAT,OXMOL,SIG)
      CALL PRINTA (NAME,MINNUM,IEL,WTPC,CPROP,NEL,TOTWT,TOTCAT,SIG)
C
C Branch to appropriate part of programme depending
C on MINNUM, determined by MINID.
C
      GOTO(200,100,300,300,300,550,400,500),MINNUM
  100  CALL GTACT(NEL,CPROP,IEL,ACTI,ACTLN,4)
      WRITE(6,1000)(ACTI(I),I=1,4),(ACTLN(I),I=1,4)
 1000 FORMAT(10X,'PYROPE',6X,'ALMANDINE',6X,'GROSSULAR',8X,'M5C1',
```

```
     1 /,1X,'ACTIVITY',2X,4(F8.6,4X),/,1X,'LNACT',4X,4(F7.3,4X))
      CALL ACTERR(ERRACT,ERRLA,PCERR,PCERLA,4,GTACT,WTPC,NEL,MINNUM,IEL,
     1 ACTI,ACTLN)
      WRITE(6,1001)(ERRACT(I),I=1,4),(PCERR(I),I=1,4)
1001 FORMAT(1X,'ERRACT',3X,4(F8.6,3X),/,1X,'%',1X,
     1 8X,4(F8.6,3X))
      WRITE(6,1002)(ERRLA(I),I=1,4),(PCERLA(I),I=1,4)
1002 FORMAT(1X,'LA',6X,4(F7.3,5X),/,1X,'%',9X,
     1 4(F7.3,4X))
      GOTO 600
 200  CALL FSPACT(NEL,CPROP,IEL,ACTI,ACTLN,3)
      WRITE(6,2000)(ACTI(I),I=1,3),(ACTLN(I),I=1,3)
2000 FORMAT(10X,'ALBITE',4X,'ORTHOCLASE',4X,'ANORTHITE',/,
     1 1X,'ACTIVITY',1X,F8.6,3X,F8.6,4X,F8.6
     2 ,/,1X,'LNACTI',4X,F7.3,5X,F7.3,6X,F7.3)
      CALL ACTERR(ERRACT,ERRLA,PCERR,PCERLA,3,FSPACT,WTPC,NEL,MINNUM,
     1        IEL,ACTI,ACTLN)
      WRITE(6,2001)(ERRACT(I),I=1,3),(PCERR(I),I=1,3)
2001 FORMAT(1X,'ERRACT'4X,F8.6,4X,F8.6,5X,F8.6,/,1X,'%',9X,
     1 F8.4,4X,F8.4,5X,F8.4)
      WRITE(6,2002)(ERRLA(I),I=1,3),(PCERLA(I),I=1,3)
2002 FORMAT(1X,'ERRLA',5X,F7.4,5X,F7.4,6X,F7.4,/,1X,'%',10X,
     1 F8.4,4X,F8.4,4X,F8.4)
      GOTO 600
 300  CALL PXACT(NEL,CPROP,IEL,ACTI,ACTLN,10)
      WRITE(6,3000)(ACTI(J),J=1,10),(ACTLN(J),J=1,10)
3000 FORMAT(1X,9X,'DIOPSIDE',2X,'ENSTATITE',2X,'JADEITE',2X,'JADEITE(L'
     1 ,'RO',2X,'CATS',2X,'CATS(1100-1300)',2X,'CATS(1300>)',2X,
     2 'XCAM2',5X,'XMGM2',5X,'XFEM2',/,10X,6(F8.6,2X),4(5X,F8.6),/,
     3 10X,6(F8.4,2X),4(5X,F8.4))
      CALL ACTERR(ERRACT,ERRLA,PCERR,PCERLA,10,PXACT,WTPC,NEL,MINNUM,
     1            IEL,ACTI,ACTLN)
      WRITE(6,3001)(ERRACT(I),I=1,10),(PCERR(I),I=1,10)
3001 FORMAT(1X,'ERRACT',4X,6(F8.6,2X),4(5X,F8.6),/,1X,'%',9X,6(F8.4
     1 ,2X),4(5X,F8.4))
      WRITE(6,3002)(ERRLA(I),I=1,10),(PCERLA(I),I=1,10)
3002 FORMAT(1X,'ERRLA',5X,6(F8.6,2X),4(5X,F8.6),/,1X,'%',6(F8.4,2X)
     1 ,4(5X,F8.4))
      GOTO 600
 400  CALL OLACT(NEL,CPROP,IEL,ACTI,ACTLN,2)
      WRITE(6,4000)(ACTI(I),I=1,2),(ACTLN(I),I=1,2)
4000 FORMAT(10X,'FORSTERITE',1X,'FAYALITE',/,1X,'ACTIVITY',2X,
     1 2(F8.6,1X),/,'LNACT',5X,2(F8.4,1X))
      CALL ACTERR(ERRACT,ERRLA,PCERR,PCERLA,2,OLACT,WTPC,NEL,MINNUM,IEL,
     1            ACTI,ACTLN)
      WRITE(6,4001)(ERRACT(I),I=1,2),(PCERR(I),I=1,2)
4001 FORMAT(1X,'ERRACT',4X,2(F8.6,1X),/,1X,'%',9X,2(F8.4,1X))
      WRITE(6,4002)(ERRLA(I),I=1,2),(PCERLA(I),I=1,2)
4002 FORMAT(1X,'ERRLA',5X,2(F8.4,1X),/,1X,'%',9X,2(F8.4,1X))
      GOTO 600
 500  CALL AMACT(NEL,CPROP,IEL,ACTI,ACTLN,2)
      WRITE(6,5000)(ACTI(I),I=1,2),(ACTLN(I),I=1,2)
5000 FORMAT(1X,9X,'TREMOLITE',2X,'PARGASITE',/,1X,'ACTIVITY',2X,2(F8.6,
     1 1X),/,1X,'LNACTI',4X,2(F8.4,1X))
      CALL ACTERR(ERRACT,ERRLA,PCERR,PCERLA,2,AMACT,WTPC,NEL,MINNUM,IEL,
     1            ACTI,ACTLN)
```

```
      WRITE(6,5001)(ERRACT(I),I=1,2),(PCERR(I),I=1,2)
 5001 FORMAT(1X,'ERRACT',4X,2(F8.6,1X),/,'%',9X,2(F8.3,1X))
      WRITE(6,5002)(ERRLA(I),I=1,2),(PCERLA(I),I=1,2)
 5002 FORMAT(1X,'ERRLA',5X,2(F8.4,1X),/,1X,'%',9X,2(F8.4,1X))
      IF (IFLAG.EQ.1) GOTO 600
C
C Amphiboles are recalculated so 40% of iron is trivalent
C
      WRITE(6,5003)
 5003 FORMAT(1X,'RECALC FOR FE3+ (40%)')
      IFLAG=1
      CALL FE3CAL(WTPC,NEL,IEL,0.2)
      GOTO 70
  550 IF (IFLAG.GT.0) GOTO 551
C
C Spinels are recalcualted so they fit the stoichiometric formula R3O4
C
      CALL FECAST(MINNUM,WTPC,NEL,IEL)
      IFLAG=1
      GOTO 70
  551 CALL SPACT (NEL,CPROP,IEL,ACTI,ACTLN,1)
      WRITE (6,5500) ACTI(1),ACTLN(1)
 5500 FORMAT(10X,'SPINEL',/,1X,'ACTIVITY',2X,F8.6,/,1X,'LNACTI',4X,F7.3)
      CALL ACTERR(ERRACT,ERRLA,PCERR,PCERLA,1,SPACT,WTPC,NEL,MINNUM,IEL,
     1            ACTI,ACTLN)
      WRITE(6,5501) ERRACT(1),PCERR(1)
 5501 FORMAT(1X,'ERRACT',4X,F8.6,/,1X,'%',9X,F8.4)
      WRITE(6,5502) ERRLA(1),PCERLA(1)
 5502 FORMAT(1X,'ERRLA',5X,F8.4,/,1X,'%',9X,F8.4)
  600 IF (MORE.LT.-1) STOP
       GOTO 10
   30 WRITE(6,35) NAME
   35 FORMAT(////,' UNKNOWN MINERAL ',20A1,/,'RENAME,EG AS "UN"')
      IF(MORE.LT.-1) STOP
      GOTO 10
      END



      SUBROUTINE ANALIN (IN,NAME,IEL,WTPC,MORE,NEL)
C
C Read in analysis from inputchannel IN
C
      DIMENSION IE(9),IEL(90),WT(9),WTPC(90),NAME(20)
      READ(IN,100,END=5) (NAME(I),I=1,20)
  100 FORMAT(20A1)
    GOTO 6
  5 STOP
  6 DO 10 I=1,10
      READ (IN,200,END=5)(IE(J),WT(J),J=1,9)
200    FORMAT(9(I3,F6.0))
     IF (IE(1).LE.-1) GOTO 20
    DO 30 IJ=1,9
     IF (IE(IJ).LT.1) GOTO 10
     NEL=(I-1)*9+IJ
      IEL(NEL)=IE(IJ)
```

```
      WTPC(NEL)=WT(IJ)
   30   CONTINUE
   10 CONTINUE
   20 MORE=IE(1)
      NEL=NEL+2
      RETURN
      END


      SUBROUTINE RECAST (IEL,WTPC,NEL,MINNUM,CPROP,TOTWT,TOTCAT,OXMOL
     1,SIG)
C
C This routine recasts a weight % analysis of 'NEL' elements to atomic
C proportions which are stored in 'CPROP'. Molecular weights and no. of
C cations/oxygen, etc. are taken from common arrays initialised in a
C BLOCK DATA Subroutine.(A.C.BARNICOAT : 1980)
C                        (MODIFIED MARCH 1982)
C
      COMMON/MINDAT/MINNAM(2,25),NOXMIN(25),MINCAT(25)/OXDATA/MOLWT(90)
     1,NOXOX(90),CATPOX(90),OXNAM(2,90),NAMION(90)
      REAL MOLWT
      DIMENSION IEL(NEL),WTPC(NEL),CPROP(NEL),OXMOL(NEL),SIG(NEL)
      TOTMOL=0.
      TOTWT=0.
      TOTCAT=0.
C
C Calculate the number of moles of oxygen from each element
C and total.
C
      DO 10 I=1,NEL
       IF (IEL(I).EQ.0) GOTO 10
      IIEL=IEL(I)
        OXMOL(I)=(WTPC(I)/MOLWT(IIEL))*NOXOX(IIEL)
        TOTMOL=TOTMOL+OXMOL(I)
        TOTWT=TOTWT+WTPC(I)
   10 CONTINUE
C
C Calculate multiplication factor to convert analysis to   'N'
C oxygens,then calculate number of cations associated
C with each oxygen,and put into 'CPROP'.
C
      FACTOR=NOXMIN(MINNUM)/TOTMOL
      DO 20 I=1,NEL
      IF(IEL(I).EQ.0) GOTO 20
         IIEL=IEL(I)
        CPROP(I)=OXMOL(I)*FACTOR*CATPOX(IIEL)
        TOTCAT=TOTCAT+CPROP(I)
   20 CONTINUE
C
C This section calculates the errors in numbers of atoms, assuming
C a 2% imprecision in anlysed wt%. It uses a generalised form (equation
C A1. ) of the equation given by Powell(1978b), pp126-7
C
      DO 30 J=1,NEL
      SIGSQ=0.
      IF (IEL (J).EQ.0) GOTO 30
```

```
      JIEL=IEL(J)
     DO 40 I=1,NEL
     IF (I.EQ.J) GOTO 35
     IF (IEL(I).EQ.0) GOTO 40
     IIEL=IEL(I)
     SIGSQ=SIGSQ+((((FACTOR*FACTOR)/NOXMIN(MINNUM)*NOXOX(IIEL)
    1/MOLWT(IIEL)*WTPC(J)*CATPOX(JIEL)/MOLWT(IIEL))**2)*(0.02*WTPC(I)
    2)**2)
     GOTO 40
35   SIGSQ=SIGSQ+((0.02*WTPC(I))**2)*((FACTOR/MOLWT(JIEL)-(CATPOX(JIEL)
    1*WTPC(J)/MOLWT(JIEL))*NOXOX(JIEL)/MOLWT(JIEL)*FACTOR*FACTOR/NOXMIN
    2(MINNUM))**2)
40   CONTINUE
     SIG(J)=SQRT(SIGSQ)
30   CONTINUE
     RETURN
     END


     SUBROUTINE MINID (NAME,MINNUM)
C
C This routine identifies the mineral species entitled 'NAME'
C and gives it an identifier number, 'MINNUM' ,used by later routines
C to select mineal-related data from labelled common 'MINDAT'.It uses
C that labelled common block to provide the standard mineral abbreviations
C used (A.C.BARNICOAT : 1980)
C
     COMMON /MINDAT/MINNAM(2,25),NOXMIN(25),MINCAT(25)
     DIMENSION NAME(20)
     NORT=0
     MINNUM=0
     DO 10 I=1,25
       IF (NAME(1).EQ.MINNAM(1,I)
    1    .AND.NAME(2).EQ.MINNAM(2,I)) MINNUM=I
      IF(MINNUM.GT.NORT) GOTO 20
10   CONTINUE
20   RETURN
     END


      SUBROUTINE PRINTA (NAME,MINNUM,IEL,WTPC,CPROP,NEL,TOTWT,TOTCAT
     1,SIG)
C
C This routine prints an analysis on the currently defined output
C channel,and also prints the calculated number of atoms and
C the weight and atom totals, together with the errors in the atom values.
C                                        (A.C.BARNICOAT : 1980(2))
C                                        (MODIFIED MARCH 1982)
C
     COMMON /OXDATA/MOLWT(90),NOXOX(90),CATPOX(90),OXNAM(2,90),NAMION
    1(90)/MINDAT/MINNAM(2,25),NOXMIN(25),MINCAT(25)
     DIMENSION NAME(20),IEL(NEL),WTPC(NEL),CPROP(NEL),SIG(NEL)
     WRITE (6,10) NAME
10   FORMAT(5X,20A1)
     WRITE (6,20) NOXMIN(MINNUM)
20   FORMAT(/,10X,'OXIDE',8X,'WT%',13X,'ATOMS FOR',I3,1X,
```

```
     1'OXYGENS',1X,'ERROR(ASSUMING 2% U/C IN WTPC)')
      DO 30 I=1,NEL
      IF(IEL(I).EQ.0) GOTO 30
       IIEL=IEL(I)
       WRITE (6,40) (OXNAM(J,IIEL),J=1,2),WTPC(I),NAMION(IIEL),CPROP(I)
     1,SIG(I)
40    FORMAT(10X,2A3,4X,F7.2,4X,A4,4X,F7.3,12X,F6.4)
30    CONTINUE
      WRITE (6,50) TOTWT,TOTCAT
50    FORMAT(20X,'-------',12X,'-------',/,12X,'TOTAL',3X,F7.3,12X,
     1F7.3)
      RETURN
      END
```

```
      SUBROUTINE FECAST(MINNUM,WTPC,NEL,IEL)
      COMMON /MINDAT/MINNAM(2,25),NOXMIN(25),MINCAT(25)/OXDATA/MOLWT(90)
     1,NOXOX(90),CATPOX(90),OXNAM(2,90),NAMION(90)
      REAL MOLWT
C
C This routine calculates the amount of FE3+ that should be present in
C a mineral to preserve its stoichiometry .Based on a routine used
C in Edinburgh,author unknown. (A.C.BARNICOAT : 1980)
C
      DIMENSION WTPC(NEL),IEL(NEL)
      IFE2=0
      IFE3=0
      CATNFE=0.
      TOTNFE=0.
C
C CALCULATE NUMBER OF NON-FE CATIONS AND OF OXYGENS IN NON-FE OXIDES
C
      DO 10 I=1,NEL
      IF(IEL(I).EQ.0) GOTO 10
      IIEL=(IEL(I))
      IF (IIEL.EQ.26.OR.IIEL.EQ.36) GOTO 15
      TOTNFE=TOTNFE+(NOXOX(IIEL)*WTPC(I)/MOLWT(IIEL))
      CATNFE=CATNFE+(CATPOX(IIEL)*NOXOX(IIEL)*WTPC(I)/MOLWT(IIEL))
      GOTO 10
   15 IF(IIEL.EQ.26) IFE2=I
      IF(IIEL.EQ.26) GOTO 10
      IFE3=I
   10 CONTINUE
      N=NEL
C
C SOLVE FOR FE2+ AND FE3+
C
      IF(IFE2.EQ.0) IEL(N-1)=26
      IF(IFE2.EQ.0) IFE2=N-1
      IF(IFE3.EQ.0) IEL(N-1) =36
      IF(IFE3.EQ.0) IFE3=N-1
      IF(IFE3.EQ.IFE2) IEL(N)=36
      IF(IFE2.EQ.IFE3) IEL(N-1)=26
      IF(IFE3.EQ.IFE2) IFE3=N
      CATRAT=FLOAT(NOXMIN(MINNUM))/FLOAT(MINCAT(MINNUM))
      R=(1.-CATRAT)/MOLWT(26)
```

```
      S=(3.-(CATRAT*2.))/MOLWT(36)
      T=.6994/.7773
      U=(CATRAT*CATNFE )-TOTNFE
      V=WTPC(IFE2)+(T*WTPC(IFE3))
      XJ=(R*T)-S
      XK=(U*T)-(S*V)
      XL=(R*V)-U
      WTPC(IFE2)=XK/XJ
      WTPC(IFE3)=XL/XJ
      RETURN
      END


      SUBROUTINE ACTERR(ERRACT,ERRLA,PCERR,PCERLA,NACT,ACTCALC,WTPC
     1                  ,NEL,MINNUM,IEL,ACTI,ACTLN)
C
C This routine calculates the error in the activity of a series of
C end-members caused by a 2% relative error in analysed wt percent. It
C does this by calculating the partial differential of activity
C with respect to wt% analysed (using a finite difference
C approximation) and then summing the products of this partial
C differential multiplied by the error in analysed wt% over all elements
C as suggested by R.Powell, and outlined in appendix 1.
C                                   A.C.Barnicoat March 1982
       DIMENSION ERRACT(NACT),ERRLA(NACT),PCERR(NACT),PCERLA(NACT),
      1           ACTI(NACT),ACTLN(NACT),WTPC(NEL),IEL(NEL),SIG(90),
      2          OXMOL(90),ACTIPL(10),ACTIMI(10),ACTLNP(10),ACTLNM(10),
      3        SIGSQ(10),SSLNA(10),PDACT(10),PDACTL(10),CPROP(90)
       INACT=NACT
       INEL=NEL
       DEL=0.00001
       DO 1 K=1,NACT
       SIGSQ(K)=0.
       SSLNA(K)=0.
     1 CONTINUE
C
C RECALCULATE THE ANALYSIS AND ACTIVITITES FOR WTPC(I)+DEL
C AND WTPC(I)-DEL
C
       DO 10 I=1,NEL
       WTPC(I)=WTPC(I)+DEL
       CALL RECAST(IEL,WTPC,INEL,MINNUM,CPROP,TOTWT,TOTCAT,OXMOL,SIG)
       CALL ACTCALC(INEL,CPROP,IEL,ACTIPL,ACTLNP,INACT)
       WTPC(I)=WTPC(I)-2.*DEL
       CALL RECAST(IEL,WTPC,INEL,MINNUM,CPROP,TOTWT,TOTCAT,OXMOL,SIG)
       CALL ACTCALC(INEL,CPROP,IEL,ACTIMI,ACTLNM,INACT)
C
C CALCULATE THE PARTIAL DIFFERENTIAL D(ACTIVITIES)/D(WTPC(I) FOR
C ALL END-MEMBERS, AND ADD THE RELEVANT CONTRIBUTION TO THE
C TOTAL ERROR FOR THAT END-MEMBER
C
        DO 5 J=1,NACT
        PDACT(J)=(ACTIPL(J)-ACTIMI(J))/(2.*DEL)
        PDACTL(J)=(ACTLNP(J)-ACTLNM(J))/(2.*DEL)
       IF(IEL(I).EQ.36) GOTO 4
        SIGSQ(J)=SIGSQ(J)+(PDACT(J)**2)*((WTPC(I)*0.02)**2)
```

```
      SSLNA(J)=SSLNA(J)+(PDACTL(J)**2)*((WTPC(I)*0.02)**2)
      GOTO 5
 4    SIGSQ(J)=SIGSQ(J)+(PDACT(J)**2)*((WTPC(I)*0.5)**2)
      SSLNA(J)=SSLNA(J)+(PDACTL(J)**2)*((WTPC(I)*0.5)**2)
 5 CONTINUE
10 CONTINUE
   DO 20 J=1,NACT
      ERRACT(J)=SQRT(ABS(SIGSQ(J)))
      ERRLA(J)=SQRT(ABS(SSLNA(J)))
      PCERR(J)=(ERRACT(J)*100.)/ACTI(J)
      PCERLA(J)=ABS((ERRLA(J)*100.)/ACTLN(J))
20 CONTINUE
   RETURN
   END
```

```
      SUBROUTINE ORDEREL(NEL,CPROP,XCAT,IEL)
      DIMENSION XCAT(90),IEL(NEL),CPROP(NEL)
C
C Insert cation proportion of each element into the
C (ie one numbered with Atomic number) array element of 'XCAT' for ease
C of access.
C
      DO 1 I=1,90
      XCAT(I)=0.0
    1 CONTINUE
      DO 2 I=1,NEL
      IF (IEL(I).EQ.0) GOTO 2
      IIEL=IEL(I)
      XCAT(IIEL)=CPROP(I)
    2 CONTINUE
      RETURN
      END
```

```
      SUBROUTINE GTACT(NEL,CPROP,IEL,ACTI,ACTLN,NACT)
C
C This routine calculates the activities of garnet end-members
C
      DIMENSION XCAT(90),ACTI(NACT),ACTLN(NACT),CPROP(NEL),IEL(NEL)
      NNEL=NEL
      CALL ORDEREL(NNEL,CPROP,XCAT,IEL)
      SUM1=XCAT(12)+XCAT(26)+XCAT(25)+XCAT(20)
      SUM2=XCAT(13)+XCAT(36)+XCAT(24)
      XMG=XCAT(12)/SUM1
      XFE=XCAT(26)/SUM1
      XCA=XCAT(20)/SUM1
      XAL=XCAT(13)/SUM2
      XALSQ=XAL*XAL
      ACTI(1)=(XMG**3)*XALSQ
      ACTI(2)=(XFE**3)*XALSQ
      ACTI(3)=(XCA**3)*XALSQ
      ACTI(4)=(XMG**(5.))*(XCA**(1.))*XALSQ
      DO 10 I=1,NACT
            ACTLN(I)=ALOG(ACTI(I))
10 CONTINUE
```

```
      RETURN
      END


      SUBROUTINE FSPACT(NEL,CPROP,IEL,ACTI,ACTLN,NACT)
C
C This routine calculates ideal activities of feldspar end-members
C
      DIMENSION XCAT(90),ACTI(NACT),ACTLN(NACT),CPROP(NEL),IEL(NEL)
      NNEL=NEL
      CALL ORDEREL(NNEL,CPROP,XCAT,IEL)
      SUM=XCAT(11)+XCAT(19)+XCAT(20)
      ACTI(1)=XCAT(11)/SUM
      ACTI(2)=XCAT(19)/SUM
      ACTI(3)=XCAT(20)/SUM
      DO 1 I=1,NACT
        ACTLN(I)=ALOG(ACTI(I))
    1 CONTINUE
      RETURN
      END


      SUBROUTINE OLACT(NEL,CPROP,IEL,ACTI,ACTLN,NACT)
C
C This routine calculates ideal activities for olivine
C
      DIMENSION XCAT(90),ACTI(NACT),ACTLN(NACT),CPROP(NEL),IEL(NEL)
      NNEL=NEL
      CALL ORDEREL(NNEL,CPROP,XCAT,IEL)
      SUM=XCAT(12)+XCAT(20)+XCAT(26)+XCAT(28)
      ACTI(1)=(XCAT(12)/SUM)**2.
      ACTI(2)=(XCAT(26)/SUM)**2.
      ACTLN(1)=ALOG(ACTI(1))
      ACTLN(2)=ALOG(ACTI(2))
      RETURN
      END


      SUBROUTINE PXACT(NEL,CPROP,IEL,ACTI,ACTLN,NACT)
C
C This routine calculates ideal activities of pyroxene end-members
C
      DIMENSION XCAT(90),ACTI(NACT),ACTLN(NACT),CPROP(NEL),IEL(NEL)
      NNEL=NEL
      CALL ORDEREL(NNEL,CPROP,XCAT,IEL)
      XSIT=XCAT(14)/2.
      XALT=1.-XSIT
      IF (XALT.LT.0.) XALT=0.
      XALM1=XCAT(13)-2.*XALT
      XCAM2=XCAT(20)
      XNAM2=XCAT(11)
      IF (XNAM2.LT.0.) XNAM2=0
      REM1=1.-(XALM1+XCAT(22)+XCAT(24)+XCAT(36))
      FM=XCAT(26)/XCAT(12)
      XMGM1=REM1/(FM+1.)
      XMGM2=XCAT(12)-XMGM1
```

```
      XFEM2=FM*(XCAT(12)-(REM1/(FM+1.)))
      ACTI(8)=XCAM2
      ACTI(9)=XMGM2
      ACTI(10)=XFEM2
C
C CALCULATE ACTIVITIES OF DIOPSIDE,ENSTATITE,JADEITE,JADEITE (MOLECULAR
C MIXING) AND CATS (WOOD FORMULA;ALSO CORRECTED FOR FE/FE+MG)
C
      ACTI(1)=XCAM2*XMGM1*XSIT*XSIT
      ACTI(2)=XMGM2*XMGM1*XSIT*XSIT
      ACTI(3)=XNAM2*XALM1*XSIT*XSIT
      ACTI(4)=XNAM2
      IF (XNAM2.GT.XALM1) ACTI(4)=XALM1
   ACTI(5)=4.*XCAM2*XALM1*XALT*XSIT
   J=0
   X=0.1
99 J=J+1
   FX=2.*X*X-X*X*X-ACTI(5)
   F1X=4.*X-3.*X*X
   DX=FX/F1X
   X=X-DX
   IF (DX.LT.1.E-7) GOTO 95
   GOTO 99
95 ACTI(5)=X
   ACTI(6)=ACTI(5)*(1.3-0.4*XCAT(26)/(XCAT(12)+XCAT(26)))
   ACTI(7)=ACTI(5)*(1.1-0.3*XCAT(26)/(XCAT(12)+XCAT(26)))
   DO 100 I=1,NACT
     IF(ACTI(I).LE.0.) ACTLN(I)=0.
     IF(ACTI(I).LE.0.) GOTO 100
       ACTLN(I)=ALOG(ACTI(I))
  100 CONTINUE
      RETURN
      END


      SUBROUTINE AMACT (NEL,CPROP,IEL,ACTI,ACTLN,NACT)
C
C Routine to calculate ideal amphiboleAactivities,using the model of
C Powell(1978),and Cameron and Papike (1979)
C
      DIMENSION XCAT(90),ACTI(NACT),ACTLN(NACT),CPROP(NEL),IEL(NEL)
      NNEL=NEL
      CALL ORDEREL(NNEL,CPROP,XCAT,IEL)
      XSIT2=1.
       XSIT1=(XCAT(14)-4.)/4.
      XALT1=1.-XSIT1
      IF (XALT1.LT.0.) XALT1=0.
      XALM2=(XCAT(13)-4.*XALT1)/2.
      REM2=1.-(XALM2+(XCAT(36)+XCAT(24)+XCAT(22))/2.)
      XCAM4=XCAT(20)/2.
      XNAM4=0.5*(7.-(XCAT(26)+XCAT(12)+(XALM2*2.)+XCAT(36)+XCAT(22)
     1 +XCAT(24)+XCAT(25)+XCAT(20)))
      IF (XNAM4.LT.0.) XNAM4=0.0
      REM4=1.-(XCAM4+XNAM4)
      XNAA=XCAT(11)-XNAM4
      XVACA=1.-XNAA-XCAT(19)
```

```
      FM=XCAT(26)/XCAT(12)
      XMGM13=1./(FM+1.)
      XMGM2=REM2/(FM+1.)
      XMGM4=REM4/(FM+1.)
C
C CALCULATE ACTIVITIES OF TREMOLITE AND PARGASITE ASSUMING IDEALITY ON SITES
C
      ACTI(1)=XVACA*(XCAM4**2.)*(XMGM13**3.)*(XMGM2**2)*(XSIT1**4.)
      ACTI(2)=64.*XNAA*(XCAM4**2.)*(XMGM13**3.)*XMGM2*XALM2*(XSIT1**2.)
     1 *(XALT1**2.)
      DO 10 I=1,NACT
        ACTLN(I)=ALOG(ACTI(I))
   10 CONTINUE
      RETURN
      END


      SUBROUTINE SPACT(NEL,CPROP,IEL,ACTI,ACTLN,NACT)
C
C Routine to calculate the activity of spinel in spinel solid solutions.
C
      DIMENSION XCAT(90),ACTI(NACT),ACTLN(NACT),CPROP(NEL),IEL(NEL)
      NNEL=NEL
      CALL ORDEREL(NNEL,CPROP,XCAT,IEL)
      SUM1=XCAT(13)+XCAT(22)+XCAT(24)+XCAT(36)
      SUM2=XCAT(12)+XCAT(20)+XCAT(25)+XCAT(26)
      ACTI(1)=XCAT(12)/SUM2 * (XCAT(13)/SUM1)**2
      ACTLN(1)=ALOG(ACTI(1))
      RETURN
      END


      SUBROUTINE FE3CAL(WTPC,NEL,IEL,FRACT)
C
C Routine to convert 'FRACT' of iron to Fe3+
C
      INTEGER FE2
       DIMENSION WTPC(NEL),IEL(NEL)
      TOTWT=0.
      NM=NEL-1
      DO 10 I=1,NM
       TOTWT=TOTWT+WTPC(I)
       II=I
       IF (IEL(II).NE.26) GOTO 10
       FEMOL=WTPC(I)/71.85
       FE2=I
   10 CONTINUE
      TOTWT2=TOTWT-WTPC(FE2)
      FE3MOL=FEMOL*FRACT
      FE2MOL=FEMOL-FE3MOL
      WTPC(FE2)=FE2MOL*71.85
      WTPC(NEL)=FE3MOL*159.70/2.
      TOTWT2=TOTWT2+WTPC(FE2)+WTPC(NEL)
      FACTOR=TOTWT/TOTWT2
      IEL(NEL)=36
      DO 15 I=1,NEL
```

```
      WTPC(I)=WTPC(I)*FACTOR
   15 CONTINUE
      RETURN
      END


      BLOCK DATA
      REAL MOLWT
      COMMON /MINDAT/MINNAM(2,25),NOXMIN(25),MINCAT(25)/OXDATA/MOLWT(90)
     1,NOXOX(90),CATPOX(90),OXNAM(2,90),NAMION(90)
      DATA MINNAM/'P','L','G','T','C','P','O','P','P','X','S',
     1'P','O','L','A','M','B','I','C','H','S','T','C','O','C',
     2'D','A','F','K','S','M','U','C','T','E','P','I','L','L','W','M','T
     5','S','A',
     3'C','A','U','N','S','U'/NOXMIN/8,12,6,6,6,4,4,23,22,28,17,18,18,8
     6,8
     4,22,12,12,3,9,4,20,3,1,0/MINCAT/5,8,4,4,4,3,3,0,0,0,6*0,8,0,2,0,3
     5,4*0/
      DATA MOLWT/18.016,0.,29.88,25.013,69.64,44.01,2*0.,19.0,0.,61.982,
     140.329,101.94,60.09,141.95,80.066,35.457,0.,94.2,56.08,
     2137.92,79.9 ,181.9,152.02,70.94,71.85,74.94,74.71,79.54,81.38,5*0.
     1,159.7,10*0.
     3,9*0.,153.6,34*0./NOXOX/1,0,1,1,3,2,4*0,1,1,3,2,5,3,2*0,1,1,3,2,5,
     43,6*1,5*0,3,19*0,1,34*0/OXNAM/'H2O',' ',' ',' ','LI2','O','BEO','
     4 '
     5,'B2O','3','CO2',' ',4*' ','F',' ',' ',' ','NA2','O ','MGO',' ',
     6'AL2','O3','SIO','2','P2O','5','SO3',' ','CL',' ',' ',' ','K2O','
     6 '
     6,'CAO',' ','SC2','O3','TIO','2','V2','O5','CR2','O3','MNO',' ',
     6'FEO',' ','COO'
     7,' ','NIO',' ','CUO',' ','ZNO',' ',10*' ','FE2','O3',38*' ',
     8'BAO',69*' '/CATPOX/2.,0.,2.,1.,.66667,.5,4*0.,2.,1.,.66667,.5,.4,
     9.33333,0.,0.,2.,1.,.66667,.5,.4,.66667,6*1.,5*0.,.66667,19*0.,1.,
     934*0./NAMION/'H+',' ','LI2+','BE2+','B3+','C4+',2*' ','F',' '
     1,'NA+','MG2+','AL3+','SI4+','P5+','S6+','CL',' '
     2,'k+','Ca2+','Sc3+','Ti4+','V 5+','Cr3+','Mn2+','Fe2+','Co2+'
     3,'Ni2+','Cu2+','Zn2+',5*' ','Fe3+',19*' ','Ba2+',34*' '/
      END
```

```
C PERROR
C Programme to calculate errors in the pressure calculated using
C the barometer of chapter 5 when given the errors in
C compositions and thermodynamic data. The method described in
C Appendix 1 is used to calculate the error.
C                                                    AC Barnicoat
C                                                        May 1982
      DIMENSION TDATA(3),TDER(3),XDATA(5),XDER(5),ACDATA(4),
     1 ACDER(4)
  999 SIGSQ=0.
      WRITE(6,200)
  200 FORMAT(1X,'XGT,XAN,XSP,XOPX,XAB')
      READ,XDATA
      WRITE (6,201)
  201 FORMAT (1X,'ERRORS IN XS')
      READ,XDER
      WRITE(6,202)
  202 FORMAT(1X,'ACTIVITY COEFFICIENTS FOR GT,PLG,SPN,CPX')
      READ,ACDATA
      WRITE(6,203)
  203 FORMAT(1X,'ACTIVITY COEFF. ERRORS')
      READ,ACDER
      WRITE(6,204)
  204 FORMAT(1X,'TEMP C')
      READ,TC
C
C Thermodynamic data and errors from regression
C
      TDATA(1)=34350
      TDATA(2)=20.0
      TDATA(3)=3.468
      TDER(1)=800
      TDER(2)=0.6
      TDER(3)=0.002
      TK=TC+273.15
C
C Calculate equilibration pressure
C
      CALL PCALC (P,TK,TDATA,XDATA,ACDATA)
C
C Calculate the share of  errors due to uncertainties in
C thermodynamic data
C
      DO 10 I=1,3
      DELT=TDATA(I)*10E-4
      TDATA(I)=TDATA(I)+DELT
      CALL PCALC (PP,TK,TDATA,XDATA,ACDATA)
      TDATA(I)=TDATA(I)-2.*DELT
      CALL PCALC (PM,TK,TDATA,XDATA,ACDATA)
      TDATA(I)=TDATA(I)+DELT
      DPDT=(PP-PM)/(2.*DELT)
      SIGSQ=SIGSQ+(DPDT**2)*(TDER(I)**2)
   10 CONTINUE
C
C Calculate share of errors due to uncertainties in
C compositions of phases
C
      DO 20 I=1,5
```

```
      DELX=0.00001
      XDATA(I)=XDATA(I)+DELX
      CALL PCALC (PP,TK,TDATA,XDATA,ACDATA)
      XDATA(I)=XDATA(I)-2.*DELX
      CALL PCALC (PM,TK,TDATA,XDATA,ACDATA)
      XDATA(I)=XDATA(I)+DELX
      DPDX=(PP-PM)/(2.*DELX)
      SIGSQ=SIGSQ+(DPDX**2)*(XDER(I)**2)
   20 CONTINUE
C
C Calculate share of errors due to uncertainties in activity
C coefficients
C
      DO 30 I=1,4
      DELAC=0.00001
      ACDATA(I)=ACDATA(I)-DELAC
      CALL PCALC (PP,TK,TDATA,XDATA,ACDATA)
      ACDATA(I)=ACDATA(I)-2.*DELAC
      CALL PCALC (PM,TK,TDATA,XDATA,ACDATA)
      ACDATA(I)=ACDATA(I)+DELAC
      DPDAC=(PP-PM)/(2.*DELAC)
      SIGSQ=SIGSQ+(DPDAC**2)*(ACDER(I)**2)
   30 CONTINUE
      WRITE(6,100) P,SQRT(SIGSQ)
  100 FORMAT(1X,'EQUILIBRATION PRESSURE=',F9.1,' VARIANCE=',
     1 F9.1)
      WRITE (6,102)
  102 FORMAT(1X,'CONTINUE? 1=YES')
      READ,ICON
      IF (ICON.EQ.1) GOTO 999
      STOP
      END



      SUBROUTINE PCALC (P,T,TDATA,XDATA,ACDATA)
C
C Routine calculates equilibration pressure. The activity
C of anorthite is calculated using the expression of
C Newton et al., 1980.
C                                                AC Barnicoat
C                                                    May 1982
C
      DIMENSION TDATA(3),XDATA(5),ACDATA(4)
      REAL K
      AAN=(0.25*XDATA(2)*(1.+XDATA(2))**2)*
     1 EXP((XDATA(5)**2*(8473.+19752.*2.*XDATA(3)))/(8.3*T))
      K=(XDATA(1)*ACDATA(1))/(XDATA(3)*ACDATA(3)*AAN
     1 *(XDATA(4)*ACDATA(4))**2)
      P=(TDATA(1) +TDATA(2)*T +8.3*T*ALOG(K))/TDATA(3)
      RETURN
      END
```

```
C          HEATFLOW
C This program calculates the temporal evolution of a 1-D
C temperature profile using the Crank-Nicholson method as
C described in appendix 2.
C     For the boundary conditions TEMP(0,J)=0.0 and d(TEMP)/dX(NX,J)
C     =-Basal flux/cond. Erosion may be either a constant rate or
C  one decreasing exponentially with time.
C
C     SUBROUTINES used are:
C      RHOLAY: to read in density, and if required the number of, and
C              base of, layers required
C      KLAY   : To read in conductivity for each layer.
C      KCALC  : To calculate temperature dependant conductivity if
C              required.
C      CPCALC : To calculate temperature dependant heat capacity if
C              required
C       TRIDG : To solve a tridiagonal set of simultaneous equations.
C       Important VARIABLES are:
C       DX: Size of distance step (CM)
C      DT: Size of time step (S)
C      J : Number of present time step
C      NX: Number of distance steps
C      ERAT: Calculated erosion rate (CMS-1)
C      LBHF: Lower boundary heat flow (HFU)
C      HF  :   "      "       "   "   (CGS UNITS
C      LN: No. of layers
C        ARRAYS used:
C      RHO: Density
C      CP: Heat capacity
C      COND: Conductivity
C      HP: Internal heat production
C      R: R=COND*DT/RHO*CP*DX*DX
C      VO: Temperature at the previous time step
C      V: Temperatures for all previous timesteps at each
        step (2D array).
C      A: Coefficients of simultaneous equations to be solved at
C         the present time step
C      TIME: Time at each time step
C      DELS: Amount of material eroded at each time step
C      LB: Position of the base of each layer
C
C                                                AC Barnicoat 1977
C                                                   Last revised March 1982
C
      REAL LAMBDA,MYS,KMCM,LBHF,P,PJP
       DIMENSION CP(100),HP(100),X(100),R(100),V(100,201),
      1TIME(202),DELS(201),VO(100),RHO(100),COND(100),LB(10 ,
      2AA(10),BB(10),CC(10),TC(10),A(100,4),CP1(100),VJM(100)
       DATA ION /'Y'/
       ICNT=0
       KMCM=1.E5
       MYS=3.15576E13
C
C Read in data,calling subroutines to set up layers and
C to calculate the values of temperature dependant
```

```
C parameters if needed
C
      READ,NX,DELX,DELT
      NXM=NX-1
      NXM2=NX-2
      DX=DELX*KMCM
      DT=DELT*MYS
      CALL RHOLAY(NX,RHOI,RHO,LN,LB)
      READ,CPI
   13 CALL KLAY(LN,LB,CONDI,COND,AA,BB,CC,TC)
      READ (5,1002) IHPO
      GOTO (18,19),IHPO
   19 READ (5,1005)(HP(I),I=1,NX)
      GOTO 9
   18 DO 10 I=1,NX
      HP(I)=0.0
   10 CONTINUE
    9 READ (5,1002) LBCO
      GOTO (20,21),LBCO
   20 READ,ERORAT
      GOTO 22
   21 READ,LAMBDA,MAXED
   22  READ (5,1003)(VO(I),I=1,NX)
      IF (CONDI.GT.0.) GOTO 23
      CALL KCALC(NX,LN,LB,AA,BB,CC,TC,VO,COND)
   23 VUP=VO(1)
       READ,LBHF
      HF=LBHF
      LBHF=LBHF*1.E-6
      DO 24 I=1,NX
      V(I,1)=VO(I)
   24 CONTINUE
      CALL CPCAL1(NX,CPI,CP,VO,COND,DT,DX,RHO)
C
C Calculate representative value of R and allow changes to
C DELX and DELT to reduce it if needed
C
      DX=DELX*KMCM
C
C   Fill 'X' array with depth of each point
C
   33 X(1)=0.0
      DO 25 I=2,NX
      IM=I-1
      X(I)=X(IM)+DELX
   25 CONTINUE
C
C Write out starting parameters if required
C
      READ (5,1004) ILIST
      IF (ILIST.NE.ION) GOTO 27
      WRITE (6,2005) DELX,DELT
      DO 34 I=1,NX
      WRITE (6,2006) X(I),RHO(I),CP(I),COND(I),HP(I)
      HP(I)=HP(I)*1.E-13
   34 CONTINUE
```

```
          GOTO (40,41),LBCO
   40 WRITE (6,2007) HF,ERORAT
      GOTO 27
   41 WRITE (6,2008) HF,MAXED,LAMBDA
   27 NXO=NX
      NXP=NX+1
      J=1
      TIT=0.0
      NT=201
      IED=0
      DELS(1)=0.0
      TIME(1)=0.0
C
C This block claculates the values of the variables which change
C at each time step.It is repeated for each time step
C
C
C
C
C
  100         J=J+1
              IF (J.GT.NT) GOTO 101
              DO 26 I=1,NX
              R(I)=COND(I)*DT/(RHO(I)*CP(I)*DX*DX)
   26         CONTINUE
              JP=J+1
              TIME(J)=TIT+DELT
              JM=J-1
C
C   Calculate the amount of erosion at this time step,modifying
C the size of arrays and reducing NX,etc. when necessary.
C Also calcualte the erosion rate.
C
  199         GOTO (200,201),LBCO
  200         DELS(J)=ERORAT*TIME(J)-IED*DELX
              GOTO 202
  201         DELS(J)=MAXED*(1.-EXP(-TIME(J)/LAMBDA))-IED*DELX
              ERORAT=EXP(-TIME(J)/LAMBDA)*MAXED/LAMBDA
  202         IF (DELS(J).GT.DELX) IED=IED+1
              IF(DELS(J).GT.DELX) GOTO 203
              GOTO 204
  203         NXP=NX
              NX=NX-1
              NXM=NX-1
              NXM2=NX-2
               DO 205 I=1,NX
              IP=I+1
              RHO(I)=RHO(IP)
              CP(I)=CP(IP)
              COND(I)=COND(IP)
              R(I)=R(IP)
              HP(I)=HP(IP)
  205         CONTINUE
              DO 206 I=1,LN
              LB(I)=LB(I)-1
  206         CONTINUE
```

```
            GOTO 199
  204       ERAT=ERORAT*KMCM/MYS
            D=ERAT*DT/DX
C
C   Set up the finite difference equations in 'A'
C
            DO 300 I=3,NXM
            IP=I+1
            IM=I-1
            B=R(I)*VO(IM)+(2.-2.*R(I)-D)*VO(I)
            C=(R(I)+D)*VO(IP)+2.*DT*HP(I)/(RHO(I)*CP(I))
            A(I,4)=B+C
            A(I,3)=-(R(I)+D)
            A(I,2)=2.+2.*R(I)+D
            A(I,1)=-R(I)
300         CONTINUE
            A(2,1)=0.0
            A(2,2)=2.+2.*R(2)+D
            A(2,3)=-(R(2)+D)
            A(2,4)=(2.-2.*R(2)-D)*VO(2)+
     *       (R(2)+D)*VO(3)+2.*HP(2)*DT/(RHO(2)*CP
     *       (2))
             P=(2.*DELX-DELS(JM))/DELX
            PJP=(2.*DELX-DELS(J))/DELX
            A(NX,1)=-R(NX)/PJP
             A(NX,2)=1.+R(NX)/PJP
             A(NX,3)=0.0
             A(NX,4)=VO(NXM)*R(NX)/P+VO(NX)
     *       *(1.-R(NX)/P)+R(NX)*DX*LBHF/COND(NX)
     *       *(1./PJP+1./P)+HP(NX)*DT/(RHO(NX)*CP(NX))
     *       +D*DX*LBHF/COND(NX)
C
C Solve the finite difference equations,then place the
C calculated temperatures into 'V' and 'VO'
C
            CALL TRIDG(A,NX)
            V(1,J)=VUP
            VO(1)=0.
            DO 301 I=2,NX
            V(I,J)=A(I,4)
            VO(I)=V(I,J)
  301       CONTINUE
C
C If necessary,call subroutines to calculate new values of CP and
C COND, using the newly calculated temperatures
C CP is calculated using an estimate of its value at the next time step
C to avoid discontinuities arising at the onset of melting,etc.
C
              CALL CPCAL1(NX,CPI,CP,VO,COND,DT,DX,RHO)
              DO 777 I=1,NX
              VJM(I)=V(I,J-1)
              VJM(I)=VO(I)+(VO(I)-VJM(I))
  777       CONTINUE
              CALL CPCAL1(NX,CPI,CP1,VJM,COND,DT,DX,RHO)
              DO 778 I=1,NX
              CP(I)=0.5*(CP(I)+CP1(I))
```

```
  778       CONTINUE
            IF (CONDI.LT.1.E-6) CALL KCALC(NX,LN,LB,AA,BB,CC,TC,VO,COND)
            TIT=TIME(J)
            DO 303 I=NXP,100
            V(I,J)=1.0
  303       CONTINUE
            GOTO 100
C
C
C
C
C
C   The last portion of the program is concerned with
C   outputting the results of the calculations and resetting
C   variables used in the previous block
C
  101 IP=1
      IF(ICNT.NE.1) GOTO 401
      IP=11
  401 WRITE(6,2000)
       WRITE(6,2001)
      WRITE(6,2002) (TIME(J),J=IP,NT,10)
      DO 500 I=1,NXO
      WRITE(6,2003)X(I),(V(I,J),J=IP,NT,10)
  500 CONTINUE
      WRITE(6,2004)(DELS(J),J=IP,NT,10)
      J=1
      DELS(1)=DELS(NT)
      ICNT=1
      NT=201
      NXO=NX
      READ (5,1004) ICON
       IF (ICON.EQ.ION) GOTO 100
      STOP
1000 FORMAT(I2)
1001 FORMAT(10F4.2)
1002 FORMAT(I1)
1003 FORMAT(10F6.0)
1004 FORMAT(A1)
1005 FORMAT(10F6.2)
2000 FORMAT(1X,//,1X,'TIME (MY)')
2001 FORMAT(1X,'DISTANCE (KM)')
2002 FORMAT(5X,21F6.2)
2003 FORMAT(F5.0,21F6.0)
2004 FORMAT(1X,'DELS',21F6.2)
2005 FORMAT(1X,'STARTING PARAMETERS USED IN THESE CALCULATIONS:',
     1/,1X,'DISTANCE STEP',21X,F4.2,' KM',/,1X,'TIME STEP',25X,
     2F4.2,' MA',//,1X,'DEPTH(KM)  DENSITY(GCM-3)  HT CAP(CALCM-3',
     3'K-1)  COND(CALCM-1K-1S-1)  HT.PRODN(HGU)')
2006 FORMAT(3X,F4.1,10X,F4.2,13X,F4.2,18X,F5.3,13X,F5.3)
2007 FORMAT(/,1X,'LOWER BOUNDARY HEAT FLOW',10X,F4.2,' HFU',/,1X
     *,'EROSION RATE',22X,F4.2,' KM/MA(=MM/YR)')
2008 FORMAT(/,1X,'LOWER BOUNDARY HEAT FLOW',10X,F4.2,' HFU',/,
     *1X'MAXIMUM EROSION DEPTH',13X,I5,' KM',/,1X'EROSION TIME
     * CONSTANT',13X,F6.2,' MA')
3000 FORMAT(1X,'NO. OF DISTANCE STEPS,SIZE OF DISTANCE STEP (KM)'
```

```
    *,/,1X,'AND SIZE OF TIME STEPS (MY)')
3002 FORMAT(1X,'HEAT CAPACITY ?')
3004 FORMAT(1X,'HEAT PRODUCTION OPTION (1 OR 2) ?')
3006 FORMAT(1X,'HEAT PRODUCTION (HGU) ?')
3008 FORMAT(1X,'LOWER BOUNDARY TYPE (1OR 2) ?')
3010 FORMAT(1X,'CONSTANT EROSION RATE (MM/YR=KM/MA) ?')
3012 FORMAT(1X,'VARIABLE EROSION RATE:TIME CONST & MAX DEPTH ?')
3014 FORMAT(1X,'INITIAL TEMPERATURE PROFILE ?')
3016 FORMAT(1X,'LOWER BOUNDARY HEATFLOW (HFU) ?')
3018 FORMAT(1X,'R=COND*DT/RHO*CP*DX*DX = ',F12.5,
    */,' EACH PASS WILL BE FOR',F7.3,'MA',
    */,' DO YOU WISH TO REDUCE R BY CHANGING DX & DT?')
3020 FORMAT(1X,'DT,DX (MA,KM) ?')
3022 FORMAT(1X,'PARAMETER LIST REQUIRED?')
 3024 FORMAT(1X'CONTINUE ?')
      END
      SUBROUTINE TRIDG(A,NX)
C
C Subroutine to solve a set of NX tridiagonal simultaneous
C equations using Gaussian elimination and back-substitution
C
      DIMENSION A(100,4)
      NXM=NX-1
      DO 1 I=3,NX
      A(I,2)=A(I,2)-A(I,1)/A((I-1),2)*A((I-1),3)
      A(I,4)=A(I,4)-A(I,1)/A((I-1),2)*A((I-1),4)
    1 CONTINUE
      NM2=NX-2
      A(NX,4)=A(NX,4)/A(NX,2)
      DO 2 I=1,NM2
      M=NX-I
      A(M,4)=(A(M,4)-A(M,3)*A(M+1,4))/A(M,2)
    2 CONTINUE
      RETURN
      END


      SUBROUTINE RHOLAY(NX,RHOI,RHO,LN,LB)
C Subroutine to read in density and to set up <10 layers if
density is first set to 0.
C
      DIMENSION DENSE(10),RHO(100),LB(10)
      READ,RHOI
      IF (RHOI.GT.0.0) GOTO 1
      READ (5,100) LN
  100 FORMAT(I2)
      DO 2 I=1,LN
      READ,LB(I),DENSE(I)
    2 CONTINUE
      GOTO 5
    1 LN=1
      DENSE(1)=RHOI
      LB(1)=NX
      NT=1
    5 DO 3 I=1,LN
      NB=LB(I)
```

```
      DO 3 K=NT,NB
      RHO(K)=DENSE(I)
      IF(K.EQ.NX) GOTO 4
      NT=LB(I)+1
    3 CONTINUE
    4 RETURN
 1000 FORMAT(1X,'DENSITY ?')
 1002 FORMAT(1X,'NO OF LAYERS ?')
 1004 FORMAT(1X,'BASE,DENSITY OF LAYER ',I2,' ?')
       END


      SUBROUTINE KLAY(LN,LB,CONDI,COND,AA,BB,CC,TC)
      DIMENSION LB(10),COND(100),AA(10),BB(10),CC(10),TC(10)
      NT=1
      DO 1 I=1,LN
      READ,CONDI
      IF (CONDI.EQ.0.0) GOTO 2
      NB=LB(I)
      DO 1  J=NT,NB
      COND(J)=CONDI*1.E-3
      NT=NB+1
    1 CONTINUE
      GOTO 4
    2 DO 3 K=1,LN
    3 READ,AA(K),BB(K),CC(K),TC(K)
    4 RETURN
 1000 FORMAT(1X,'CONDUCTIVITY(MCAL ETC) ?')
 1002 FORMAT(1X,'PARAMETERS A,B,C,TC FOR CONDUCTIVITY ?')
      END


SUBROUTINE KCALC(NX,LN,LB,AA,BB,CC,TC,VO,COND)
DIMENSION LB(10),AA(10),BB(10),CC(10),TC(10),VO(100),COND(100)
NT=1
DO 1 K=1,LN
AB=AA(K)
B=BB(K)
C=CC(K)
CT=TC(K)
NB=LB(K)
DO 1 I=NT,NB
IF(VO(I).LT.CT) C=0.0
COND(I)=1./(AB+(VO(I)+273.15)*B)+C*(VO(I)-CT)
C=CC(K)
IF(K.EQ.NX) GOTO 2
NT=NB+1
    1 CONTINUE
    2 RETURN
      END


      SUBROUTINE CPCAL1 (NX,CPI,CP,VO,COND,DT,DX,RHO)
C
C Subroutine to calculate heat capacity, temperature dependant
C if initial value is set to zero, and to calculate latent heat
```

```
C of melting crystallisation, with a solidus of 800 C and
C a liquidus of 1000 C (increasing at 2.5 and 2 degrees per km respectively)
C
C
      REAL L
      DIMENSION CP(100),VO(100),COND(NX),RHO(NX)
      IF(CPI.NE.0.) GOTO 10
      DO 5 I=1,NX
      CP(I)=0.18*(1.+6.14E-4*(VO(I)+273.15)-1.928E4/((VO(I)+273.15
     *)**2))
    5 CONTINUE
      GOTO 20
   10 DO 15 I=1,NX
      CP(I)=CPI
   15 CONTINUE
   20 L=80.
      DO 30 I=1,NX
      TMIN=800.+(2.5*I*DX/100000.)
      TMAX=1000.0+(2.*I*DX/100000.)
      IF (VO(I).LT.TMIN
     1 .OR.VO(I).GT.TMAX) GOTO 30
      CP(I)=CP(I)+(L/(TMAX-TMIN))
   30 CONTINUE
      DO 40 I=2,NX
      CP(I)=0.5*(CP(I-1)+CP(I))
   40 CONTINUE
      RETURN
      END
```

## References


Allen JC and Boettcher AL (1978) Amphiboles in andesite and basalt. II. Stability as a function of P-T-$f_{H_2O}$-$f_{O_2}$. Am.Mineral. 63,1074-1087

Arndt NT (1977) Mineralogical and chemical variation in two thick, layered komatiitic lava flows. Carnegie Institution of Washington Yearbook 76,494-502

Arth JG and Barker F (1976) Rare-earth partitioning between hornblende and dacitic liquid and implications for the genesis of trondhjemitic-tonalitic magmas. Geology 4,534-536

Barooah BC (1970) Significance of calc-silicate rocks and meta-arkose in the Lewisian complex south east of Scourie. Scot.J.Geol. 6,221-225

Barton CM and England PC (1979) Shear heating at the Olympos (Greece) thrust and the deformation properties of carbonates at geological strain rates. Geol.Soc.Am.Bull. 90,483-492

Beach A (1973) The mineralogy of high temperature shear zones at Scourie, Sutherland. J.Petrol. 14,231-248

Beach A (1974) The measurement and significance of displacements on Laxfordian shear zones NW Scotland. Proc.Geol.Ass. 85,13-21

Beach A (1976) The interrelations of fluid transport, deformation, geochemistry and heat flow in early Proterozoic shear zones in the Lewisian complex. Phil.Trans.Roy.Soc.Lond. A280,569-604

Beach A, Coward MP and Graham RH (1974) An interpretation of the structural evolution of the Laxford front, NW Scotland. Scot.J.Geol. 9,297-308

Best NF (1979) A preliminary study of the tremolite-edenite solid solution series. Progr.Expt.Petrol.NERC. 4,162-163

Bevington PR (1969) Data reduction and error analysis for the physical sciences. McGraw-Hill, New York

Bickle MJ (1978) Heat loss from the Earth: a constraint on Archaean tectonics from the relation between geothermal gradients and the rate of plate production. Earth Planet.Sci.Lett. 40,301-315

Bonnichson B (1969) Metamorphic pyroxenes and amphiboles in the Biwabik Iron Formation, Dunka river area Minnesota. Mineral.Soc.Am.Spec.Pap. 2,217-239

Bostwick TR (1976) The effect of Mn in the stability and phase relations of iron-rich pyroxenes. MS thesis, State Univ. of New York at Stony Brook

Bott MHP, Holland JG, Storry PG and Watts AB (1972) Geophysical evidence concerning the structure of the Lewisian of Sutherland NW Scotland. J.Geol.Soc.Lond. 128,599-612

Bowdidge CR (1969) Petrological studies of the Lewisian basic and ultrabasic rocks near Scourie,Sutherland. Ph.D. thesis Edinburgh Univ.

Bowes DR (1978) Shield formation in early Precambrian times: the Lewisian complex. In DR Bowes and BE Leake (eds.) 'Crustal evolution in NW Britain'. Geol.J.Spec.Issue. 10,39-80

Bowes DR, Wright AE and Park RG (1964) Layered intrusive rocks in the Lewisian of NW Highlands of Scotland. Q.J.Geol.Soc.Lond. 120,159-192

Boyd FR (1959) Hydrothermal investigations of amphibole stability. In PH Abelson (ed) 'Researches in geochemistry. Vol. 1.' Wiley and Sons, New York. 377-396

Bridgewater D, McGregor VR and Myers JS (1974) A horizontal tectonic regime in the Archaean of Greenland and its implications for early crustal thickening. Precambrian Res. 1,179-197

Burns DJ (1966) Chemical and mineralogical changes associated with the Laxfordian metamorphism of dolerite dykes in the Scourie - Loch Laxford area, Sutherland, Scotland. Geol.Mag. 103,20-35

Cameron M and Papike JJ (1979) Amphibole crystal chemistry: a review. Fortschr.Mineral. 57,28-67

Carslaw HS and Jaeger JC (1959) Conduction of heat in solids. 2nd edition Oxford University Press, Oxford

Chapman HJ (1979) 2390 myr Rb-Sr whole rock age for the Scourie dykes of north-west Scotland. Nature. 277,642-643

Chapman HJ and Moorbath S (1977) Lead isotope measurements from the oldest recognised Lewisian gneiss of NW Scotland. Nature. 268,41-42

Charlu TV, Newton RC and Kleppa OJ (1975) Enthalpies of formation of compounds in the systm $MgO-Al_2O_3-SiO_2$ from high temperature solution calorimetry. Geochim.Cosmochim.Acta. 39,1487-1497

Charlu TV, Newton RC and Kleppa OJ (1978) Enthalpy of formation of some lime silicates by high temperature solution calorimetry, with discussion of high pressure phase equilibria. Geochim.Cosmochim.Acta. 42,367-376

Chisolm JE (1973) Planar defects in fibrous amphiboles. J.Mater.Sci. 8,475-483

Copley PA, Champness PE and Lorimer GW (1974) Electron petrography of exsolution textures in an iron-rich clinopyroxene. J.Petrol. 15,41-57

Coward MP (1974) Flat lying structures within the Lewisian basement gneiss complex, NW Scotland. Proc.Geol.Ass. 85,459-472

Coward MP, Lintern BC and Wright LI (1976) The pre-cleavage deformation of the sediments and gneisses of the northern Limpopo belt. In BF Windley (ed) 'The early history of the Earth' Wiley and Sons. 323-330

Coward MP, Kim JH and Parke J (1980) A correlation of Lewisian structures and their displacement across the lower thrusts of the Moine thrust zone, NW Scotland. Proc.Geol.Ass. 91,327-337

Crank J and Nicholson P (1947) A practical method for numerical evaluation of solutions of partial differential equations of the heat conduction type. Proc.Camb.Phil.Soc. 43,50-67

Cullers RL, Medaris LG and Haskin LA (1973) Experimental studies of rare earths as trace elements among silicate minerals and liquids and water. Geochim.Cosmochim.Acta 37,1499-1512

Danckwerth PA and Newton RC (1978) Experimental determination of the spinel peridotite to garnet peridotite reaction in the system $MgO-Al_2O_3-SiO_2$ in the range 900-1100°C and $Al_2O_3$ isopleths of enstatite in the spinel field. Contrib.Mineral.Petrol. 66,189-201

Davies FB (1974) A layered basic complex in the Lewisian south of Loch Laxford, Sutherland. J.Geol.Soc.Lond. 130,279-284

Davies FB (1975) Origin and ancient history of gneisses older than 2800 my in the Lewisian complex. Nature. 258,589

Davies FB (1976) Early Scourian structures in the Scourie-Laxford region and their bearing on the evolution of the Laxford front. J.Geol.Soc.Lond. 132,543-554

Davies FB (1978) Progressive simple shear on the Laxford shear zone, Sutherland. Proc.Geol.Ass. 89,177-196

Deer WA, Howie RA and Zussman J (1962) Rock forming mineral. 1. Ortho- and ring silicates. Longmans,London

De Waard D (1965) A proposed sub-division of the granulite facies. Am.J.Sci. 263,455-461

Dickinson BR and Watson J (1976) Variations in crustal level and geothermal gradient during the evolution of the Lewisian complex of northwest Scotland. Precambrian Res. 3,363-374

Dodson MH (1976) Kinetic processes and thermal history of slowly cooling solids. Nature. 259,551-553

Doolan BL, Zen E-An and Bence AE (1978) Highly aluminous hornblendes: compositions and occurences from southwestern Massachusetts. Am.Mineral. 63,1088-1099

Drake MJ and Weill DF (1975) Partition of Sr, Ba, Ca, Y, $Eu^{2+}$, $Eu^{3+}$ and other REE between plagioclase feldspar and magmatic liquid: an experimental study. Geochim.Cosmochim.Acta. 39,689-712

Drury SA (1973) TThe geochemistry of precambrian granulite facies rocks from the Lewisian complex of Tiree, Inner Hebrides, Scotland. Chem. Geol. 11,167-188

Duckworth S and Freer R (1981) Cation diffusion studies in garnet-garnet and garnet-pyroxene couples at high temperatures and pressures. Progr.Expt.Petrol.NERC. 5,36-39

Eggler DH (1978) The effect of $CO_2$ upon partial melting in the system $Na_2O$-CaO-$Al_2O_3$-MgO-$SiO_2$-$CO_2$ to 35kbar, with an analysis of melting in a peridotite-$H_2O$-$CO_2$ system. Am.J.Sci. 278,305-343

Eggler DH and Burnham CW (1973) Crystallisation and fractionation trends in the system Andesite-$H_2O$-$CO_2$-$O_2$ at pressures to 10kb. Geol.Soc.Am.Bull. 84,2517-2532

Ellis DJ and Green DH (1979) An experimental study of the effect of Ca upon garnet-clinopyroxene Fe-Mg exchange equilibria. Contrib.Mineral.Petrol. 71,13-22

England PC and Richardson SW (1977). The influence of erosion upon the mineral facies of rocks from different metamorphic environments. J.Geol.Soc.Lond. 134,201-213

Evans CR (1965). Geochronology of the Lewisian basement near Lochinver, Sutherland. Nature. 207,54-56

Evans CR and Lambert RStJ (1974) The Lewisian of Lochinver, Sutherland; the type area for the Inverian metamorphism. J.Geol.Soc.Lond. 130,125-150

Finger LW and Burt DM (1972). REACTION, a Fortran IV computer program to balance chemical reactions. Carnegie Institution of Washington Yearbook 71,616-620

Ford CE (1972) Furnace design, temperature distribution, calibration and seal design in internally heated pressure vessels. Progr.Expt.Petrol.NERC. 2,89-96

Fraser DG and Lawless PJ (1978) Palaeogeotherms: implications of disequilibrium in garnet lherzolite xenoliths. Nature. 273,220-222

Freer R (1981) Diffusion in silicate minerals and glasses: a data digest and guide to the literature. Contrib.Mineral.Petrol. 76,440-454

Fyfe WS (1973) The granulite facies, partial melting and the Archaean crust. Phil.Trans.Roy.Soc.Lond. A273,457-461

Ganguly J (1979) Garnet and clinopyroxene solid solutions, and geothermometry based on Fe-Mg distribution coefficient. Geochim.Cosmochim.Acta. 43,1021-1029

Gasparik T and Lindsley (1981) Phase equilibria at high pressure of pyroxenes containing monovalent and trivalent ions. In CT Prewitt (ed) Reviews in mineralogy (Mineral.Soc.Am.) 7,309-339

Gerald CF (1978) Applied numerical analysis. 2nd edition. Addison-Wesley, Reading,Mass.

Giletti BJ, Moorbath S and Lambert RStJ (1961) A geochronological study of the metamorphic complexes of the Scottish Highlands. Q.J.Geol.Soc.Lond. 117,233-272

Gole MJ and Klein C (1981) High-grade Archaean banded iron-formations, Western Australia: assemblages with coexisting pyroxenes fayalite. Am.Mineral. 66,87-99

Graham CM and England PC (1976) Thermal regimes and regional metamorphism in the vicinity of overthrust faults: an example of shear heating and inverted metamorphic zonation from southern California. Earth Planet.Sci.Lett. 31,142-152

Gross GA (1980) A classification of iron formations based on depositional environment. Can.Mineral. 18 215-222

Gross GA and McLeod CR (1980) A preliminary assessment of the chemical composition of iron formations in Canada. Can.Mineral. 18,223-229

Hamilton PJ, Evensen NM, O'Nions RK and Tarney J (1979) Sm-Nd systematics of Lewisian gneisses: implications for the origin of granulites. Nature. 277,25-28

Hanson GN (1980) Rare earth elements in petrogenetic studies of igneous rocks. Ann.Rev.Earth Planet.Sci. 8,371-406

Hansen B (1981) The transition from pyroxene granulite facies to garnet clinopyroxene facies. Experiments in the system $CaO-MgO-Al_2O_3-SiO_2$. Contrib.Mineral.Petrol. 76,234-242

Haselton HT and Newton RC (1980) Thermodynamics of pyrope-grossular garnets and their stabilities at high temperatures and pressures. J.Geophys.Res. 85,6973-6982

Harte B, Jackson PM and Macintyre RM (1981) Age of mineral equilibria in granulite facies nodules from kimberlites. Nature. 291,147-148

Hawkesworth CJ (1974) Vertical distribution of heat production in the basement of the eastern Alps. Nature. 249,535

Helz RT (1973) Phase relations of basalts in their melting range at $P_{H_2O}$=5kb as a function of oxygen fugacity. Part I. Mafic phases. J.Petrol. 14,249-302

Helz RT (1976) Phase relations of basalts in their melting range at $P_{H_2O}$=5kb. Part II. Melt compositions. J.Petrol. 17,139-193

Hensen BJ (1976) The stability of pyrope-grosular garnet with excess silica. Contrib.Mineral.Petrol. 55,279-292

Herzberg CT (1972) Stability fields of plagioclase and spinel lherzolite. Progr.Expt.Petrol.NERC. 2,145-148

Herzberg CT (1975) The stability of pyrope-rich garnet within the spinel-lherzolite facies. Progr.Expt.Petrol.NERC. 3,235-237

Herzberg CT (1978) Pyroxene geothermometry and geobarometry: experimental and thermodynamic evolution of subsolidus phase relations in the system $CaO-MgO-Al_2O_3-SiO_2$. Geochim.Cosmochim.Acta. 42,945-958

Herzberg CT and O'Hara MJ (1972) Temperature and pressure calibration and reproducibility of pressure in solid media equipment. Progr.Expt.Petrol.NERC. 2,97-98

Holland JG and Lambert RStJ (1973) Comparative major element geochemistry of the Lewisian of the mainland of Scotland. In RG Park and J Tarney (eds) 'Early precambrian rocks of Scotland and related rocks of Greenland.' Univ. of Keele. 51-62

Holland JG and Lambert RStJ (1975) The chemistry and origin of the Lewisian gneisses of the Scottish mainland: the Scourie and Inver assemblages and sub-crustal accretion. Precambrian Res.2,161-188

Holland TJB (1981) Thermodynamic analysis of simple mineral systems. In RC Newton, A Navrotsky and BJ Wood (eds) 'Thermodynamics of minerals and melts'. Springer-Verlag. 19-34

Holland TJB, Navrotsky A and Newton RC (1979) Thermodynamic parameters of $CaMgSi_2O_6-Mg_2Si_2O_6$ pyroxenes based on regular solution and cooperative disordering models. Contrib.Mineral.Petrol. 69,317-344

Holloway JR (1973) The system pargasite-$H_2O-CO_2$: a model for melting of a hydrous mineral with a mixed-volatile fluid - I. Experimental results to 8Kbar. Geochim.Cosmochim.Acta. 37,651-666

Holloway JR and Burnham CW (1972) Melting relations of basalts with equilibrium water pressure less than total pressure. J.Petrol. 13,1-29

Hollister LA and Burruss RC (1976) Phase equilibria in fluid incusions from the Khatada Lake metamorphic complex. Geochim.Cosmochim.Acta. 40,163-175

Huang WL and Wyllie PJ (1975) Melting reactions in the system $NaAlSi_3O_8$-$KAlSi_3O_8$-$SiO_2$ to 35 kilobars, dry and with excess water. J.Geol. 83 737-748

Humphries FJ and Clif RA (1982) Sm-Nd dating and cooling history of Scourian granulites, Sutherland. Nature. 295,515-517

Irving AJ and Frey FA (1978) Distribution of trace elements between garnet megacrysts and host volcanic liquids of kimberlitic to rhyolitic composition. Geochim.Cosmochim.Acta. 42,771-788

Jackson PM (1981) Experimental studies of the reaction: orthopyroxene + plagioclase = garnet + clinopyroxene + quartz. Progr.Expt.Petrol.NERC. 5,201-203

Jaffe HW, Robinson P and Tracey RJ (1975) Orientation of pigeonite exsolution lamellae in metamorphic augite: correlation with composition and calculated optimal phase boundaries. Am.Mineral. 66,9-28

Jenkins DM (1981) Experimental phase relations of hydrous peridotites modelled in the system $H_2O$-CaO-MgO-$Al_2O_3$-$SiO_2$. Contrib.Mineral.Petrol. 77,166-176

Jenkins DM and Newton RC (1979) Experimental determination of the spinel peridotite to garnet peridotite inversion at 900°C and 1100°C in the system CaO-MgO-$Al_2O_3$-$SiO_2$, and at 900°C with natural garnet and olivine. Contrib.Mineral.Petrol 68,407-419

Kerrick DM and Darken LS (1975) Statistical themodynamic models for ideal oxide and silicate solid solutions, with applications to plagioclase. Geochim.Cosmchim.Acta. 39,1431-1442

Kushiro I and Yoder HS (1966) Anorthite-forsterite and anorthite-enstatite reactions and their bearing on the basalt-eclogite transformation. J.Petrol. 7,337-362

Lambert IB and Wyllie PJ (1972) Melting of a gabbro (quartz eclogite) with excess water to 35 kbars, with geological applications. J.Geol. 80,693-708

Leake BE (1978) Nomenclature of amphiboles. Mineral.Mag. 42,533-563

Lindh A (1974) Manganese distribution between coexisting pyroxenes. Neues.Jahrb.Mineral.Monatsheft. 1974 335-345

Lindsley DH, Grover JE and Davidson PM (1981) The thermodynamics of the $Mg_2Si_2O_6$ - $CaMgSi_2O_6$ join: a review and an improved model. In RC Newton, A Navrotsky and BJ Wood (eds) 'Themodynamics of minerals and melts' Springer-Verlag. 149-175

McGregor VR and Mason B (1977) Petrogenesis and geocheistry of metabasaltic and metasedimentary enclaves in the Amitsoq gneisses, west Greenland. Am.Mineral. 62,887-904

Miyashiro A (1973) Metamorphism and metamorphic belts. Allen and Unwin, London

Moorbath S, Welke H and Gale NH (1969) The significance of Pb isotope studies in acsient high-grade metamorphic basement, as exemplified by the Lewisian rocks of NW Scotland. Earth Planet.Sci.Lett. 6,245-256

Mori T (1978) Experimental study of pyroxene equilibria in the system $CaO-MgO-FeO-SiO_2$. J.Petrol. 19,45-65

Muecke GK (1969) Petrogenesis of granulite facies rocks from the Lewisian of north-west Scotland D.Phil. thesis Oxford Univ.

Muecke GK, Pride C and Sarkhar P (1979) Rare-earth element geochemistry of regionally metamorphosed rocks. Phys.Chem.Earth 11,449-464

Newton RC (1978) Experimental and thermodynamic evidence for the operation of high pressures in Archaean metamorphism. In BF Windley and SM Naqvi (eds) 'Archaean geochemistry' Elsevier. 221-240

Newton RC, Charlu TV and Kleppa OJ (1977) Thermochemistry of high pressure garnets and clinopyroxenes in the system $CaO-MgO-Al_2O_3-SiO_2$. Geochim.Cosmochim.Acta. 41,369-377

Newton RC, Charlu TV Anderson PAM and Kleppa OJ (1979) Thermochemistry of synthetic clinopyroxenes on the join $CaMgSi_2O_6-Mg_2Si_2O_6$. Geochim.Cosmochim.Acta. 43,55-60

Newton RC, Charlu TV and Kleppa OJ (1980) Thermochemistry of high structural state plagioclases. Geochim.Cosmochim.Acta. 44,933-941

Newton RC and Haselton HT (1981) Thermodynamics of the garnet-plagioclase-quartz geobarometer. In RC Newton, A Navrotsky and BJ Wood (eds) 'Thermodynamics of minerals and melts' Springer-Verlag. 131-147

Nicholls IA and Harris KL (1980) Experimental rare earth element partition coefficients for garnet, clinopyroxene and amphibole coexisting with andesitic and basaltic liquids. Geochim.Cosmochim.Acta. 44,287-308

Nisbet EG, Bickle MJ and Martin A (1977) The mafic and ultramafic lavas of the Belingwe greenstone belt, Rhodesia. J.Petrol. 18,521-566

Oba T (1978) Phase relationship of $Ca_2Mg_3Al_2Si_6Al_2O_{22}(OH)_2$ - $Ca_2Mg_3Fe^{3+}_2Si_6Al_2O_{22}(OH)_2$ join at high temperature and pressure - the stability of tschermakite. J.Fac.Sci.Hokkaido Univ. Ser.IV 18,339-350

Obata M and Thompson AB (1981) Amphibole and chlorite in mafic and ultramafic rocks in the lower crust and upper mantle: a theoretical approach. Contrib.Mineral.Petrol. 77,74-81

O'Hara MJ (1960) The metamorphic petrology of the Scourie district, Sutherland. Ph.D. thesis Cambridge Univ.

O'Hara MJ (1961a) Petrology of the Scourie dyke. Mineral.Mag 32,848-865

O'Hara MJ (1961b) Zoned ultrabasic and basic gneiss masses in the early Lewisian metamorphic complex at Scourie, Sutherland. J.Petrol. 2,248-276

O'Hara MJ (1962) Some intrusions in the Lewisian complex near Badcall, Sutherland. Trans.Edin.Geol.Soc. 19,201-207

O'Hara MJ (1965) Origin of ultrabasic and basic gneiss masses in the Lewisian. Geol.Mag. 102,296-314

O'Hara MJ (1967a) Mineral facies in ultrabasic rocks. In PJ Wyllie (ed) 'Ultramafic and related rocks'. Wiley and Sons, New York. 7-18

O'Hara MJ (1967b) Mineral parageneses in ultrabasic rocks. In PJ Wyllie (ed) 'Ultramafic and related rocks'. Wiley and Sons, New York. 393-403

O'Hara MJ (1977) Thermal history of excavation of Archaean gneisses from the base of the continental crust. J.Geol.Soc.Lond. 134,185-200

O'Hara MJ and Yarwood G (1978) High pressure-temperature point on an Archaean geotherm, implied magma genesis by crustal anatexis, and consequences for garnet-pyroxene thermometry and barometry. Phil.Trans.Roy.Soc.Lond. A288,441-456

O'Neill HStC (1981) The transition between spinel lherzolite and garnet lherzolite, and its use as a geobarometer. Contrib.Mineral.Petrol. 77,185-194

O'Neill HStC and Wood BJ (1979) An experimental study of Fe-Mg partitioning between garnet and olivine and its calibration as a geothermometer. Contrib.Mineral.Petrol. 70,59-70

Oxburgh ER and Turcotte DL (1974) Thermal gradients and regional metamorphism in overthrust terrains wth special reference to the eastern Alps. Schweiz.Mineral.Petrogr.Mitt. 54,641-662

Park RG (1970) Observations on Lewisian chronology. Scot.J.Geol 6,379-399

Peach BN, Horne J, Gunn W, Clough CT and Hinxman LW (1907) The geological structure of the north-west Highlands of Scotland. Mem.Geol.Surv.Great Britain

Phillips GN (1980) Water activity changes across an amphibolite-granulite facies transision, Broken Hill, Australia. Contrib.Mineral.Petrol. 75,377-368

Perkins D and Newton RC (1980) The composition of coexisting pyroxenes and garnets in the system $CaO-MgO-Al_2O_3-SiO_2$ at 900 -1100°C and high pressures. Contrib.Mineral.Petrol. 75,291-300

Pidgeon RT and Bowes DR (1972) Zircon U-Pb ages of granulites from the central region of the Lewisian, north west Scotland. Geol.Mag. 109,247-258

Pitcher WS (1979) The nature, ascent and emplacement of granitic magmas. J.Geol.Soc.Lond. 136,627-662

Powell R (1975) Thermodynamics of coexisting cumingtonite-hornblende pairs. Contrib.Mineral.Petrol. 51,29-37

Powell R (19789) The thermodynamics of pyroxene geotherms. Phil.Trans.Roy.Soc.Lond. A288,457-469

Powell R (1978b) Equilibrium thermodynamics in petrology. Harper and Row, London

Pride C and Muecke GK (1980) Rare earth element geochemistry of the Scourian complex NW Scotland - evidence for the granite granulite link. Contrib.Mineral.Petrol. 73,403-412

Pride C and Muecke GK (1981) Rare eath element distribution among coexisting granulite facies minerals, Scourian complex, NW Scotland. Contrib.Mineral.Petrol 76,463-471

Richardson SW and England PC (1979) Metamorphic consequences of crustal eclogite production in overthrust orogenic zones. Earth Planet.Sci.Lett. 42,183-190

Robie RA, Hemingway BS and Fishe JR (1978) Thermodynamic properties of minerals and related substances at 298.15K and 1bar ($10^5$ pascals) pressure and higher temperatures. Geol.Surv.Am.Bull. 1452

Robinson P, Jaffe HW, Ross M and Klein C (1971) Orientation of exsolution lamellae in clinopyroxene and clinoamphiboles: consideration of optimal phase boundaries. Am.Mineral. 56,909-939

Robinson P, Ross M, Nord GL, Smyth JR and Jaffe HW (1977) Exsolution lamellae in augite and pigeonite: fossil indicators of lattice parameters at high temperatures and pressures. Am.Mineral. 62,857-873

Rollinson HR (1979) Ilmenite-magnetite geothermometry in trondhjemites from the Scourian complex of NW Scotland. Mineral.Mag. 43,165-170

Rollinson HR (1980a) Iron-titanium oxides as an indicator of the role of the fluid phase during the cooling of granites metamorphosed to granulite grade. Mineral.Mag. 43,623-631

Rollinson HR (1980b) Mineral reactions in a granulite facies calc-silicate rock from Scourie. Scot.J.Geol. 16,153-164

Rollinson HR (1981) Garnet-pyroxene thermometry and barometry in the Scourie complex, NW Scotland. Lithos 14,225-238

Rollinson HR and Windley BF (1980a) Selective elemental depletion during metamorphism of Archaean granulites, Scourie, NW Scotland. Contrib.Mineral.Petrol. 72,257-263

Rollinson HR and Windley BF (1980b) An Archaean granulite-grade tonalite-trondhjemite-granite suite from Scourie, NW Scotland. Contrib.Mineral.Petrol. 72,265-281

Ross M, Huebner JS and Dowty E (1973) Delineation of the one atmosphere augite-pigeonite miscibility gap for pyroxenes from Lunar basalt 12021. Am.Mineral. 58,619-635

Ross MJ and Huebner JS (1975) A pyroxene geothermometer based on composition-temperature relationships of naturally occuring orthopyroxene, pigeonite and augite. International conference on goethermometry and geobarometry abstracts. Penn.State.Univ.

Ross M, Papike JJ and Shaw KW (1969) Exsolution textures in amphiboles as indicators of sub-solidus thermal histories. Mineral.Soc.Am.Spec.Pap. 2 275-299

Savage D and Sills JD (1980) High pressure metamorphism in the Scourian of NW Scotland: evidence from garnet granulites. Contrib.Mineral.Petrol. 74,153-163

Saxena SK (1979) Garnet-clinopyroxene geothermometer. Contrib.Mineral.Petrol. 70,229-235

Sheraton JW (1970) The origin of the Lewisian gneisses of north-west Scotland, with particular reference to the Drumbeg area, Sutherland. Earth Planet.Sci.Lett. 8,301-310

Sheraton JW, Skinner AC and Tarney J (1973) The geochemistry of the Scourian gneisses of the Assynt district. In RG Park and J Tarney (eds) 'Early precambrian rocks of Scotland and related rocks of Greenland' Univ.of Keele 13-30

Smith GD (1978) Numerical solution of partial differential equations: finite difference methods. 2nd edition. Oxford University Press, Oxford

Sutton J and Watson J (1951) The pre-Torridonian history of the Loch Torridon and Scourie areas in the north-west Highlands and its bearing on the chronological classification of the Lewisian. Q.J.Geol.Soc.Lond. 106,241-296

Tarney J (1963) Assynt dykes and their metamorphism. Nature. 199,672-674

Tarney J (1973) The Scourie dyke suite and the nature of the Inverian event in Assynt. In RG Park and J Tarney (eds) 'Early precambrian rocks of Scotland and related rocks of Greenland'. Univ. of Keele. 105-118

Tarney J (1976) Geochemistry of Archaean high-grade gneisses, with implications as to the origin and evolution of the pre-cambrian crust. In BF Windley (ed) 'The early history of the Earth'. Wiley and Sons, New York 405-417

Tarney J, Weaver B and Drury SA (1979) Geochemistry of Archaean trondhjemitic and tonalitic gneisses from Scotland and East Greenland. In F Barker (ed) 'Trondhjemites, dacites and related rocks'. Elsevier. 175-199

Tarney J and Windley BF (1977) Chemistry, thermal gradients and evolution of the lower crust. J.Geol.Soc.Lond. 134,153-172

Teall JJH (1885) The metamorphism of dolerite to hornblende schist. Q.J.Geol.Soc.Lond. 41,133-144

Turner FJ (1981) Metamorphic petrology. 2nd edition. McGraw Hill, New York

Ujike O (1980) Petrology and petrochemistry of Shirotori-Hiketa dike swarm, northeastern Shikoku, Japan: products of amphibole-dominated fractional crystallisation. J.Petrol. 21,721-741

Walsh JN, Buckley F and Barker J (1981) The simultaneous determination of rare-earth elements in rocks using inductively coupled plasma source spectroscopy. Chem.Geol. 33,141-154

Walsh JN and Howie RA (1980) An evaluation of the performance of an inductively coupled plasma source spectrometer for the determination of major and trace constituents of silicate rocks and minerals. Mineral.Mag. 43,967-974

Sheraton JW, Skinner AC and Tarney J (1973) The geochemistry of the Scourian gneises of the Assynt district. In RG Park and J Tarney (eds) 'Early precambrian rocks of Scotland and related rocks of Greenland' Univ.of Keele 13-30

Smith GD (1978) Numerical solution of partial differential equations: finite difference methods. 2nd edition. Oxford University Press, Oxford

Sutton J and Watson J (1951) The pre-Torridonian history of the Loch Torridon and Scourie areas in the north-west Highlands and its bearing on the chronological classification of the Lewisian. Q.J.Geol.Soc.Lond. 106,241-296

Tarney J (1963) Assynt dykes and their metamorphism. Nature. 199,672-674

Tarney J (1973) The Scourie dyke suite and the nature of the Inverian event in Assynt. In RG Park and J Tarney (eds) 'Early precambrian rocks of Scotland and related rocks of Greenland'. Univ. of Keele. 105-118

Tarney J (1976) Geochemistry of Archaean high-grade gneisses, with implications as to the origin and evolution of the pre-cambrian crust. In BF Windley (ed) 'The early history of the Earth'. Wiley and Sons, New York 405-417

Tarney J, Weaver B and Drury SA (1979) Geochemistry of Archaean trondhjemitic and tonalitic gneisses from Scotland and East Greenland. In F Barker (ed) 'Trondhjemites, dacites and related rocks'. Elsevier. 175-199

Tarney J and Windley BF (1977) Chemistry, thermal gradients and evolution of the lower crust. J.Geol.Soc.Lond. 134,153-172

Teall JJH (1885) The metamorphism of dolerite to hornblende schist. Q.J.Geol.Soc.Lond. 41,133-144

Turner FJ (1981) Metamorphic petrology. 2nd edition. McGraw Hill, New York

Ujike O (1980) Petrology and petrochemistry of Shirotori-Hiketa dike swarm, northeastern Shikoku, Japan: products of amphibole-dominated fractional crystallisation. J.Petrol. 21,721-741

Walsh JN, Buckley F and Barker J (1981) The simultaneous determination of rare-earth elements in rocks using inductively coupled plasma source spectroscopy. Chem.Geol. 33,141-154

Walsh JN and Howie RA (1980) An evaluation of the performance of an inductively coupled plasma source spectrometer for the determination of major and trace constituents of silicate rocks and minerals. Mineral.Mag. 43,967-974

Watson J (1975) The Lewisian complex. In 'Precambrian'. Spec.Rept.Geol.Soc.Lond. 6,15-29

Weaver BL and Tarney J (1980) Rare earth geochemistry of Lewisian granulite-facies gneisses, northwest Scotland: implications for the petrogenesis of the Archaean lower crust. Earth Planet.Sci.Lett. 51,279-296

Weaver BL and Tarney J (1981a) Chemical changes during dyke metamorphism in high-grade basement terrains. Nature. 289,47-49

Weaver BL and Tarney J (1981b) The Scourie dyke suite: petrogenesis and geochemical nature of the Proterozoic sub-continental mantle. Contrib.Mineral.Petrol. 78,175-188

Wells PRA (1976) Late Archaean metamorphism in the Buksefjorden region SW Greenland. Contrib.Mineral.Petrol. 59,229-242

Wells PRA (1977) Pyroxene thermometry in simple and complex systems. Contrib.Mineral.Petrol. 62,129-139

Wells PRA (1979) Chemical and thermal evolution of Archaean sialic crust, SW Greenland. J.Petrol. 20,187-226

Wells PRA (1980) Thermal models for the magmatic accretion and subsequent metamorphism of continental crust. Earth Planet.Sci.Lett. 46,253-265

Wells PRA (1981) Accretion of continental crust: thermal and geochemical consequences. Phil.Trans.Roy.Soc.Lond. A301,347-357

Wood BJ (1974) Solubility of alumina in orthopyroxene coexisting with garnet. Contrib.Mineral.Petrol. 46,1-15

Wood BJ (1975) The influence of pressure, temperature and bulk composition on the appearance of garnet in ortho-gneisses - an example from South Harris, Scotland. Earth Planet.Sci.Lett. 26,299-311

Wood BJ (1977) The activities of components in clinopyroxene and garnet solid solutions and their application to rocks. Phil.Trans.Roy.Soc.Lond. A286,331-342

Wood BJ (1979) Activity-composition relationships in $Ca(Mg,Fe)Si_2O_6$ - $CaAl_2SiO_6$ clinopyroxene sold solutions. Am.J.Sci. 279,854-875

Wood BJ and Kleppa OJ (1981) Thermochemistry of forsterite-fayalite olivine solutions. Geochim.Cosmochim.Acta. 45,529-534

Wyllie PJ (1971) The dynamic Earth. Wiley and Sons, New York

Wyllie PJ (1977) Crustal anatexis: an experimental review. Tectonophysics 43,41-71

Wyllie PJ (1979) Magmas and volatile components. Am.Mineral. 64,469-500

Yamaguchi Y, Akai J and Tomita K (1978) Clinoamphibole lamellae in diopside of garnet lherzolite from Alpe Arami, Bellinzona, Switzerland. Contrib.Mineral.Petrol. 66,263-270

## Additional references

England PC (1978) Some thermal considerations of alpine metamorphism, past, present and future. Tectonophysics 46,21-40

England PC (1979) Continental geotherms during the Archaean. Nature 277,556-558